**Oceano Dunes State Vehicular Recreation Area (ODSVRA) Dust Control Program**
**Provisional Final 2026 Annual Report and Work Plan (ARWP)**

## ATTACHMENTS

Attachment 01: 2011 to 2026 Dust Control Projects

Attachment 02: 2025/2026 ODSVRA Dust Control Program Vegetation Restoration Projects (State Parks' ARWP Work Product)

Attachment 03: Report of Findings: ODSVRA Meteorological and $PM_{10}$ Monitoring Network, 2025

- Report of Findings: ODSVRA Meteorological and $PM_{10}$ Monitoring Network, 2025 (DRI Document)
- SAG Review of Desert Research Institute (DRI) "Report of Findings: ODSVRA Meteorological and $PM_{10}$ Monitoring Network, 2025" (SAG Memo)

Attachment 04: ODSVRA Emissivity PI-SWERL Update Report (2025):

- ODSVRA Emissivity PI-SWERL Update Report (2025) (SAG Memo)

Attachment 05: UCSB 2025-2026 ODSVRA Foredune Restoration Area UAS Monitoring Report

- UCSB 2025-2026 ODSVRA Foredune Restoration Area UAS Monitoring Report (UCSB Report)
- SAG Review of UCSB Report "2025-2026 ODSVRA Foredune Restoration Area UAS Monitoring Report" (SAG Memo)

Attachment 06: Summary of Vegetation Monitoring of Restoration Sites at ODSVRA (2025) (State Parks' ARWP Work Product)

Attachment 07: Increments of Progress Toward Air Quality Objectives, ODSVRA Dust Control 2025 Update

- Increments of Progress Toward Air Quality Objectives, ODSVRA Dust Control 2025 Update (DRI Document)
- SAG Review of DRI "Increments of Progress Toward Air Quality Objectives, ODSVRA Dust Control 2025 Update" (SAG Memo)

Attachment 08: SAG Recommendations for Parameterizing Vegetative Grid Cells

- Recommendations for Reconciling DRI Model Assumptions with Ground Evidence in Respect of Vegetated Grid Cells (SAG Memo)
- Incorporating Vegetation Cover into the DRI Model (SAG Memo)
- Contemplating DRI Model Refinements in Anticipation of the 2026 ARWP (SAG Memo)

- Synthetic Power Relations for Vegetation Islands (SAG Memo)
- Restoration Project Maturation Timeline (State Parks Memo)

Attachment 09: Modeling to Determine the Condition of Excess Emissions for 2026 ODSVRA (DRI Document)

Attachment 10: 2026 PMRP Evaluation Metrics

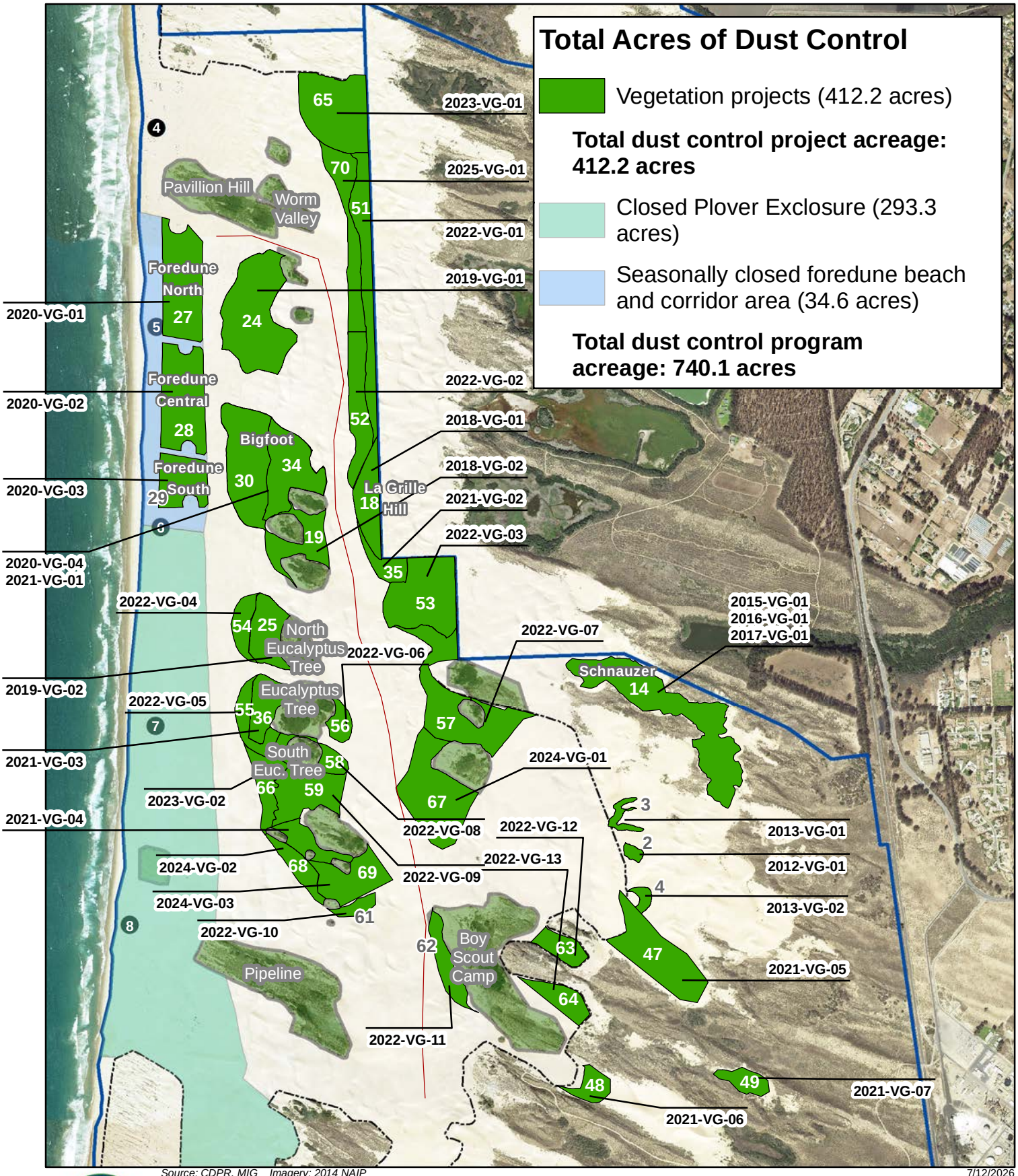
Attachment 11: 2026/2027 ODSVRA Dust Control Program Vegetation Restoration Projects

**ODSVRA Dust Control Program SAG Review Draft 2026 ARWP**

**ATTACHMENT 01**

**2011 to 2026 Dust Control Projects**

*THIS PAGE WAS INTENTIONALLY LEFT BLANK*




# A01-01: Cumulative Dust Control as of 7/31/2026

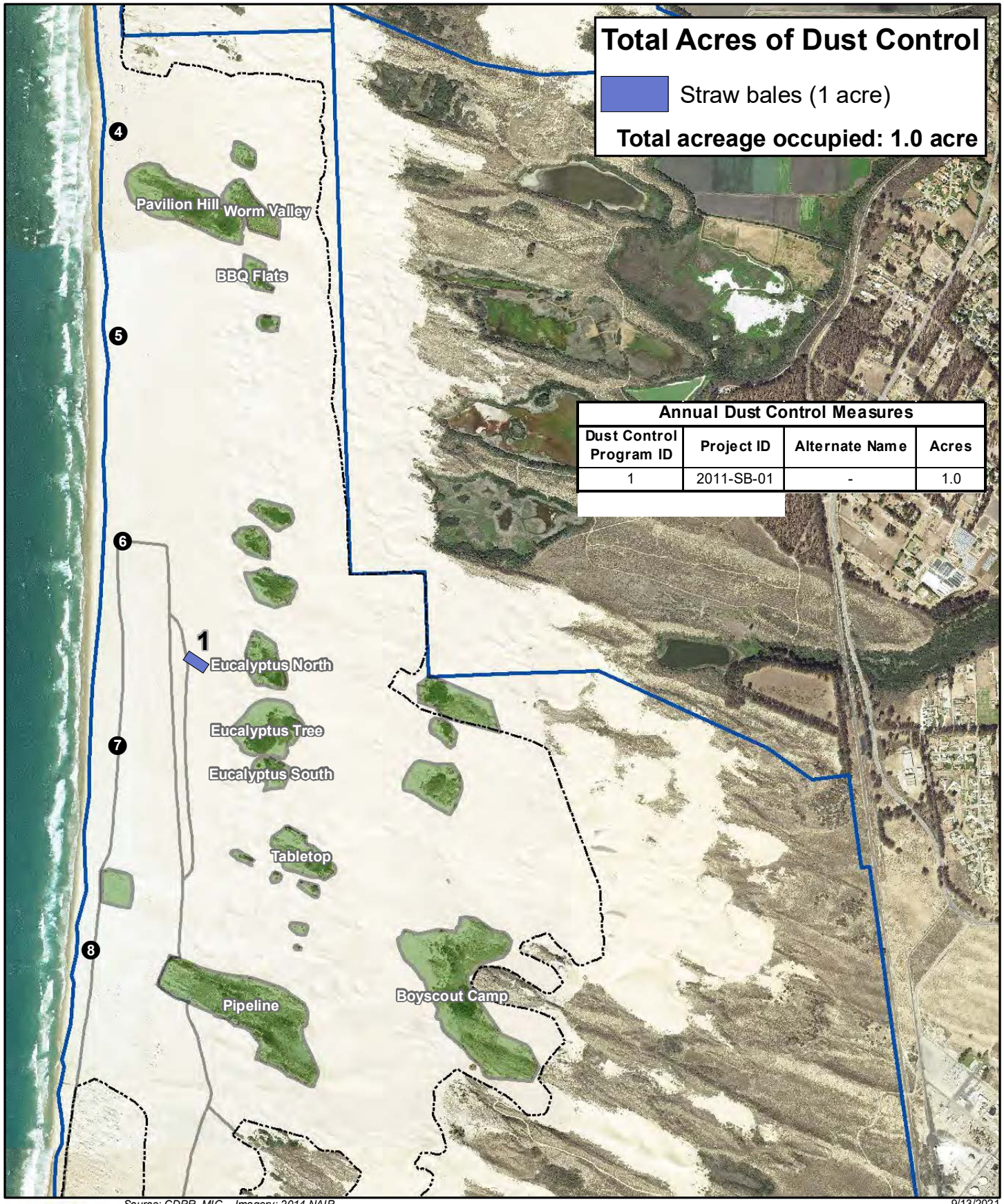
*2026 ARWP*

Sand Highway, approx. | Marker post | Existing fenced vegetated islands

Park boundary | Open riding and camping area boundary fence

N

0 500 1,000 2,000 Feet




Source: CDPR, MIG Imagery: 2014 NAIP

9/13/2021

Feet
0 500 1,000 2,000

N

# A01-02: 2011 Dust Control Treatment Areas

*2026 ARWP*

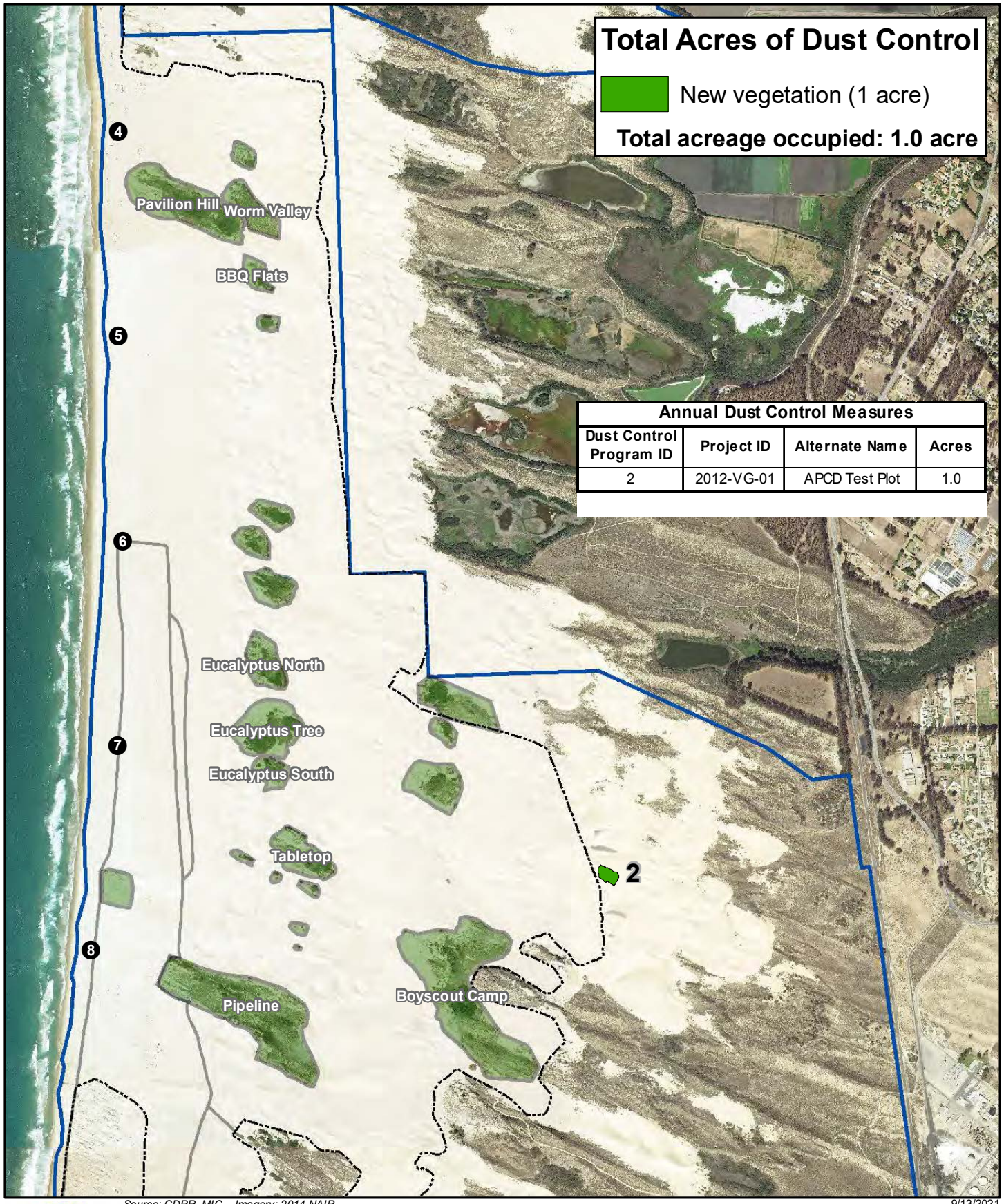
Marker post

Existing fenced vegetated islands

Park boundary

Nesting exclosure from 2020

Open riding and camping area boundary fence




Source: CDPR, MIG Imagery: 2014 NAIP

9/13/2021

Feet
0 500 1,000 2,000

N

# A01-03: 2012 Dust Control Treatment Areas

*2026 ARWP*

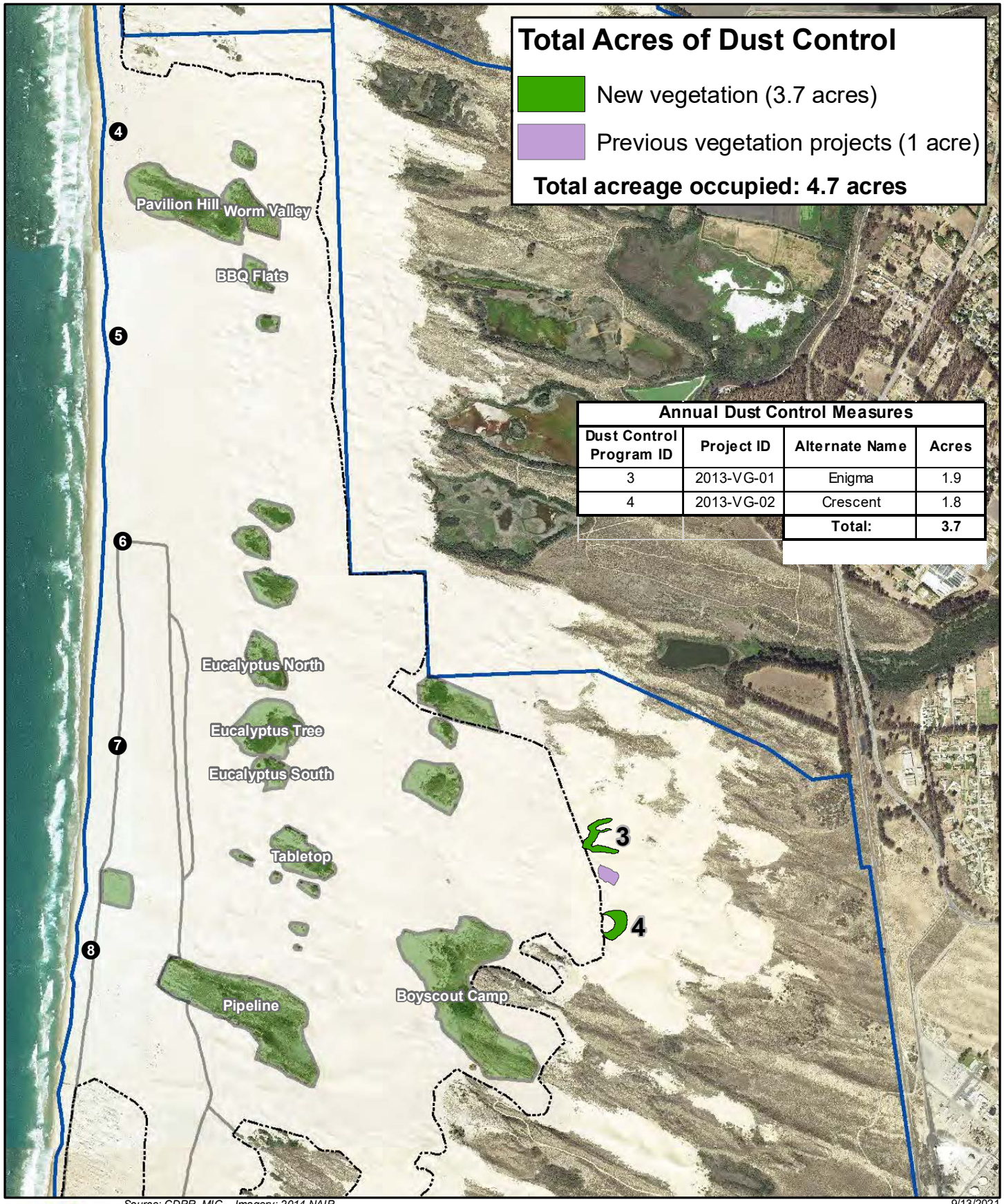
Marker post

Existing fenced vegetated islands

Park boundary

Nesting exclosure from 2020

Open riding and camping area boundary fence




Source: CDPR, MIG Imagery: 2014 NAIP

9/13/2021

Feet
0 500 1,000 2,000

N

# A01-04: 2013 Dust Control Treatment Areas

*2026 ARWP*

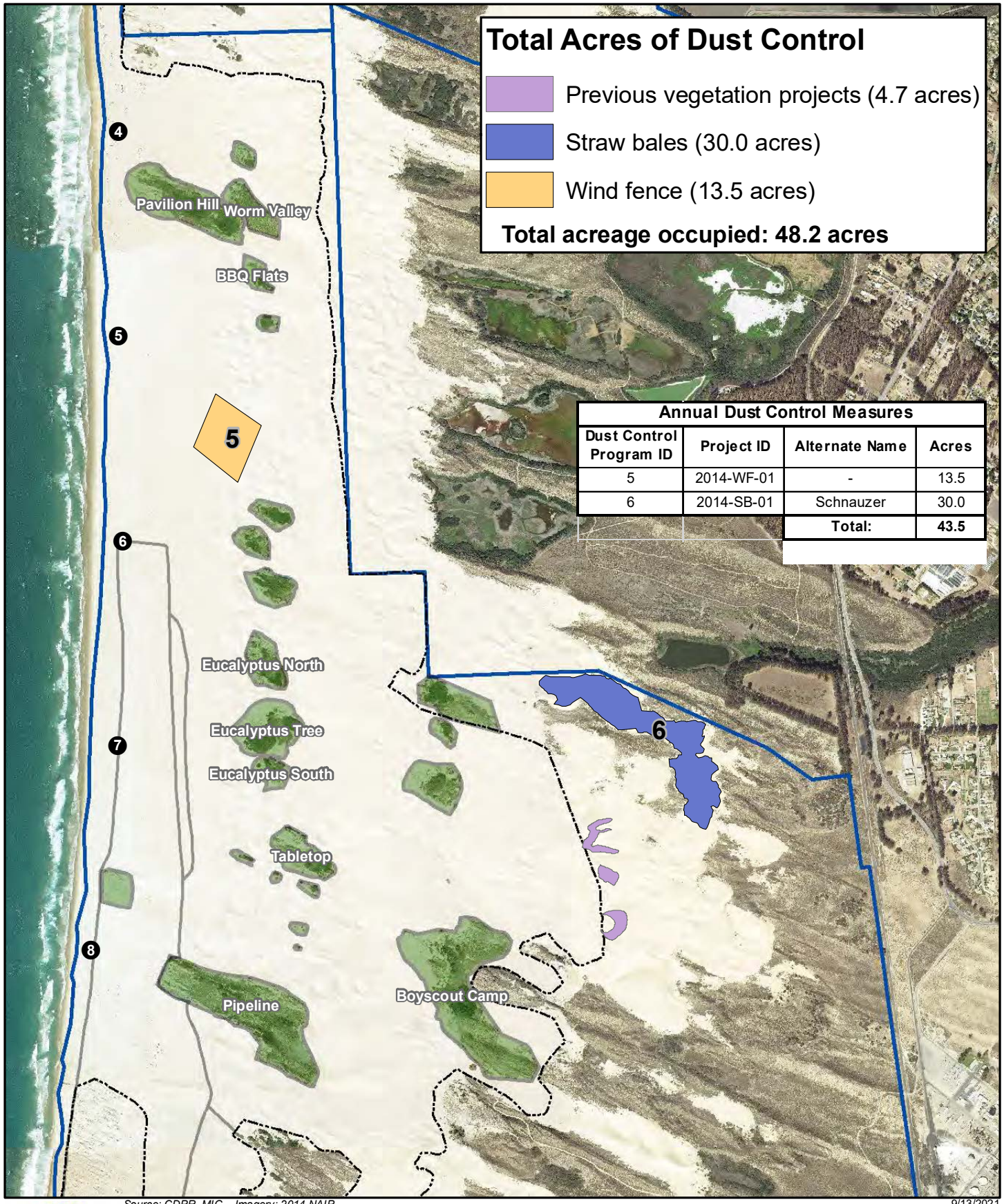
Marker post

Existing fenced vegetated islands

Park boundary

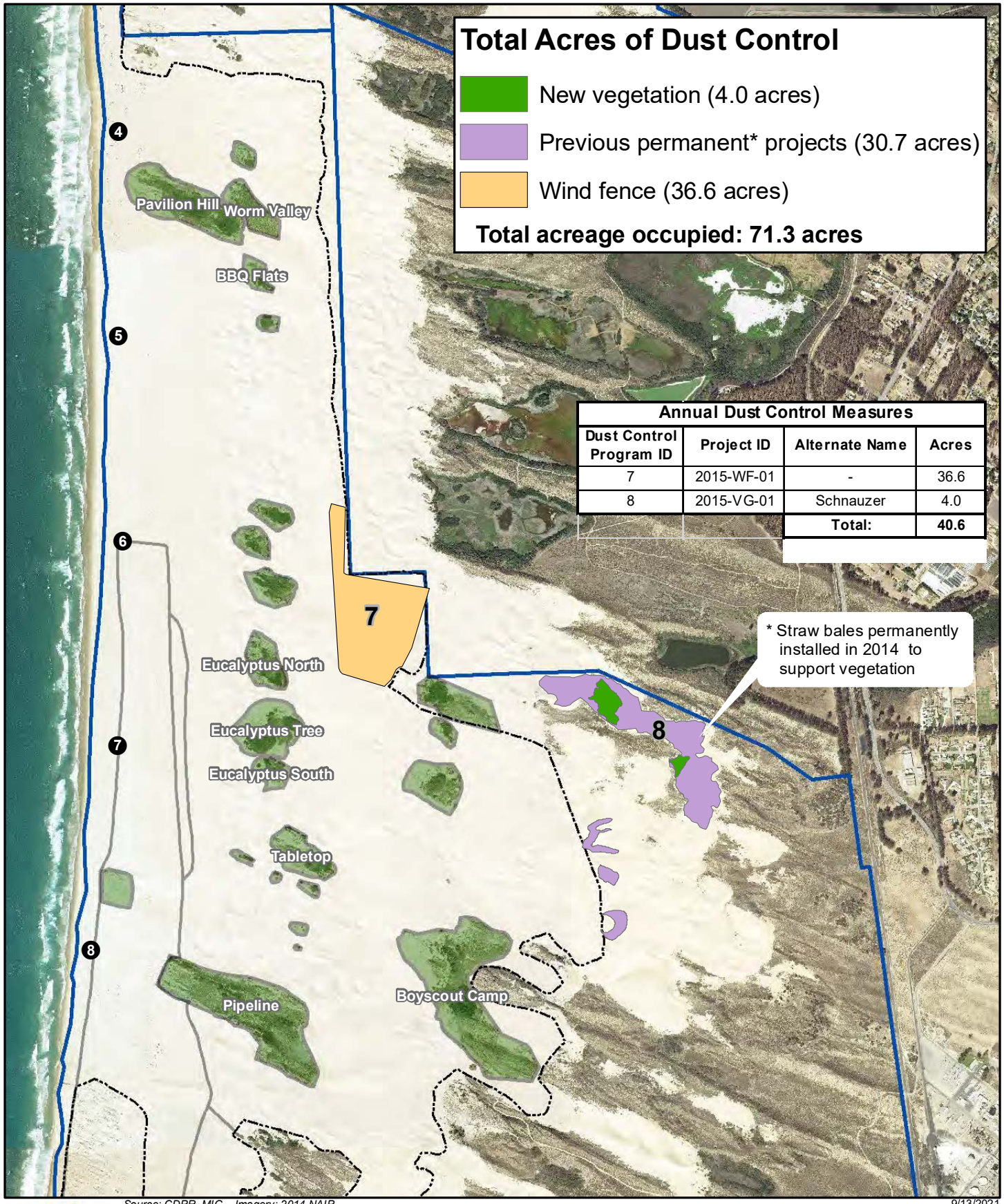
Nesting exclosure from 2020

Open riding and camping area boundary fence




# A01-05: 2014 Dust Control Treatment Areas

*2026 ARWP*




Source: CDPR, MIG Imagery: 2014 NAIP

9/13/2021

Feet
0 500 1,000 2,000

N

# A01-06: 2015 Dust Control Treatment Areas

*2026 ARWP*

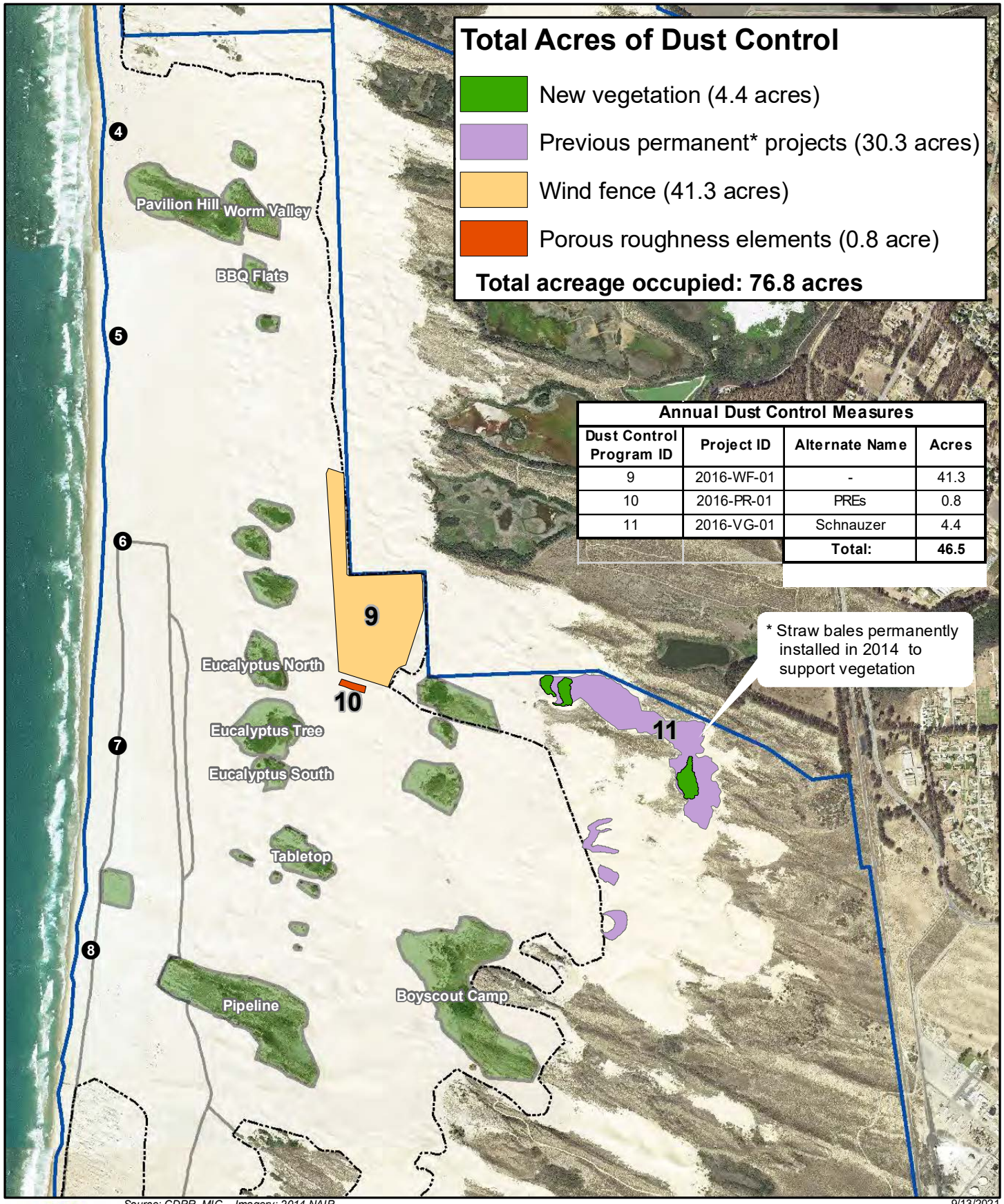
Marker post

Existing fenced vegetated islands

Park boundary

Nesting exclosure from 2020

Open riding and camping area boundary fence




Source: CDPR, MIG Imagery: 2014 NAIP

9/13/2021

Feet
0 500 1,000 2,000

N

# A01-07: 2016 Dust Control Treatment Areas

*2026 ARWP*

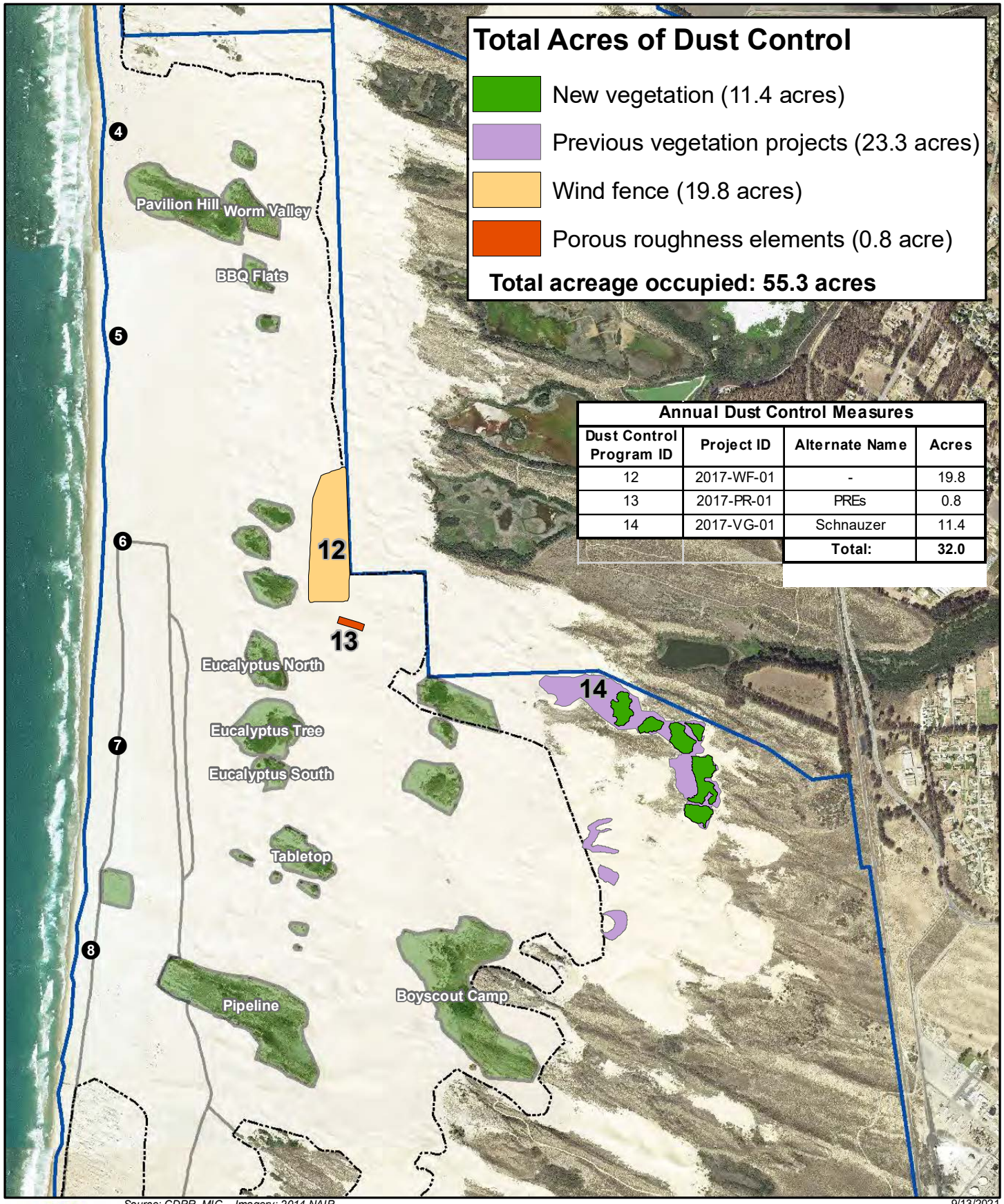
Marker post

Existing fenced vegetated islands

Park boundary

Nesting exclosure from 2020

Open riding and camping area boundary fence




Source: CDPR, MIG Imagery: 2014 NAIP

9/13/2021

Feet
0 500 1,000 2,000

N

# A01-08: 2017 Dust Control Treatment Areas

*2026 ARWP*

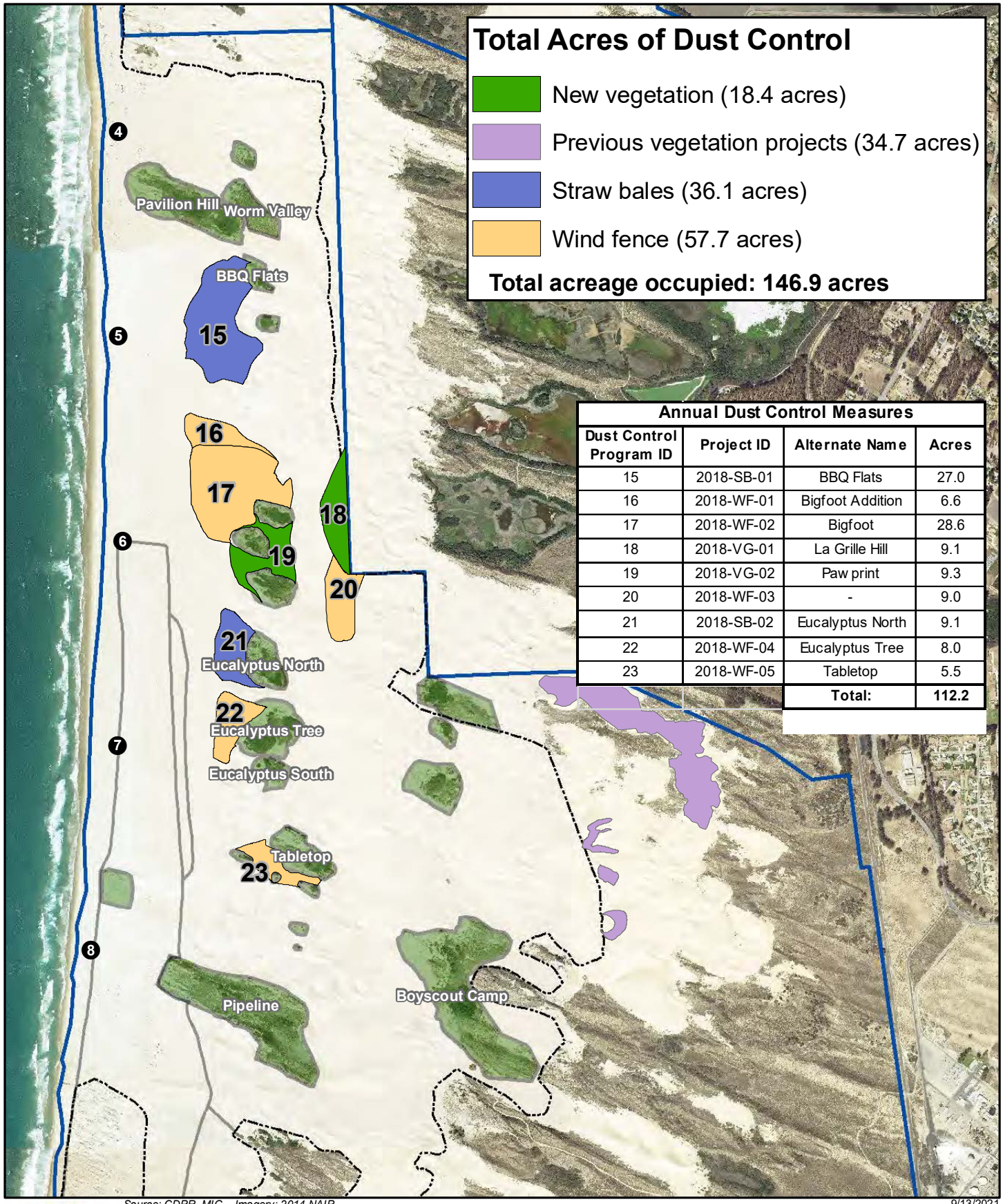
Marker post

Existing fenced vegetated islands

Park boundary

Nesting exclosure from 2020

Open riding and camping area boundary fence




| Annual Dust Control Measures | | | |
|---|---|---|---|
| Dust Control Program ID | Project ID | Alternate Name | Acres |
| 15 | 2018-SB-01 | BBQ Flats | 27.0 |
| 16 | 2018-WF-01 | Bigfoot Addition | 6.6 |
| 17 | 2018-WF-02 | Bigfoot | 28.6 |
| 18 | 2018-VG-01 | La Grille Hill | 9.1 |
| 19 | 2018-VG-02 | Paw print | 9.3 |
| 20 | 2018-WF-03 | - | 9.0 |
| 21 | 2018-SB-02 | Eucalyptus North | 9.1 |
| 22 | 2018-WF-04 | Eucalyptus Tree | 8.0 |
| 23 | 2018-WF-05 | Tabletop | 5.5 |
| | | **Total:** | **112.2** |

*Source: CDPR, MIG  Imagery: 2014 NAIP*

9/13/2021

Feet
0 500 1,000 2,000

N

# A01-09: 2018 Dust Control Treatment Areas

*2026 ARWP*

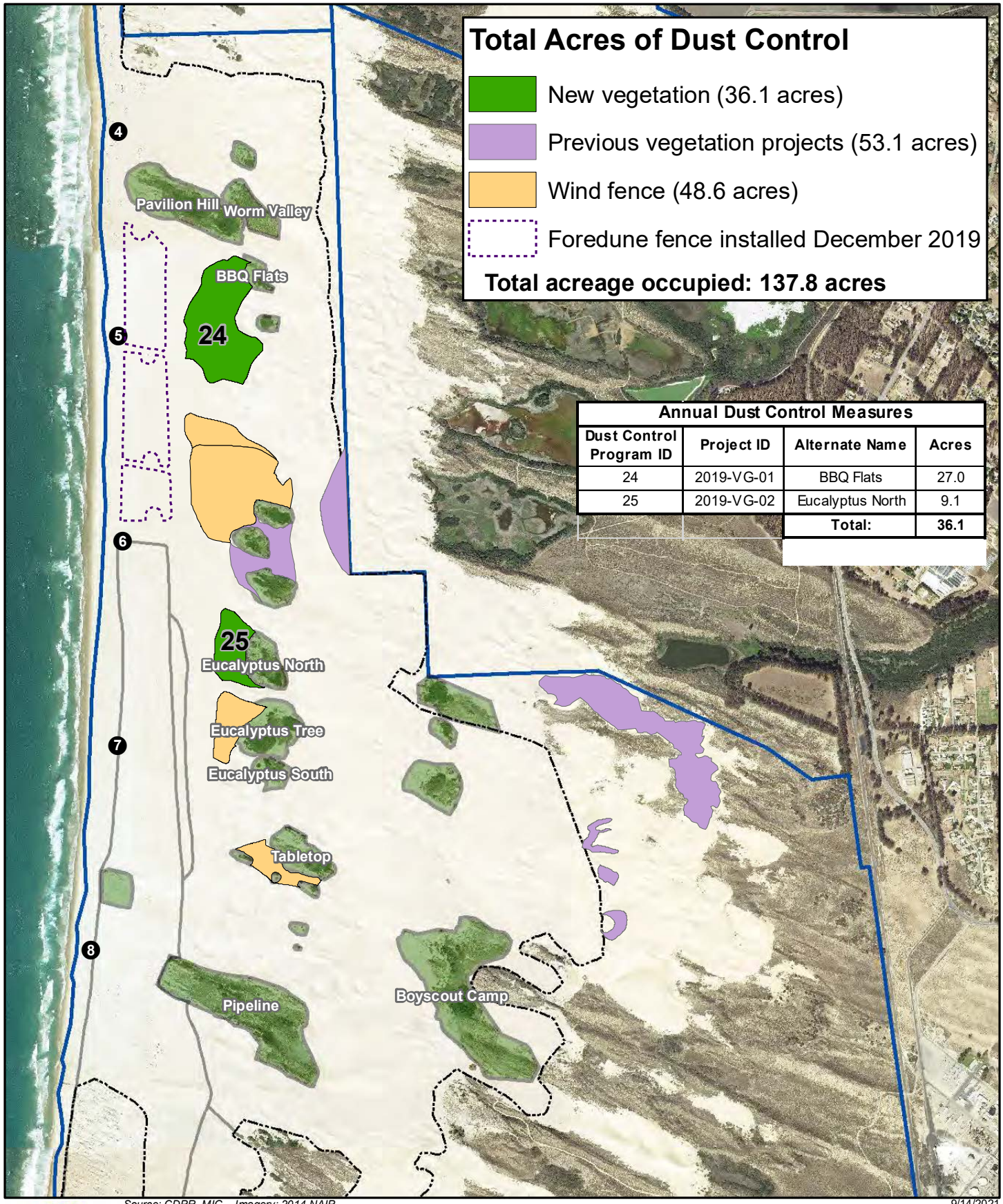
Marker post

Existing fenced vegetated islands

Park boundary

Nesting exclosure from 2020

Open riding and camping area boundary fence




Source: CDPR, MIG Imagery: 2014 NAIP

9/14/2021

Feet
0 500 1,000 2,000

N

# A01-10: 2019 Dust Control Treatment Areas

*2026 ARWP*

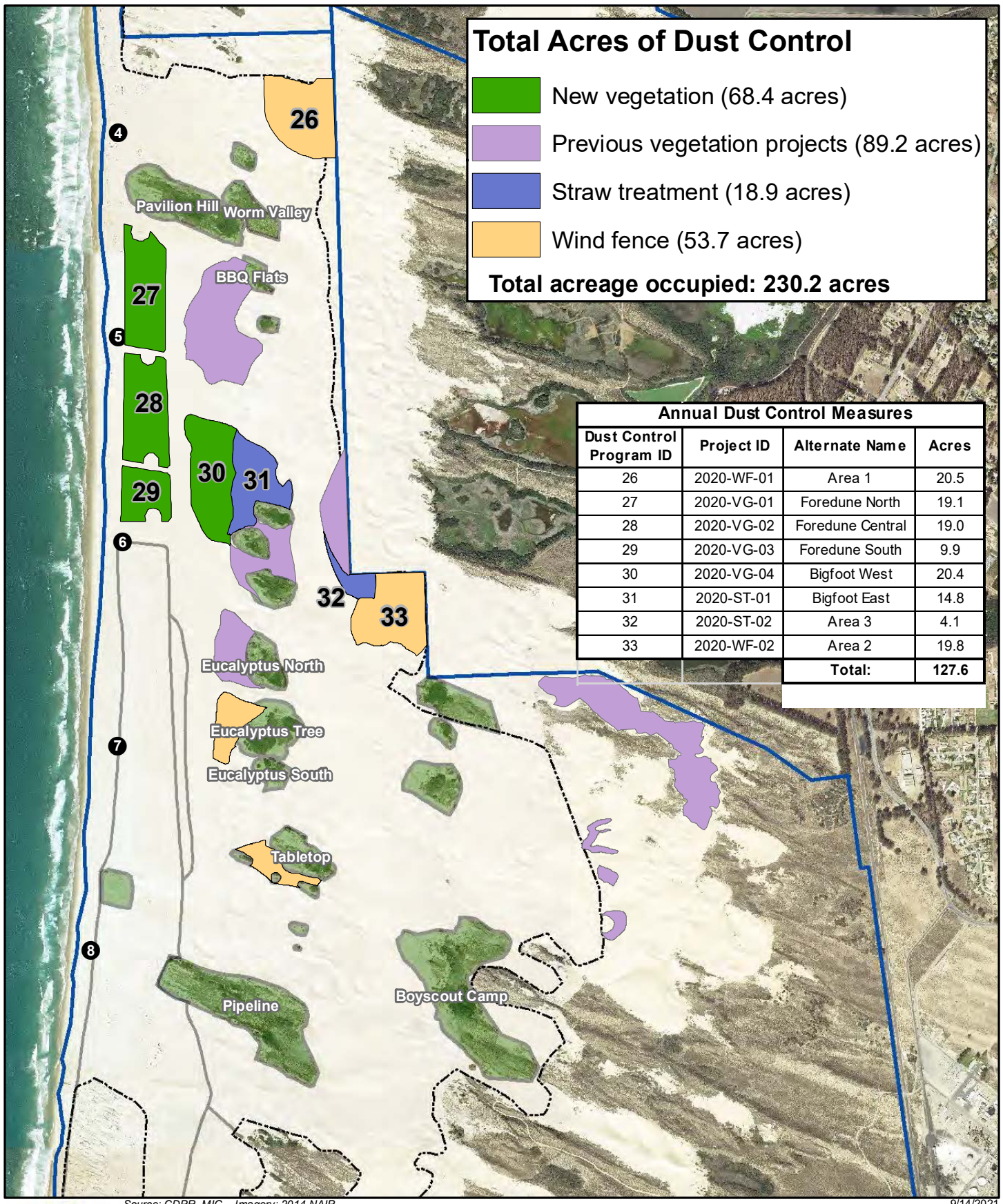
Marker post

Existing fenced vegetated islands

Park boundary

Nesting exclosure from 2020

Open riding and camping area boundary fence




| Annual Dust Control Measures | | | |
|---|---|---|---|
| Dust Control Program ID | Project ID | Alternate Name | Acres |
| 26 | 2020-WF-01 | Area 1 | 20.5 |
| 27 | 2020-VG-01 | Foredune North | 19.1 |
| 28 | 2020-VG-02 | Foredune Central | 19.0 |
| 29 | 2020-VG-03 | Foredune South | 9.9 |
| 30 | 2020-VG-04 | Bigfoot West | 20.4 |
| 31 | 2020-ST-01 | Bigfoot East | 14.8 |
| 32 | 2020-ST-02 | Area 3 | 4.1 |
| 33 | 2020-WF-02 | Area 2 | 19.8 |
| | | **Total:** | **127.6** |

*Source: CDPR, MIG  Imagery: 2014 NAIP*

9/14/2021

Feet
0 500 1,000 2,000

N

# A01-11: 2020 Dust Control Treatment Areas

*2026 ARWP*

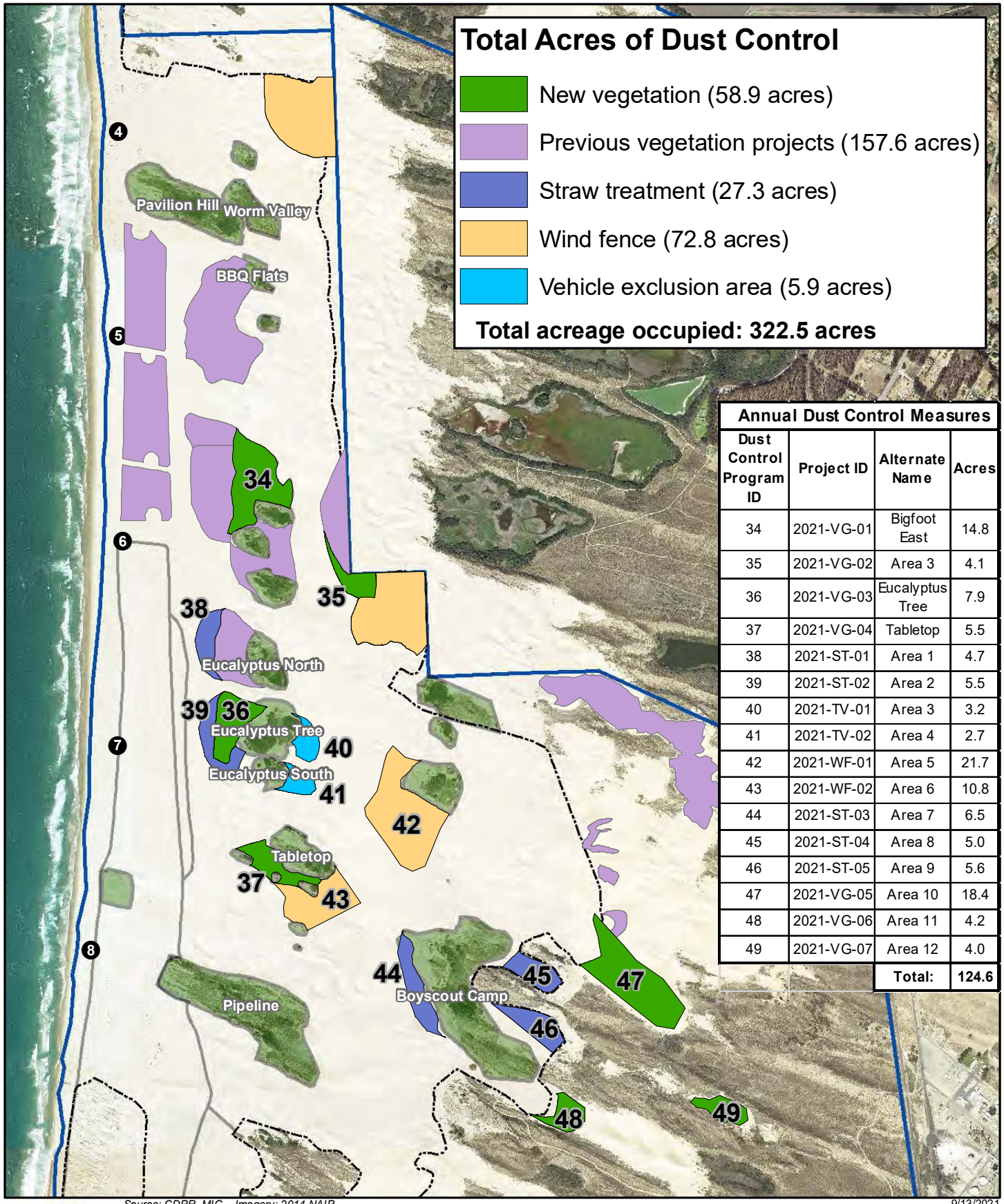
Marker post

Existing fenced vegetated islands

Park boundary

Nesting exclosure from 2020

Open riding and camping area boundary fence




| Annual Dust Control Measures | | | |
|---|---|---|---|
| Dust Control Program ID | Project ID | Alternate Name | Acres |
| 34 | 2021-VG-01 | Bigfoot East | 14.8 |
| 35 | 2021-VG-02 | Area 3 | 4.1 |
| 36 | 2021-VG-03 | Eucalyptus Tree | 7.9 |
| 37 | 2021-VG-04 | Tabletop | 5.5 |
| 38 | 2021-ST-01 | Area 1 | 4.7 |
| 39 | 2021-ST-02 | Area 2 | 5.5 |
| 40 | 2021-TV-01 | Area 3 | 3.2 |
| 41 | 2021-TV-02 | Area 4 | 2.7 |
| 42 | 2021-WF-01 | Area 5 | 21.7 |
| 43 | 2021-WF-02 | Area 6 | 10.8 |
| 44 | 2021-ST-03 | Area 7 | 6.5 |
| 45 | 2021-ST-04 | Area 8 | 5.0 |
| 46 | 2021-ST-05 | Area 9 | 5.6 |
| 47 | 2021-VG-05 | Area 10 | 18.4 |
| 48 | 2021-VG-06 | Area 11 | 4.2 |
| 49 | 2021-VG-07 | Area 12 | 4.0 |
| | | Total: | 124.6 |

*Source: CDPR, MIG  Imagery: 2014 NAIP*

9/13/2021

Feet
0 500 1,000 2,000

N

# A01-12: 2021 Dust Control Treatment Areas

*2026 ARWP*

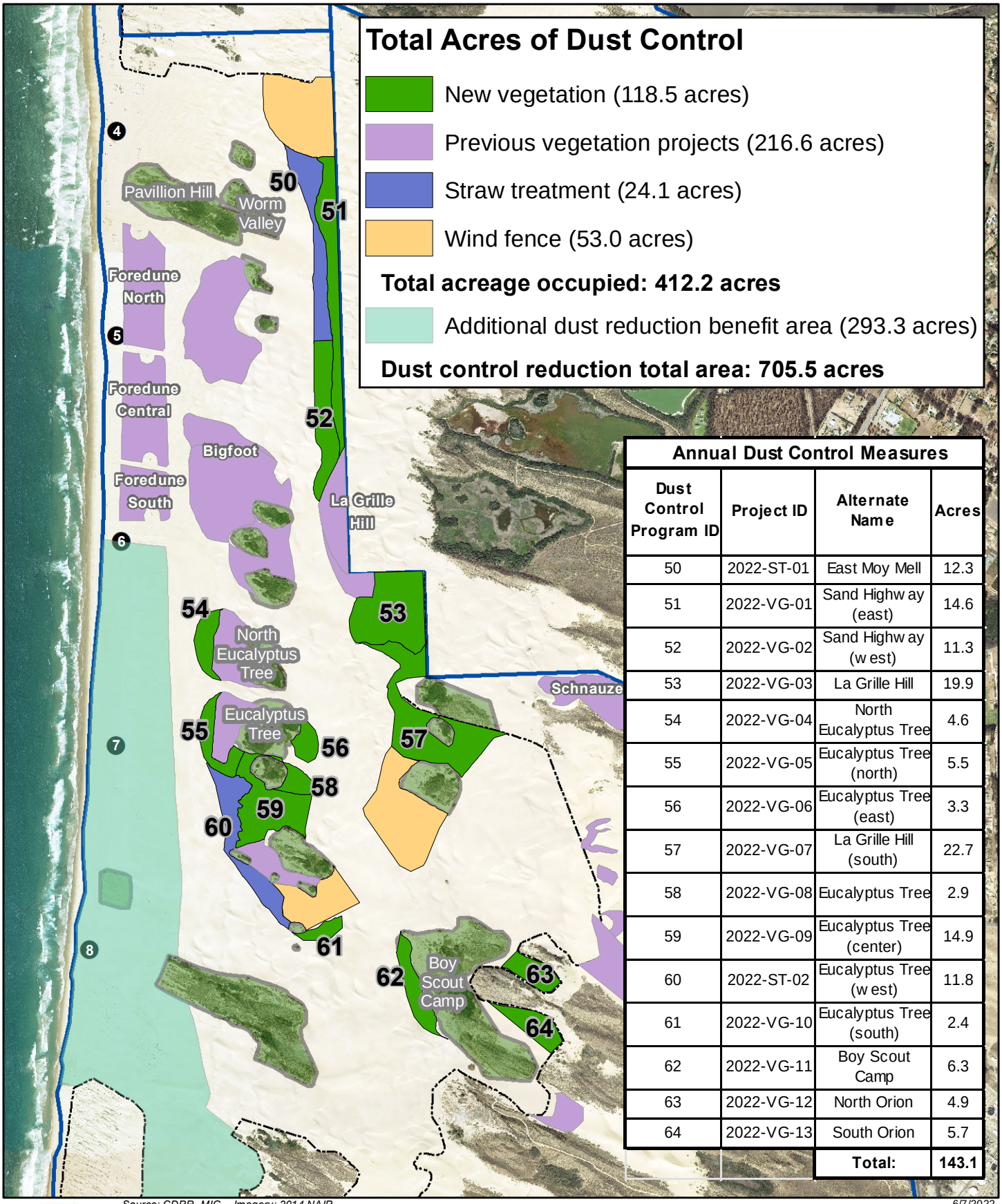
Marker post

Existing fenced vegetated islands

Park boundary

Nesting exclosure from 2020

Open riding and camping area boundary fence




| Annual Dust Control Measures | | | |
|---|---|---|---|
| Dust Control Program ID | Project ID | Alternate Name | Acres |
| 50 | 2022-ST-01 | East Moy Mell | 12.3 |
| 51 | 2022-VG-01 | Sand Highway (east) | 14.6 |
| 52 | 2022-VG-02 | Sand Highway (west) | 11.3 |
| 53 | 2022-VG-03 | La Grille Hill | 19.9 |
| 54 | 2022-VG-04 | North Eucalyptus Tree | 4.6 |
| 55 | 2022-VG-05 | Eucalyptus Tree (north) | 5.5 |
| 56 | 2022-VG-06 | Eucalyptus Tree (east) | 3.3 |
| 57 | 2022-VG-07 | La Grille Hill (south) | 22.7 |
| 58 | 2022-VG-08 | Eucalyptus Tree | 2.9 |
| 59 | 2022-VG-09 | Eucalyptus Tree (center) | 14.9 |
| 60 | 2022-ST-02 | Eucalyptus Tree (west) | 11.8 |
| 61 | 2022-VG-10 | Eucalyptus Tree (south) | 2.4 |
| 62 | 2022-VG-11 | Boy Scout Camp | 6.3 |
| 63 | 2022-VG-12 | North Orion | 4.9 |
| 64 | 2022-VG-13 | South Orion | 5.7 |
| | | **Total:** | **143.1** |

Source: CDPR, MIG  Imagery: 2014 NAIP

6/7/2022

0 500 1,000 2,000 Feet

N

# A01-13: 2022 Dust Control Treatment Areas

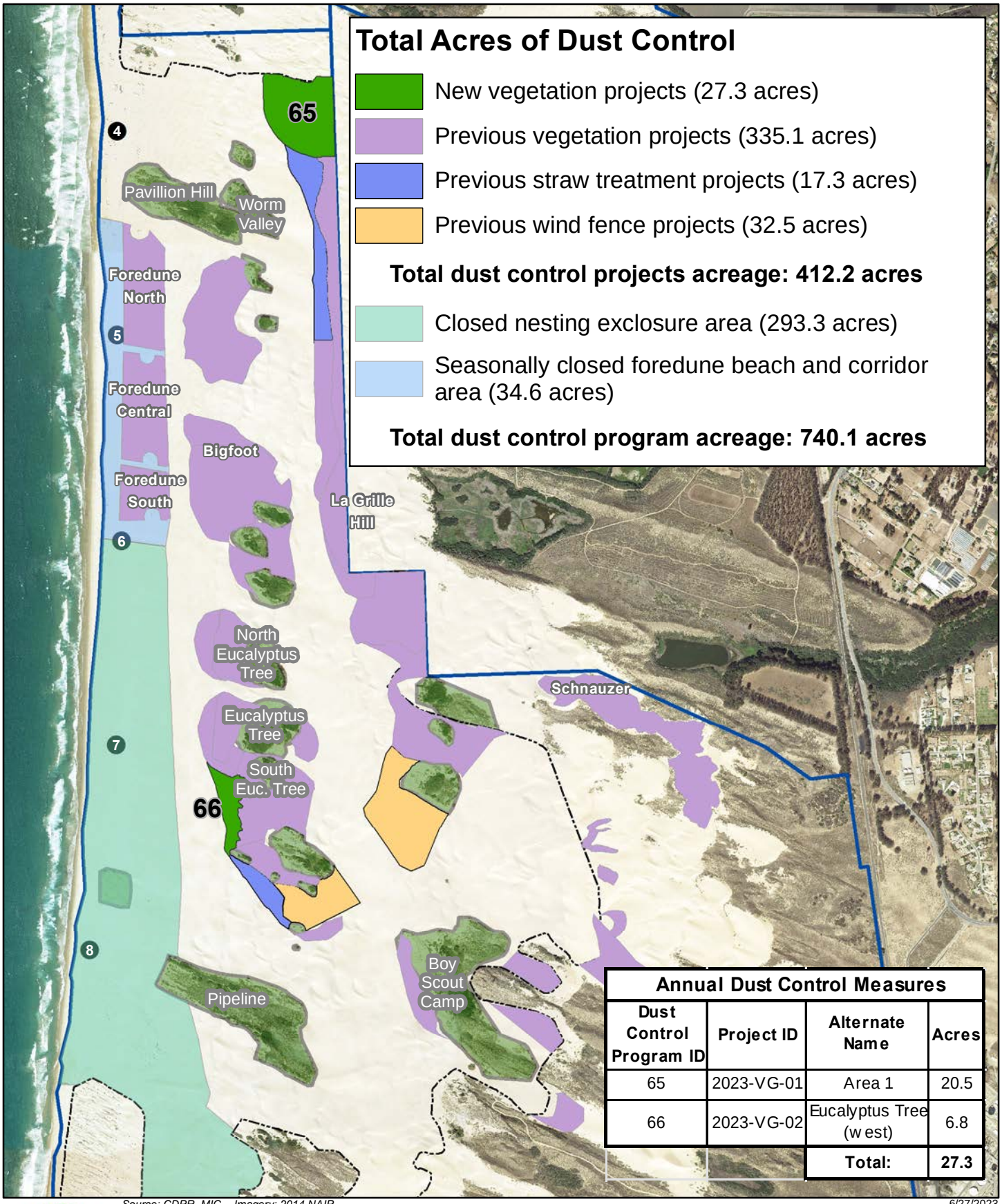
*2026 ARWP*

Marker post

Existing fenced vegetated islands

Park boundary

Open riding and camping area boundary fence




| Annual Dust Control Measures | | | |
|---|---|---|---|
| Dust Control Program ID | Project ID | Alternate Name | Acres |
| 65 | 2023-VG-01 | Area 1 | 20.5 |
| 66 | 2023-VG-02 | Eucalyptus Tree (west) | 6.8 |
| | | Total: | 27.3 |

Source: CDPR, MIG Imagery: 2014 NAIP

6/27/2023

0 500 1,000 2,000 Feet

N

# Figure A01-14: 2023 Dust Control Treatment Areas

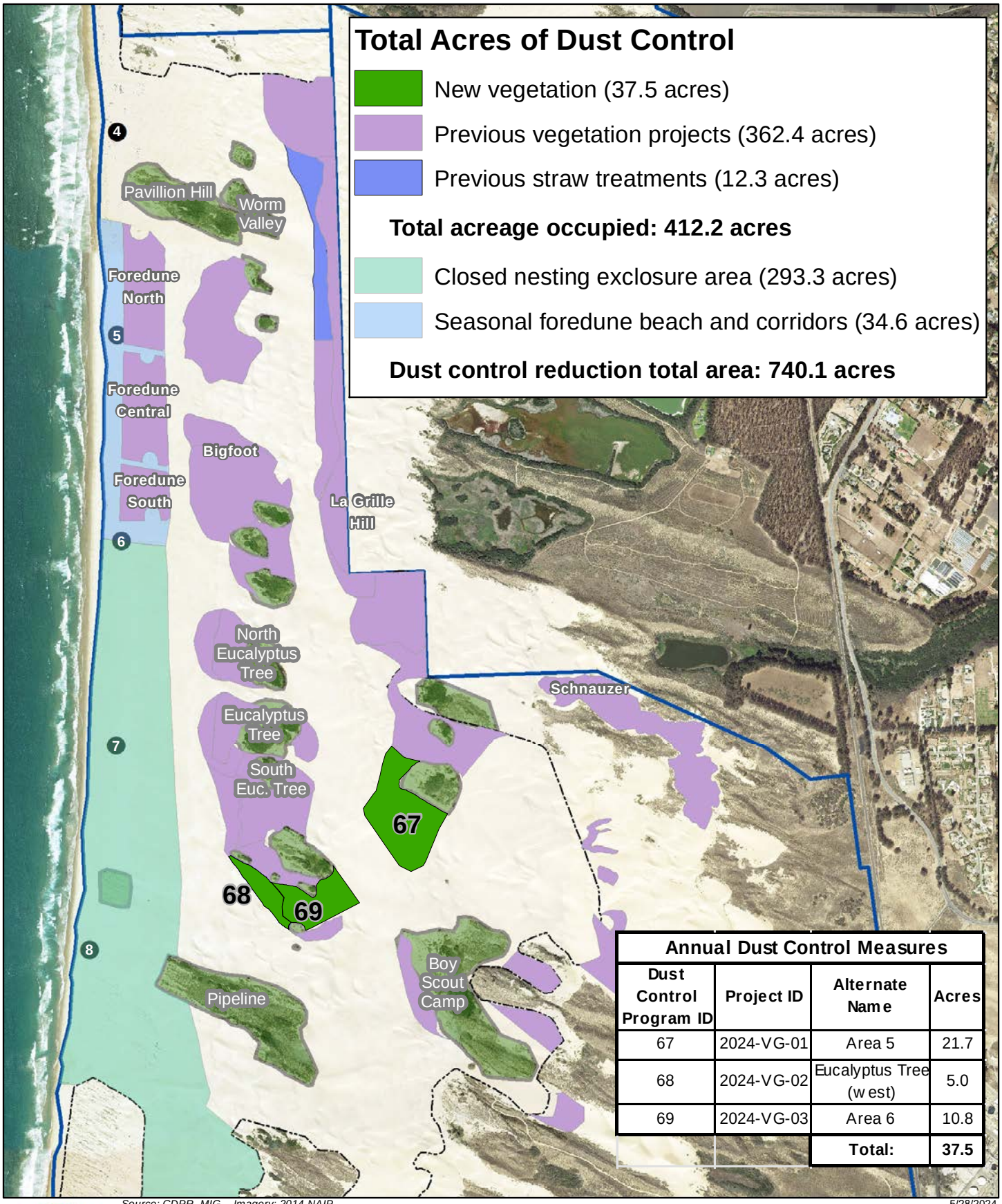
*2026 ARWP*

Marker post

Existing fenced vegetated islands

Park boundary

Open riding and camping area boundary fence




| Annual Dust Control Measures | | | |
|---|---|---|---|
| Dust Control Program ID | Project ID | Alternate Name | Acres |
| 67 | 2024-VG-01 | Area 5 | 21.7 |
| 68 | 2024-VG-02 | Eucalyptus Tree (west) | 5.0 |
| 69 | 2024-VG-03 | Area 6 | 10.8 |
| | | Total: | 37.5 |

Source: CDPR, MIG Imagery: 2014 NAIP 5/28/2024

0 500 1,000 2,000 Feet

N

# Figure A01-15: 2024 Dust Control Treatment Areas

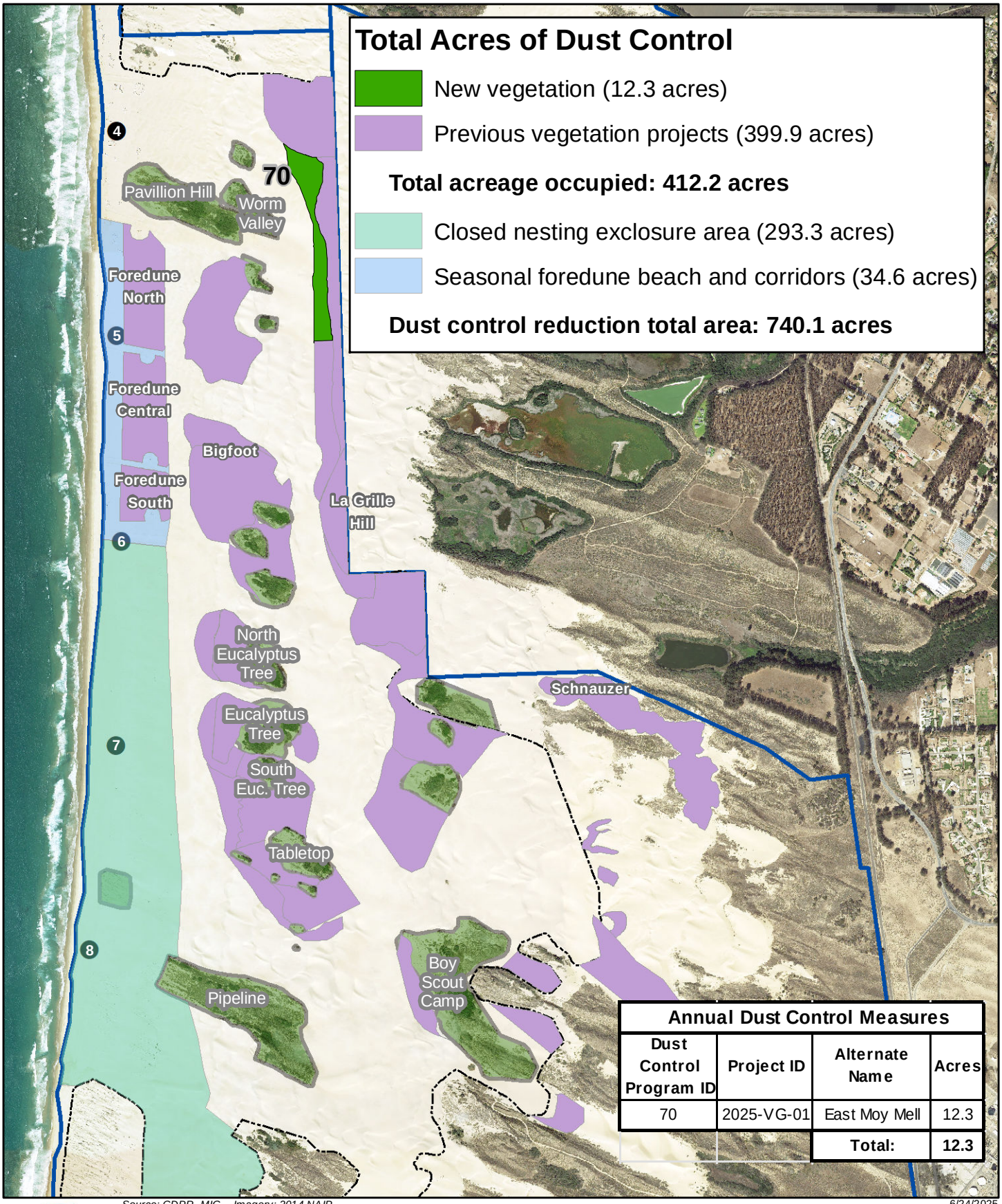
*2026 ARWP*

Marker post

Existing fenced vegetated islands

Park boundary

Open riding and camping area boundary fence




| Annual Dust Control Measures | | | |
|---|---|---|---|
| Dust Control Program ID | Project ID | Alternate Name | Acres |
| 70 | 2025-VG-01 | East Moy Mell | 12.3 |
| | | Total: | 12.3 |

Source: CDPR, MIG Imagery: 2014 NAIP

6/24/2025

0 500 1,000 2,000 Feet

N

# Figure A01-16: 2025 Dust Control Treatment Areas

*2026 ARWP*

Marker post

Existing fenced vegetated islands

Park boundary

Open riding and camping area boundary fence

**ODSVRA Dust Control Program SAG Review Draft 2026 ARWP**

**ATTACHMENT 02**

**2025/2026 ODSVRA Dust Control Program Vegetation Restoration Projects**

**(State Parks' ARWP Work Product)**

*THIS PAGE WAS INTENTIONALLY LEFT BLANK.*

| 2025/2026 ODSVRA Dust Control Program - Restoration Projects | | | | | | | | |
|---|---|---|---|---|---|---|---|---|
| *Scientific Name*<br>Common Name | Plant Counts<br>Native Seed (lbs) | Season Totals | La Grille Hill (south) 2022-VG-07 (New Planting) | South Crescent 2021-VG-05 (New Planting) | Jack Lake West 2021-VG-06 (New Planting) | Boyscout North 2024-VG-01 (Supplemental Planting) | La Grille Hill 2022-VG-03 (Supplemental Planting) | Area 3 2021-VG-02 (Supplemental Planting) |
| Acreage | | 44.2 | 23.6 | 10.3 | 4.4 | 4.2 | 1.0 | 0.7 |
| Straw - (large bales) | | 528 | 313 | 109 | 48 | 44 | 4 | 10 |
| Fertilizer (lbs) - 15-15-15 | | 2150 | 1200 | 500 | 200 | 175 | 50 | 25 |
| Triticale Seed (lbs) - sterile | | 1025 | 600 | 250 | 100 | 50 | 15 | 10 |
| *Total plants* | | 109,657 | 58,799 | 26,916 | 10,880 | 10,024 | 2,014 | 1,024 |
| Total Native Seed (lbs) | | 408.1 | 231.7 | 80.5 | 35.1 | 43.4 | 10.1 | 7.3 |
| *Abronia latifolia* | | 167 | 91 | - | - | 56 | 13 | 7 |
| Yellow sand verbena | | 0.92 | 0.52 | - | - | 0.28 | 0.07 | 0.05 |
| *Abronia maritima* | | 231 | 117 | - | - | 80 | 23 | 11 |
| Sticky sand verbena | | 35.55 | 19.50 | - | - | 11.40 | 2.70 | 1.95 |
| *Abronia umbellata* | | 25 | 25 | - | - | - | - | - |
| Beach sand verbena | | 0.78 | 0.28 | 0.50 | - | - | - | - |
| *Acmispon glaber* | | 2,676 | 1,715 | 490 | 392 | - | 30 | 49 |
| Deerweed | | 12.78 | 7.10 | 4.00 | 1.68 | - | - | - |
| *Acmispon tomentosus* | | - | - | - | - | - | - | - |
| Woolly lotus | | 1.49 | 0.78 | 0.50 | 0.21 | - | - | - |
| *Achillea millefolium* | | 7,839 | 4,067 | 1,960 | 784 | 784 | 146 | 98 |
| Common yarrow | | 21.44 | 10.79 | 7.50 | 3.15 | - | - | - |
| *Ambrosia chamissonis* | | 2,279 | 1,274 | - | - | 784 | 147 | 74 |
| Beach bur | | 35.55 | 19.50 | - | - | 11.40 | 2.70 | 1.95 |
| *Amsinckia spectabilis* | | - | - | - | - | - | - | - |
| Seaside fiddleneck | | 3.20 | 3.20 | - | - | - | - | - |
| *Astragalus nuttallii* | | 856 | 238 | 490 | 128 | - | - | - |
| Nuttall's milkvetch | | 0.42 | 0.42 | - | - | - | - | - |
| *Castilleja affinis* | | 123 | 57 | 50 | 16 | - | - | - |

| 2025/2026 ODSVRA Dust Control Program - Restoration Projects | | | | | | | | |
|---|---|---|---|---|---|---|---|---|
| *Scientific Name*<br>Common Name | Plant Counts<br>Native Seed (lbs) | Season Totals | La Grille Hill (south) 2022-VG-07 (New Planting) | South Crescent 2021-VG-05 (New Planting) | Jack Lake West 2021-VG-06 (New Planting) | Boyscout North 2024-VG-01 (Supplemental Planting) | La Grille Hill 2022-VG-03 (Supplemental Planting) | Area 3 2021-VG-02 (Supplemental Planting) |
| Indian paintbrush | | 0.75 | 0.57 | 0.10 | 0.08 | - | - | - |
| *Camissoniopsis cheiranthifolia* | | 3,773 | 1,862 | 980 | 392 | 392 | 98 | 49 |
| Beach evening-primrose | | 0.50 | 0.50 | - | - | - | - | - |
| *Carex praegracilis* | | 203 | 203 | - | - | - | - | - |
| Field sedge | | - | - | - | - | - | - | - |
| *Castilleja exserta* | | - | - | - | - | - | - | - |
| Owl's clover | | 0.64 | 0.36 | 0.20 | 0.08 | - | - | - |
| *Cirsium occidentale* | | 258 | 146 | 80 | 32 | - | - | - |
| Cobweb thistle | | - | - | - | - | - | - | - |
| *Chenopodium californica* | | - | - | - | - | - | - | - |
| California goosefoot | | 2.37 | 1.66 | 0.50 | 0.21 | - | - | - |
| *Corethrogyne filaginifolia* | | 6,860 | 3,577 | 1,960 | 784 | 392 | 98 | 49 |
| Common sandaster | | 8.88 | 5.28 | 2.00 | 0.84 | 0.76 | - | - |
| *Cryptantha spp.* | | - | - | - | - | - | - | - |
| Cryptantha species | | 1.21 | 0.93 | 0.20 | 0.08 | - | - | - |
| *Dudleya lanceolata* | | 405 | 245 | - | - | 160 | - | - |
| Southern California dudleya | | - | - | - | - | - | - | - |
| *Erigeron blochmaniae* | | 5,869 | 3,337 | 1,470 | 588 | 392 | 57 | 25 |
| Blochman's leafy daisy | | 5.39 | 3.26 | 1.50 | 0.63 | - | - | - |
| *Eriastrum densifolium* | | 913 | 227 | 490 | 196 | - | - | - |
| Giant eriastrum | | - | - | - | - | - | - | - |
| *Ericameria ericoides* | | 6,508 | 3,176 | 1,960 | 784 | 392 | 147 | 49 |
| Mock heather | | 72.23 | 39.25 | 20.00 | 8.40 | 3.80 | 0.45 | 0.33 |
| *Eriogonum parvifolium* | | 9,065 | 4,704 | 2,450 | 980 | 784 | 98 | 49 |
| Coastal buckwheat | | 54.48 | 34.15 | 10.00 | 4.20 | 3.80 | 1.35 | 0.98 |

| 2025/2026 ODSVRA Dust Control Program - Restoration Projects | | | | | | | | |
|---|---|---|---|---|---|---|---|---|
| *Scientific Name*<br>Common Name | Plant Counts<br>Native Seed (lbs) | Season Totals | La Grille Hill (south) 2022-VG-07 (New Planting) | South Crescent 2021-VG-05 (New Planting) | Jack Lake West 2021-VG-06 (New Planting) | Boyscout North 2024-VG-01 (Supplemental Planting) | La Grille Hill 2022-VG-03 (Supplemental Planting) | Area 3 2021-VG-02 (Supplemental Planting) |
| *Eriophyllum staechadifolium* | | 8,617 | 4,214 | 2,450 | 980 | 784 | 140 | 49 |
| Seaside golden yarrow | | 33.11 | 18.45 | 7.50 | 3.15 | 2.85 | 0.68 | 0.49 |
| *Erysimum suffrutescens* | | 5,660 | 3,405 | 1,470 | 392 | 320 | 49 | 24 |
| Suffrutescent wallflower | | 0.49 | 0.49 | - | - | - | - | - |
| *Eschscholzia californica* | | - | - | - | - | - | - | - |
| California poppy | | 0.06 | 0.06 | - | - | - | - | - |
| *Horkelia cuneata* | | 245 | 245 | - | - | - | - | - |
| Wedge leaved horkelia | | 1.65 | 1.65 | - | - | - | - | - |
| *Juncus lescurii* | | 459 | 459 | - | - | - | - | - |
| Dune rush | | 0.85 | 0.85 | - | - | - | - | - |
| *Linanthus californicus* | | 10 | - | 10 | - | - | - | - |
| Prickly phlox | | - | - | - | - | - | - | - |
| *Lupinus chamissonis* | | 23,422 | 12,152 | 5,880 | 2,352 | 2,352 | 441 | 245 |
| Dune bush lupine | | 39.80 | 22.20 | 9.00 | 3.78 | 3.42 | 0.81 | 0.59 |
| *Monardella undulata ssp crispa* | | 7,397 | 3,575 | 1,960 | 784 | 784 | 196 | 98 |
| Crisp monardella | | 10.30 | 6.13 | 2.00 | 0.84 | 0.95 | 0.23 | 0.16 |
| *Penstemon centranthifolius* | | 610 | 330 | 200 | 80 | - | - | - |
| Scarlet bugler | | - | - | - | - | - | - | - |
| *Phacelia distans* | | - | - | - | - | - | - | - |
| Common phacelia | | 0.61 | 0.61 | - | - | - | - | - |
| *Phacelia ramosissima* | | 11,775 | 7,291 | 1,960 | 784 | 1,372 | 245 | 123 |
| Branching phacelia | | 47.65 | 26.00 | 10.00 | 6.30 | 3.80 | 0.90 | 0.65 |
| *Salvia columbariae* | | - | - | - | - | - | - | - |
| Chia sage | | 1.28 | 1.28 | - | - | - | - | - |
| *Salix lasiolepis* | | 361 | 205 | 116 | 40 | - | - | - |

| 2025/2026 ODSVRA Dust Control Program - Restoration Projects | | | | | | | | |
|---|---|---|---|---|---|---|---|---|
| *Scientific Name*<br>Common Name | Plant Counts<br>Native Seed (lbs) | Season Totals | La Grille Hill (south) 2022-VG-07 (New Planting) | South Crescent 2021-VG-05 (New Planting) | Jack Lake West 2021-VG-06 (New Planting) | Boyscout North 2024-VG-01 (Supplemental Planting) | La Grille Hill 2022-VG-03 (Supplemental Planting) | Area 3 2021-VG-02 (Supplemental Planting) |
| Arroyo Willow | | - | - | - | - | - | - | - |
| *Senecio blochmaniae* | | 3,051 | 1,862 | 490 | 392 | 196 | 86 | 25 |
| Dune ragwort | | 13.78 | 5.97 | 5.00 | 1.47 | 0.95 | 0.23 | 0.16 |

**ODSVRA Dust Control Program Draft 2026 ARWP**

**ATTACHMENT 03**

**Report on Findings: ODSVRA Meteorological and $PM_{10}$ Monitoring Network, 2025**

- Report of Findings: ODSVRA Meteorological and $PM_{10}$ Monitoring Network, 2025 (DRI Document)
- SAG Review of Desert Research Institute (DRI) "Report of Findings: ODSVRA Meteorological and $PM_{10}$ Monitoring Network, 2025" (SAG Memo)

*THIS PAGE WAS INTENTIONALLY LEFT BLANK.*

**Report of Findings: ODSVRA Meteorological and $PM_{10}$ Monitoring Network, 2025**

J.A Gillies* and G. Nikolich**
Division of Atmospheric Sciences, Desert Research Institute, *Reno and **Las Vegas, Nevada

State Parks' meteorological and $PM_{10}$ monitoring network varies slightly from year to year depending on specific goals, objectives, and dust control measures identified in the annual ARWP cycle. In 2025, a reduction in the number of monitoring stations was undertaken in response to budgetary considerations by California State Parks. The network of stations was reduced from 15 to 12 and new station locations are shown in Fig. 1. Each station has a MetSens500 instrument that measures wind speed and wind direction (ultrasonically), ambient temperature, atmospheric pressure, and relative humidity (RH), paired with a MetOne 212 particle profiler to measure hourly $PM_{10}$. The measurement height above ground level (AGL) for both instruments is 3.5 m. The MetOne instrument is calibrated against a Beta Attenuation Monitor (BAM) in a dust chamber prior to deployment and after removal from the field in October.

Some of the original stations were maintained (e.g., NDP, Lagrande, Acacia, Scout, Phillips 66, CDF, and Pipeline) while five new station locations were created: Northern Foredune (NFRA), ST125 (eastern side of foredune restoration area #5), S1 Wind Tower (S1 Tower), Midden, and Independence Hill. All stations were operated from approximately May 15 to September 30, 2025. Unfortunately, in 2025, the deployment was delayed from the usual start date of April 1 as the instrument supplier MetOne (Grants Pass, OR) was unable to service the MetOne 212 particle profilers used to measure particulate matter (i.e., $PM_{10}$) in a timely fashion.

The environmental data collected by these stations provides a means to examine spatial trends in $PM_{10}$ concentrations ($\mu g\ m^{-3}$) across the ODSVRA in relation to wind speed ($m\ s^{-1}$) and wind power density ($W\ m^{-2}$), and to evaluate if these relations have changed through time.

Wind power density (WPD, $W\ m^{-2}$) is defined as (e.g., Kalmikov, 2017):

$$WPD=0.5\ \rho_a\ u_z^3 \quad (1)$$

where $\rho_a$ is air density (assumed to be a constant 1.225 $kg\ m^{-3}$), and $u_z$ ($m\ s^{-1}$) is wind speed at the measurement height z (m) above ground level (AGL), a unit area of 1 $m^2$ is assumed in this application. For comparison among different locations and between different years, the height of measurement of wind speed and the lower limit of mean hourly wind speed for summation of Total Wind Power Density (TWPD) must be the same. To standardize the calculation of TWPD a lower limit of wind speed is chosen that corresponds with the lowest speed where the relation between increasing wind speed and simultaneous increase in $PM_{10}$ is observed at a

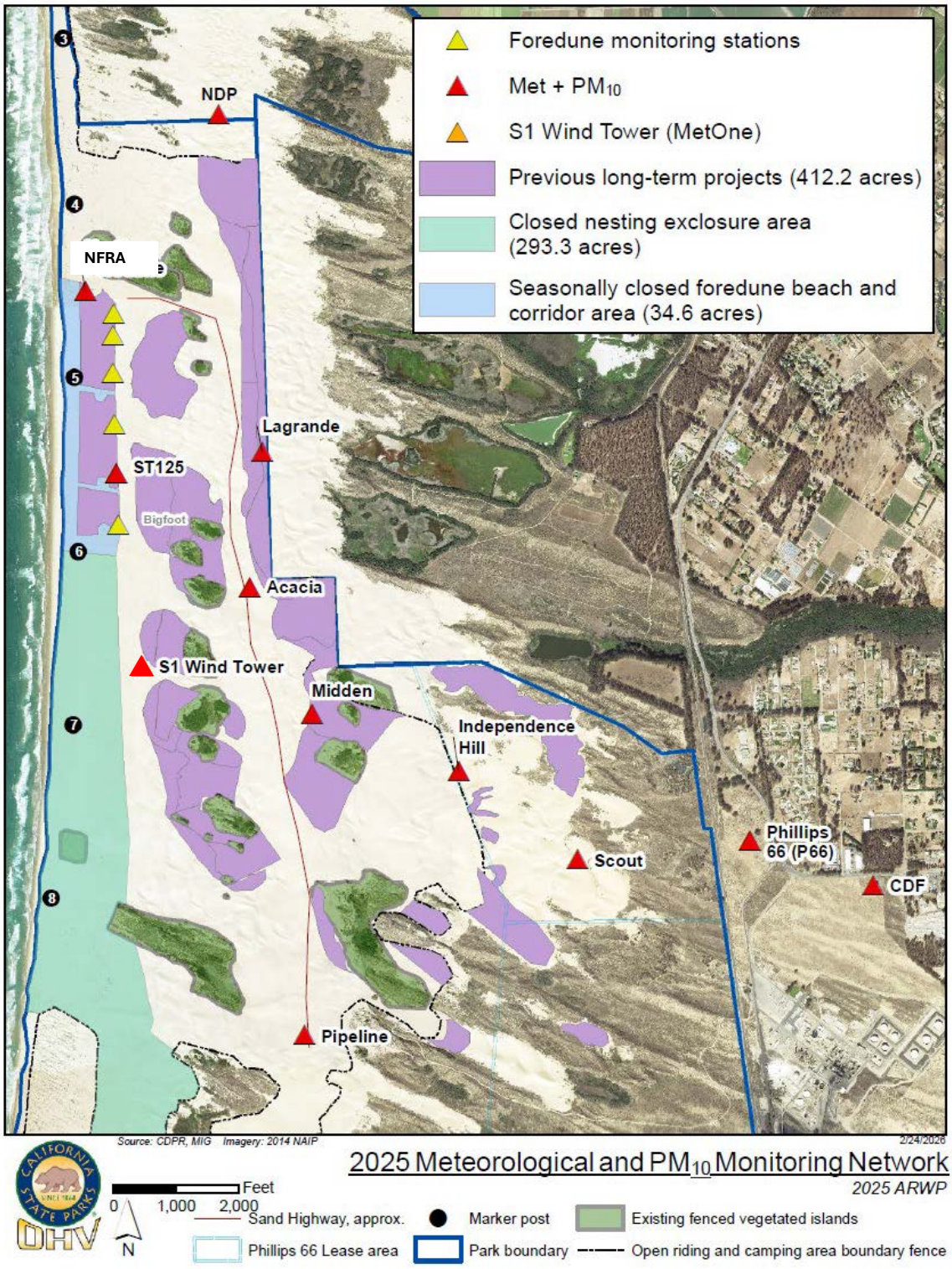



**Figure 1**. The locations of the monitoring stations in 2025. Note S1 Tower had a MetOne 212 particle profiler and a MetSens500 positioned at 3.5 m AGL in 2025 similar to the other stations.

monitoring station. For the stations on open sand areas of the ODSVRA this wind speed is chosen to be 5.5 m $s^{-1}$ measured at 3.5 m AGL. Figure 2 shows typical response relations between mean hourly wind speed measured at 3.5 m AGL for four stations on sand-sheet areas of the ODSVRA covering the north to south extent of the monitoring network in 2025 for the period May through September. A wind speed of 5.5 m $s^{-1}$, measured at 3.5 m AGL is indicative of a wind speed of ≈ 8.5 m $s^{-1}$ measured at 10 m AGL at the S1 tower. The 10 m AGL wind speed had been used previously to define a lower limit wind speed that indicates a correlation with increasing $PM_{10}$ concentration observed at CDF and Mesa2 as noted in the Increments of Progress reporting (Gillies et al., 2024a, 2024b, 2025).

Total $PM_{10}$ ($TPM_{10}$), is the summation of hourly mean $PM_{10}$ concentration values for the hours when MetOne 212 $PM_{10}$ concentrations are paired with the station-measured wind speed for the same hours. The lower limit for summation was set at 5.5 m $s^{-1}$ for mean hourly wind speed, as this wind speed indicates that $PM_{10}$ concentration begins to increase and correlate with increasing wind speed with further increases in wind speed (Fig. 2). A wind directional filter of 248°to 326° was applied to ensure that the $PM_{10}$ measured at the stations was being transported from the ODSVRA towards the air quality monitoring locations CDF and Mesa2.

TWPD, by month, for the period May to September in 2025 for each station on open sand areas of the ODSVRA (i.e., NDP, NFRA, Lagrande, ST125, Acacia, S1 Tower, Midden, Independence Hill, and Pipeline) is shown in Fig. 3. Through this period higher TWPD was observed in May and June as compared with the months July, August, and September. Higher wind speeds in the south gave rise to higher TWPD than was observed in the northern stations, which is illustrated by the stations Lagrande, Acacia, Midden, and Pipeline (Fig. 4) that are roughly in a north to south alignment (≈353°).

The trend in TWPD by month for the period May to September in 2025 for the stations located along an approximately west to east alignment from the S1 Tower through to CDF (≈287°) is shown in Fig. 5. The same seasonal pattern, i.e., greater TWPD in May and June as compared with July, August, and September, was observed in these stations as occurred for the stations on open sand areas. The TWPD gradient in this west to east direction shows that the TWPD decreased substantially for stations Scout, P66 and CDF, compared with the more westerly stations. The wind speed is slowed moving eastward due to the increasing frictional resistance at the surface particularly due to the vegetated surfaces at P66 and around CDF. The CDF

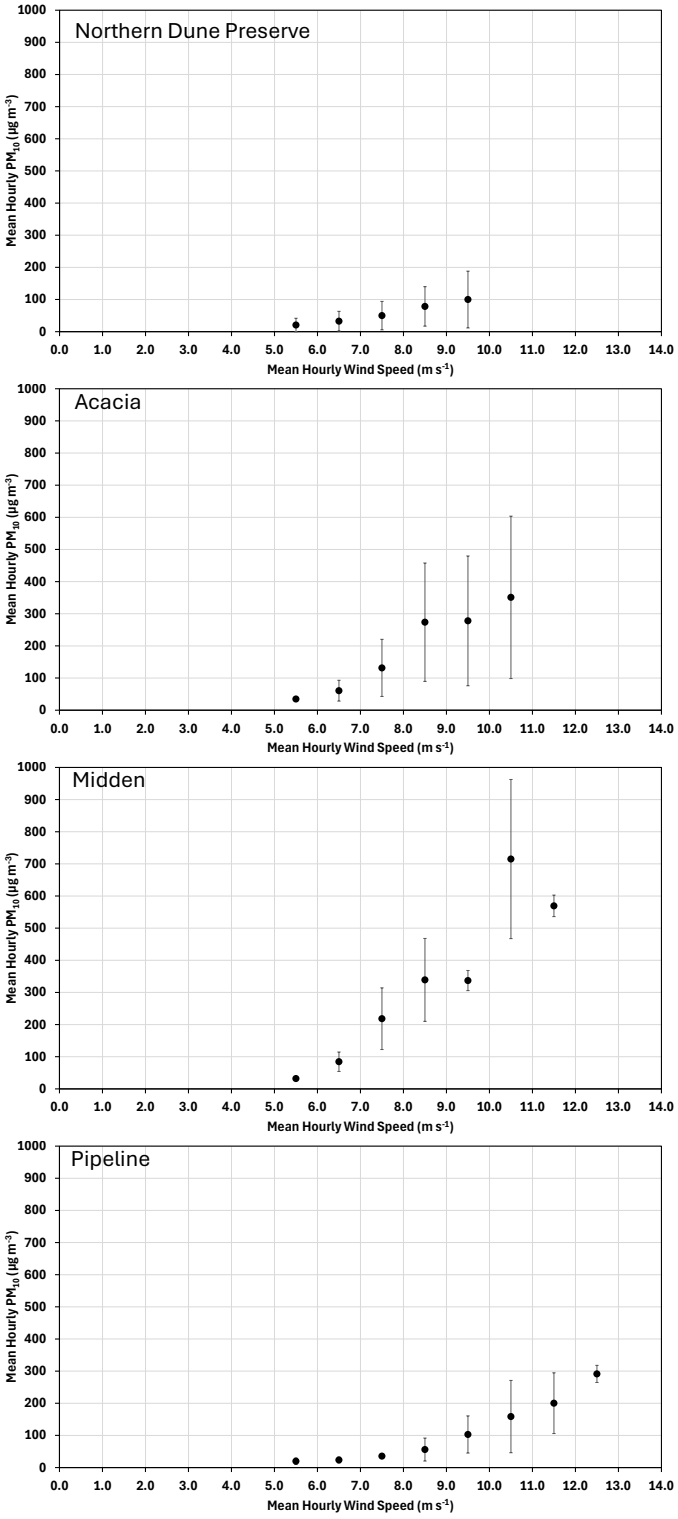



**Figure 2**. Relation between mean hourly $PM_{10}$ concentration and mean hourly wind speed for select stations on open sand areas of the ODSVRA (May-September 2025) spanning the network distance from north (Northern Dune Preserve, NDP) to south (Pipeline).

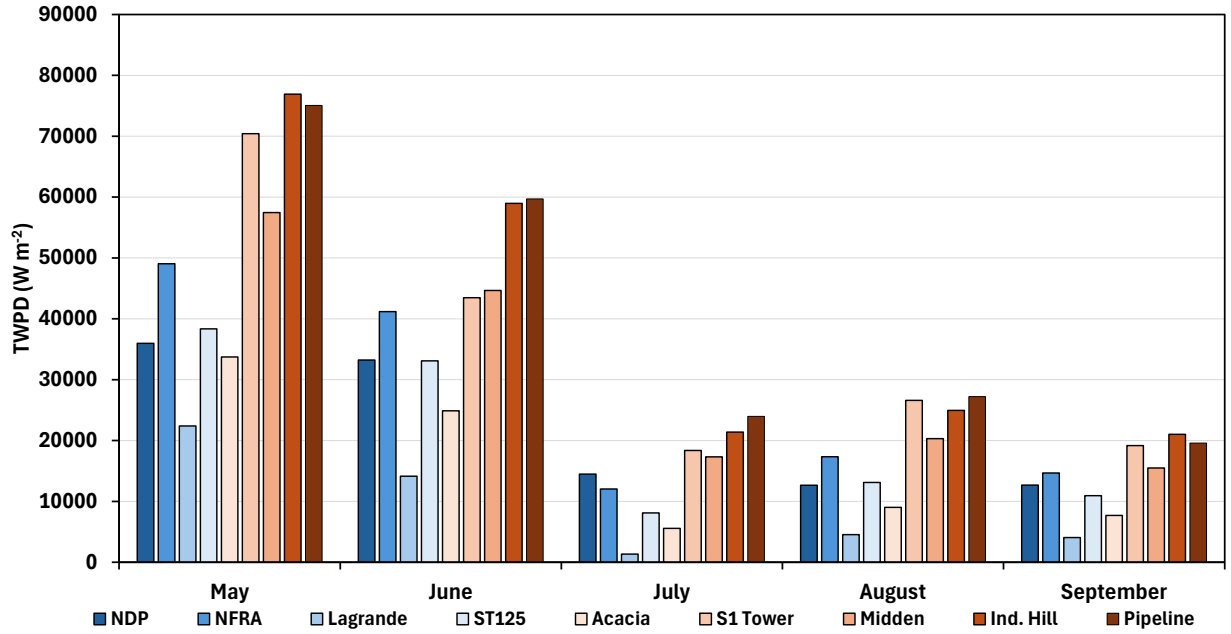



**Figure 3**. The monthly TWPD (W $m^{-2}$) for the stations on open sand areas within the ODSVRA, 2025. The order of stations is approximately north to south, from the left.

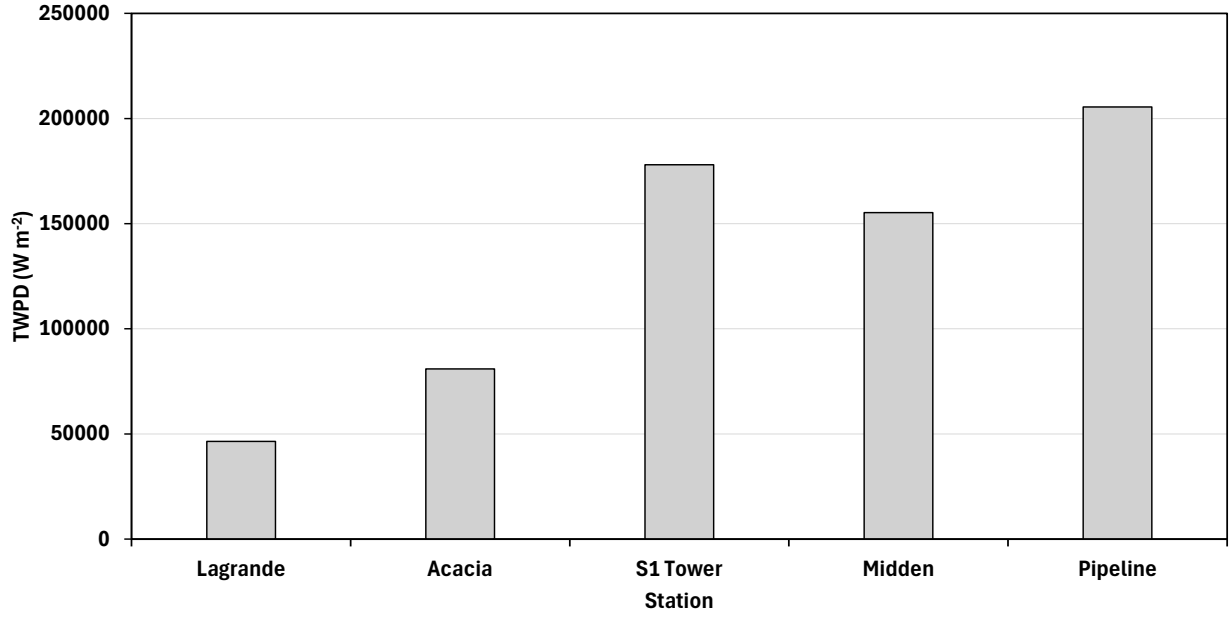



**Figure 4**. The TWPD (W $m^{-2}$), hourly summation from May through September, for stations along a north-south alignment on open sand areas within the ODSVRA, 2025. The order of stations is north to south from the left.

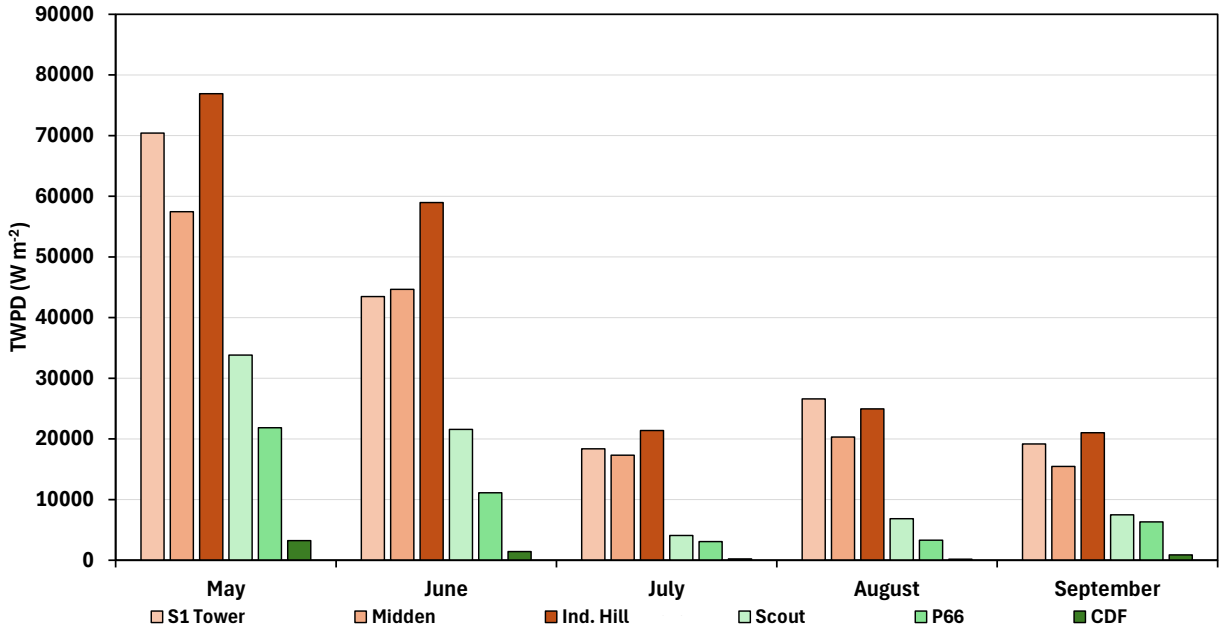



**Figure 5**. The monthly TWPD (W $m^{-2}$) for stations along an approximately west to east alignment from S1 Tower to P66 and CDF, which are downwind of ODSVRA open sand areas.

station, located farthest inland, had the lowest range of TWPD compared with the other three stations to the west. The increase in TWPD at Independence Hill is likely due to the long open fetch to the west as well as an increase in elevation with respect to the Midden station.

The $TPM_{10}$:TWPD for stations located on the open sand areas of the ODSVRA (operated in 2025) for available data from April to September 2021 through 2024[1] and May through September 2025 is shown in Fig. 6. The $TPM_{10}$:TWPD ratio for stations on open sand areas (including NDP) was variable as a function of position. The stations with the greatest $TPM_{10}$:TWPD ratio have consistently been the northern stations and this is still the case in 2025 for Lagrande and Acacia stations, now including the Midden station as well. These stations are all on the downwind (eastern) side of the "sand highway" route that is consistently used by OHV riders to access the ODSVRA riding areas that meet their personal preferences. The Lagrande and Midden stations have longer upwind fetches of open sand than Acacia. NDP station in the non-riding area dune preserve, which is also in an open sand area, had lower ratio values than the stations in the northern zone of the ODSVRA where OHV activity is allowed (Fig. 6).

The $TPM_{10}$:TWPD values along an approximately west to east alignment from the S1 Tower through to CDF (≈287°) for the period May to September in 2025 is shown in Fig. 7. CDF registered the highest mean monthly $TPM_{10}$:TWPD ratio as it had the lowest TWPD values on a monthly basis but still had $PM_{10}$ concentration levels similar to the monitoring stations

[1]Note WPD was incorrectly calculated in 2024 reporting (it was doubled). This is corrected in Fig. 6.

farther to the west that experience higher wind speeds. The $TPM_{10}$:TWPD ratio for CDF, based on using the MetOne Particle profiler data, was not directly comparable to the ratio reported in the Increments of Progress Reporting (Gillies et al., 2022, 2023, 2024a 2024b, 2025) as the measurement instruments, measurement heights, and measurement locations of the wind speed instruments were different (see Gillies and Nikolich, 2024 for further explanation).

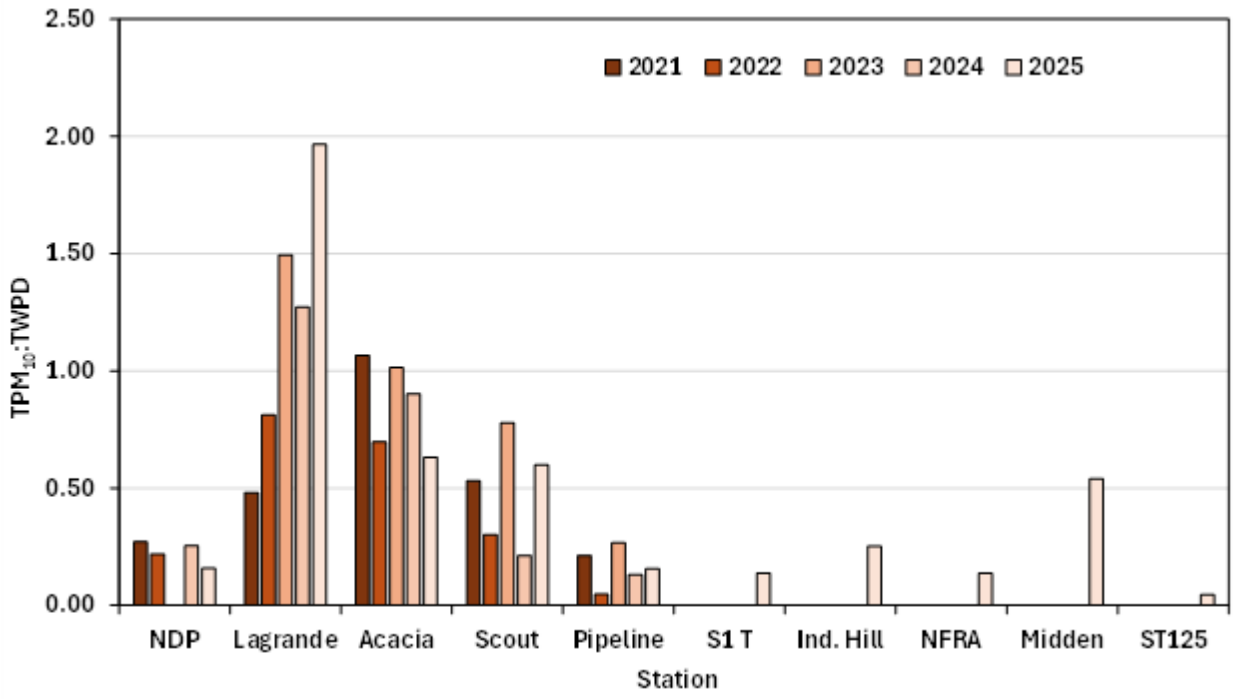



**Figure 6**. The $TPM_{10}$:TWPD ratio, 2021-2025, (based on the summation of mean hourly data) for the stations that are located on sand-sheet areas of the ODSVRA (not including the stations that were removed prior to 2025). The values represent the ratio based on a five (2025) or 6 month period (2021-2024).

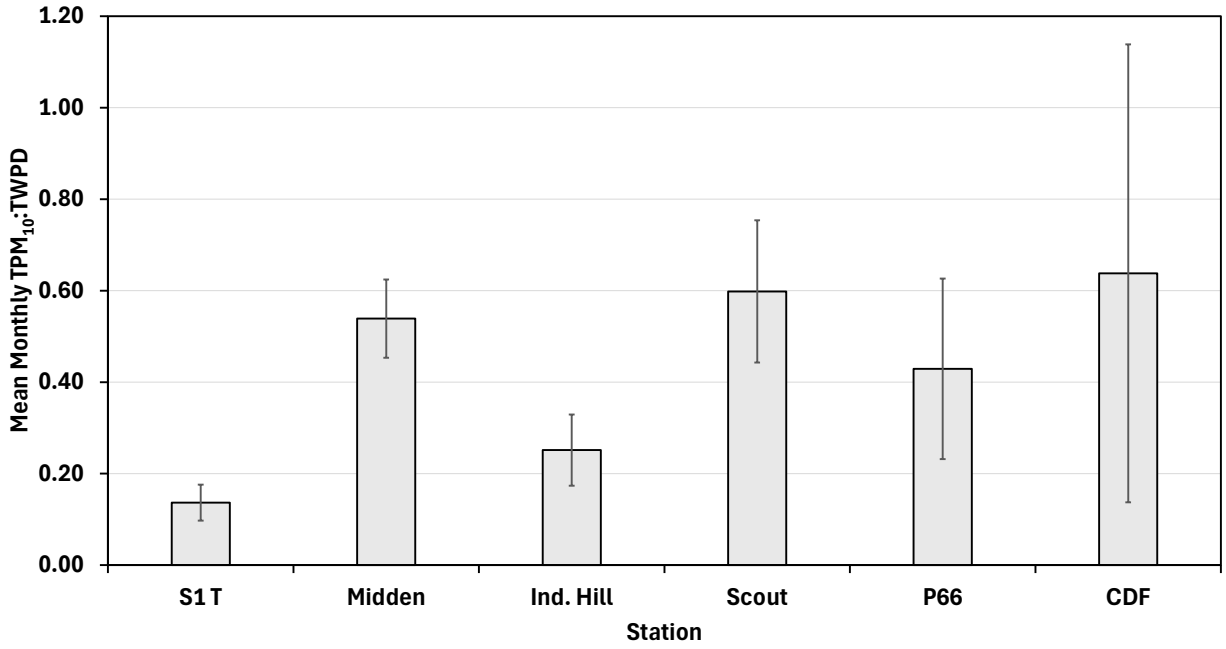



**Figure 7**. The $TPM_{10}$:TWPD for the stations located along an approximately west to east alignment from S1 Tower to P66 and CDF, which are downwind of ODSVRA sand-sheet areas. The error bars represent the standard deviation of a mean monthly $TPM_{10}$:TWPD ratio value.

A representation of the change in $PM_{10}$ moving from west to east from open sand areas to the monitoring stations downwind of the ODSVRA that better revealed the spatial trend was produced by normalizing the mean hourly $PM_{10}$ concentration data at each location by the hourly mean $PM_{10}$ for the Midden station (Fig. 8), which had the consistently highest hourly concentration values. Moving from west to east, the mean hourly $PM_{10}$ concentrations increase from S1 Tower to Midden and then decline as a function of increasing distance east of Midden. Emissions of $PM_{10}$ from sand areas cease approximately 300 m east of Scout, after which the $PM_{10}$ particles were dispersed and deposited as they traveled towards P66 and CDF. At CDF the mean hourly normalized concentration diminished to 0.28 relative to Midden. For the 2024 station data, CDF $PM_{10}$ mean hourly concentration was a third of that observed at the Acacia station, which is relatively consistent with the change in 2025 between Midden and CDF.

A question that has been posed by a group of stakeholders is that consideration should be given to the potential contribution of oceanic sources to the regional $PM_{10}$ burden. Several lines of evidence can be used to examine the significance of potential contributions from this source. Wang et al. (2023) quantified the chemical composition of $PM_{10}$ collected at the CDF site in

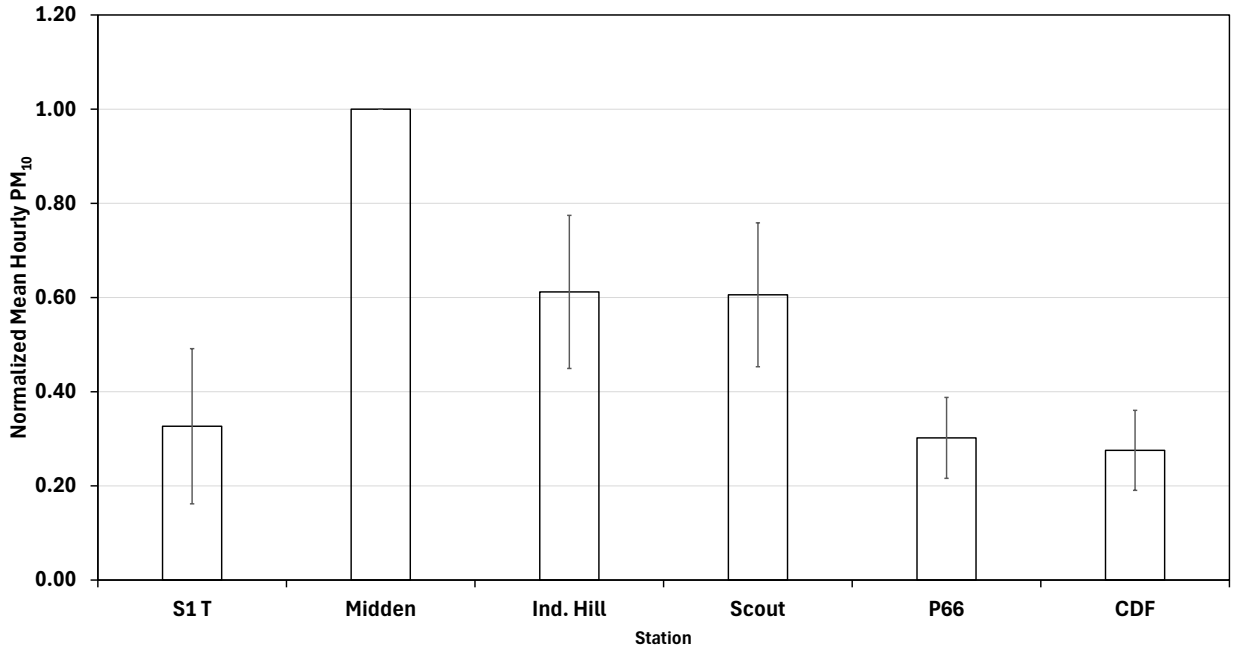



**Figure 8**. The hourly mean $PM_{10}$ concentration, normalized to the hourly mean $PM_{10}$ concentration at the Midden station, for the stations located along an approximately west to east alignment from S1 Tower to P66 and CDF, which are downwind of ODSVRA open sand areas. The error bars represent the standard deviation of a normalized mean hourly $PM_{10}$ value.

2021 and found mineral dust comprised the largest fraction of the particles, which they attributed to wind-driven saltation and dust emission processes within the ODSVRA. In 2025 three monitoring stations, NFRA, ST125 and S1 Tower were located relatively close to the shoreline. NFRA is located west of the northern limit of foredune restoration area #1. To the west of the NFRA station is the beach approximately 100 m wide. The beach area is closed to OHV activity for the duration of the Snowy Plover breeding period. West of ST125 is foredune restoration area #5 and a narrow beach zone to the west of the restoration area. West of S1 tower is a narrow area that has riding activity with the plover exclosure farther west of this narrow area. These stations are located downwind of areas of low emissivity, except for the narrow riding area zone to the west of the S1 Tower, based on multiple years of PI-SWERL measurements. Comparing the mean (May-September) $TPM_{10}$:TWPD ratio values from these two stations with the stations Lagrande, Acacia, Midden and Pipeline, which are located well within the ODSVRA and in open riding areas, the data show that the interior stations produce much higher $PM_{10}$ values for equivalent WPD (Fig. 9). The increase in $PM_{10}$ produced per unit WPD with increasing distance from the shoreline indicates that the $PM_{10}$ concentrations cannot be a result of an initial input of high $PM_{10}$ concentrations from Oceanic sources

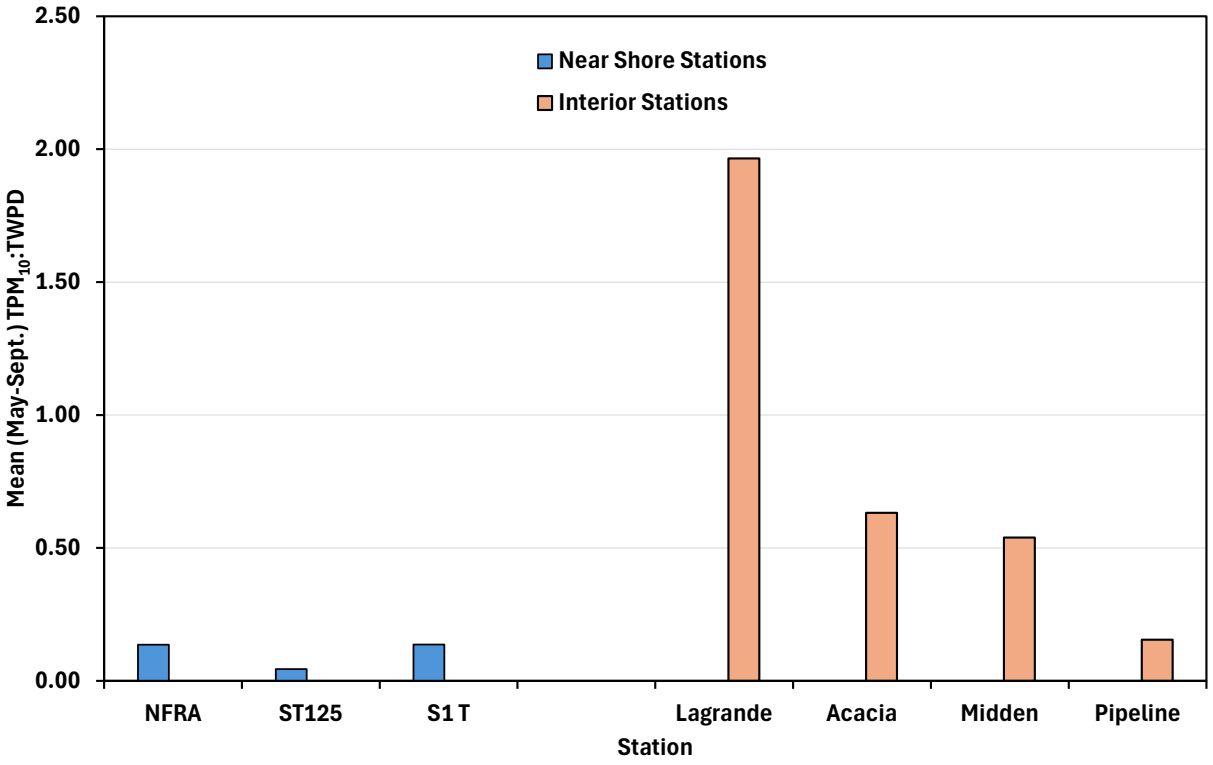



**Figure 9**. The $TPM_{10}$:TWPD for stations NFRA, ST125 and S1 Tower (S1 T) near the shoreline and for stations Lagrande, Acacia, Midden and Pipeline located within the riding area of the ODSVRA.

## Conclusions

The stations on the opens sand sheet areas show that the concentration of $PM_{10}$ along an approximately 3.8 km west to east transect (S1 T to CDF) showed a consistent peak concentration occurring at the Midden station, reflecting the greater emissivity of the sand in this area that is highly influenced by the sand highway to the west of this station. The concentration of $PM_{10}$ diminished compared to the Midden station by, on average, 70% (±9%) in May-September 2025 for the Phillips 66 station, and 72% (±8%) at CDF, which are east of the open sand areas of the riding and non-riding areas of the ODSVRA. This decrease in normalized reflects the change from an area where emissions of $PM_{10}$ are occurring on sand sheet areas, to one in which dispersion and deposition dominate the transport process. Beginning east of the Scout station (≈300 m) and extending to CDF, the surface becomes non-emissive with respect to dust emissions as it is covered by vegetation. Across the distance from Scout to CDF dispersion and deposition processes will tend to decrease particulate matter concentration with increasing travel distance.

The 2025 wind speed and wind power density data (Figs. 2) show that for the north-south distance covered by the network the wind speed was higher in the south than the north, which

corroborates what has previously been reported and indicates that this pattern has persisted since monitoring was initiated. The station $PM_{10}$ and wind speed data combined also showed (Fig. 6) that the $PM_{10}$ concentrations for the same wind power density were higher in the northern stations indicating that the emissivity of the sand surfaces upwind of these stations remains high in relation to the other stations and is still a rich source area for $PM_{10}$ emissions. The high $PM_{10}$ concentrations and emissivity in this area may be due to the presence of the "sand highway", which remains a high use area for OHV. The gradient of decreasing emissivity from north to south has also been observed in the PI-SWERL data. The 2025 $TPM_{10}$:TWPD data (Fig. 6) indicates that this pattern has persisted since the monitoring was initiated.

The $PM_{10}$ data from the monitoring network for its period of operation, 2021-2025, has consistently shown that $PM_{10}$ concentrations increase from the shore area to the interior of the ODSVRA, and decline moving from the eastern boundary to the two easternmost stations Phillips 66 and CDF. This argues against the conjecture that high $PM_{10}$ concentrations downwind of the ODSVRA can be attributed to oceanic sources.

**References**


Etyemezian, V., J.A. Gillies, D. Zhu, A. Pokharel, G. Nikolich (2014). 2013 Intensive Wind Erodibility measurements at and Near the Oceano Dunes State Vehicular Recreation Area. Prepared for California State Parks, ODSVRA, Oceano, CA and OHMVR Division, Sacramento, CA, 07-08-2014.

Gillies, J.A., V. Etyemezian (2014a). Wind and $PM_{10}$ Characteristics at the ODSVRA from the 2013 Assessment Monitoring Network. Prepared for California State Parks, ODSVRA, Oceano, CA and OHMVR Division, Sacramento, CA, 01-14-2014.

Gillies, J.A., V. Etyemezian (2014b). Addendum to the PI-SWERL Report of Etyemezian et al. (2014): Particle Size Distribution Characteristics and PI-SWERL$^{TM}$ $PM_{10}$ Emission Measurements: Oceano Dunes State Vehicular Recreation Area. Prepared for California State Parks, ODSVRA, Oceano, CA and OHMVR Division, Sacramento, CA, 02-03-2015.

Gillies, J.A., E. Furtak-Cole, G, Nikolich (2022). Increments of Progress Towards Air Quality Objectives - ODSVRA Dust Controls, 2021. Prepared for California State Parks, ODSVRA, Oceano, CA and OHMVR Division, Sacramento, CA, 09-14-2022.

Gillies, J.A., E. Furtak-Cole, G, Nikolich (2023). Increments of Progress Towards Air Quality Objectives - ODSVRA Dust Controls, 2022. Prepared for California State Parks, ODSVRA, Oceano, CA and OHMVR Division, Sacramento, CA, 02-08-2023.

Gillies, J.A., E. Furtak-Cole, G, Nikolich (2024). Increments of Progress Towards Air Quality Objectives - ODSVRA Dust Controls, 2023. Prepared for California State Parks, ODSVRA, Oceano, CA and OHMVR Division, Sacramento, CA, 02-15-2024.

Gillies, J.A., E. Furtak-Cole, G, Nikolich (2025). Increments of Progress Towards Air Quality Objectives - ODSVRA Dust Controls, 2024. Prepared for California State Parks, ODSVRA, Oceano, CA and OHMVR Division, Sacramento, CA, 05-22-2025.

Gillies, J.A., G. Nikolich (2024c) Report of Findings: ODSVRA Meteorological and $PM_{10}$ Monitoring Network, 2023. Prepared for California State Parks, ODSVRA, Oceano, CA and OHMVR Division, Sacramento, CA, 06-20-2024.

Kalmikov, A. (2017). Wind power fundamentals. In Wind Power Engineering, ed. T.M. Letcher. Elsevier Science Publishing Co., Inc.

Wang, X., J.A. Gillies, S. Kohl, E. Furtak-Cole, K. Tupper, D. Cardiel (2023). Quantifying the source attribution of PM10 measured downwind of the Oceano Dunes State Vehicular Recreation Area. Atmosphere 14, 718, doi: 10.3390/atmos14040718.

June 9, 2026

**Memo: SAG Review of Desert Research Institute (DRI) "Report of Findings: ODSVRA Meteorological and $PM_{10}$ Monitoring Network, 2025"**

**From**: Scientific Advisory Group (SAG)

**To:** Jon O'Brien, California Department of Parks and Recreation

**Cc**: Ronnie Glick, California Department of Parks and Recreation

The Scientific Advisory Group (SAG) received a copy of the Desert Research Institute (DRI) "Report of Findings: ODSVRA Meteorological and $PM_{10}$ Monitoring Network, 2025" on June 1, 2026 via e-mail, and SAG members have had the opportunity to review the document. This memo provides feedback on the DRI report[1].

The report summarizes the latest results, acquired in 2025, from the wind and dust monitoring network, which comprises multiple stations distributed within the ODSVRA and supplemented with additional stations downwind of the ODSVRA. The results from 2025 are contextualized using similar data collected in 2021 through 2024. The data were presented in summary form using hourly values that are averaged over monthly and seasonal (May – September) periods.

The key findings of the report are that:

1. In 2025, the number of monitoring stations was reduced in response to budgetary pressures. The network was reduced from 15 to 12 stations. Five stations were re-deployed in different locations in an effort to capture west to east gradients in wind and dust concentrations. The typical deployment period is from April through September, but because of instrument calibration delays by the vendor, the deployment period was from May through September;
2. The data trends in 2025 are consistent with those from earlier years (2021 – 2024), recognizing that there is year-to-year variability in wind strength as represented by Total Wind Power Density (TWPD);
3. Similar to previous years, greater TWPD was observed in May and June compared to lesser values observed in the summer months of July, August, and September;
4. Also similar to previous years, there was a general increase in wind speed from the north to the south, leading to higher TWPD at southern stations;
5. A west-east gradient in TWPD was observed, with lower TWPD at eastern sites due to increased frictional resistance from vegetated surfaces and topographic features upwind;
6. There was a general decrease in normalized $PM_{10}$ concentrations from north to south, as represented by the ratio of Total $PM_{10}$ divided by Total Wind Power Density ($TPM_{10}$/TWPD). This is consistent with results from previous years;

[1] Standard procedure for SAG review of DRI reports is for Dr. Jack Gillies to recuse himself from the discussions due to a potential conflict of interest. Despite being a SAG member in good standing, Dr. Gillies did not participate in this review in any manner nor was DRI consulted about any aspect of this review.

7. There was a general west-east trend in $TPM_{10}$/TWPD that indicated that dust emissions increased moving inland from the shoreline across the ODSVRA and then decreased beyond the park boundary toward monitoring stations such as CDF. Normalized $PM_{10}$ concentrations were highest at the new Midden station and then decreased eastward. The Midden station is downwind of the sand highway, which experiences significant OHV activity.
8. The mean (May-September) $TPM_{10}$/TWPD ratio for the two shoreline stations (ST125 and S1 Tower) were significantly lower than at stations in open riding areas (e.g., Lagrande, Acacia, Midden, and Pipeline).

SAG members make the following recommendations for possible improvement of the DRI report. Some of these recommendations were made in previous SAG reviews of earlier reports, but these recommendations were not acted upon in this report:

A. It would be helpful to organize the report such that results are presented from straightforward to more complicated parameters, such as $PM_{10}$ concentrations and wind speeds, followed by TWPD and $TPM_{10}$/TWPD ratios. This organization would allow the reader to have a more physical interpretation of the $TPM_{10}$/TWPD ratios. Similarly, organizing the discussion to focus separately on spatial variability and temporal variability would help with interpretation of the data and conclusions. The current report seems to use a 'mix and match' approach, which is difficult for the reader to follow.
B. In future reports (or as a separate exercise), an analysis should be undertaken of dust dynamics during specific wind events. This might involve using hourly values across a 24-hour period or perhaps 10-minute averages across an 8-hour period when dust concentrations are particularly high. The intent would be to understand how and where dust plumes are generated and eventually make their way to inland monitoring stations such as CDF. Such an analysis would help to identify west-east transport dynamics during actual dust events rather than on a seasonal average basis.
C. In future reports, it would be useful to tie the metrics used in the current report (e.g., monthly averages of TWPD and $TPM_{10}$/TWPD) to measures used by regulatory agencies to define exceedance events (i.e., 24-hr $PM_{10}$ concentrations). The objective is to use the scientific results to inform management and regulatory efforts directly in ways that are meaningful and easy to understand.

A marked-up copy of the original report will be sent under separate cover, which will indicate where in the document improvements are possible. The final report will be a welcome addition to the body of knowledge that informs the air quality program at the ODSVRA.

Respectfully,

The Scientific Advisory Group

Bernard Bauer (Chair), Jenny Hand, Leah Mathews, Ian Walker

**ODSVRA Dust Control Program Draft 2026 ARWP**

**ATTACHMENT 04**

**ODSVRA Emissivity PI-SWERL Update Report (2025) (SAG Report)**

*THIS PAGE WAS INTENTIONALLY LEFT BLANK.*

February 12, 2026

**Memo: ODSVRA PI-SWERL Emissivity Measurements Update Report (2025)**

**From**: Scientific Advisory Group (SAG)

**To:** Jon O'Brien, California Department of Parks and Recreation

**Cc**: Ronnie Glick, California Department of Parks and Recreation
Karl Tupper, SLO Air Pollution Control District

The Desert Research Institute (DRI) undertook an extensive sampling campaign in 2024 consisting of PI-SWERL measurements at 808 locations distributed across the Oceano Dunes State Vehicular Recreation Area (ODSVRA). The SAG analyzed those data and provided a comprehensive report that summarized the results from all PI-SWERL campaigns between 2013 and 2024, inclusive[1]. In September, 2025, the DRI conducted another PI-SWERL campaign focused on the Plover Exclosure (PE) with control measurements taken in the Non-Riding Area Central (NRA-C) zone. This memorandum summarizes the results from the 2025 campaign and presents updated emissivity power relations for use in the DRI simulation model.

For the 2025 PI-SWERL campaign, a total of 57 measurements were taken in the PE. Another 24 measurements were made in the NRA-C for purposes of investigating potential spatio-temporal biases. Figure 1 shows the measurement locations for 2025, with PI-SWERL sites along the beach in front of the foredunes, within the foredunes to the extent feasible, and toward the landward (eastern) margins of the PE. In prior years, particularly 2022 (n = 23) and 2024 (n = 30), the measurement locations were dominantly along a north-south transect situated approximately in the middle of the PE, to the lee of the foredunes. Despite the broader spatial coverage in 2025, the measurements collectively provide similar statistical results (i.e., means, medians, ranges) to those made in 2024 and 2022 (see Figure 2).

[1] SAG Memorandum (May 11, 2025) with accompanying report entitled "ODSVRA PI-SWERL Emissivity Measurements Update Report (2013-2024)."

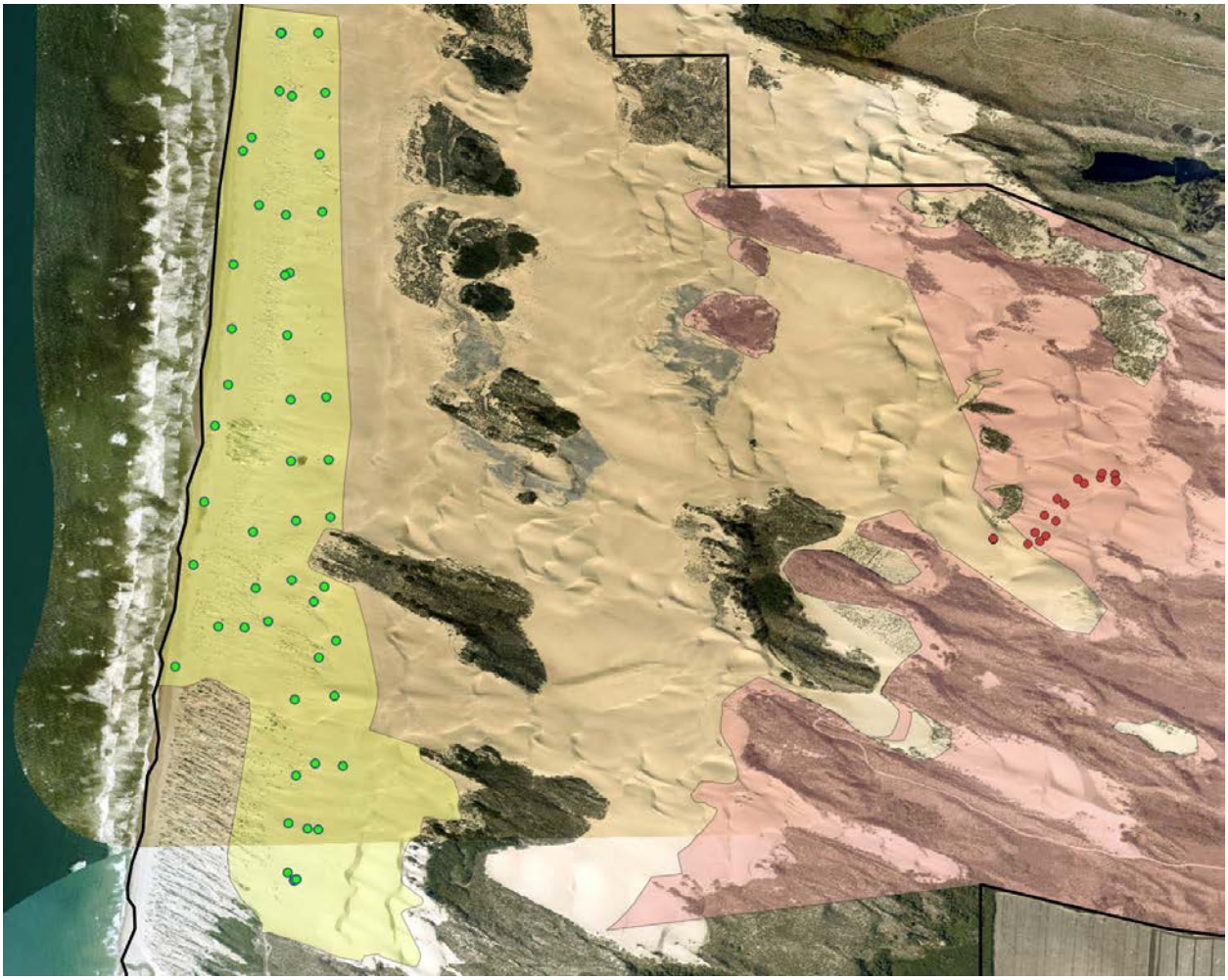


**Figure 1 – PI-SWERL sampling locations in September 2025. The Plover Exclosure locations are indicated by green circles and the extent of the PE zone is shown in pale yellow. Control measurement locations in the Non-Riding Area Central are indicated by red circles, and the extent of the NRA-C zone is shown in pale pink.**

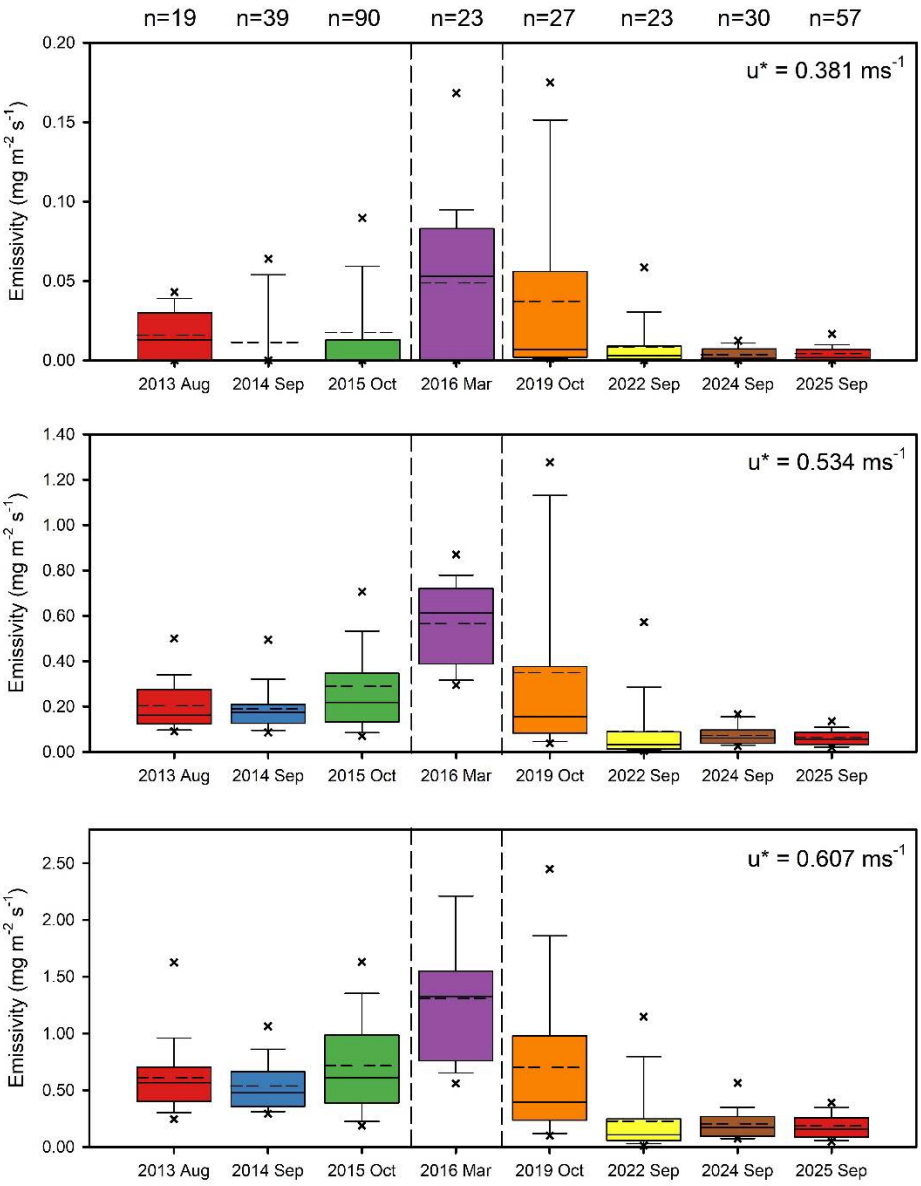



**Figure 2 - Box-and-whisker plots of PI-SWERL emissivity measurements in the PE for all sampling campaigns between 2013 and 2025, inclusive. Horizontal axes show dates given as year and month. The three panels (upper middle, lower) correspond to the three RPM speeds (low, medium, high) used in the PI-SWERL device to characterize dust emissions at any single measurement location. The colored boxes define the range of the 25$^{th}$ and 75$^{th}$ percentiles; the whiskers correspond to the 10$^{th}$ and 90$^{th}$ percentiles; and the outer symbols (x) indicate the 5$^{th}$ and 95$^{th}$ percentiles (note that 95$^{th}$ percentile for 2016 in the lower panel falls above the graph range). The median value is given by the horizontal solid line within the box, whereas the arithmetic mean (average value) is shown by the horizontal dashed line. Note that the PE was closed permanently in 2021, so earlier campaigns reflect seasonal exclosure with OHV access between October 1 and February 28. Vertical dashed lines isolate the March, 2016, measurements from all others as being different (see SAG Memorandum, May 11, 2025, for details).**

PI-SWERL measurements made in the NRA-C provide a means to assess whether differences in results from year-to-year are due to spatial biases as opposed to meteorological controls on emissivity potential. A comprehensive analysis has not been conducted given the limited data available, but Figure 3 shows the temporal trends in emissivity for the middle speed of the PI-SWERL ($u_* = 0.534$ m $s^{-1}$) for both the PE and the NRA-C. As noted in reference to Figure 2, the 2025 values for the PE are similar to the 2024 and 2022 values (all taken in September), suggesting little temporal variation in environmental controls on emissivity recently. Similarly, the NRA-C values in September of 2025 align well with those in May 2024 and September 2024. However, the May 2022 NRA-C values were higher, as were all previous measurements back to 2013. Note that the 2022 measurements for the NRA-C aren't directly comparable to those for the PE in the same year because measurements were taken at different times of the year (May vs September, respectively). Given that there were no measurements taken in the PE in May of 2022 and 2024, and none taken in the NRA-C in September 2022, it is difficult to reach conclusions about spatio-temporal trends other than the recent reduction in emissivity (since approximately September 2022) in both the PE and NRA-C.

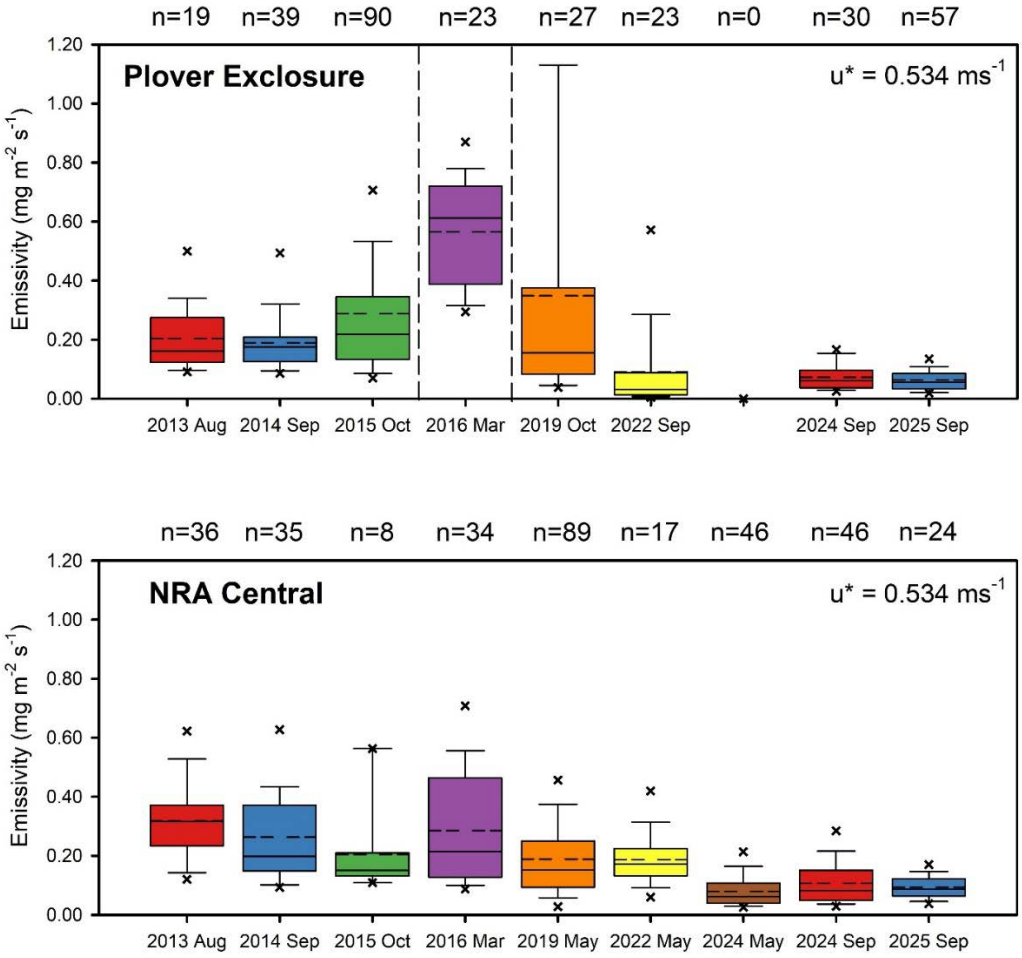



**Figure 3 – Box-and-whisker plots of mid-speed PI-SWERL emissivity measurements in the PE (upper panel) for all sampling campaigns between 2013 and 2025, inclusive, contrasted with those from the NRA Central (lower panel). No data were collected in the PE for May 2024. See Figure 2 for explanation of symbols.**

The data trends shown in Figures 2 and 3 suggest three things: (1) there was a noticeable reduction in emissivity in the PE after 2021 when seasonal riding was no longer allowed in that zone (i.e., after all-year closure); (2) there was a similar reduction in emissivity in the NRA-C since approximately 2022, which cannot be ascribed to management interventions; and (3) even though closure of the PE after about 2021 led to evident reductions in emissivity potential, a parallel decrease in emissivity in the NRA-C since May 2022 suggests that there may be other factors at play. It may be that broad environmental controls (e.g., atmospheric humidity, surface moisture) have influenced the emissive properties of the entire ODSVRA in similar fashion, although providing conclusive proof is confounded by several factors such as semi-random PI-SWERL measurement locations and limited operational access during certain times of the year.

The 2025 data for the PE and the NRA-C have been integrated into the global data set (2013-2025) to calculate new median values for those zones, and accordingly, new emissivity power relations were derived. Table 1 shows the updated values. Note that the parameters for all other zones are identical to those provided in the previous report (and used for purposes of the 2025 ARWP).

| | **NRA North** | **NRA Central** | **NRA South** | **RA C-North** | **RA C-South** | **FRA** | **PE** | | **SE Average** |
|---|---|---|---|---|---|---|---|---|---|
| ***n =*** | ***170*** | ***337*** | ***109*** | ***495*** | ***828*** | ***177*** | ***110*** | | ***72R + 74NR*** |
| **$u_*$ (m $s^{-1}$)** | median | median | median | median | median | median | median | | median |
| **0.381** | 0.033 | 0.013 | 0.001 | 0.093 | 0.024 | 0.006 | 0.002 | | 0.024 |
| **0.534** | 0.277 | 0.14 | 0.09 | 0.651 | 0.317 | 0.072 | 0.055 | | 0.166 |
| **0.607** | 0.755 | 0.45 | 0.251 | 1.296 | 0.752 | 0.205 | 0.15 | | 0.348 |
| | | | | | | | | | |
| **a** | 35.646 | 41.170 | 14.411 | 19.732 | 22.635 | 11.858 | 7.752 | | 6.197 |
| **b** | 7.724 | 9.048 | 8.111 | 5.451 | 6.817 | 8.129 | 7.901 | | 5.768 |
| **Rsqr** | 0.999 | 1 | 0.999 | 1 | 1 | 1 | 1 | | 1 |

**Table 1: Median emissivity (mg $m^2$ $s^{-1}$) values for each of the three PI-SWERL speeds (shear velocities, $u_*$) used to fit power relations characterizing the eight (8) distinct management zones in the simulation model. Power function coefficients (a, b) are for the power relation, $F = a\,(u_*)^b$ where F is the flux (emissivity) magnitude (mg $m^{-2}$ $s^{-1}$). Power regression results calculated using SigmaPlot© software.**

Respectfully,

The Scientific Advisory Group
Bernard Bauer (Chair), Jack Gillies, Jenny Hand, Leah Mathews, Ian Walker

*THIS PAGE WAS INTENTIONALLY LEFT BLANK.*

**ODSVRA Dust Control Program Draft 2026 ARWP**

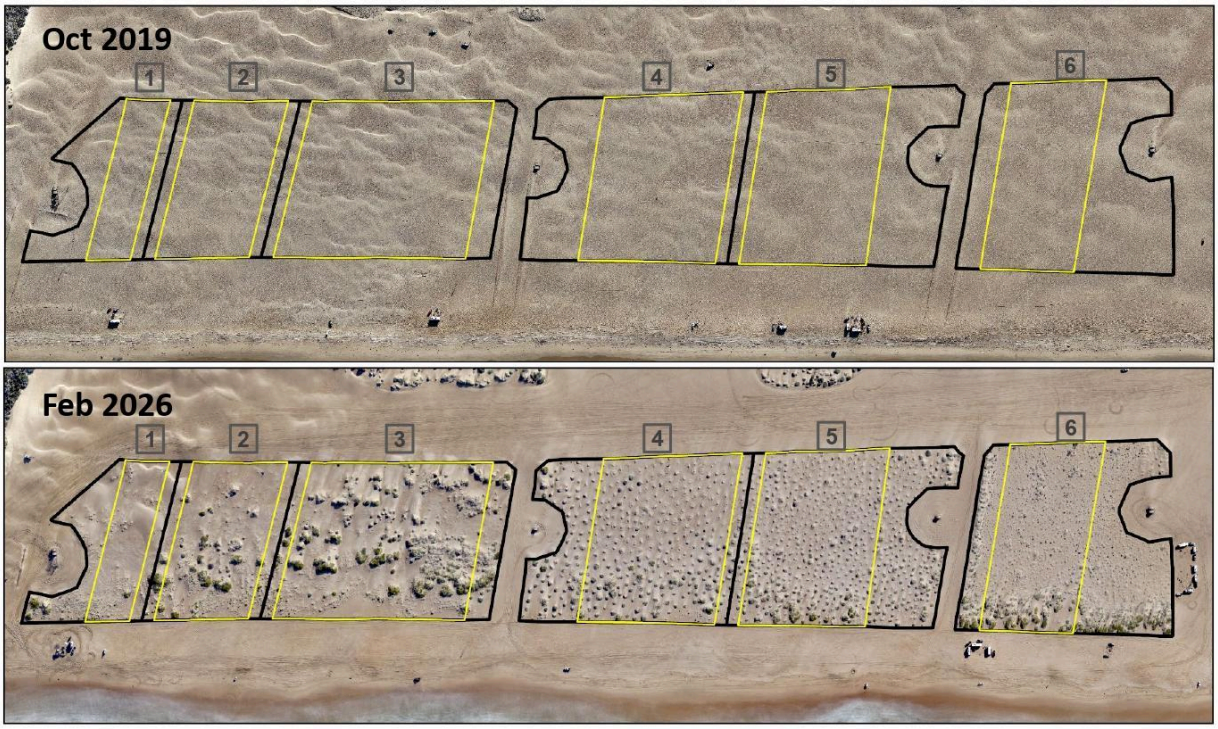
**ATTACHMENT 05**

**UCSB 2025-2026 ODSVRA Foredune Restoration Area UAS Monitoring Report**

- UCSB 2025-2026 ODSVRA Foredune Restoration Area UAS Monitoring Report (UCSB Report)
- SAG Review of UCSB Report "2025-2026 ODSVRA Foredune Restoration Area UAS Monitoring Report" (SAG Memo)

*THIS PAGE WAS INTENTIONALLY LEFT BLANK.*

# 2025-2026 ODSVRA
# Foredune Restoration Area UAS Monitoring Report




*Aerial image mosaics of the foredune restoration area in ODSVRA prior to implementation of restoration treatments in Oct. 2019 (upper) and after 6 years of development in Feb. 2026 (lower). Numbers indicate treatment plots and their analytical areas are outlined in yellow.*

**Prepared by: Chloe Daudon[1,2], Madison Heffentrager[1], Maya Bernstein[2], Zach Hilgendorf[3], and Ian Walker[1,2]**

[1]Department of Geography, University of California Santa Barbara
[2]Marine Sciences Institute, University of California Santa Barbara
[3]Department of Geography & Anthropology, University of Wisconsin - Eau Claire

July 2026

## List of Acronyms:

California Department of Parks and Recreation – CDPR

Desert Research Institute – DRI

Digital Terrain Model – DTM

Foredune Restoration Area – FRA

Geomorphic Change Detection – GCD

Ground Sampling Distance – GSD

Light Detection and Ranging – LIDAR

Multispectral – MS

Near Infrared – NIR

Normalized Difference Vegetation Index – NDVI

North Oso Flaco – NOF

Oceano Dunes State Vehicular Recreation Area – ODSVRA

Off-Highway Vehicles – OHV

Particulate Matter – PM

Particulate Matter Reduction Plan - PMRP

Portable In-Situ Wind Erosion Laboratory – PI-SWERL

Post-Processing Kinematic - PPK

Red-Edge – RE

Red-Green-Blue Spectral Bands – RGB

San Luis Obispo Air Pollution Control District – SLO-APCD

Scientific Advisory Group – SAG

Structure-from-Motion – SfM

Stipulated Order of Abatement – SOA

Treatment Plot - TP

Uncrewed Aerial System – UAS

University of California Santa Barbara – UCSB

# EXECUTIVE SUMMARY

The foredune restoration project was established in Feb. 2020 as a nature-based solution to mitigate dust emissions from a highly emissive 48-acre site by promoting sand deposition, vegetation growth, and dune development. The foredune restoration area (FRA) consists of 6 treatment plots (TPs), including (north-south): TP1, a control plot only textured by a sheepsfoot roller; TP2, sheepsfoot texture and broadcast native seeds; TP3, sheepsfoot texture and broadcast native plant and sterile rye grass seeds; TP4, low-density straw planting circles with nodes of juvenile native plants; TP5, high-density straw planting circles with nodes of juvenile native plants; and TP6, complete straw cover with high density of juvenile plants.

An uncrewed aerial system (UAS) with high resolution cameras has been flown biannually (Oct. and Feb.) since Oct. 2019 to monitor and detect geomorphic and vegetation changes in the FRA and adjoining beach and back dune areas. To date, 12 campaigns have been conducted and resulting datasets include: georeferenced orthomosaics, plant cover maps, digital terrain models (DTMs), topographic change maps, and sand volumetric change estimates. These datasets are used to examine quantities and patterns of sand erosion/deposition, dune development responses, and changes in vegetation across the TPs through time. These results were then used to assess the performance of the treatments based on indicators of dune development, sediment budget response, vegetation trends, and dust mitigation potential.

This report provides results from 6 years of development through to Feb. 2026. The results reflect modifications to the analytical approach, on advice of SAG and CDPR, that include: 1) new analytical sub-areas within the TPs to remove edge effects from fences and structures, 2) a new reference site at North Oso Flaco (NOF) against which observations from the TPs are normalized and compared, and 3) modification of the performance assessment to focus solely on 3 simpler metrics derived from sediment budget responses, plant cover change, and a new terrain roughness index (TRI) that describes evolving roughness of dunes and plant cover as a more quantitative measure of flow sheltering and dust emissions control potential of the TPs.

In terms of sediment budget responses, sand supply to the beach, which feeds aeolian transport into the TPs to promote dune development, remains highly variable due to seasonal changes in wave energy, beach erosion/rebuilding, and moving rip current embayments. Generally, beach sediment budgets trended from positive in the pre-restoration baseline (Oct. 2019 to Feb. 2020), negative by Feb. 2023, then back to less variable positive values since. Net (i.e., cumulative) changes in beach sediment volumes indicate slight erosion in the northern two plots (TPs 1-2) and accretion in the southern four plots (TPs 3-6).

Despite fluctuations in beach sand supply, the TPs continue to maintain net positive sediment budgets, albeit with some erosional intervals. Net change in the TP1 control site remained neutral while the neighboring TP2 showed the lowest rates of accumulation due to sediment bypassing and longer-term declines in sand inputs from the beach. TP4 showed the third lowest accumulation rate, but with less bypassing to the landward dunes. TP5 showed moderate rates of sand accumulation, while TP6 exhibited the second highest accumulation rates. Overall, TP 3

continues to have the highest net sand accumulation rate.

Plant cover, on average, has increased in the FRA since Feb. 2020, but with significant variation and a marked period of decline following a very wet, stormy year in 2023. Since Feb. 2025, this trend has reversed with all TPs resuming positive trends in plant cover. Currently, the TP1 control site has increased slightly to 3.17% following prolonged minimal plant cover, and is the only plot to remain below the historical peak value within the foredune zone of ODSVRA of 5.3% in 1966. To date, TP6, the most intensive treatment, has shown the greatest net increase in plant cover (14.71%), followed by TP3 (10.27%), TP2 (8.62%), TP5 (8.00%), and TP4 (7.43%). Compared to the NOF reference site, however, all TPs remain well below average (21.89%) and minimum (16.99%) plant cover values. The NOF site provides an important reference condition for plant cover for a foredune ecosystem that has seen limited disturbance and at least 40 years of development. NOF also captures variations in plant cover and dune development that reflect regional variability in climatological and ecogeomorphic controls. Some species, namely *Abronia latifolia*, have shown rapid establishment and growth, and appear to play a leading role in dune development at the site.

Dust control potential of the FRA, estimated through the new topographic roughness index (TRI), has increased across all TPs over time as dunes and plant communities have developed. For instance, the TRI values of TPs have increased by factors ranging from 2.3 (TP1, lowest) to 3.4 (TP5, highest) between Feb. 2020 and Oct. 2023. This was followed by a decline between Oct. 2023 and Oct. 2024 (by a factor of about 1.3), likely associated with reduced plant cover, after which TRI values stabilized or increased slightly for most treatments, while the TP1 control site continued to decline after Feb. 2025. Since Feb. 2022, TP3, TP5, and TP6 have consistently shown the greatest roughness, with TP5 having the highest TRI by Feb. 2026, followed by TP4, TP2, and TP1. However, the roughness of all FRA treatment plots remains below the relatively stable TRI observed at the NOF reference site, which varied only slightly over the monitoring period. Comparatively, the roughness of the treatment plots reached just 30 to 60% of NOF roughness by Feb. 2026, suggesting further development is needed to reach comparable surface roughness and dust control potential of a fully developed dune state (Figure 10, Table 4).

After 6 full wind and plant growth seasons, the TPs continue to evolve on different trajectories as a function of initial treatments and variability in sand supply, plant cover, and dune development. From this report forward, performance is only assessed based on sediment budget, plant cover, and roughness (TRI) metrics. Despite this new methodology, the relative rankings of treatment performance have not changed significantly since Oct. 2022, with TP3, TP6, and TP5 (in order) ranked as top performers. These treatments show the largest net positive sediment budgets, greatest plant cover values, and highest terrain roughness and, as such, offer the greatest dust emission control potential. TP4 has shown a recent decline in sediment budget, but maintains increasing plant cover and roughness. Next to the TP1 (control) site, TP2 maintains the lowest performance due to modest amounts of accretion and dune development, low plant cover, and correspondingly low dust emissions control potential. Monitoring will continue as the treatments evolve to detect further responses indicative of success or concern for adaptive management and for longer-term sustainability of the FRA as a dust control mitigation site.

# 1. Introduction

The purpose of the foredune restoration project is to help reduce dust emissions in the ODSVRA and downwind through the implementation of a nature-based foredune restoration area (FRA) on a formerly highly emissive site near the beach. To monitor and assess the performance of the FRA, a team from UC Santa Barbara, in collaboration with CDPR, have conducted biannual UAS flights since Oct. 2019 (Figure 1).

This report presents results from 6 years of dune development following implementation of the FRA treatments in Feb. 2020 through to Feb. 2026. On advice of SAG and CDPR, the analytical methodology was also refined to include: 1) new analytical sub-areas within the TPs to remove edge effects from fences and structures (Figure 2), 2) a new reference site at North Oso Flaco (NOF) against which observations from the TPs are normalized and compared, and 3) modification of the performance assessment to focus only on 3 simpler metrics derived from sediment budget responses, plant cover change, and a new terrain roughness index (TRI) that describes evolving roughness of dunes and plant cover as a more quantitative measure of flow sheltering and dust emissions control potential of the TPs.

The UAS imagery datasets are used to create the following data products:

1. Fourteen (14) visual (RGB) georeferenced aerial orthomosaic images of the FRA and NOF at ~1.5 cm resolution,
2. Twelve (12) MS (multi-spectral: RGB-RE-NIR-Pan) georeferenced orthomosaic images of the FRA and NOF at ~3.0-7.5 cm resolution collected concurrently with the RGB datasets since Oct. 2020,
3. Twelve (12) NDVI orthomosaics used to assess vegetation cover in the FRA and NOF at ~3.0-7.5 cm resolution derived from the MS orthomosaic datasets,
4. Twelve (12) georeferenced, orthorectified maps of vegetation cover derived from RGB and NDVI imagery used to track changes in plant cover within the FRA and NOF,
5. Fourteen (14) three-dimensional point clouds of surface topography within the FRA and NOF at a decimated resolution of 10 cm,
6. Fourteen (14) three-dimensional rasterized digital terrain models (DTMs) of topography within the FRA and NOF at 10 cm pixel resolution,
7. Thirteen (13) topographic change maps derived from statistically significant pixels of erosion and deposition between DTM intervals to assess geomorphic and sediment volume changes.

Data collected from the UAS flights allows for high resolution, three-dimensional DTM surfaces to be constructed and compared using geospatial statistics to quantify sand volume changes and dune development over time. MS orthomosaics and DTM surfaces allow for examination of the growth of vegetation and the development of dune forms within the FRA and NOF.

This report also explains the methods used for data collection and processing, as well as the new analytical methodology, but focuses mainly on interpreting new results from 2025-2026 in the context of longer-term trends through Feb. 2026. This report also focuses on the updated results based on new FRA polygon boundaries and reference site at NOF (Figure 2). As in previous reports,

we also assess the performance of the restoration treatments at ODSVRA, but now using only 3 simpler metrics. The original metrics and performance assessment approach is described in Walker et al. (2023)[1]. These revised indicators characterize the re-establishment of dynamic ecological and geomorphic conditions required to improve dune ecosystem form and function in relation to an established foredune site at NOF that has experienced minimal disturbance to dune development for at least 40 years.




***Figure 1.*** *Map showing the typical extent of the UAS surveys (North to the left). The FRA TPs 1-6 and foredune (FD) zone at NOF are shown with adjoining beach (B), landward dune (LD), and foredune lee (FL, at NOF only). New analytical sub-zones within the FRA are shown in yellow with the original TP boundaries shown in black. The underlying image is from NAIP 2024.*

## 2. Methods

Full details on the methods used for this work are documented in prior reports by Hilgendorf et al. (2023[2], 2024[3]). Since Oct. 2019, a fixed-wing, fully autonomous WingtraOne UAS platform has been flown biannually with surveys bracketing the nesting season of the Western Snowy Plover, typically in Oct. and Feb. UAS imagery was processed using Structure-from-Motion (SfM) photogrammetry in Agisoft Metashape to produce georeferenced orthomosaics and 3D point

[1] Walker, I.J., Hilgendorf, Z., Gillies, J.A., Turner, C.M., Furtak-Cole, E., Nikolich, G. (2023). Assessing performance of a "nature-based" foredune restoration project, Oceano Dunes, California, USA. Earth Surface Processes and Landforms, 48(1), 143-162.

[2] Hilgendorf, Z. Walker, I.J., Swet, N., Heffentrager, M. (2023). UCSB 2022-2023 ODSVRA Foredune Restoration Survey Report. Research report to the Oceano Dunes Scientific Advisory Group (SAG) and the State of California Department of Parks and Recreation. 44 p.

[3] Hilgendorf, Z., Walker, I.J., Heffentrager, M. (2024). 2023-2024 ODSVRA Foredune Restoration UAS Monitoring Report. Technical Report to the Oceano Dunes Scientific Advisory Group (SAG) and the State of California Department of Parks and Recreation (CDPR). 37 p.

clouds to derive DTMs and maps of vegetation cover. These products were then used to monitor and characterize changes in sediment volumes, geomorphic responses, and vegetation cover within and beyond the restoration treatments and NOF (Figure 1). Given the new analytical sub-areas of the TPs and inclusion of the new NOF reference site, all results from prior reports were redone, using the same fundamental methods, but with the new analytical sub-areas and referenced to the NOF site (Figure 2). Locations and extents of the new TP analytical areas and the NOF reference site were designed in consultation with CDPR and SAG to reduce edge effects from fences and structures and to provide a regional reference site for dune development to allow comparative assessment of FRA performance.

This report provides updated sediment budget, vegetation cover, and dune development results from Oct. 2019 to Feb. 2026 . The UAS is typically flown at altitudes over 100 m above ground level and is equipped with on board, survey-grade GPS with PPK correction capabilities. During data collection, a GPS base station is operated in static collection mode and occupation datasets are used to refine UAS photo locations to within millimeters of their real-world locations. Surveys are flown in full compliance with FAA regulations and as reviewed and approved by the University of California Unmanned Aircraft System Safety Program[4]. CDPR wildlife monitors were present to ensure safe conditions for wildlife during the UAS flights as necessary.

To date, 14 UAS survey campaigns have been flown producing 14 RGB datasets since Oct. 2019 and 12 MS datasets since Oct. 2020 (Table 1). Resulting high resolution (<2 cm) orthomosaic imagery was then converted in SfM software to three-dimensional point clouds of the underlying surfaces. Point clouds between campaigns were aligned to one another using static features in the landscape (e.g., structures, roads, etc.). Point clouds were then used to produce gridded (rasterized) DTMs. Raster surfaces were gridded to 0.1 m/pixel and assigned an elevation value by averaging all points within that 0.1 $m^2$ cell. MS surveys were flown separately from the RGB flights.

Successive DTMs were imported into ArcGIS Pro and the Geomorphic Change Detection (GCD) toolset[5] was used to detect locations of statistically significant elevation change and associated volumes between co-located raster grid cells. The method applies a spatial statistical filter to remove changes that fall below a threshold uncertainty value with 95% confidence[6] based on a total uncertainty budget that includes the accuracy of the GPS station, the calculated uncertainty of the point cloud, and the root mean square error from the alignment of each point cloud with static features in the landscape. Significant pixels were used to create elevation change maps and topographic differencing between successive maps was used to estimate volumetric changes and interpret corresponding geomorphic responses. Results were partitioned into the new analytical units to monitor plot-based changes through time (Figure 2).

Two multi-spectral sensors have been used to date: a Micasense RedEdge-MX (Oct. 2020 - Feb.

[4]https://www.ucop.edu/safety-and-loss-prevention/environmental/program-resources/unmanned-aircraft-systems-safety.html

[5] Wheaton, J.M., Brasington, J., Darby, S.E., Sear, D.A. (2009). Accounting for uncertainty in DEMs from repeat topographic surveys: improved sediment budgets. Earth Surface Processes and Landforms, 35(2), 136-156.

[6] Hilgendorf, Z., Marvin, M.C., Turner, C.M., Walker, I.J. (2021). Assessing Geomorphic Change in Restored Coastal Dune Ecosystems Using a Multi-Platform Aerial Approach. Remote Sensing, 13(3), 354.

2022) and a Micasense RedEdge-P (Oct. 2022 to present). The RedEdge-MX is a 5-band sensor that captures visual (RGB), red-edge (RE), and near-infrared (NIR) bands. This sensor was replaced with the RedEdge-P, which contains the same five bands and an additional panchromatic (Pan) band that is used to improve the resolution of the dataset from ~7 to ~3.5 cm/pix. From these bands, NDVI-derived vegetation maps were produced.

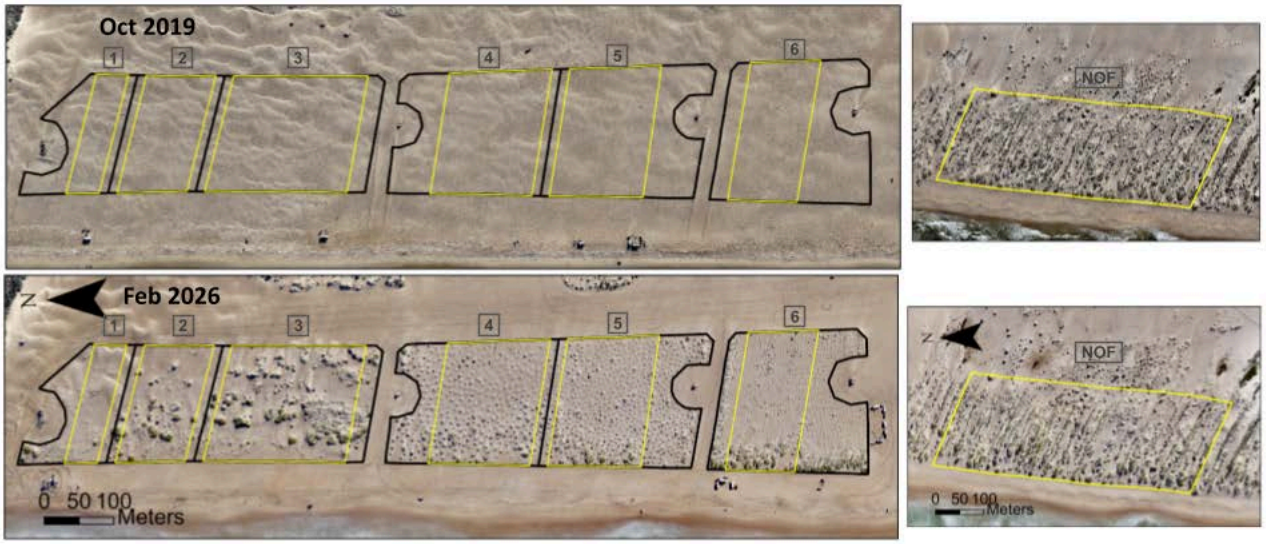



***Figure 2.*** *Visible (RGB) orthophoto mosaics of the FRA and NOF reference site from the initial baseline survey (Oct. 2019) during installation of restoration treatments in Feb. 2020, and the latest Feb. 2026 UAS survey. Numbers represent the different TP plots. Notable dune development and plant community re-establishment is observed in all plots, except within the TP1 control plot.*

***Table 1.*** *Specifications for the UAS monitoring campaigns. Multi-spectral sensors were only used after installation of the vegetation treatments in Feb. 2020. GSD (ground sample distance) is the distance between the center of adjacent pixels and describes the cell size (pixel resolution). Total uncertainty values are the calculated vertical uncertainty for datasets used in DTM development and for detecting and quantifying significant volumetric changes. No uncertainty value is shown for MS datasets that were not used for volumetric analyses.*

| UAS Survey Campaign | Survey Date | Sensor Payload | Average Altitude (m) | GSD (cm/pix) | Total Uncertainty (m) |
|---|---|---|---|---|---|
| 1. Baseline pre-restoration survey | 1-2 Oct. 2019 | Sony RX1RII | 114 | 1.45 | 0.038 |
| 2. Initial treatment installations | 10-11 Feb. 2020 | Sony RX1RII | 123 | 1.56 | 0.033 |
| 3. First post-treatment survey and growing season | 13-15 Oct. 2020 | Sony RX1RII | 121 | 1.54 | 0.037 |
| | 16 Oct. 2020 | Micasense RedEdge-MX | 113 | 7.53 | — |
| 4. End of first year of development | 17-18 Feb. 2021 | Sony RX1RII | 120 | 1.52 | 0.030 |
| | 18-21 Feb. 2021 | Micasense RedEdge-MX | 118 | 7.89 | — |
| 5. Second growing season | 4-5 Oct. 2021 | Sony RX1RII | 121 | 1.54 | 0.025 |
| | 5-7 Oct. 2021 | Micasense RedEdge-MX | 119 | 7.82 | — |
| 6. End of second year of development | 23-25 Feb. 2022 | Sony RX1RII | 112 | 1.42 | 0.043 |
| | 25-26 Feb. 2022 | Micasense RedEdge-MX | 116 | 7.71 | — |
| 7. Third growing season | 17-18 Oct. 2022 | Sony RX1RII | 125 | 1.66 | 0.026 |
| | 19-21 Oct. 2022 | Micasense RedEdge-P | 111 | 3.67 | — |
| 8. End of third year of development | 23 Feb. 2023 | Sony RX1RII | 121 | 1.59 | 0.034 |
| | 20-21 Feb. 2023 | Micasense RedEdge-P | 120 | 3.97 | 0.105 |
| 9. Fourth growing season | 9 Oct. 2023 | Sony RGB61 | 108 | 1.65 | 0.049 |
| | 10-13 Oct. 2023 | Micasense RedEdge-P | 135 | 4.42 | — |
| 10. End of fourth year of development | 23 Feb. 2024 | Sony RGB61 | 116 | 1.78 | 0.071 |
| | 21-23 Feb. 2024 | Micasense RedEdge-P | 133 | 4.38 | 0.071 |
| 11. Fifth growing season | 29-30 Oct. 2024 | Sony RGB61 | 107 | 1.65 | 0.047 |
| | 14-18 Oct. 2024 | Micasense RedEdge-P | 121 | 3.96 | — |
| 12. End of fifth year of development | 20-21 Feb. 2025 | Sony RGB61 | 125 | 1.89 | 0.030 |
| | 18-19 Feb. 2025 | Micasense RedEdge-P | 123 | 4.05 | — |
| 13. Sixth growing season | 14-15 Oct. 2025 | Sony RGB61 | 109 | 1.68 | 0.055 |
| | 13-15 Oct. 2025 | Micasense RedEdge-P | 123 | 4.06 | — |
| 14. End of sixth year of development | 12-13 Feb. 2026 | Sony RGB61 | 106 | 1.64 | 0.056 |
| | 9-12 Feb. 2026 | Micasense RedEdge-P | 121 | 4.00 | — |

In addition to the usual sediment budget and vegetation cover change results, we also quantified the evolving surface roughness of the treatment plots and at the NOF site as a proxy for their dust control potential using a new Terrain Roughness Index (TRI). TRI characterizes the topographic

complexity and aerodynamic roughness of a surface based on the spatial variability in elevation derived from DTMs. This fairly simple and effective quantitative metric has been used in other aeolian studies[7,8]. Here, we use the method developed by Riley et al. (1999)[9], which computes TRI using the RMS difference between cell elevation and the elevation of neighbouring cells in an array. This is calculated in ArcGIS using the equation below:

$$TRI = \sqrt{\sum_{\substack{i=1 \\ j=1}}^{n} (x_{22} - x_{ij})^2}$$

equation 1

where $x_{22}$ represents a central cell within a spatial array of pixels (e.g., for the 8 surrounding pixels, or 3x3 array, n=3). The pixel size of the DTM is 10 cm, which makes the roughness estimation of sufficiently fine scale (i.e., 3x3 pixels or 30 x 30 cm) to detect and quantify decimeter-scale roughness of the smallest observed nebkha. At this size of spatial array, the TRI value provides the cumulative elevation difference between a DTM cell and its surrounding neighbors, in meters. Riley et al. (1999) provide a wide range of TRI values that approach 1000 for extremely rugged (mountainous) terrain using a much coarser DEM (1-km pixel size). So, their categorical ranges (e.g., 0-80 for level terrain) do not apply for this study, as the neighborhood used to compute the TRI value is much smaller (30 x 30 cm instead of 3 x 3 km). Regardless, the method is valid at finer spatial scales. Mean roughness for each treatment plot in this study is then computed. These mean values are then compared to the mean roughness at NOF as a ratio, which indicates the state of roughness of each of the TPs as compared to that of the fully-developed dunes at the reference site.

# 3. Results

### 3.1 Visible (RGB) imagery and orthophoto mosaics

Figure 1 shows the typical extent of the UAS visual (RGB) orthophoto campaigns. Figure 2 shows the FRA and NOF sites wherein the analyses are conducted. Appendix A shows all biannual UAS RGB orthophoto mosaics of the FRA and NOF back to Oct. 2019. These images were used to interpret geomorphic responses within the TP, such as aeolian sand transport corridors (ripples), deflation surfaces (coarse lag deposits), and general dune development.

[7]Nield, J.M., Wiggs, G.F.S., Squirrell, R.S. (2011). Aeolian sand strip mobility and protodune development on a drying beach: examining surface moisture and surface roughness patterns measured by terrestrial laser scanning. Earth Surface Processes and Landforms, 36(4), 513-522.

[8] Sankey, J.B., Eitel, J.U., Glenn, N.F., Germino, M.J., Vierling, L.A. (2011). Quantifying relationships of burning, roughness, and potential dust emission with laser altimetry of soil surfaces at submeter scales. Geomorphology, 135(1-2), 181-190.

[9] Riley, S., DeGloria, S.D., Elliot, R. (1999). A terrain ruggedness index that quantifies topographic heterogeneity. Intermountain Journal of Sciences, 5(1-4), 23-27.

### 3.2 UAS multispectral imagery and measurement of changes in vegetation cover

To detect and quantify vegetation cover at the landscape scale in the FRA treatment areas, MS imagery has been collected since Oct. 2020 (Figure 3). The initial survey focused primarily on the seaward extent of the ODSVRA, including the FRA, seasonal plover exclosure, and NOF. The Feb. 2021 survey covered a larger extent to match that of the RGB surveys and this coincident survey strategy has been followed since (Figures 1 and 3), with minor variations due to logistical and weather constraints. MS sensors were calibrated pre- and post-flight with a calibration panel so that, while some imagery in Figure 3 may appear to have variable contrast, individual pixels are properly scaled and the extracted indices are accurate.

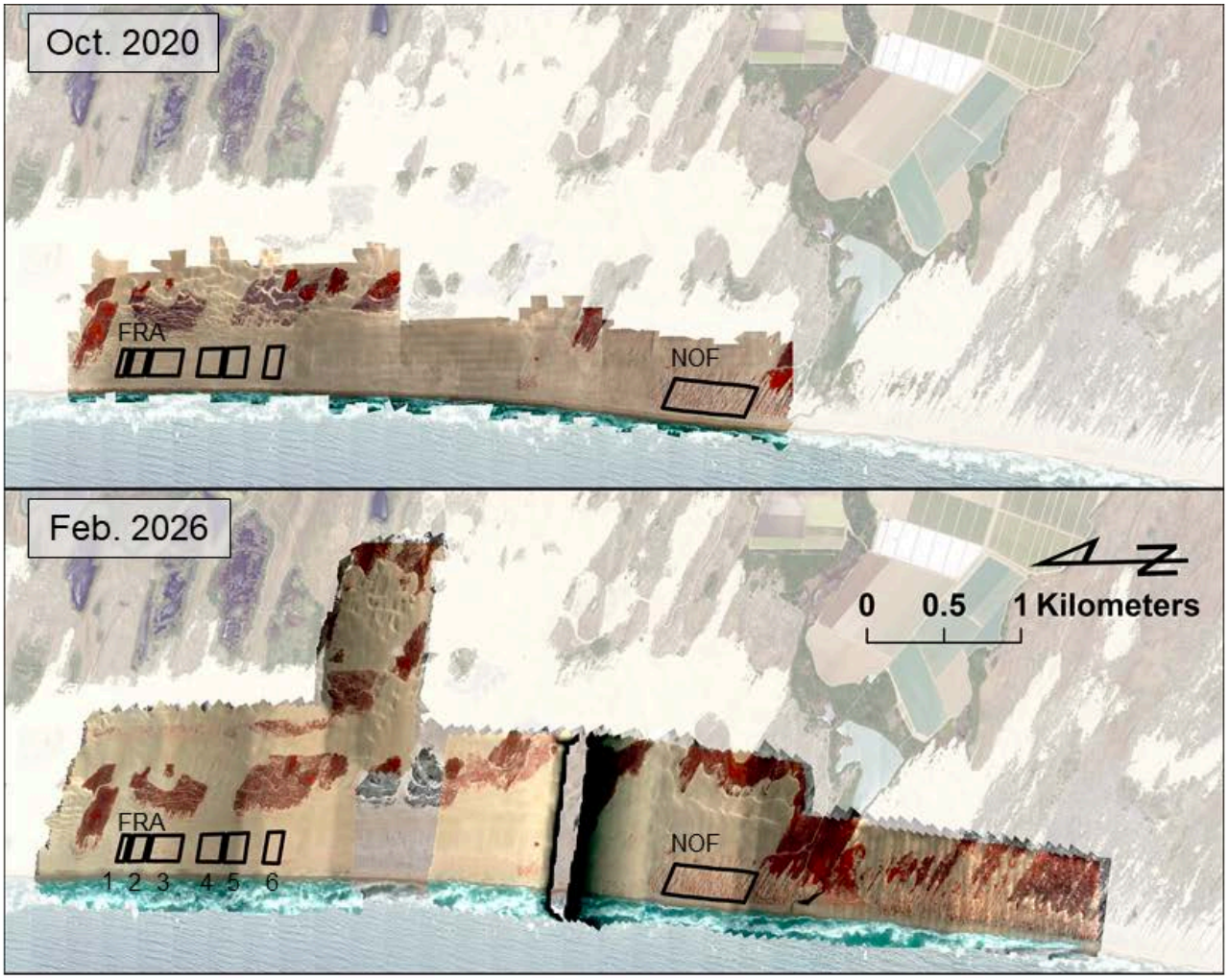



***Figure 3.*** *MS false-color (G, B, NIR) UAS orthomosaics captured from a Micasense RedEdge-MX 5-band sensor (R, G, B, RE, NIR) in Oct. 2020 and a Micasense RedEdge-P 6-band sensor (RGB, Pan, RE, NIR) in Feb. 2026, used to map vegetation cover. Contrast differences are only visual. An environmental anomaly during the Feb. 2026 MS flight resulted in gaps in the dataset south of the FRA. However, the FRA and NOF areas were not impacted. Locations of the revised FRA TP*

*analytical areas and the NOF reference site are outlined.*

NDVI values were calculated for all MS surveys to detect and map vegetation and its changes through time. Percent plant cover (normalized by total area of each treatment plot) has generally increased through time in all TPs with some variability (Figure 4, Table 2). The NOF reference site maintained a slightly positive trend from Oct. 2020 to Feb. 2026 but generally remains more stable over time given its fully developed state compared to the variability observed in the TPs. By Feb. 2026, TP1-4 and TP6 reached their highest plant cover since the implementation of the FRA. TP5 still shows increasing vegetation cover in Oct. 2025 and Feb. 2026, but the highest value was observed in Oct. 2022. Overall, TP6 had the greatest plant cover change (from 2.2% in Oct. 2020 to 16.9% by Feb. 2026), followed by TP3 (2.3 to 12.5%), TP2 (0.4 to 9.0%), TP5 (1.5 to 9.5%), TP4 (0.8 to 8.2%) and TP1 (0.0 to 3.2%). From Oct. 2020 to Feb. 2026, NOF saw 23.0% to 26.1% cover, respectively, with a total change of 3.1%. The range in observed plant cover change at NOF (10.5%) indicates that significant interannual variations in vegetation are not uncommon within foredune ecosystems in the region (Table 2, Figure 4).

Figure 4 shows general increasing trends in plant cover with notable seasonal variability between spring and fall cover that bracket the plant growth season. Most treatments and the NOF reference site showed a notable decline in cover in recent monitoring intervals (Oct. 2023 - Feb. 2025), while TP1 and TP2 saw subtle increases over this time. Since Oct. 2025 or Feb. 2026, depending on the treatment site, all sites have shown increasing plant cover (Table 2, Figure 4).

For historical context, plant cover observed in aerial imagery back to 1939 within the ODSVRA averaged about 25% in 1939 with a peak at 37% in 2012 followed by a slight decline to 35% by 2020 prior to implementation of the FRA[10]. Recent imagery shows extensive backdune shrub and forest ecosystems, and other new restoration sites. Within the foredune zone of the OHV riding area, in particular, plant cover was low (2.6 %) in 1939, rose to a peak of 5.3% in 1966[10], then declined steadily to ~1% from 1985 to 1998. These lower values reflect the influence of decades of vehicular recreation and camping activities in the dunes. Within the FRA specifically, plant cover declined to a negligible amount by 1985 until after installation of the treatments in 2020. In contrast, at the nearby South Oso Flaco (SOF) site, plant cover was 26% in 1939, decreased to a low of 24% in 1949, increased to a peak of 66% in 2012, and remained >60% by 2020. At the NOF reference site, plant cover was <1% in the 1930s, but increased notably after 1985 to over 24% by 2012. Plant cover estimates at SOF and NOF partly reflect the influence of invasive species (SOF) and more recent restoration efforts in these areas. Following restoration in the FRA, plant cover has increased to an average of 9.8% across all treatments by Feb. 2026 (Table 2), which exceeds the historic maximum cover in all TPs, except the TP1 control plot (no treatment), which remains at 3.2% as of Feb. 2026.

[10] Swet, N, Hilgendorf, Z, Walker, IJ (2022). UCSB Historical Vegetation Cover Change Analysis (1930-2020) within the Oceano Dunes SVRA. Technical report to the Oceano Dunes Scientific Advisory Group (SAG) and the State of California Parks and Recreation Department Off-Highway Vehicle Division. Feb. 2022.

***Table 2.*** *Vegetation cover (%) in each treatment plot and in NOF as shown in Figure 4. *Note: a multi-spectral sensor was not available for the Feb. 2020 campaign. MS-derived NDVI calculations began in Oct. 2020.*

| Survey Date | TP1 | TP2 | TP3 | TP4 | TP5 | TP6 | NOF |
|---|---|---|---|---|---|---|---|
| 10-11 Feb. 2020* | n/a | n/a | n/a | n/a | n/a | n/a | n/a |
| 16 Oct. 2020 | 0.01 | 0.38 | 2.25 | 0.76 | 1.46 | 2.19 | 22.96 |
| 18-21 Feb. 2021 | 0.02 | 0.64 | 3.11 | 1.30 | 2.36 | 4.56 | 18.83 |
| 5-7 Oct. 2021 | 0.06 | 1.64 | 3.95 | 1.74 | 3.03 | 2.49 | 18.76 |
| 25-26 Feb. 2022 | 0.02 | 1.74 | 4.23 | 2.19 | 3.94 | 9.26 | 16.99 |
| 19-21 Oct. 2022 | 0.12 | 3.55 | 10.32 | 5.94 | 9.55 | 12.73 | 24.58 |
| 20-21 Feb. 2023 | 0.06 | 2.71 | 8.18 | 5.71 | 9.28 | 12.40 | 24.21 |
| 10-13 Oct. 2023 | 0.42 | 3.65 | 10.09 | 7.32 | 9.08 | 16.61 | 27.50 |
| 21-23 Feb. 2024 | 0.32 | 3.00 | 6.37 | 4.57 | 5.54 | 8.93 | 22.61 |
| 14-18 Oct. 2024 | 0.32 | 4.57 | 8.06 | 4.34 | 5.84 | 11.13 | 22.44 |
| 18-19 Feb. 2025 | 0.91 | 3.51 | 4.38 | 2.93 | 2.82 | 5.90 | 19.56 |
| 13-15 Oct. 2025 | 1.21 | 5.55 | 9.55 | 7.81 | 8.80 | 10.34 | 18.17 |
| 9-12 Feb. 2026 | 3.18 | 9.00 | 12.52 | 8.19 | 9.46 | 16.90 | 26.05 |

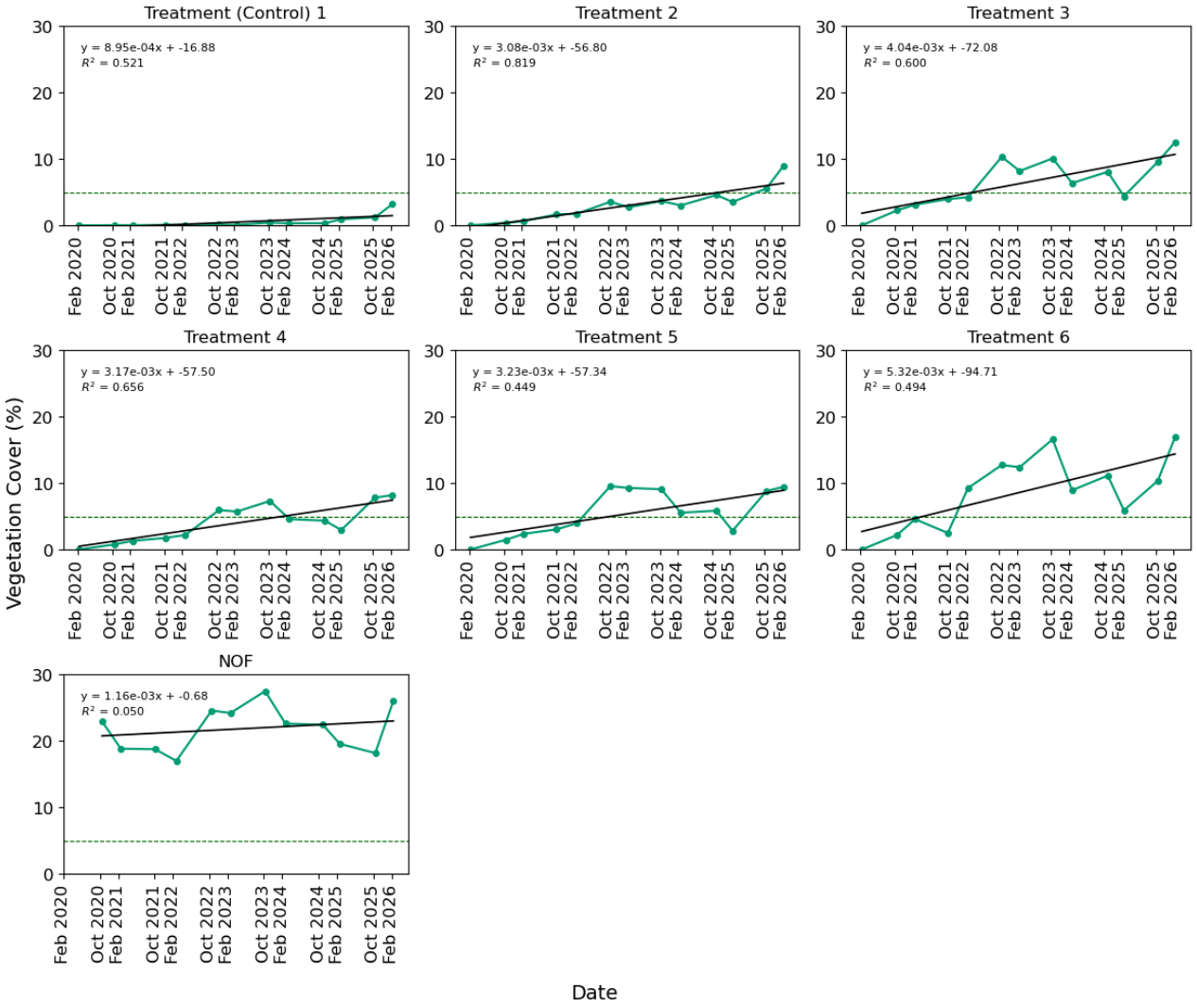



***Figure 4.*** *Time series of percent vegetation cover by treatment plot derived from the UAS surveys from Feb. 2020 for the FRA treatment plots and Oct. 2020 for the NOF reference site. Dashed line is the peak historic vegetation cover in 1966 (5.3%) within the foredune zone of the broader OHV riding area (Swet et al. 2022). Corresponding values are shown in Table 2.*

### 3.3 Topographic Differencing and Volumetric Change Trends

The topographic difference maps (Figures 5-7) show areas of significant elevation change that are used to calculate volumes of sediment erosion or deposition between surveys in cubic meters ($m^3$), that are normalized by area and over time ($m^3$ $m^{-2}$ $month^{-1}$), which effectively provides an average depth of change (m) over the entire surface averaged over the observation periods (see Table 3). Locations of statistically insignificant change are not shown in the change maps and are not used to calculate sediment volumes. The raster grid from which volume estimates are determined remains fixed in position and size (0.10 m x 0.10 m) across all surveys. Pixels of statistically insignificant change, as determined by a two-tailed t-test at a 95% confidence interval in the GCD package (Section 2), are not used to calculate sediment volumes.

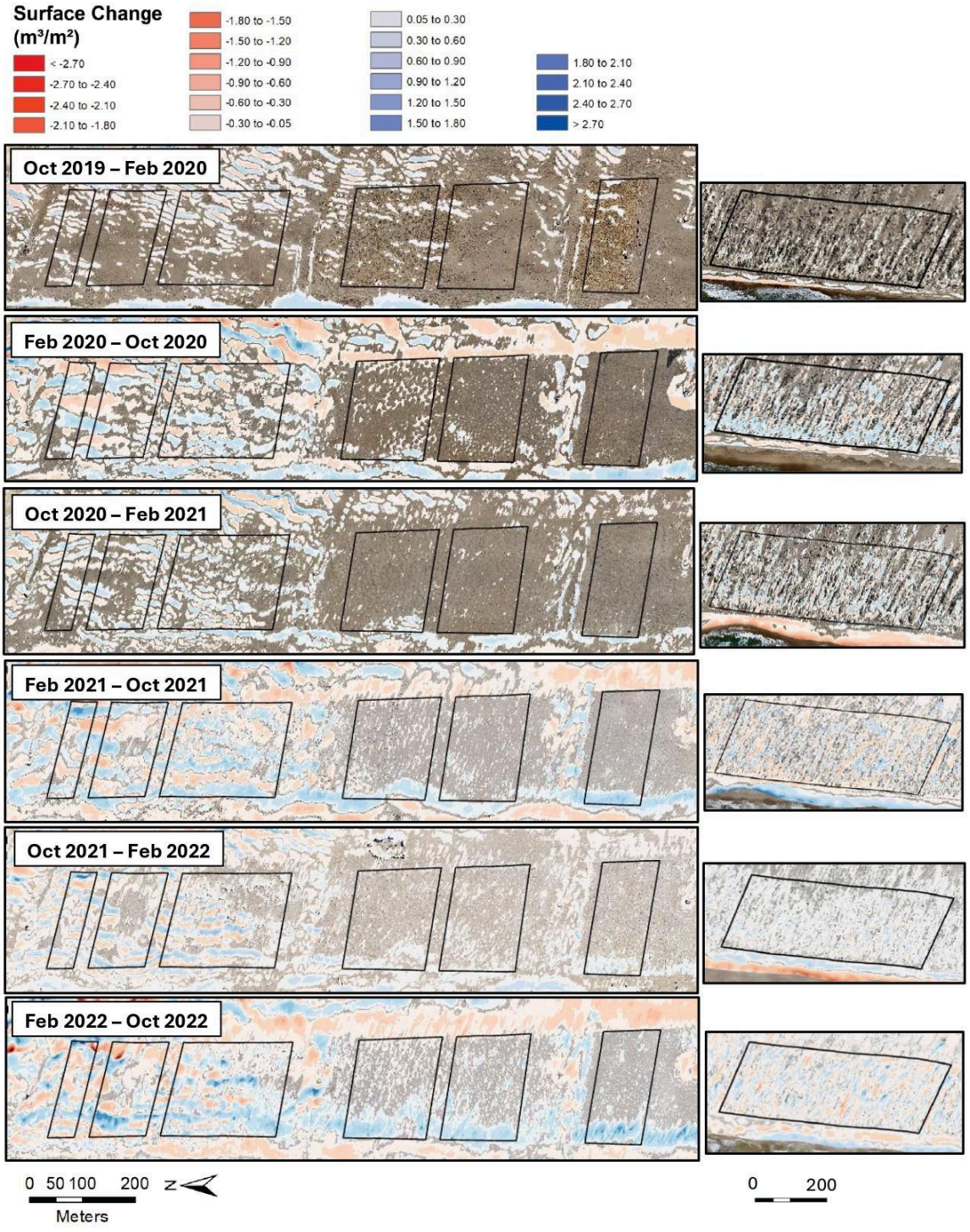



***Figure 5.*** *Topographic change maps showing pixels of significant area-normalized volumetric changes (reds = erosion, blues = deposition) for survey intervals from Oct. 2019 to Oct. 2022 overlain on the UAS photomosaics for the second time step in each interval. New analytical areas for each restoration treatment plot are outlined in black (from left, TP1 to TP6, then NOF on right panel; note different scale). Intervening spaces are not included in the analysis.*

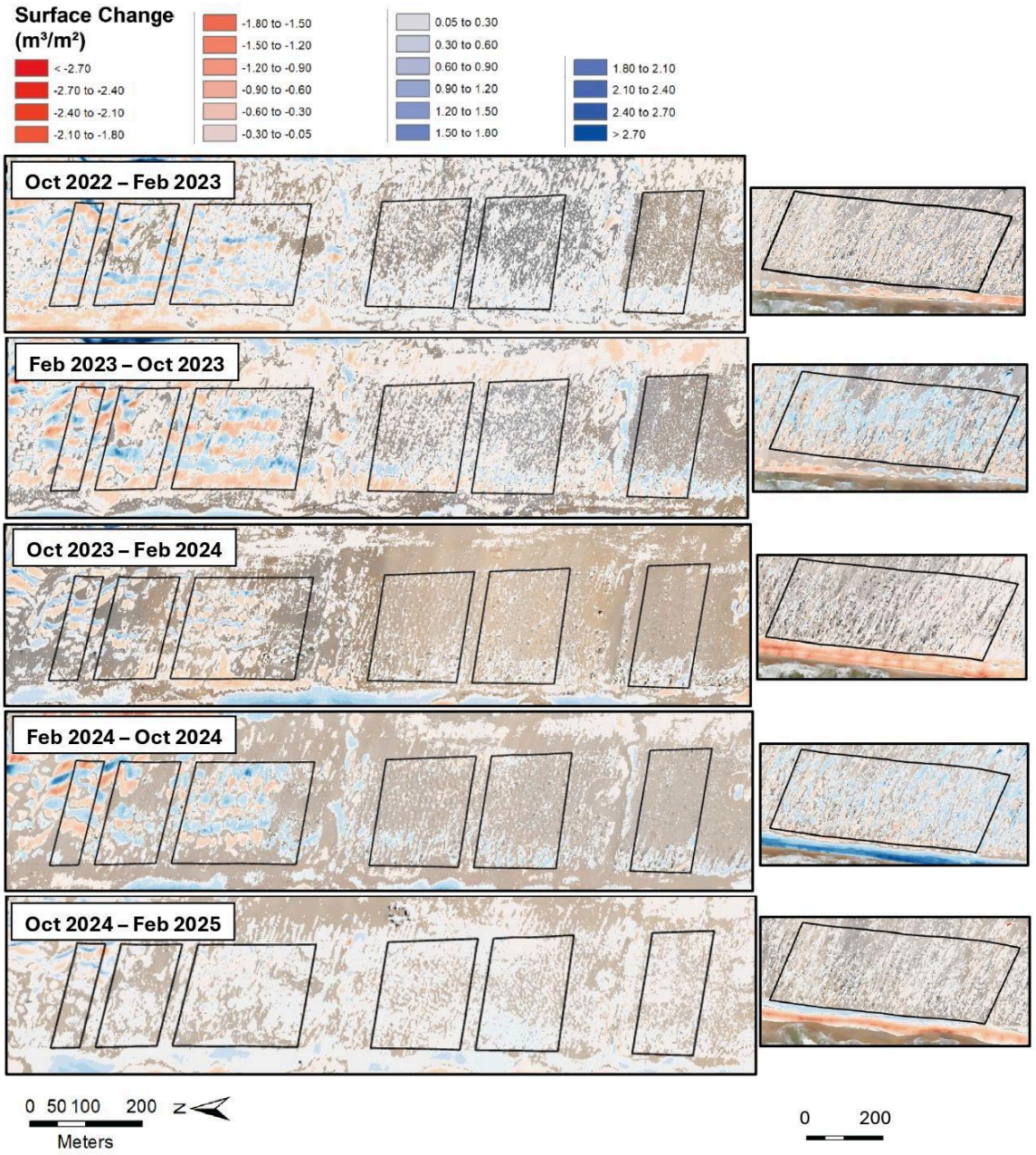



***Figure 6.*** *Topographic change maps showing pixels of significant area-normalized volumetric changes (reds = erosion, blues = deposition) for survey intervals from Oct. 2022 to Feb. 2025 overlain on the UAS photomosaics for the second time step in each interval. New analytical areas for each restoration treatment plot are outlined in black (from left, TP1 to TP6, then NOF on right panel; note different scale). Intervening spaces are not included in the analysis.*

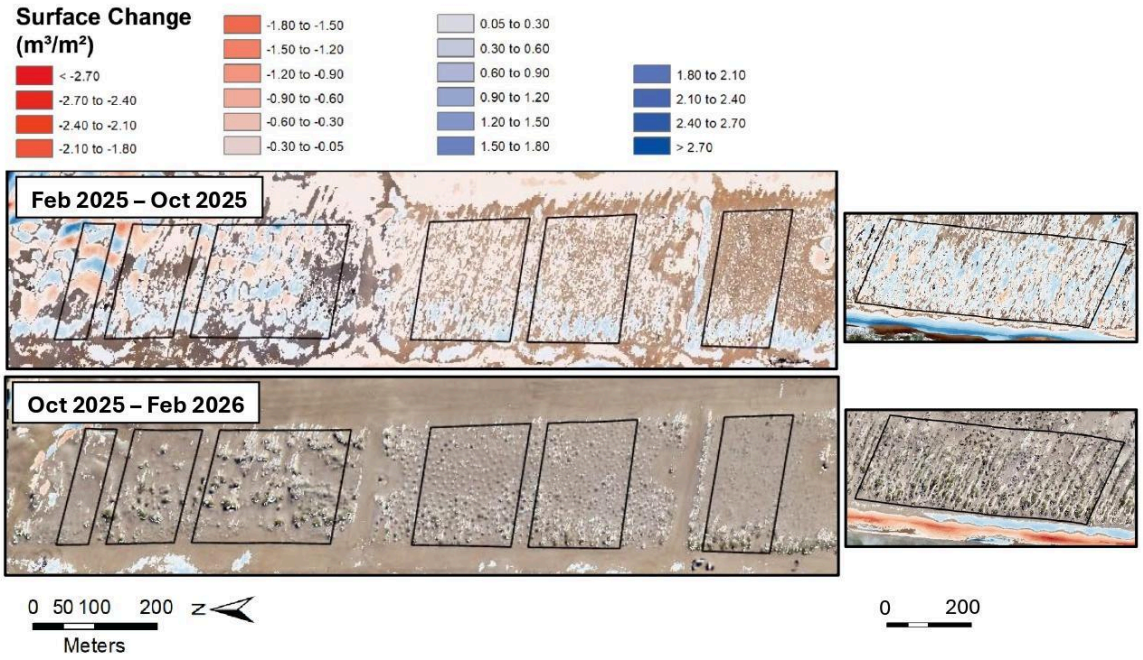



***Figure 7.*** *Topographic change maps showing pixels of significant area-normalized volumetric changes (reds = erosion, blues = deposition) for survey intervals from Feb. 2025 to Feb. 2026 overlain on the UAS photomosaics for the second time step in each interval. New analytical areas for each restoration treatment plot are outlined in black (from left, TP1 to TP6, then NOF on right panel; note different scale). Intervening spaces are not included in the analysis.*

Figure 8 shows a time series of normalized volumetric changes within the treatment plots and their adjoined geomorphic units from Oct. 2019 and Feb. 2026 (values provided in Table 3). The first interval (Oct. 2019 to Feb. 2020) provides baseline reference conditions prior to implementation of the restoration treatments. Geomorphic units include each of the foredune treatment areas (FD), an adjoining beach area (B), and landward backdune areas (LD) (Figure 1). Within the NOF reference site, an additional foredune lee zone (FL) was identified that is a non-riding area with limited dune development that backs the established foredune and connects to the backdune riding area. For simplicity, and because the FRA TP units lack a comparable zone, volumetric change data for this FL zone are not included in the analysis.

A key control on the volumetric and geomorphic responses in the foredune zone is the amount of sand that enters the upwind beach from the nearshore, which provides supply for aeolian delivery to the treatment plots. Beach units fronting the plots saw variable trends of positive (depositional) and negative (erosional) change in sediment volumes that relate to seasonal variations (e.g., winter storm erosion signals) and migration of rip current embayments.

Generally, the beach units show a highly variable trend in sand volumes from positive values in the initial Oct. 2019 to Feb. 2020 baseline interval to distinctly negative values by Feb. 2023. More recently, the beach units fronting the FRA have mostly shown positive trends since 2024 (Table 3), except for slight erosion at TP3 to TP6 in 2025. The northern 2 plots (TP1-2) experienced more

pronounced erosive intervals compared to the southern 4 plots (TP3-6), suggesting a slight trend toward erosion in the northern beach units, transitioning to a slightly more depositional state in the southern units. Further south at the NOF site, the beach unit shows significantly greater volumes of erosion and deposition with a cumulative change (erosional) of -304.16 x $10^{-3}$ $m^3$ $m^{-2}$ $mo^{-1}$, which is roughly triple the magnitude of the highest net (i.e., cumulative) sediment change at TP4 (Table 3). This high variation in the sediment budget of the beach at NOF is partly due to the persistence of large rip cell embayments and a generally narrower beach at this location.

Within the foredune zone, all FRA plots experienced net positive gains in sediment volumes since installation and, with some exceptions, most intervals showed positive sediment budgets (Figure 7, Table 3). Distinct negative (erosional) volumetric responses occurred in all TPs from Feb. to Oct. 2023, but shifted back to depositional conditions following Oct. 2023, except for TP2 and TP3. TP2 and TP4 also showed small negative sediment losses from Feb. to Oct, 2020 and from Feb 2025 to Oct. 2025. The TP1 control site and TP2 continue to show the lowest rates of accumulation, reflecting significant beach erosion and sediment bypassing due to lower plant cover and limited nebkha dune development. TP4 and TP5 experienced the fourth and third highest accumulation, respectively, with relatively low accumulation rates since Feb. 2024. TP6 is the only plot that has not yet experienced an erosive interval and now has the second highest net deposition. In the previous report, T6 had the highest accumulation, but this was biased by deposits along a sand fence on the northern side of the plot, which has since been removed from analysis. As a result, TP3 is now the treatment with the greatest net sand accumulation. Since Feb. 2024, all treatment plots have shown neutral to slightly positive trends in normalized sediment volumes.

The FRA TPs vary notably in their sediment budget responses due to differences in vegetation establishment and/or treatment method. TP1 and TP2 were least altered by treatment interventions and have maintained similar change patterns across all intervals until Oct. 2025, when TP2 began to develop more nebkha. Sand transport within these plots generated low-lying (0.4 to 0.6 m), slowly migrating semi-continuous transverse and barchanoid dune ridges and protodunes from the establishment of the FRA until Feb. 2025. Limited plant cover established in TP1 except for a few plants near the seaward edge of the plot, first observed in Oct. 2022. Some shadow dunes were present in the landward half of these plots, but these were not associated with vegetation (i.e., nebkha), rather with nodes of cemented sand and anthropogenic debris[11]. Following the winter storm season of 2023-2024, vegetation wrack and propagules that washed into the plot led to an increase in plant cover by Oct. 2024. TP2 exhibited a developing nebkha cluster in the center of the plot, which had not expanded notably until Oct. 2025, when shadow dunes in the wake of the nebkha were observed (Figure 7) and with recent increases in plant cover (from 3.51% in Feb. 2025 to 9.00% in Feb. 2026, Table 2). Overall, TP1 and TP2 have shown the smallest net changes in sand volume over the monitoring period (Table 3).

TP3 has developed extensive nebkha, predominantly with *Abronia latifolia*, and these dunes have coalesced to form appreciable discontinuous ridges >2 m high, which are the tallest dunes in

[11] Hilgendorf, Z. Walker, I.J., Swet, N., and Heffentrager, M. (2023). UCSB 2022-2023 ODSVRA Foredune Restoration Survey Report. Research report to the Oceano Dunes Scientific Advisory Group (SAG) and the State of California Department of Parks and Recreation. 44 p.

the FRA. The latest two intervals showed positive to neutral volumetric changes within TP3 at rates slower than in prior intervals (Table 3). TP3 has had among the highest and most consistent positive sediment budget responses of the sites, and the largest overall net depositional change (Table 3).

TP4 and TP5 experienced localized erosion between planting nodes during early intervals. Although some of these 'erosional streets' formed between the straw planting nodes persist, nebkha are growing and slowly coalescing in both plots. TP4 and TP5 experienced the fourth and third highest net deposition amounts, respectively, to date (Table 3). Nebkha dunes in TP5 are larger than in TP4 and closer in height to the larger dunes in TP3, with some dunes now >1.5 m tall. In the most recent surveys, however, dunes in TP4 had grown notably, particularly along the seaward half of the plot. Nebkha coalescence was observed in both treatments along the seaward half of the plot by Oct. 2023.

TP6 had the most intensive treatment with the highest planting density and complete surface straw cover on installation. TP6 maintains the highest plant coverage (Figure 4, Table 2), large depositional volumes, and the second highest cumulative positive sediment budget to date, following TP3 (Table 3). However, the development of taller nebkha is largely constrained to the seaward portion of the plot, compared to plots TP2-5 which exhibit nebkha development to a greater inland extent. Nebkha within TP6 downwind of the sand fencing or inland from the seaward edge, have yet to exhibit significant development despite recent increases in vegetation cover in Oct. 2025 and Feb. 2026 (Table 2, Figure 4).

In contrast to the largely positive sediment volumes observed in most intervals in the FRA, the foredune at the NOF reference site has shown intermittent periods of erosion and deposition (Figure 8, Table 3). Periods of erosion tend to occur in winter while depositional intervals often occur in summer. In terms of cumulative sediment budgets, TP3, 6, and 5, in decreasing order, have had larger net amounts than the NOF site by factors of 2.02, 1.64, and 1.26, respectively (Table 3). Normalized net sediment volume values >1 suggest that these treatments are accumulating at faster rates than the NOF reference site, which is expected for developing dunes. Values < 1 suggest that these sites (TP1, TP2, TP4) are under performing in sediment accumulation rates. Generally, NOF has a much larger magnitude of change in the beach unit compared to the beach unit at the FRA, with a cumulative (erosional) change of $-304.16 \times 10^{-3}$ $m^3$ $m^{-2}$ $mo^{-1}$, which is more than triple the net sediment change of the FRA beach unit. As mentioned above, this is potentially due to the presence of large rip-cell embayments and the typically narrower beach width at NOF.

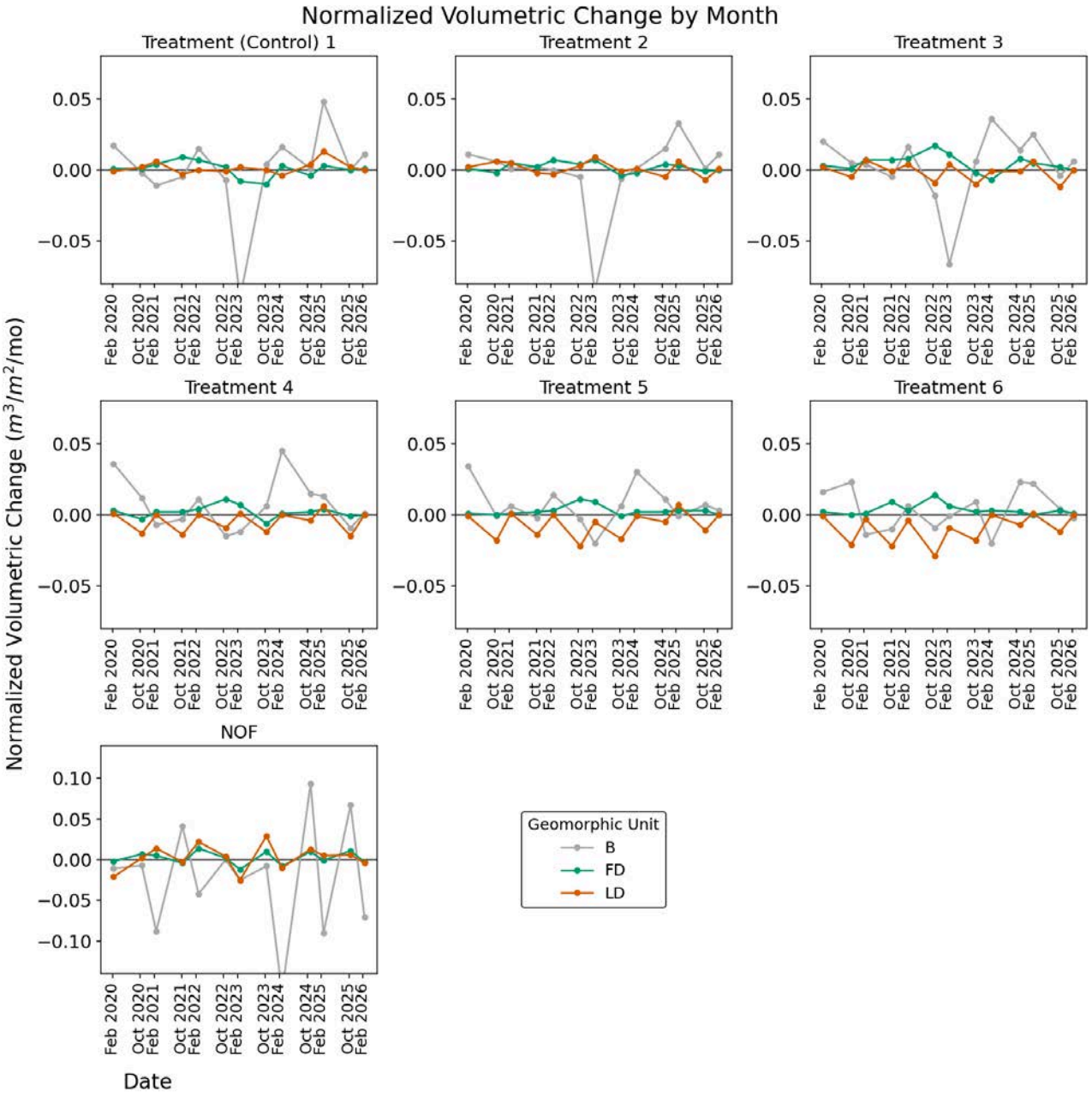



***Figure 8.*** *Time series of area-normalized volumetric changes derived from successive survey intervals for each foredune restoration treatment plot (FD), adjacent beach (B), and landward dune (LD) units. Each point represents results of volumetric change for the preceding interval (e.g., first point represents change between Oct. 2019 and Feb. 2020, etc.).*

***Table 3.*** *Normalized surface volumetric changes for the beach (B), foredune treatment plots (FD) in bold, and landward dune (LD) zones for all the TP and NOF, using the new polygons. Note that values are scaled by a factor of 1000 for presentation. Blue text indicates sand accumulation, red text indicates erosion. The last column indicates the TP foredune area-normalized cumulative (i.e., net) volumetric change and the green value is the one closer to NOF (i.e., closer to one). Uncertainty values are provided in Table 1.*

| Area-normalized volumetric changes (m3 m-2 mo-1) x 1000 | | | | | | | | | | | | | | | | |
|---|---|---|---|---|---|---|---|---|---|---|---|---|---|---|---|---|
| | Landscape Unit | Oct 2019 to Feb 2020 | Feb 2020 to Oct 2020 | Oct 2020 to Feb 2021 | Feb 2021 to Oct 2021 | Oct 2021 to Feb 2022 | Feb 2022 to Oct 2022 | Oct 2022 to Feb 2023 | Feb 2023 to Oct 2023 | Oct 2023 to Feb 2024 | Feb 2024 to Oct 2024 | Oct 2024 to Feb 2025 | Feb 2025 to Oct 2025 | Oct 2025 to Feb 2026 | Cumulative Change | Net change/Net change (NOF) |
| TP 1 | B | 17.24 | -1.60 | -10.89 | -4.92 | 15.01 | -6.51 | -89.71 | 3.67 | 16.23 | 0.94 | 47.87 | -0.22 | 10.68 | *-1.40* | |
| | **FD** | **1.23** | **1.19** | **4.18** | **8.61** | **7.15** | **1.61** | **-7.56** | **-9.54** | **3.35** | **-3.85** | **3.18** | **-0.32** | **0.74** | ***9.97*** | **0.35** |
| | LD | -1.02 | 2.41 | 5.77 | -3.37 | 0.44 | -1.35 | 1.68 | -0.30 | -3.56 | 3.50 | 12.60 | 1.75 | -0.20 | *1.80* | |
| TP 2 | B | 11.37 | 6.42 | 1.16 | 2.19 | -0.17 | -5.08 | -85.05 | -6.07 | 0.63 | 15.27 | 33.12 | 1.14 | 10.92 | *-2.70* | |
| | **FD** | **1.08** | **-2.02** | **5.22** | **1.70** | **7.31** | **3.99** | **6.76** | **-3.60** | **-2.23** | **4.23** | **2.70** | **-1.38** | **-0.03** | ***23.73*** | **0.82** |
| | LD | 1.85 | 6.14 | 4.83 | -2.20 | -2.65 | 3.26 | 9.13 | -0.56 | 0.69 | -5.13 | 5.89 | -6.75 | 0.76 | *2.10* | |
| TP 3 | B | 20.19 | 5.25 | 4.04 | -4.85 | 16.09 | -17.68 | -65.80 | 5.85 | 35.82 | 14.38 | 25.50 | -3.71 | 5.60 | *3.70* | |
| | **FD** | **2.98** | **1.18** | **6.53** | **7.24** | **7.86** | **17.07** | **10.50** | **-2.45** | **-7.37** | **7.86** | **4.95** | **1.69** | **0.35** | ***58.39*** | **2.02** |
| | LD | 2.33 | -4.84 | 7.01 | -1.31 | 3.69 | -8.87 | 4.23 | -10.13 | -1.27 | -1.38 | 5.85 | -11.98 | 0.25 | *-0.40* | |
| TP 4 | B | 35.54 | 11.78 | -6.95 | -3.30 | 11.31 | -15.19 | -12.09 | 5.86 | 45.09 | 15.16 | 13.27 | -8.57 | 1.49 | *10.10* | |
| | **FD** | **3.47** | **-2.86** | **2.28** | **2.31** | **3.83** | **10.54** | **7.36** | **-5.98** | **0.65** | **1.80** | **3.83** | **-0.59** | **0.32** | ***26.96*** | 0.93 |
| | LD | 0.90 | -12.80 | -0.40 | -13.66 | 0.07 | -8.90 | 1.01 | -11.82 | -0.24 | -3.65 | 6.19 | -15.03 | 0.20 | *-4.40* | |
| TP 5 | B | 34.01 | -0.93 | 6.28 | -2.32 | 14.16 | -2.64 | -19.58 | 5.91 | 29.60 | 10.59 | -1.23 | 6.73 | 2.58 | *7.40* | |
| | **FD** | **1.30** | **0.26** | **0.98** | **1.61** | **3.18** | **11.01** | **8.65** | **-1.45** | **2.32** | **2.41** | **2.90** | **2.75** | **0.34** | ***36.26*** | **1.26** |
| | LD | -1.12 | -18.12 | 1.26 | -13.89 | 0.01 | -21.58 | -5.19 | -16.76 | -0.53 | -5.31 | 6.94 | -11.33 | 0.18 | *-7.50* | |
| TP 6 | B | 15.54 | 23.18 | -13.86 | -9.52 | 6.39 | -8.96 | -0.52 | 8.98 | -20.00 | 22.66 | 21.84 | 4.43 | -2.27 | *4.50* | |
| | **FD** | **2.38** | **0.29** | **0.80** | **9.06** | **3.47** | **14.28** | **6.20** | **1.95** | **3.26** | **2.01** | **-0.12** | **3.12** | **0.50** | ***47.20*** | **1.64** |
| | LD | -0.59 | -21.21 | -3.23 | -22.36 | -4.19 | -28.57 | -8.84 | -17.52 | -0.36 | -6.57 | 0.74 | -11.99 | -0.16 | *-11.30* | |
| NOF | B | -11.15 | -6.64 | -88.13 | 41.33 | -42.37 | -0.14 | **-25.36** | *-8.32* | *-163.30* | *93.28* | -89.85 | 66.61 | -70.12 | *-304.16* | |
| | **FD** | **-1.68** | **6.73** | **5.28** | **-4.11** | **13.67** | **1.97** | **-11.55** | **9.68** | ***-7.55*** | ***9.85*** | **-1.31** | **10.86** | **-2.99** | ***28.85*** | **1.00** |
| | LD | -20.99 | 1.89 | 13.59 | -2.70 | 21.62 | 4.24 | *-25.03* | *28.94* | *-10.28* | *12.98* | 4.84 | 6.20 | -3.78 | *31.52* | |

### 3.4 Topographic Roughness Index (TRI) Trends

The topographic roughness index (TRI) was computed for every DTM using the Terrain Ruggedness Index tool in ArcGIS, which uses equation 1. Besides roughness, TRI values also depend on the pixel size and the neighborhood over which TRI is calculated. For this study, TRI values range from 0 to 1.5 m, although values exceeding 0.5 m are rare, with the vast majority concentrated between 0 and 0.5 m.

High value pixels indicate rough terrain while smooth terrain is represented by values close to 0,

as shown by the color scale maps of TRI values in Figure 9. For each treatment, we extract the mean(TRI) and these means are then normalized by mean(TRI) of NOF (Table 4) to provide a ratio that indicates how each treatment plot compares to the roughness of the established dunes at the NOF reference site (discussed further in section 4.3, Figure 11).

All TPs show a progressive increase in roughness (i.e., a positive trend in TRI values) until Oct. 2023, then decline through Oct. 2024, followed by slight increases in most sites, except TP1 and TP2 (Table 4). Roughness increases to Oct. 2023 range from ~127% of initial TRI values for the TP1 control site to 239% for TP5. This is followed by a widespread decline in roughness from Oct. 2023 to Oct. 2024, ranging from -25% (TP5) to -30% (TP1), which could reflect corresponding declines in plant cover[12]. By Feb. 2026, the sites with the highest roughness were, in decreasing order, TP5, TP3, and TP6, followed by TP4, TP2 and TP1. As expected, the NOF reference site has the highest mean TRI values, given the roughness offered by fully developed dunes, yet it also showed a slight decrease (-6%) from Oct. 2023 to Feb. 2024, but remains mostly stable with slight increases (up to 12%) otherwise. By Feb. 2026, the FRA treatment plots had reached roughly 30 to 60% of the roughness observed at the NOF reference site.

***Table 4.*** *Mean TRI values for each foredune restoration treatment plot (TP1 to TP6) and the NOF reference site in bold (TRI $m^{-2}$). Mean TRI values are multiplied by 100 for presentation. Mean TRI for each TP divided by mean NOF is shown in brackets. The 3 highest mean TRI values observed are shown in red, while the 3 highest values in the latest survey are in blue and italicized.*

| | mean(TRI)*100 | | | | | | | | | | | | |
|---|---|---|---|---|---|---|---|---|---|---|---|---|---|
| | Oct-19 | Feb-20 | Oct-20 | Feb-21 | Oct-21 | Feb-22 | Oct-22 | Feb-23 | Oct-23 | Feb-24 | Oct-24 | Feb-25 | Oct-25 | Feb-26 |
| TP 1 | 1.92 (0.24) | 2.25 (0.29) | 2.07 (0.26) | 2.00 (0.25) | 2.75 (0.32) | 2.31 (0.27) | 3.76 (0.44) | 3.08 (0.35) | 4.37 (0.49) | 3.10 (0.37) | 2.75 (0.31) | 3.31 (0.37) | 2.87 (0.33) | 2.69 (0.31) |
| TP 2 | 1.80 (0.22) | 2.07 (0.26) | 2.07 (0.26) | 2.10 (0.26) | 3.01 (0.35) | 2.65 (0.31) | 3.94 (0.46) | 3.51 (0.40) | 4.95 (0.55) | 3.46 (0.41) | 3.52 (0.39) | 3.92 (0.44) | 3.83 (0.44) | 3.65 (0.42) |
| TP 3 | 1.93 (0.24) | 2.08 (0.27) | 2.31 (0.29) | 2.73 (0.34) | 3.94 (0.45) | 3.72 (0.44) | 4.75 (0.55) | 4.54 (0.51) | 5.79 (0.65) | 4.63 (0.55) | 4.75 (0.53) | 5.11 (0.57) | 5.25 (0.60) | *4.86 (0.56)* |
| TP 4 | 1.78 (0.22) | 2.09 (0.27) | 2.19 (0.27) | 2.54 (0.31) | 3.21 (0.37) | 3.02 (0.36) | 3.04 (0.35) | 3.95 (0.45) | 5.51 (0.62) | 4.49 (0.53) | 4.55 (0.50) | 4.70 (0.53) | 4.75 (0.55) | 4.41 (0.51) |
| TP 5 | 1.73 (0.22) | 1.85 (0.24) | 1.95 (0.24) | 2.57 (0.32) | 3.62 (0.42) | 3.22 (0.38) | 4.06 (0.47) | 4.52 (0.51) | 5.86 (0.66) | 4.73 (0.56) | 4.75 (0.53) | 5.17 (0.58) | 5.35 (0.62) | *4.98 (0.58)* |
| TP 6 | 1.76 (0.22) | 2.12 (0.27) | 1.94 (0.24) | 2.83 (0.35) | 3.53 (0.41) | 3.65 (0.43) | 4.05 (0.47) | 4.48 (0.51) | 5.15 (0.58) | 4.87 (0.58) | 4.75 (0.53) | 5.12 (0.58) | 5.09 (0.59) | *4.81 (0.56)* |
| **NOF** | **8.03** | **7.84** | **8.04** | **8.1** | **8.66** | **8.48** | **8.61** | **8.82** | **8.92** | **8.4** | **9.01** | **8.9** | **8.69** | **8.63** |

[12] Note: DTMs used for roughness parameterization include both plant cover and dune forms.

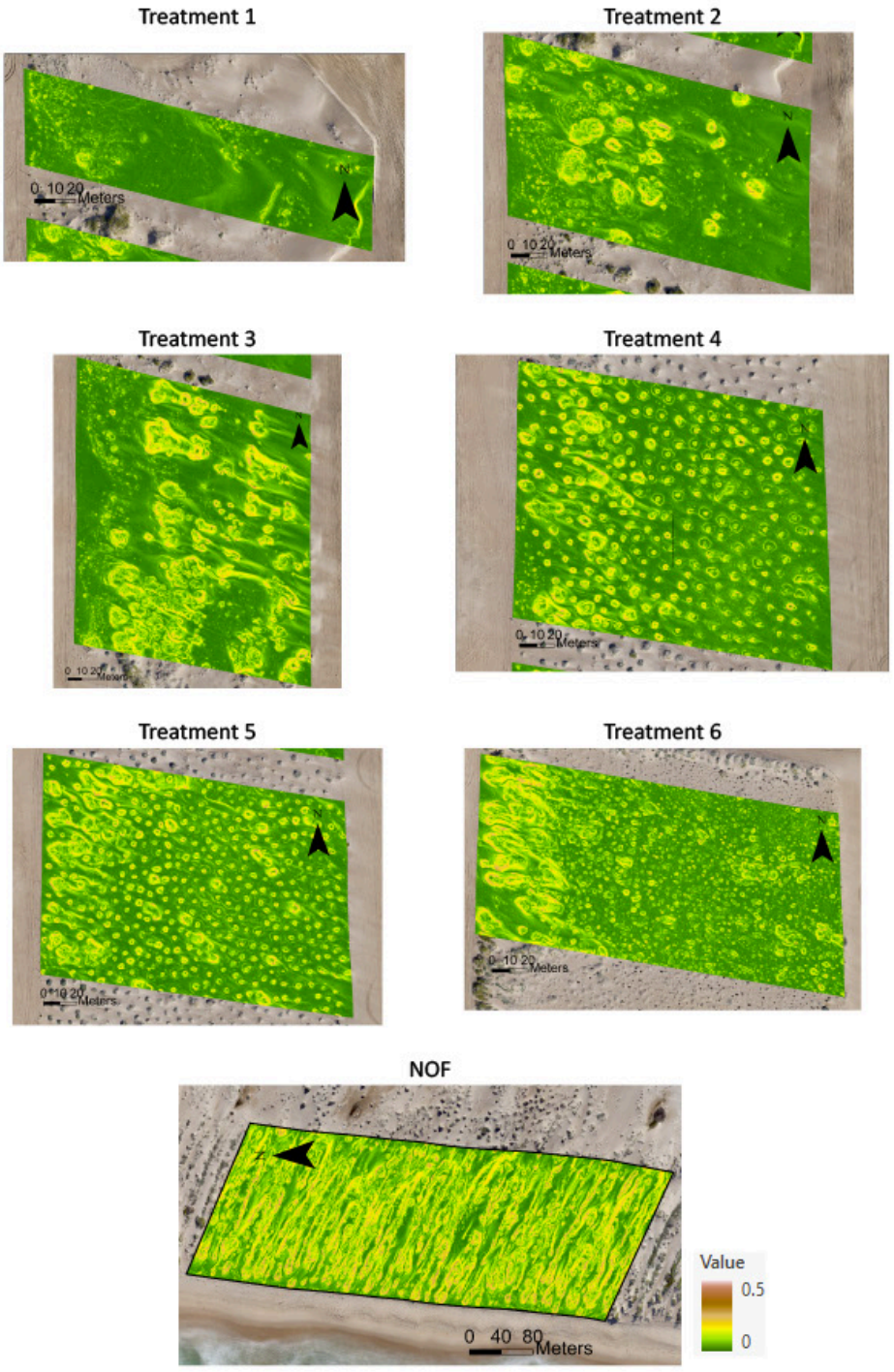



***Figure 9.*** *Topographic roughness index (TRI) maps for each FRA treatment plot and for the NOF foredune reference site, computed using the February 2026 DTM. Generally, greener colors represent smoother surfaces (e.g., interdune corridors, blowouts) and warmer colors are rougher terrain (e.g., dune ridges, vegetated nebkha). All maps are scaled similarly for comparison.*

# 4. Discussion

Most coastal dunes owe their form and function to the presence of vegetation. In turn, sand loving (psammophytic) plants require the conditions and disturbance processes offered by aeolian processes for their success[13,14]. These interactions are particularly important to recognize when designing and assessing foredune restoration projects. In addition, variability in sand inputs from the upwind beach, variations in other supply- and transport-limiting factors can also influence treatment responses and resulting dune evolution. At ODSVRA, sand volume and resulting geomorphic changes within the TPs show seasonal and interannual responses related to variations in factors that limit either the supply of sand to, or transport capacity of, aeolian transport, including: a) surface moisture, which acts as a supply-limiting factor that is highest in wetter winter months, b) the frequency of transporting winds, a transport-limiting factor that is highest in the April-June wind season, c) sand supply to the beach (and/or beach width), a supply-limiting factor that varies on seasonal to interannual scales, and d) the extent and type of treatment modifications, such as plant establishment and straw cover, which can act as both a supply- and/or transport-limiting factor on seasonal to interannual scales. Below, we interpret these interactions and responses within the FRA treatment plots with respect to sand volume and geomorphic changes, vegetation cover, and roughness. We relate the observations to changes at NOF that serves as a reference site. Following this, an assessment of performance of the treatments based on identified indicators is provided.

### 4.1 Vegetation Change and Dune Development

From implementation of the FRA to Feb. 2026, all restoration treatment plots (TP2-6) experienced an increase in plant cover that now exceeds the peak extent of historic vegetation cover in 1966 within the foredune zone of the broader OHV riding area (Figure 4). The TP1 control site showed negligible to slow rates of plant cover to values that remain below the historical average, although the trend in TP1 has slightly increased over time. TP6 and TP3, respectively, had the fastest rates of vegetation establishment and had the highest vegetation cover compared to other treatments to date (Table 2, Figure 4). Most plots experienced a decrease in plant cover in the Oct. 2023 to Feb. 2025 interval, but had begun to increase over the most recent survey intervals. TP1 and TP2 plots did not seem to show the same decline during the Oct. 2023 to Feb. 2025 interval. Overwash events in the preceding year deposited debris and some vegetation propagules within the seaward portions of the plots, allowing the establishment and expansion of vegetation and the initial development of some nebkha within TP1, and notable increases in smaller vegetation along the seaward edge of the TP2 and TP3 plots. Comparatively, NOF vegetation cover also declined during the Oct. 2023 to Feb. 2025 interval and increased in vegetation cover in Feb. 2026, suggesting a regional trend in vegetation cover that is likely influenced by sediment transport dynamics, vegetation burial, and vegetation health due to

[13] Hesp, PA, and Martinez, M. (2007) Disturbance in coastal dune ecosystems. In: Johnson EA and Miyanishi K (eds.) Plant Disturbance Ecology: The Process and the Response, pp. 217–247. Elsevier.

[14] Wiedemann, A, and Pickart, A. (2007). Temperate Zone Coastal Dunes. Ch. 4 in Martinez, M. and Psuty, N. *Coastal Dunes: Ecology and Conservation. Ecological Studies 171*, 53-66. Elsevier.

environmental changes. Vegetation losses appeared to correspond with an erosional interval from Feb. 2023 to Feb 2024 in the FRA (Table 3). However, NOF has had intermittent periods of erosion and deposition and vegetation losses occurred during the same period in the FRA, so vegetation loss due to erosion is speculative.

Dune development continued to differ distinctly across the treatment plots. At the TP1 control site, protodunes and transverse/barchanoid ridges continue to migrate through the plot, ranging in height from 0.3 m near the seaward edge to 1.3 m at the landward edge, with minor nebkha development near the seaward edge of the plot in recent surveys. Combined with a relatively neutral sediment budget, this indicates appreciable sand bypassing through the control plot due to limited vegetation cover. The recent increase in vegetation in TP2 has led to more nebkha development central to the plot. These nebkha are formed predominantly with *Abronia latifolia*. TP3 is distinct in that larger nebkhas have formed in the seaward, central, and inland portions of the foredune plot compared to TP4-6, which have nebkha concentrated on the seaward portion of the plot. TP6 began as the roughest of all the plots (full straw cover, many randomly distributed plants), but only the seaward edge has shown appreciable dune development, while the size and development of nebkha in the central portion of the plot remains limited. TP3 is the leading plot in positive sediment budget followed by TP6, while TP6 leads in vegetation cover followed by TP3. These plots have top critical elements in their performance assessment (Section 4.3) but have distinctly different nebkha development patterns. Dune development in TP3 is comparatively most similar to dunes observed at NOF, however, the net area-normalized sediment budget of NOF is more similar to TP4 (Table 3).

Feedbacks between dune and vegetation roughness, secondary flow patterns, surface shear stress, and sand transport will continue to evolve and influence dune development[15]. While beyond the scope of this report, ongoing work comparing wind data from the meteorological stations at the eastern edge of the plots, nebkha development, and geomorphic change suggests that the more geomorphically developed TP3, TP5, and TP6 sites have the greatest impact on the wind fields. Variations in roughness patterns between these plots have resulted in notably different dune development pathways.

### 4.2 Sediment Budget Trends

For dunes to establish and be maintained following erosive events, they require net positive sediment budgets. Absolute volumes of sand inputs to the beach, foredune, and landward dune units at each treatment site over the 6-year monitoring period indicate relatively small changes in TP1 and TP2 in contrast to large changes in TP3, TP5 and TP6, which could be due to several factors. First is the observed north-south gradient in sand supply to the beach as well as an increasing trend in wind strength. In addition, notable erosion is evident in the landward units behind TP4-6, which reflects lower sediment bypassing, an erosional wake effect that is not as pronounced in the more northern treatment plots, and the north-south gradient in increasing wind

[15] Walker, I.J., Hesp, P. and Smyth, T. (2022). Airflow dynamics over unvegetated and vegetated dunes. Chapter 7.16 in Aeolian and Desert Geomorphology in Shroder, J. F. (Ed.) and Lancaster, N. (Section Ed). *Treatise on geomorphology*, *7*(2), pp.415-453. London, United Kingdom: Elsevier.

speeds. Furthermore, the evolving morphology and roughness of the new foredunes in the FRA exert a positive (self-amplifying) feedback on sediment accumulation, so those treatments with larger dunes and higher plant cover, such as TP3-6, are more effective than TP1-2 at trapping sand.

Seasonal to interannual variations in volumetric change are also evident at many locations, including NOF, reflecting the combined influences of the spring wind season, winter beach erosion and/or movement of rip cell embayments that reduce beach width, and spring/summer bar welding on to the upper beach (see also erosion/deposition patterns and trends in Figures 5 to 8). Figure 8 also shows that, despite high variability in beach sand volumes and a general net erosional trend, the FRA plots have maintained a net positive sediment budget response, indicative of continued accretion in developing vegetated dunes.

Significant declines in beach volumes and widths during fall/winter 2023 (Oct. 2022 to Feb. 2023) were not mirrored in the adjoined foredune treatment plots, yet most showed a continued or increasing negative trend in sand volume in the following interval (to Oct. 2023). The Feb. 2025 to Oct. 2025 interval showed consistent increased deposition between both the beach and foredune geomorphic units except for TP2-4 that showed some erosion in the beach unit and a very small decrease in the foredune unit. The most recent Oct. 2025 to Feb. 2026 interval showed very limited deposition or erosion within all sites, suggesting very low aeolian activity during this time. Most of the FRA plots (TP3-6) have had larger net sediment budgets compared to the net positive change at NOF (Table 3), which is not surprising given the continued and early evolutionary state of the FRA plots, as well as the fully-developed, quasi-equilibrium state of the NOF foredune. As for the fronting beach units, they continue to accrete except at TP6. Compared to NOF, erosional beach intervals tended to correspond with erosional foredune events, which could signify that the larger erosive events at the NOF beach might be impacting sediment supply available to the foredune unit.

Changes in the landward dune units (LD) are variable given the lack of vegetation and continued influence of OHV traffic. Areas downwind of TP3-6 show seasonally alternating (peak-valley) trends in their sediment budgets, whereas areas downwind of TP1-2 do not show this trend, although TP2 started to develop this trend in Feb. 2025. Though speculative, this could relate partly to the greater and seasonally varying influence of plant growth/roughness, sand accretion, and dune development within TP3-6 compared to TP1-2. For TP3-6, this seasonal pattern alternates between positive budgets in fall/winter (Oct. to Feb.) and negative budgets during the wind and plant growth season (Feb. to Oct.) when more sediment accreted in the upwind treatment plot. The longer-term trend of this cycle is predominantly negative in the LD units behind TP4-6 (Table 3), which have developed increasingly larger dunes and more extensive plant cover. In NOF, the behavior is different as the foredune and landward dunes follow this seasonal pattern simultaneously. Increases and decreases in foredune volume are mirrored by corresponding changes in the landward dune, as shown in Figure 8. We could thus expect the TP to act the same when more established.

### 4.3 Performance Assessment of Restoration Treatments

The foredune restoration project at ODSVRA was designed to re-establish a foredune ecosystem

with dust emissions mitigation benefits using a 'nature-based' approach with an assortment of treatment types of increasing levels of intervention. To inform potential adaptive management by CDPR, it is important to recurrently evaluate the relative performance of the treatments. The goal of the FRA is to grow and maintain dunes with positive sediment budgets (i.e., sand sinks), self-sustaining plant communities, and enhanced roughness to collectively reduce dust emissions.

In previous reports, performance assessment was based on a cumulative score derived from 6 indicators whereby lower total values indicated higher overall performance[1]. In consultation with SAG and APCD, we refined and simplified the assessment approach to focus only on 3 indicators (metrics): 1) plant cover (% cover), 2) sediment budgets (area-normalized volumetric change ($m^3$ $m^{-2}$ $mo^{-1}$), and 3) topographic roughness (TRI). Metrics are also now derived from within smaller analytical areas to reduce bias from edge effects and performance is assessed in comparison to the more fully-developed dune conditions at the NOF reference site. Summaries for each of the assessment indicators are as follows:

1. **Net positive plant cover trends persist for all FRA treatment plots** since installation, with some variability, and despite a concerning declining trend at most sites, including the NOF reference site, that began in Oct. 2023. Declines were most pronounced in TP6 and less so within TP3-TP5. This trend has since reversed with the most recent surveys in Oct. 2025 and Feb. 2026 showing increases in plant cover in all TPs and at NOF. These corresponding declines, followed by increases in vegetation within the FRA and NOF, suggests a regional trend that is likely driven by variability in regional climate, sediment transport, vegetation burial, plant health, and/or plant community dynamics. Currently, **the three top performers for plant cover are TP6 (16.9%), TP3 (12.5%), and TP5 (9.5%) with TP1-4 reaching their highest cover values to date**. With the exception of the TP1 control site, all plots have surpassed the peak historical observed plant cover in the foredune zone (5.3% in 1966). However, vegetation cover within the FRA has not yet reached the target cover state at the NOF reference site (26.1%). At NOF, vegetation trends have been relatively stable, yet fluctuate by as much as 9%, which could be typical of the quasi-equilibrium state of fully-developed dune ecosystems in the region. Observations of trends in plant cover in the FRA and NOF reinforce that more time is required for the treatments to re-establish and sustain dune plant communities, which has important implications for maintaining dune development and growth and, in turn, dust emissions control potential (see also #3 below).

2. **Net positive sediment budgets continue within all FRA treatment plots** (Table 3) and the last two monitoring intervals saw mostly positive budgets that exceed those of the TP1 control plot. To assess how these changes compare with conditions at NOF, we standardized area-normalized values for each TP by the same value for NOF to provide a proportionally differenced volume score, $DV_{TP\#,\ NOF}$, for each treatment plot:

$$DV_{TP\#,\ NOF} = \left|\frac{TP\ area-normalized\ volumetric\ change}{NOF\ area-normalized\ volumetric\ change}\right| \qquad \text{Equation 3}$$

As such, DV values closest to 1 indicate conditions that closely match the volumetric changes observed at NOF (Table 5) and DV values < 1 suggest that a TP is underperforming by

accumulating less sediment than the NOF reference site. Generally, there are two distinct intervals where most TPs exceeded accumulation amounts at NOF (Oct. 2022, Feb. 2025), which indicate rapid phases of dune growth also reflected in higher NOF accretion amounts. For instance, in Oct. 2022, accumulation rates in the treatment plots were 2 to 8 times higher than NOF and roughly 2 to 4 times greater in Feb. 2025. Over time, TP DV values alternate above and below those at NOF, which is not unexpected given variations in beach sediment supply across sites and because the treatment areas should be accumulating sediment at faster rates as the dunes continue to develop (vs. maintaining large, quasi-equilibrium dunes at NOF). Comparison of overall (net) volumetric gains of each TP against those NOF (Figure 10) shows that TP4 has the closest net sediment budget (~11% lower) to that of NOF, however, as it is expected that the FRA should have higher rates of accumulation than NOF as the TPs continue to develop, **the three top performers with respect to exceeding NOF net accumulation values are TP3 (+106%), TP6 (+60%), and TP5 (+25%)**.

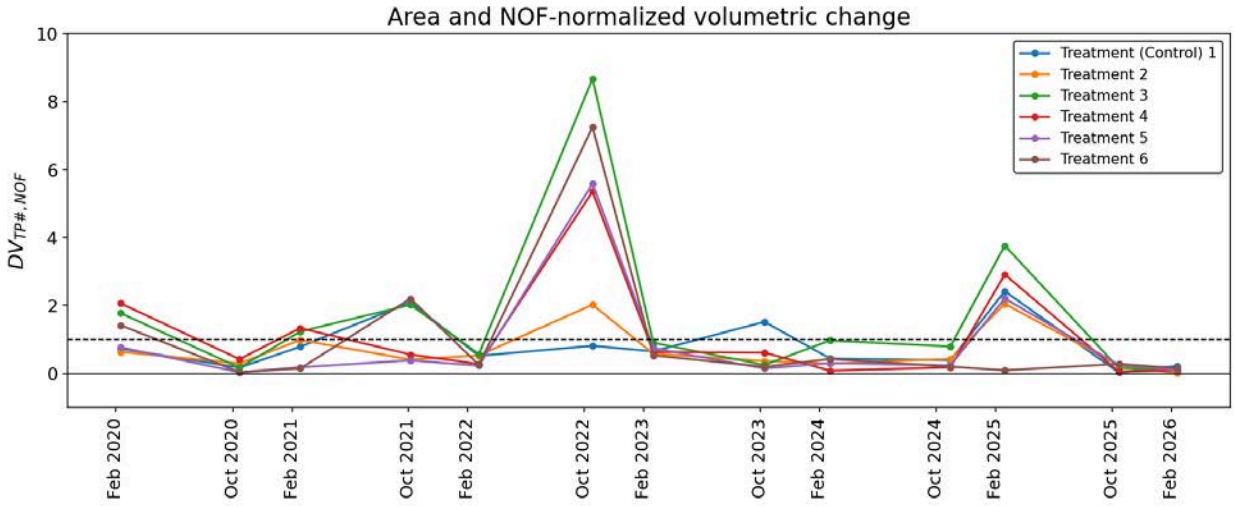



***Figure 10.*** *Time series of normalized differenced volume scores, $DV_{TP\#,\ NOF}$, for each treatment plot with the dashed line representing conditions at NOF (i.e., DV = 1).*

***Table 5:*** *Normalized volumetric change ($DV_{TP\#,\,NOF}$) values for all FRA treatment plots as a function of the ratio of observed area-normalized quantities at each TP to concurrent volumetric change at the NOF reference site. Green values indicate those closest to NOF conditions (i.e., $DV_{TP\#,\,NOF}$ = 1.00) for each observation interval.*

| NOF-normalized volumetric change | | | | | | | | | | | | | |
|---|---|---|---|---|---|---|---|---|---|---|---|---|---|
| | Oct 2019 to Feb 2020 | Feb 2020 to Oct 2020 | Oct 2020 to Feb 2021 | Feb 2021 to Oct 2021 | Oct 2021 to Feb 2022 | Feb 2022 to Oct 2022 | Oct 2022 to Feb 2023 | Feb 2023 to Oct 2023 | Oct 2023 to Feb 2024 | Feb 2024 to Oct 2024 | Oct 2024 to Feb 2025 | Feb 2025 to Oct 2025 | Oct 2025 to Feb 2026 |
| TP1 | 0.73 | 0.18 | 0.79 | 2.09 | 0.52 | 0.82 | 0.65 | 0.99 | 0.44 | 0.39 | 2.43 | 0.03 | 0.25 |
| TP2 | 0.64 | 0.30 | 0.99 | 0.41 | 0.53 | 2.03 | 0.59 | 0.37 | 0.30 | 0.43 | 2.06 | 0.13 | 0.01 |
| TP3 | 1.77 | 0.18 | 1.24 | 1.76 | 0.57 | 8.66 | 0.91 | 0.25 | 0.98 | 0.80 | 3.78 | 0.16 | 0.12 |
| TP4 | 2.07 | 0.42 | 0.43 | 0.56 | 0.28 | 5.35 | 0.64 | 0.62 | 0.09 | 0.18 | 2.92 | 0.05 | 0.11 |
| TP5 | 0.77 | 0.04 | 0.19 | 0.39 | 0.23 | 5.59 | 0.75 | 0.15 | 0.31 | 0.24 | 2.21 | 0.25 | 0.11 |
| TP6 | 1.42 | 0.04 | 0.15 | 2.20 | 0.25 | 7.25 | 0.54 | 0.20 | 0.43 | 0.20 | 0.09 | 0.29 | 0.17 |

3. **<u>Dust control potential for all FRA treatment plots continues to increase</u>**. The new topographic roughness index (TRI) metric characterizes the combined effects of terrain complexity and vegetation surface roughness within TPs and, as such, provides a proxy measure of their aerodynamic roughness and surface sheltering effects. Higher TRI values and positive TRI trends indicate enhanced dust control potential. Since installation, all TPs, as well as the T1 control site, have shown net positive trends in roughness (Table 4), albeit with some variability. Coincident with observed declines in plant cover, a period of declining roughness occurred across all sites from Oct. 2023 to Oct. 2024, which persisted through Feb. 2025. Since, roughness trends for all TPs are slightly positive (TP2-6) while the TP1 control site has shown decreasing roughness. By comparing mean TRI values for the TPs against those for fully-developed dunes at NOF (Figure 11), TPs 3, 5 and 6 have consistently shown the highest normalized roughness since Feb. 2022, with TP3 and TP5 often leading, while TP6 remained very close and slightly less variable over this time. Since early stages of development in Oct. 2020, the FRA TPs have generally increased from 20 to 30% of the roughness at NOF to over 60% during peak observations in Oct. 2023. Currently, the treatments range from 43% (TP2) to 58% (TP5) of the NOF roughness (Figure 10) with the TP1 control site at 31%. **As of Feb. 2026, the three top performers for dust control potential based on TRI scores are, in decreasing order, TP5 (57.7%), TP3 (56.3%), and TP6 (55.7%).** Despite continued net positive roughness trends since installation, none of the TPs have reached the scale of roughness at NOF, which has remained largely stable during the 6 year monitoring period. As with vegetation cover, this reinforces that more time is required for the FRA treatments to continue their morphological development and maximize their dust emissions control potential.

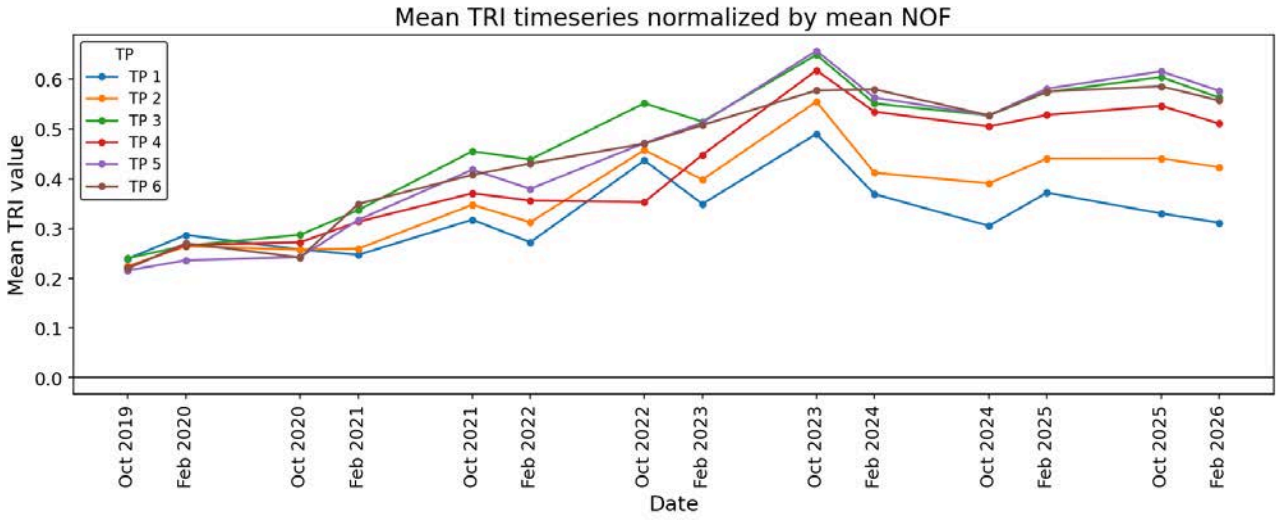



***Figure 11.*** *Time series of mean topographic roughness index (TRI) of each foredune restoration treatment plot (TP1 to TP6) normalized by area and by the corresponding mean NOF TRI value.*

Based on these 3 indicators and their metrics, TP6 maintains top performance for plant cover (at roughly 65% of NOF), TP3 for sediment accumulation (at rates exceeding NOF), and TP5 for dust control potential (at about 58% of NOF). **Overall, as TP3 also placed second for vegetation cover and dust control potential, it narrowly outperformed TP6 and TP5 as the most effective treatment to date** toward developing established foredunes with a self-sustaining plant community while offering enhanced dust control potential.

## 5. Summary and Conclusions

To monitor and assess the performance of the foredune restoration dust mitigation project at the ODSVRA, biannual uncrewed aerial system (UAS) surveys of the FRA have been conducted from Oct. 2019 through to Feb. 2026. Results presented in this report provide interpretations of 6 years of geomorphic and plant community development at the FRA.

Prior to implementation of the restoration treatments in Feb. 2020, there was negligible vegetation at the site and geomorphology was primarily driven by: i) aeolian processes moving sand landward by saltation and low transverse dune migration, and ii) the impacts of vehicle activity and camping. From the baseline surveys (Oct. 2019 to Feb. 2020), supply to the beach was variable, but net positive and deposition within the FRA generally was low to negligible over the barren sand surfaces. Following restoration, sand accretion, plant growth, and resulting dune development has continued steadily, yet differently, within the treatment plots.

The restoration plots continue to evolve on different trajectories as a function of the initial treatments and variability in other controlling factors such as sand supply to the beach, plant cover, and roughness effects.

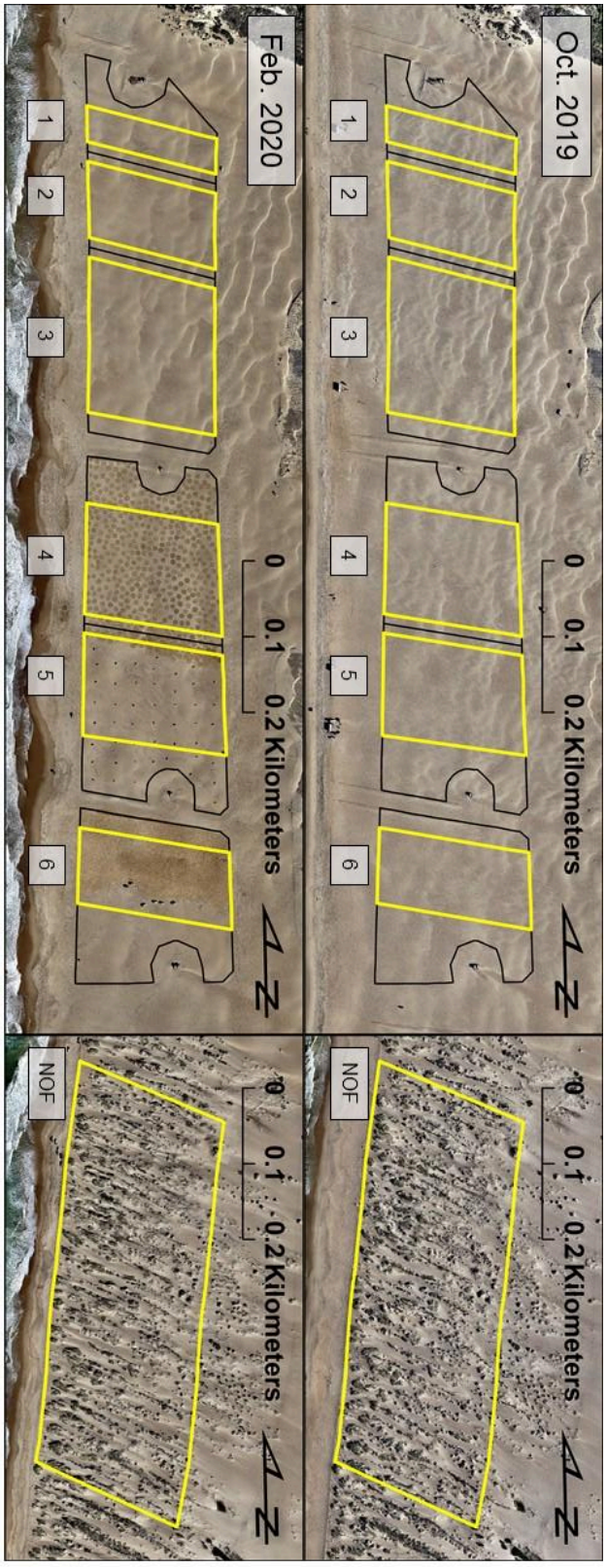
All treatment plots except the control (TP1) have exceeded their historical peak vegetation cover but have not yet reached the vegetation cover observed at the NOF reference site, which is considered to be in dynamic equilibrium and exhibits a stable trend with seasonal variability. The continued increase in vegetation cover within the FRA, compared with the stable cover at NOF, suggests that FRA foredunes are still developing, whereas the more mature NOF foredunes have likely reached equilibrium. Recent changes in vegetation trajectories indicate that longer-term monitoring is needed to assess foredune ecosystem recovery and sustainability.

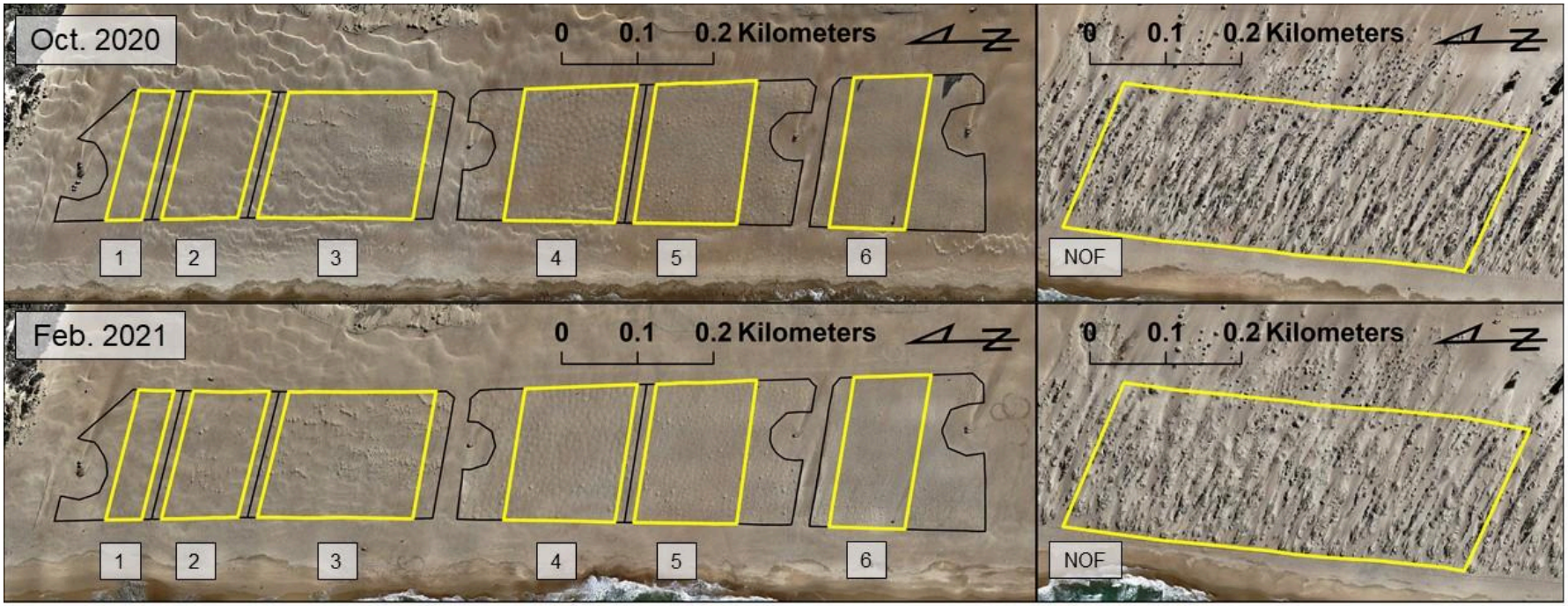
Seasonal to interannual variability in sediment budgets are evident across all sites, including NOF. Despite fluctuations in beach sand volumes and an overall erosional beach trend, the FRA plots maintained a net positive sediment budget, reflecting continued accretion in developing vegetated dunes. TP3–6 exhibited greater net sediment gains than NOF, likely because the NOF foredune has reached a state of dynamic equilibrium and therefore accumulates sediment more slowly. At NOF, changes in foredune and landward dune volumes occur synchronously, with increases and decreases in foredune volume mirrored by corresponding changes in the landward dune (Figure 8). As the treatment plots mature, they may be expected to exhibit similar behavior.

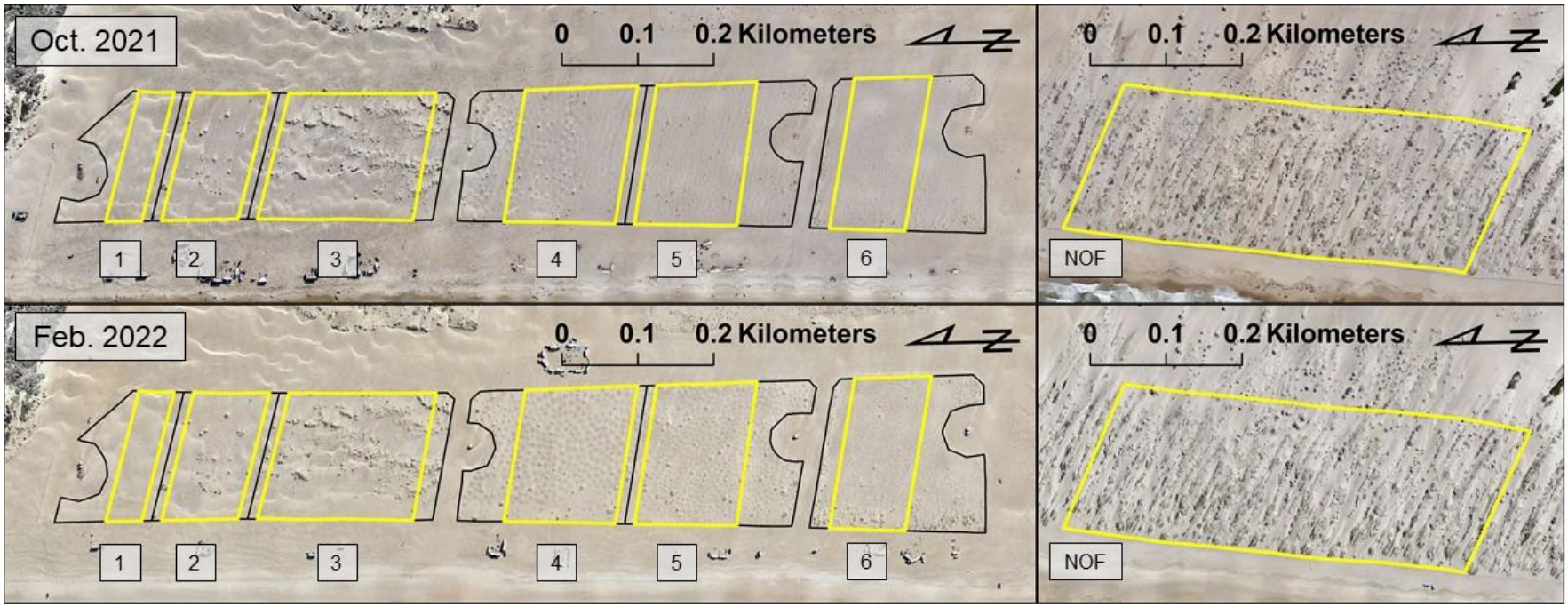
The dust control potential, estimated through the new topographic roughness index (TRI), has generally increased across all treatment plots. Following a decline in roughness between Oct. 2023 and Oct. 2024, likely associated with reduced vegetation cover, TRI values stabilized or increased slightly for most treatments, while the control site continued to decline after Feb. 2025. Since Feb. 2022, TP3, TP5, and TP6 have consistently exhibited the greatest roughness, with TP5 showing the highest TRI by Feb. 2026. However, all treatment plots remain below the relatively stable roughness observed at the NOF reference site, suggesting further development is needed to reach comparable surface roughness and dust control potential.

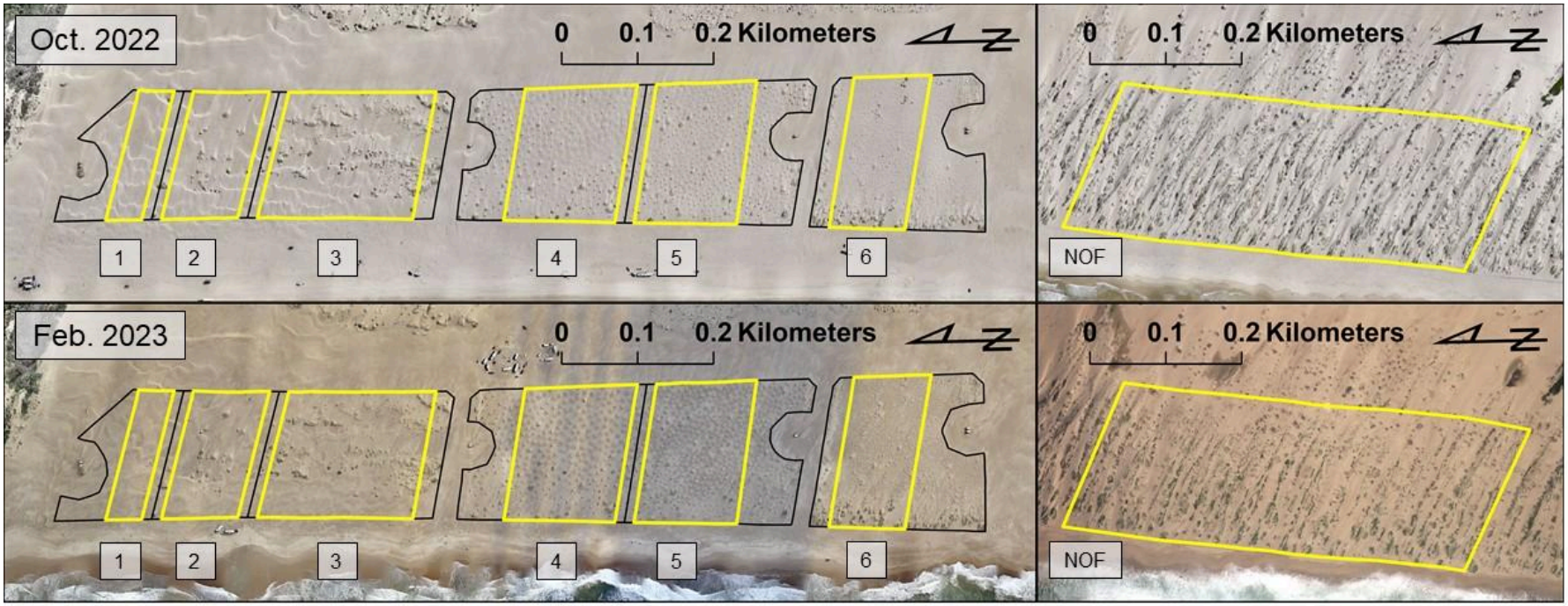
Based on these 3 indicators, TP6 maintains top performance for plant cover (at ~65% of NOF), TP3 for sediment accumulation (at rates exceeding NOF), and TP5 for dust control potential (at about 58% of NOF). As TP3 also placed second for vegetation cover and dust control potential, it narrowly outperformed TP6 and TP5 as the most effective treatment to date toward developing established foredunes with a self-sustaining plant community while offering enhanced dust control potential. This modified performance assessment is consistent with the previous assessment, which showed that TP1 (control) and TP2 have been consistently performing poorly, TP5 and TP6 showed similar performance and slightly better than TP4, while TP3 consistently maintains the highest performance since installation. Next to the TP1 control plot, which received no vegetation treatment, TP2 maintains the lowest performance due to modest amounts of accretion and dune development, low plant cover, and correspondingly low dust emissions control potential. Monitoring will continue as the treatments evolve to detect further responses indicative of success or concern for adaptive management and for longer-term sustainability of the FRA as a dust control mitigation site.

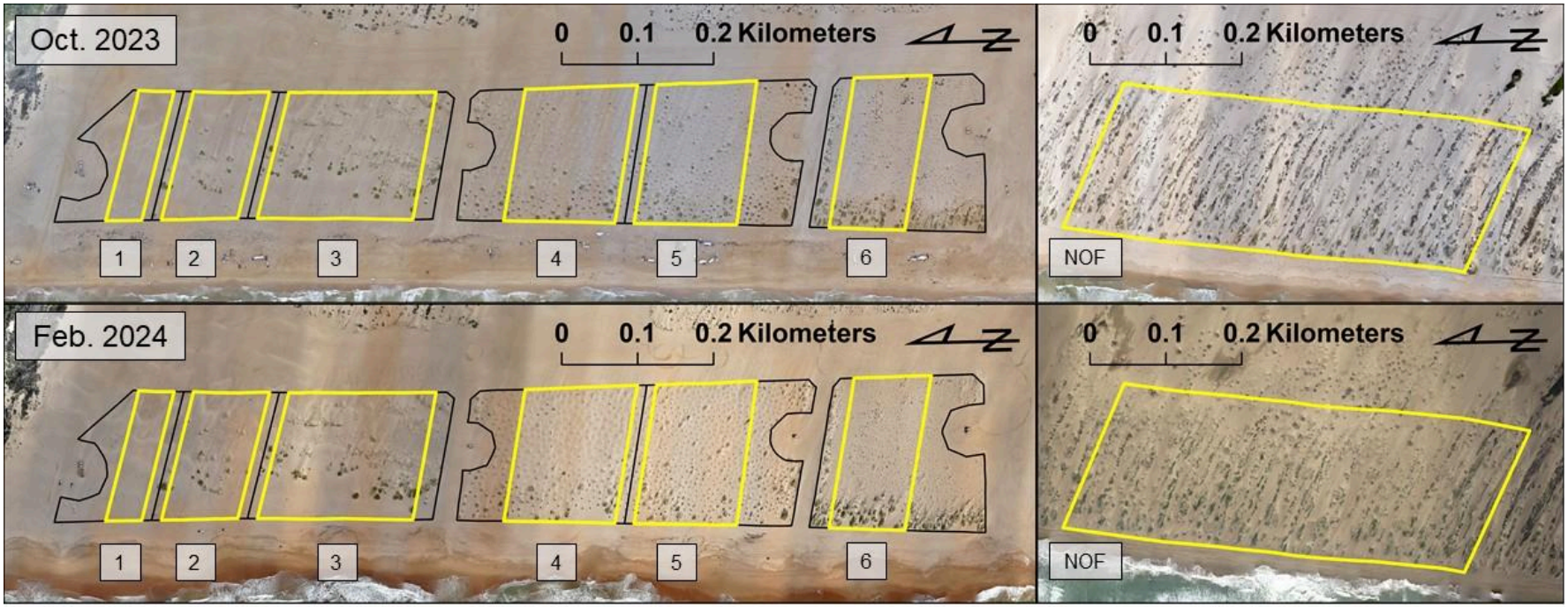
**Appendix A:** Biannual RGB orthomosaics of the FRA and NOF from Oct. 2019 to Feb. 2026. The orthomosaics in NOF from Feb. 2023 to Feb. 2024 are MS.

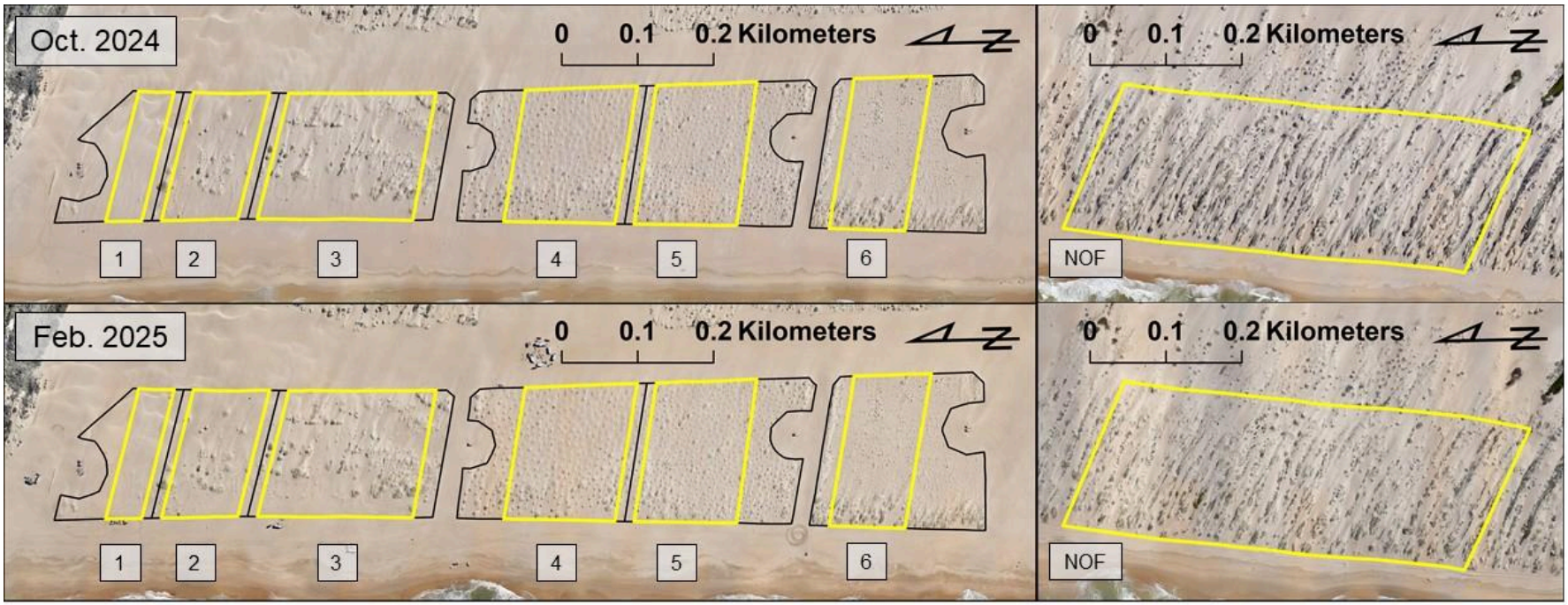


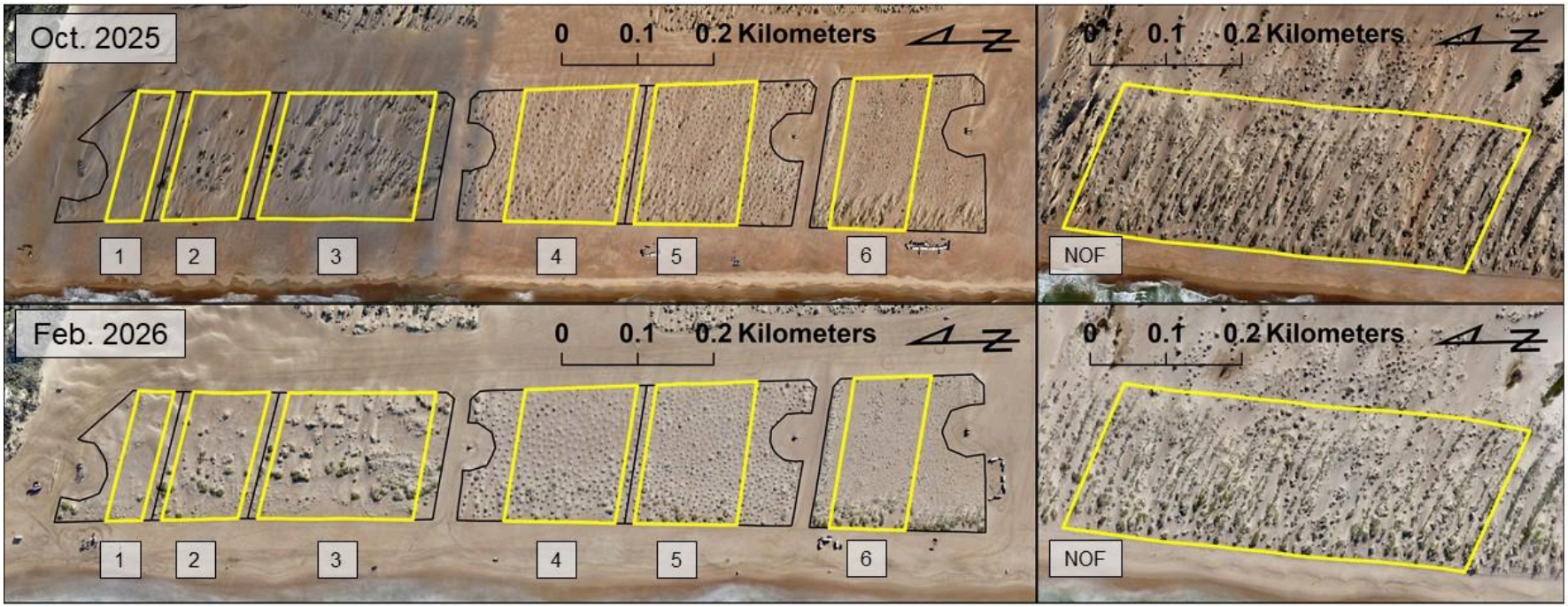

Oct. 2020
0 0.1 0.2 Kilometers
N
1
2
3
4
5
6
0 0.1 0.2 Kilometers
N
NOF
Feb. 2021
0 0.1 0.2 Kilometers
N
1
2
3
4
5
6
0 0.1 0.2 Kilometers
N
NOF


Oct. 2021
0 0.1 0.2 Kilometers
N
1
2
3
4
5
6
0 0.1 0.2 Kilometers
N
NOF
Feb. 2022
0 0.1 0.2 Kilometers
N
1
2
3
4
5
6
0 0.1 0.2 Kilometers
N
NOF

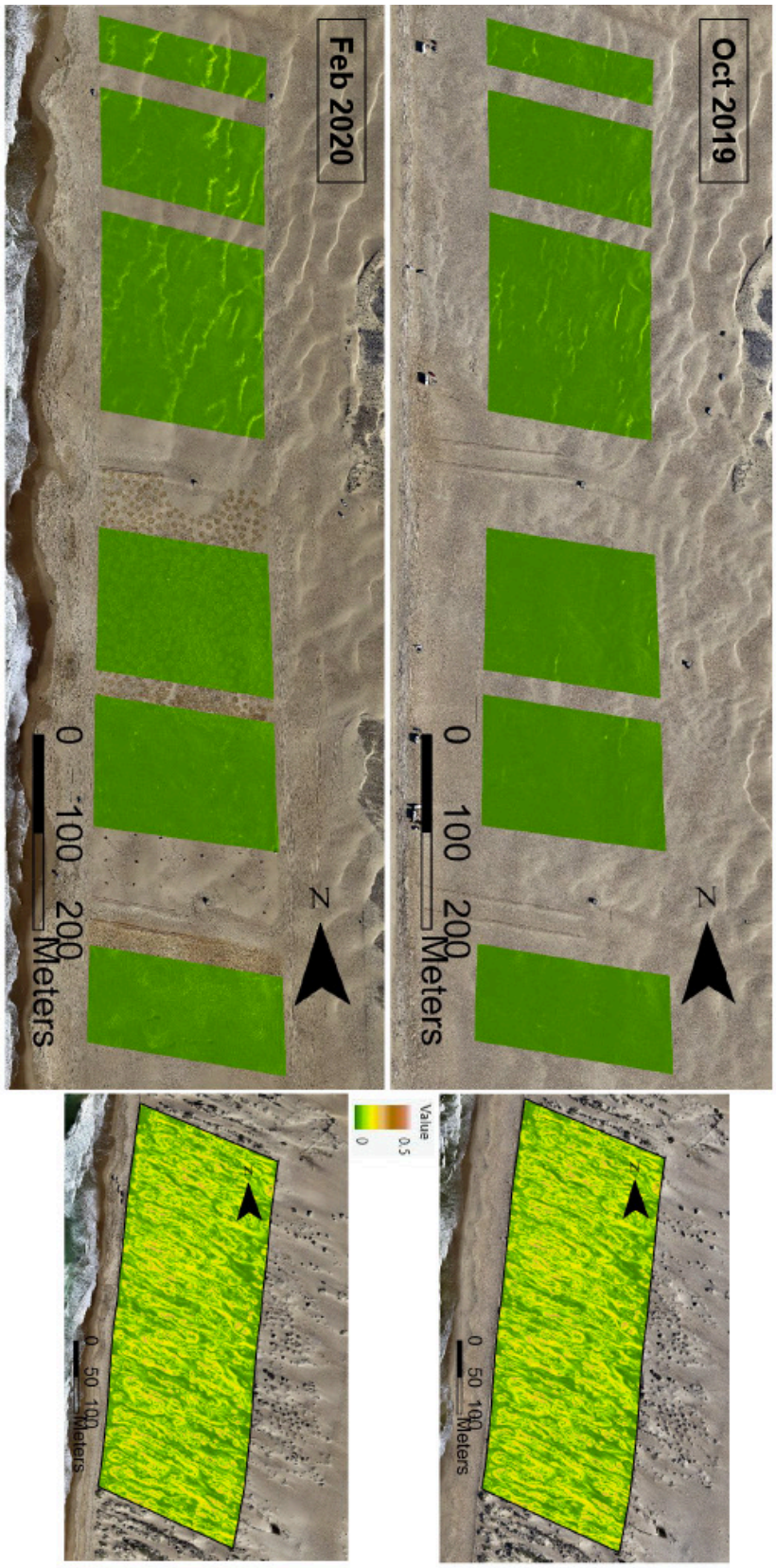

Oct. 2022
0 0.1 0.2 Kilometers
N
1
2
3
4
5
6
0 0.1 0.2 Kilometers
N
NOF
Feb. 2023
0 0.1 0.2 Kilometers
N
1
2
3
4
5
6
0 0.1 0.2 Kilometers
N
NOF

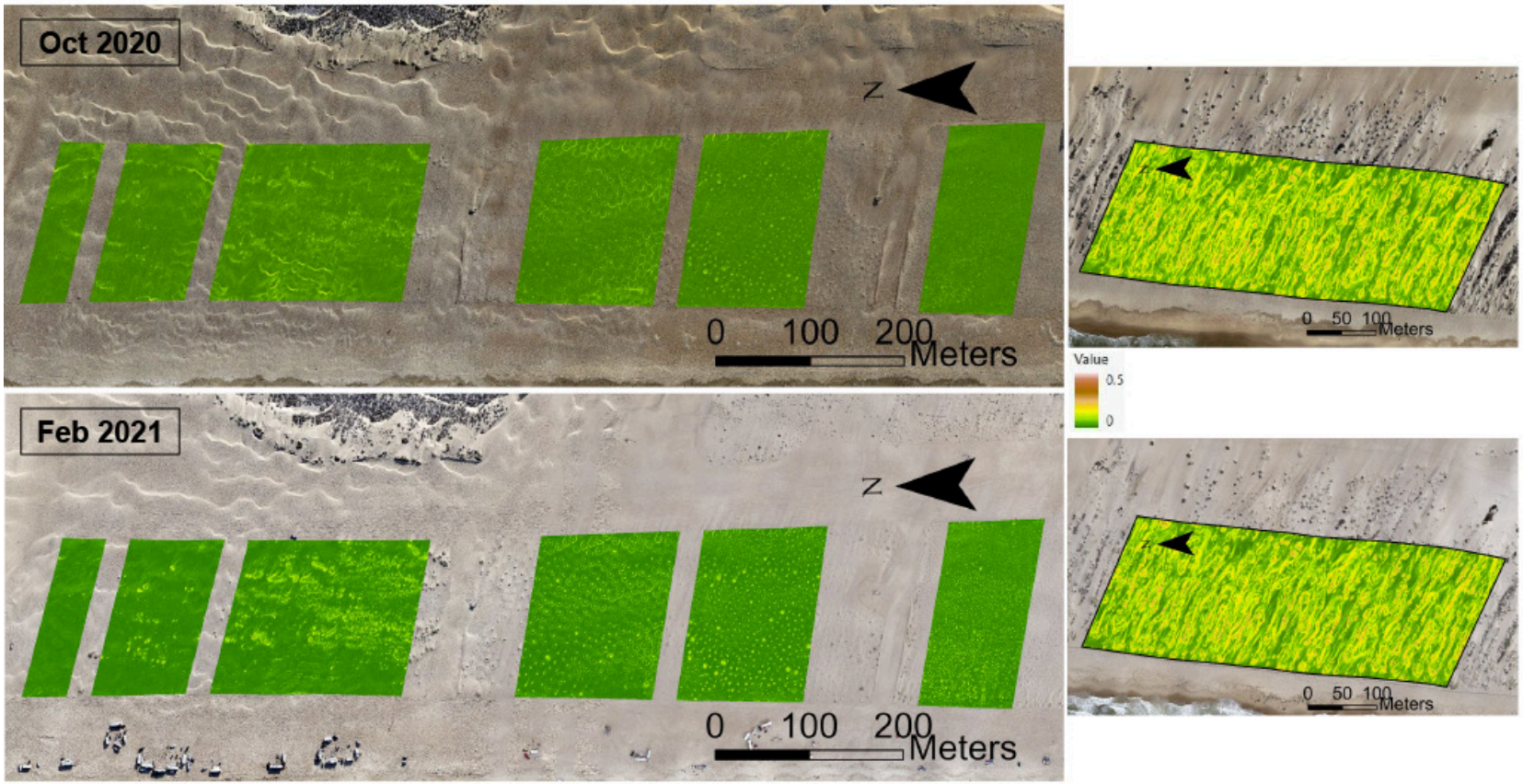

Oct. 2023
0 0.1 0.2 Kilometers
N
1
2
3
4
5
6
0 0.1 0.2 Kilometers
N
NOF
Feb. 2024
0 0.1 0.2 Kilometers
N
1
2
3
4
5
6
0 0.1 0.2 Kilometers
N
NOF

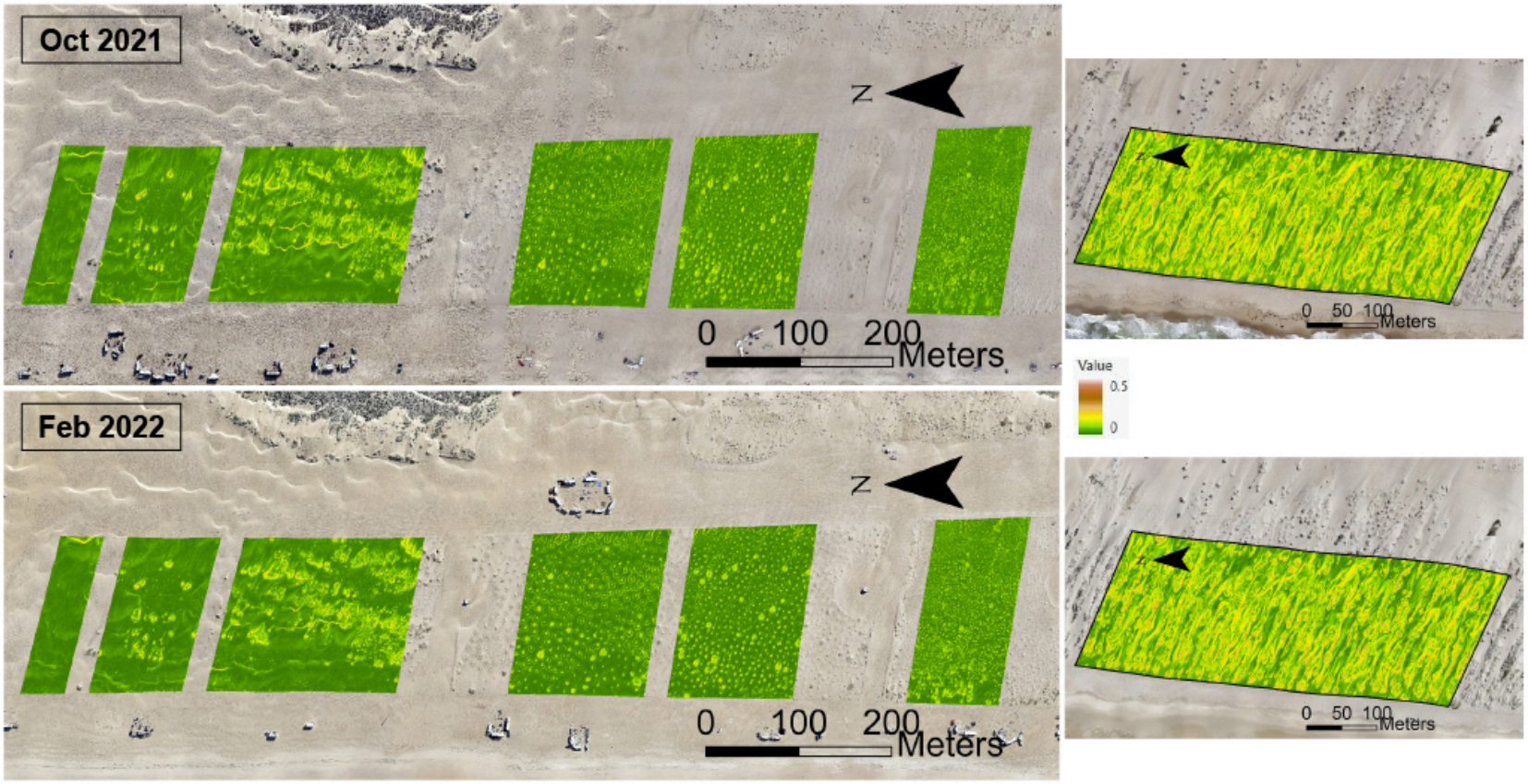

Oct. 2024
0 0.1 0.2 Kilometers
N
1
2
3
4
5
6
0 0.1 0.2 Kilometers
N
NOF
Feb. 2025
0 0.1 0.2 Kilometers
N
1
2
3
4
5
6
0 0.1 0.2 Kilometers
N
NOF

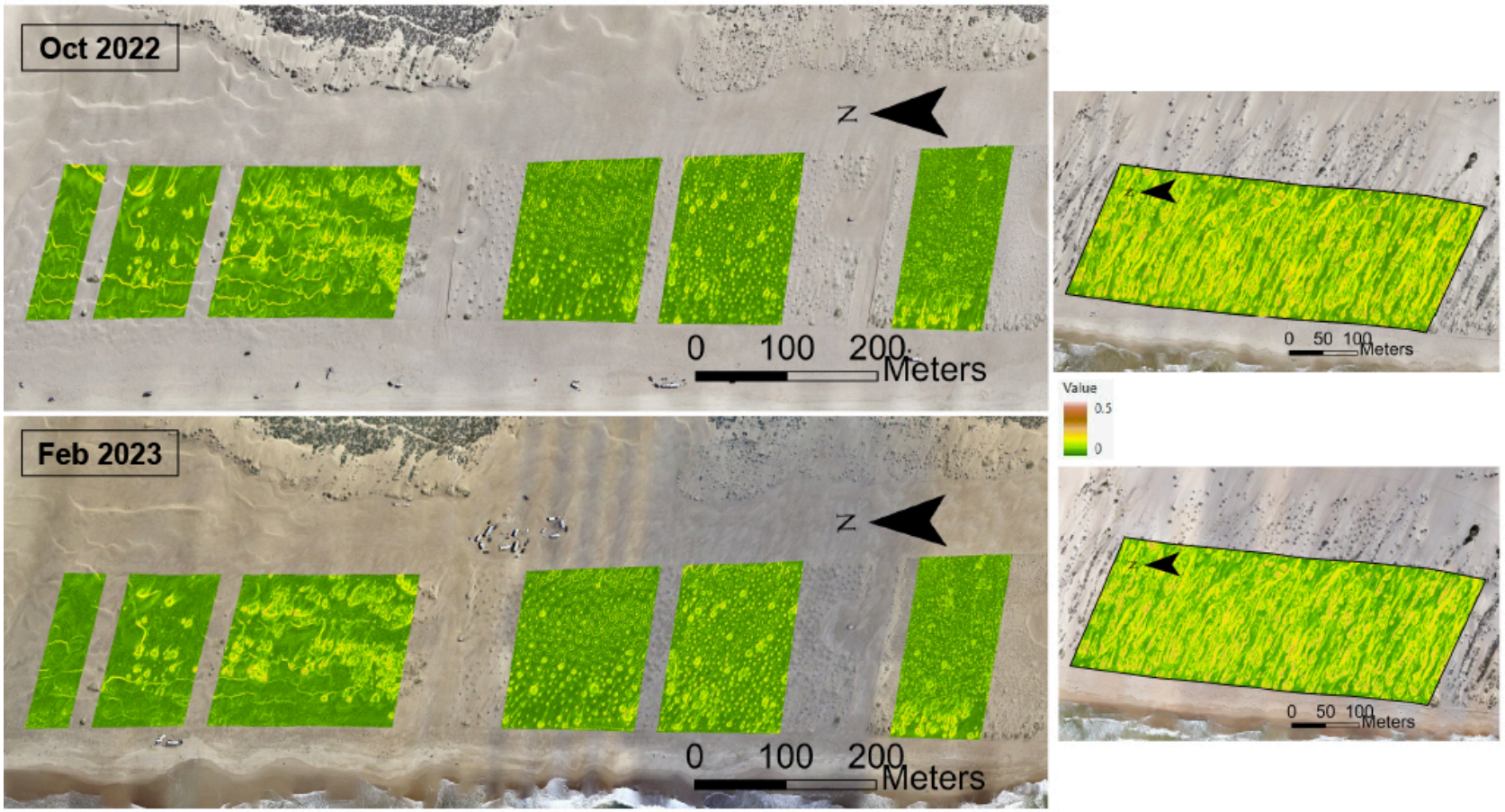

Oct. 2025
0 0.1 0.2 Kilometers
N
1
2
3
4
5
6
0 0.1 0.2 Kilometers
N
NOF
Feb. 2026
0 0.1 0.2 Kilometers
N
1
2
3
4
5
6
0 0.1 0.2 Kilometers
N
NOF

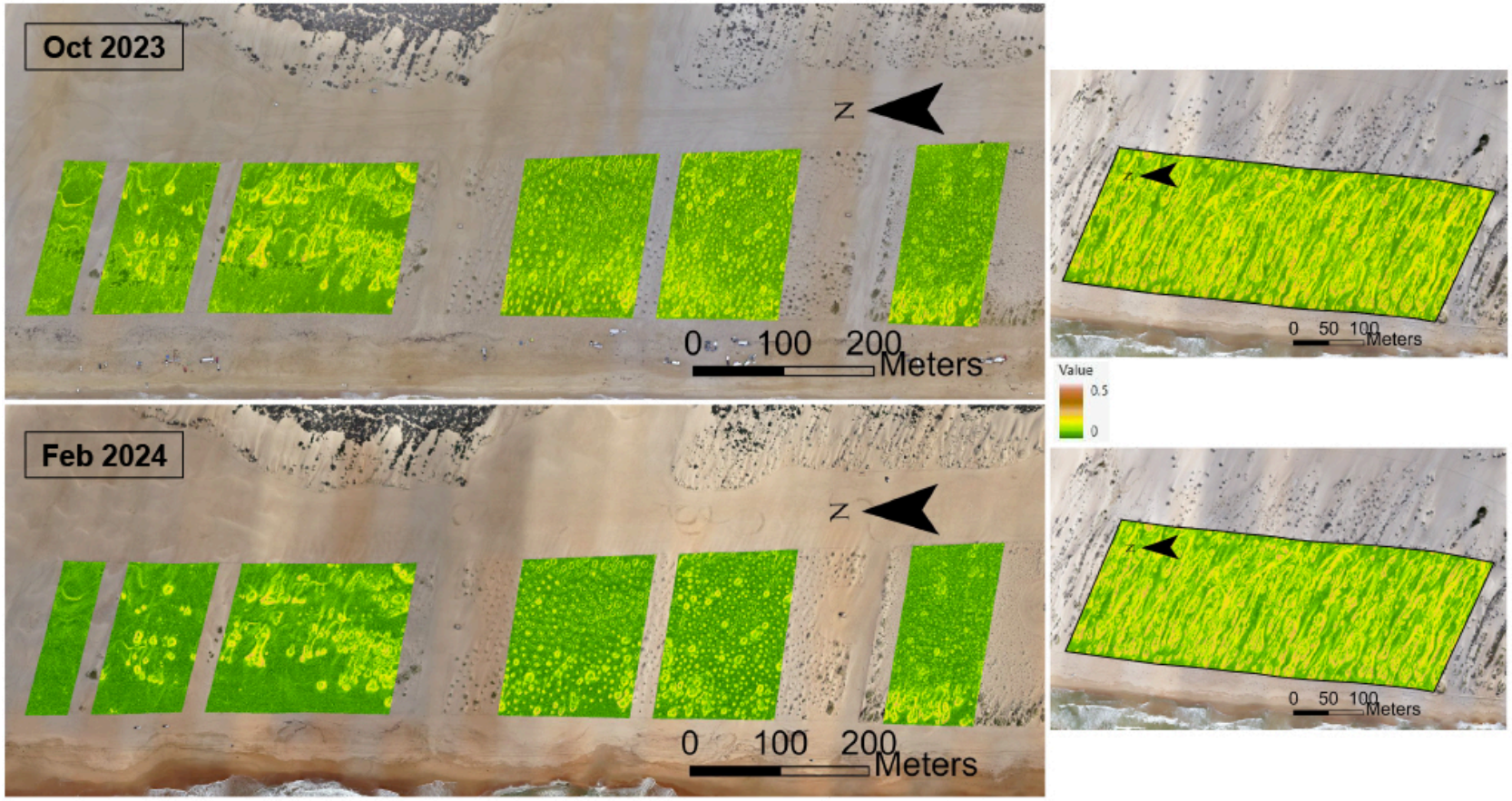
**Appendix B:** Biannual TRI maps of the FRA and NOF from Oct. 2019 to Feb. 2026.

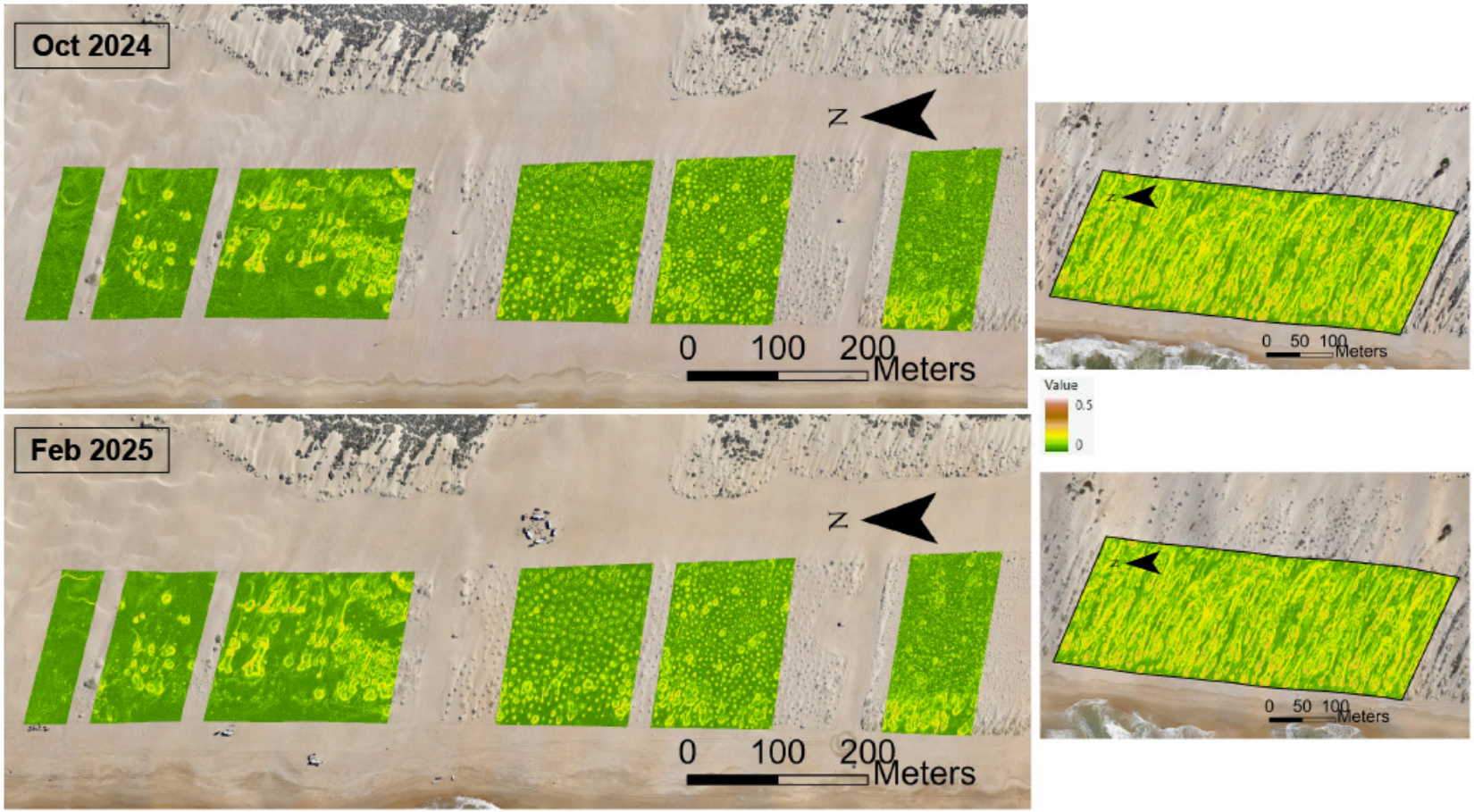


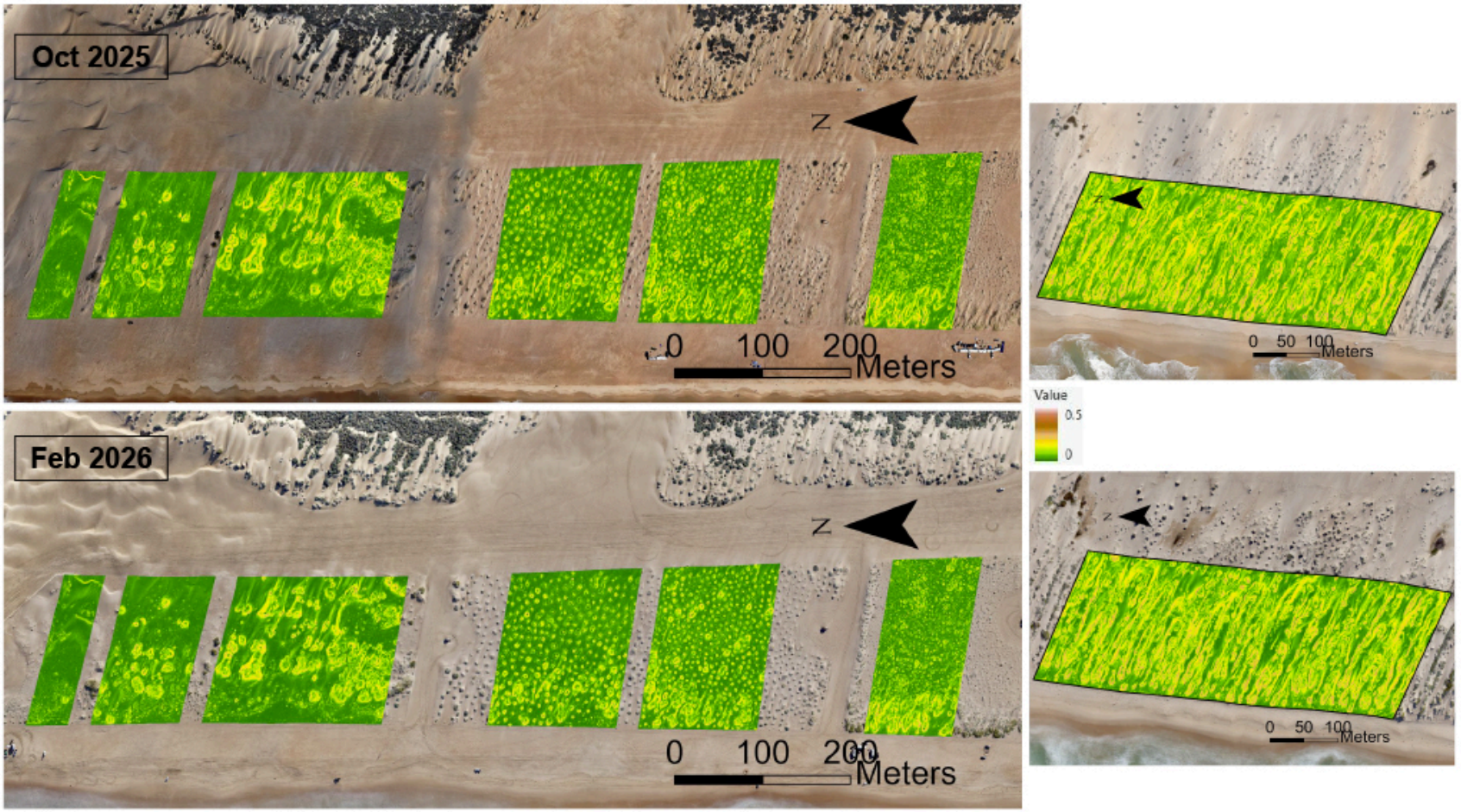

Oct 2020
N
0 100 200
Meters
Feb 2021
N
0 100 200
Meters
Value
0.5
0
0 50 100
Meters
0 50 100
Meters


Oct 2021
N
0 100 200
Meters
Feb 2022
N
0 100 200
Meters
N
0 50 100
Meters
Value
0.5
0
N
0 50 100
Meters


Oct 2022
N
0 100 200
Meters
Feb 2023
N
0 100 200
Meters
0 50 100
Meters
Value
0.5
0
0 50 100
Meters


Oct 2023
N
0 100 200
Meters
Feb 2024
N
0 100 200
Meters
N
0 50 100
Meters
Value
0.5
0
N
0 50 100
Meters


Oct 2024
N
0 100 200
Meters
Feb 2025
N
0 100 200
Meters
N
0 50 100
Meters
Value
0.5
0
N
0 50 100
Meters


Oct 2025
N
0 100 200
Meters
Feb 2026
N
0 100 200
Meters
N
0 50 100
Meters
Value
0.5
0
N
0 50 100
Meters

*THIS PAGE WAS INTENTIONALLY LEFT BLANK.*

July 16, 2026

**Memo: SAG Review of UCSB Report "2025-2026 ODSVRA Foredune Restoration Area UAS Monitoring Report" (UCSB)**

**From**: Scientific Advisory Group (SAG)[1]

**To:** Jon O'Brien, California Department of Parks and Recreation (CDPR)

**Cc**: Ronnie Glick, California Department of Parks and Recreation (CDPR)

The Scientific Advisory Group (SAG) received a copy of the University of California, Santa Barbara (UCSB) report *"**2025-2026 ODSVRA Foredune Restoration UAS Monitoring Report**"* on July 10, 2026. SAG members have had the opportunity to review the document and this memo provides feedback on the UCSB report.

UCSB has produced a well-written and very informative report that discusses changes to the Foredune Restoration Area (FRA) since the area was closed to Off-Highway Vehicle (OHV) traffic in October, 2019 and subsequently treated with various combinations of surface treatments, seeding, and plantings in February, 2020. The *Executive Summary* is particularly well-written, concise, and factual. As with previous reports on the same topic, the methods are clearly outlined and the results presented with the aid of graphics and tables.

Major differences between this report and those from previous years include: (1) re-sizing the analytical sub-areas within each of the six Treatment Plots (TPs) so as to avoid potential bias from 'edge' effects such as sand fences and human structures; (2) identification of a reference site (North Oso Flaco or NOF) against which changes and trends within each of the TPs can be evaluated as they evolve towards more natural conditions (as represented by NOF); and (3) utilization of a new set of three metrics to assess TP performance (sediment budget changes, percent plant cover change, and terrain roughness index or TRI). The new metrics are considered to be more useful in assessing 'dynamic equilibrium' conditions within the foredune area given that there has been six years of foredune development and vegetation growth. In previous reports, six metrics were used, and these largely assessed performance on the basis of the early evolution of the foredunes from an essentially barren sand surface. Thus, the initial six metrics are less relevant now than when they were first applied, as noted in the SAG review of the 2024-2025 report. These changes are a very positive development in the monitoring and analysis of the FRA.

SAG members had the following specific queries or comments:

1) Page 2. Add "TRI" to the list of abbreviations.
2) Page 2, paragraph 4. Consider removing "less variable" before "positive values", since the degree of variability has not been defined.

[1] SAG member Dr. Ian Walker recused himself from SAG review of this document due to conflict of interest.

3) Page 3, paragraph 1. The percentage values reported do not need this many significant digits.
4) Page 3, paragraph 2. Please clarify the acronym TRI: this section states 'TRI' is topographic roughness index, while elsewhere the paper defines TRI as terrain roughness index.
5) Page 3, paragraph 2. Is TRI influenced by vegetation cover or does it consider only a bare-earth surface? If the former, is there duplicity given that percent vegetation cover is also a metric? How can this avoided/managed?
6) Page 4, second last paragraph. "dune development over through time…" Strike 'over.'
7) Page 9. The pixel size is reported as 10 cm, yielding a search window that is 30 cm by 30 cm. Have you performed tests to determine whether a larger search window provides different results because it would 'see' greater variation in topography corresponding to larger dune elements? Does the size of the search window matter?
8) Page 9, Equation 1. "xoo" represents the elevation of the central cell. (add 'elevation')
9) Page 9. What is the uncertainty in TRI?
10) Page 9, Section 3.1. "…NOF sites wherein the analyses were conducted" Awkward sentence construction.
11) Page 12, Table 2. Check consistency and number of significant digits.
12) Page 13. Locations of statistically insignificant change are not shown in the change maps and are not used to calculate sediment volumes. This seems sensible, but could you provide some sense of what constitutes an 'insignificant change' so that the reader has a better idea of the scales involved. The legend in Figure 5 seems to suggest that pixels with volume changes between -0.05 m and +0.05 m are not shown. Are these the insignificant ones. Can you provide a sense of the number of insignificant pixels as a percentage of the total number of pixels in the DEM (i.e., less than 1%, approximately 5%, as much as 20%)?
13) Page 13, first paragraph. Consider moving the sentence beginning with "Pixels of statistically significant…" before the sentence beginning with "Locations of statistically insignificant change…" so that the reader knows what the significance level is.
14) Page 13, Section 3.3. "…that are normalized by area and over time…" Strike 'over.'
15) Pages 14-16; Figures 5, 6, and 7. The colors on the map look brown and don't seem to correspond to the color palette in the legend. This makes it very hard to interpret these maps. Perhaps there are too many divisions, and it might be better to reduce them down to, say 10 rather than 20. The eye can't easily differentiate the shades or red and blue, and all we really see is light brown and tan with the occasional blotch of blue or red.
16) Page 18, last paragraph. Are these numbers correct? It seems like they are off by a decimal point or two. Specifically, the narrative says that the NOF had a net positive budget change of 2.9 $m^3m^{-2}mo^{-1}$, and this translates to a net depth change of 2.9 meters in one month! More striking is a net change in the beach area in front of the NOF of -29 m. This can't be. Table 3 indicates that all the values as shown are multiplied by 100, which seems to explain the confusion in the paragraph on page 18. Figure 8 shows the same data (?) in graphical form, and the volumetric changes are much more sensible (i.e., less than 5 cm or 0.05 m in most TPs). Also, with respect to Table 3, what does 'Net Change' actually mean, and how was it calculated? It doesn't seem like it is the cumulative change since October 2019 nor is it the average change. How do you get a value of -29

for NOF when all the other numbers bounce between positive and negative values, with the largest being -16?

17) Page 20. High value pixels, close to 1, indicate rough terrain while smooth terrain is represented by values close to 0 (as in Figure 9). This is odd because Riley et al. (1999) suggest that level terrain is between 0-80 whereas a highly rugged surface has values of 498-958. Note also that equation 1 in the report divides the sum by 'n' (the number of values) whereas the original equation in Riley et al (1999) does not. It seems evident from equation 1 that there can't be an upper limit of 1, and the values used to indicate how rough a surface is will depend on the units of measure (e.g., m, cm, feet, etc.). Please clarify.
18) Page 25, last paragraph. "…although TP2 starts to develop…" Change 'starts' to 'started.'
19) Page 27, Figure 10. The caption and the vertical axis have different titles ("$DV_{area}$" versus "$DV_{TP\#}$")
20) Page 28, Table 5. The caption reads that green values indicate those closest to NOF (~1) but there are green values less than 1 and down to 0.00. And there are other cells with values less than 1 that are not colored green. Please clarify.

Respectfully,

The Scientific Advisory Group

Bernard Bauer (Chair), Jack Gillies, Jenny Hand, Leah Mathews

*THIS PAGE WAS INTENTIONALLY LEFT BLANK.*

**ODSVRA Dust Control Program SAG Review Draft 2026 ARWP**

**ATTACHMENT 06**

**Summary of Vegetation Monitoring of Restoration Sites at ODSVRA (2025)**

**(State Parks' ARWP Work Product)**

*THIS PAGE WAS INTENTIONALLY LEFT BLANK.*

# Summary of Vegetation Monitoring of Restoration Sites at ODSVRA

**Monitoring Species Composition Within Restoration Sites**

Background

Ground monitoring surveys were conducted in October 2025 to determine species richness and relative species cover within a sample of previously treated restoration sites. Reconnaissance-level surveys recorded species richness (number of species present) and the line-intercept survey method measured relative cover between species. Both methods were completed within all treatment areas of the 48-acre Foredune Restoration Area (FRA), the North Oso Flaco Foredune Reference Site (NOF), and three back dune project areas. Back dune project areas that had been planted with native container plants and native seeds two and three years prior, in late 2022 or early 2023, were chosen for sampling, including, 2023-VG-01, 2022-VG-09 and 2022-VG-13. Areas with two- to three-year-old plantings are chosen to allow the plants and seeds enough time to begin establishment before surveys are conducted. The results from these surveys are used to prioritize planting and seedling supplementation for improved species diversity and cover within project sites.

Changes to Monitoring and Reporting

In past Annual Report and Work Plans (ARWP), the line intercept surveys were used to provide an assessment of total vegetative cover within the FRA and the results were compared to the UAS vegetation cover assessment. In consultation with key members of the Scientific Advisory Group (SAG), it was determined that this was redundant and provided little utility, given that the UAS surveys measure total vegetative cover over the entire FRA at a fine scale while the line intercept surveys measure only a small sample of the FRA (four 30-meter transects per Treatment Plot). Furthermore, the line intercept surveys have shown similar results to the UAS surveys since 2022. For this reason, an assessment of total vegetative cover and a comparison with the UAS surveys is not provided for this monitoring report. However, State Parks will continue reporting the other results, including species richness and relative species cover, as they are not currently being evaluated with the UAS surveys. An assessment of species richness and relative species cover is important in evaluating biodiversity of the FRA and the progression of species composition toward a natural and healthy foredune habitat. Furthermore, evaluating species distribution provides insight into the resilience of the site toward environmental changes and ultimately its influence on emissions reduction.

In consultation with members of the SAG, it was determined that altering the placement of the transect lines to run in the direction of the prevailing wind could better inform species distribution within the FRA and provide a better comparison to other sites that use the same line intercept method. For this reason, in accordance with recommendations by members of the SAG, beginning in 2026, State Parks plans to modify the location and direction of all of the FRA transect lines to run in the direction of the prevailing wind for the entire width of the FRA within each of the Treatment Plots (previously randomized placement and direction). With this modification, the surveys will better capture the change in species composition along the prevailing wind and provide better insight into the interaction of species with environmental factors including, dune development, deflation surfaces, wind exposure, tidal events and exposure to salt spray. State Parks will continue in consultation with members of the SAG to refine the survey protocol, specifically to determine the number and placement of the transect lines.

Methods

For reconnaissance-level surveys, the entire project area is visually searched as the surveyors walk in belt transects of no more than 15-meters apart so that full visual coverage of the project area is obtained. All species observed are identified and documented to determine species richness within the project area. For the reference sites, reconnaissance level surveys follow the same methodology and cover the area within 50-meters of the line-intercept transects.

For the line-intercept surveys, relative species cover within each project area is estimated by measuring vegetation cover using a measuring tape along 30-meter transect lines. Three lines were sampled in back dune project areas and four lines were sampled in the FRA in 2025. Line intercept method is defined by the following: (percent cover = distance a+b+c+d+e+f / total transect length), where a, b, c, etc. are the intercept lengths of species cover. Starting points for the transect lines were randomly selected using GIS software. The direction of the transect lines were randomly selected from the eight cardinal and intermediate directions (i.e., north, northeast, east, southeast, south, southwest, west, and northwest). Within the FRA and the NOF, the directions of three of the four lines in each area were randomly selected and the fourth line was run in the direction of the prevailing wind. Transect starting locations and directions for these areas have remained the same each year. Photo documentation of the transect line from the starting point and ending point is taken for every transect.

To conduct sampling, the pre-determined starting and ending points are located using a hand-held GPS unit with sub-meter accuracy. Wooden stakes are then placed at the starting and ending points of the transect line, a measuring tape is fastened to the stake at the starting point and run along the transect so that it lies flat on the ground and/or slack over the top of the vegetation canopy and is then secured to the wooden stake at the end point. Stakes are re-installed each year as stakes become buried or dislodged by sand movement between sampling years. Because of this, there is some variability in the transect beginning and ending points between years, estimated to be less than 1-meter variability based on the reported GPS unit accuracy and reviewing reference photos between years. As the tape crosses vegetation, the species is noted on the datasheet along with the beginning and ending measurements of the vegetation cover under rows labeled “Start” and “Stop”. If vegetation cover of two different species overlaps, the vegetation cover of both species is documented separately. A “Stop” in cover for a given species is not recorded until gaps in vegetation cover exceed 5 cm. This is done to improve sampling efficiency as there can be many small gaps between individual leaves and branches. Cover of dead woody vegetation is documented in the same way and noted as “dead” unless it was clearly the result of seasonal dieback of a perennial plant that is still viable.

Note, that for sampling that occurred in 2020 and 2021, gaps in branches or leaves of an individual plant were recorded as continuous cover. In 2022 and subsequent years, a “Stop” in cover was recorded if the gap in cover exceeded 5 cm regardless of whether the gap was between branches of the same individual plant or a different plant. As a result, cover in 2020 and 2021 appears to be inflated for species that can have wide spreading branches, particularly red sand verbena (*Abronia maritima*) and beach primrose (*Camissoniopsis cheiranthifolia*). When comparing the results of the transect surveys to the Uncrewed Aerial System (UAS) surveys for those years, the transect surveys showed substantially greater total cover particularly in areas where red sand verbena and beach primrose were abundant, notably TP3 (Native Seed and Sterile Seed Treatment) and TP6 (Parks Classic). When a strict 5 cm gap threshold was implemented in 2022 and in subsequent years, the results between the transect surveys and the UAS

surveys showed similar vegetation cover (refer to 2025 ARWP – Attachment 07). For this reason, the results from 2020 and 2021 transect sampling are not used to evaluate trends in cover for this report.

For this assessment both the foredune restoration area and back dune project areas were sampled in October 2025. A reference site for foredune vegetation was selected in the NOF and was also sampled in October 2025 and had previously been sampled in 2023 and 2024. Reference sites for back dune areas were last sampled in October 2024. Reference sites for both foredune and back dune vegetation were selected in areas that have been closed to vehicular activity for at least 20 years and have not been subject to restoration plantings in the past. Within back dune habitats, early succession communities (early seral) and climax communities (late seral) can vary considerably in species composition and percent cover. For this reason, both early seral and late seral reference sites were sampled for comparison.

2025 Results

48-acre Foredune Project Area (FRA) and Foredune Reference Site

In 2025, after the sixth growing season for the FRA, richness increased in every treatment area from the previous year. Four species, beach bur (*Ambrosia chamissonis*), red sand verbena, yellow sand verbena (*Abronia latifolia*) and sea rocket (*Cakile maritima*), were present within all treatment areas, including the TP1 (Control) and the reference site. TP6 (Parks Classic) had the greatest richness with 12 species present, matching the richness of the reference site. TP5 (High Density Nodes) and TP4 (Low Density Nodes) followed closely behind with 11 species and 10 species respectively. The full FRA shared 10 species with the reference site with only two species from the reference site not represented, specifically, beach morning glory (*Calestegia soldanella*) and mock heather (*Ericameria ericoides*). Within the FRA, 6 species were present that were not included in the original seed and container plant mix that was used during project installation. Of these, 2 species are non-native including sea rocket and sea fig (*Carpobrotus chilensis*). Refer to Table 1. Results from the FRA line intercept transect sampling.

Table 1. Results from the FRA line intercept transect sampling.

| **Foredune Restoration Area Vegetation Assessment (Oct 2025)** | | | | | | | |
|---|---|---|---|---|---|---|---|
| | **Area 1 Control** | **Area 2 Native Seed** | **Area 3 Native Seed & Grain Seed** | **Area 4 Low Density Nodes** | **Area 5 High Density Nodes** | **Area 6 Parks Classic** | **Reference North Oso Flaco Foredune** |
| **Age of Planting (years)** | **5.5** | **5.5** | **5.5** | **5.5** | **5.5** | **5.5** | **-** |
| **2025 Species Richness** | **5** | **4** | **8** | **10** | **11** | **12** | **12** |
| **2024 Species Richness** | **4** | **3** | **5** | **9** | **10** | **10** | **12** |
| **Number of Species in 2020 Plant/Seed Palette** | **0** | **8** | **8** | **9** | **9** | **10** | **-** |
| **Species** | **2025 Mean Percent Cover** | | | | | | |
| *Abronia latifolia* | P | P | P | P | 0.04% | P | P |
| *Abronia maritima* | 0.18% | 1.94% | 6.09% | 0.14% | 2.13% | 1.27% | 4.54% |
| *Achillea millefolium* | - | - | - | - | P | - | - |
| *Ambrosia chamissonis* | 0.13% | 2.50% | 3.68% | 2.93% | 2.07% | 6.08% | 4.96% |
| *Atriplex leucopylla* | P | - | - | 0.20% | P | P | - |

| Foredune Restoration Area Vegetation Assessment (Oct 2025) | | | | | | | |
|---|---|---|---|---|---|---|---|
| | **Area 1 Control** | **Area 2 Native Seed** | **Area 3 Native Seed & Grain Seed** | **Area 4 Low Density Nodes** | **Area 5 High Density Nodes** | **Area 6 Parks Classic** | **Reference North Oso Flaco Foredune** |
| *Camissoniopsis cheiranthifolia* | - | - | P | 0.08% | 0.13% | 1.63% | 0.79% |
| *Eriogonum parvifolium* | - | - | - | - | - | P | P |
| *Eriophyllum staechadifolium* | - | - | P | P | P | 0.96% | - |
| *Fragaria chiloensis* | - | - | - | - | - | P | - |
| *Malicothrix incana* | - | - | - | P | P | - | 0.28% |
| *+*Cakile maritima* | 1.88% | 0.46% | 0.10% | 0.03% | 0.41% | 0.05% | 3.07% |
| *+Calestegia soldanella* | - | - | - | - | - | - | 0.89% |
| *+*Carpobrotus chilensis* | - | - | - | - | - | P | 0.71% |
| *+Ericameria ericoides* | - | - | - | - | - | - | P |
| *+Erigeron blochmaniae* | - | - | - | - | - | P | P |
| *+Monardella undulata ssp. crispa* | - | - | P | P | P | P | - |
| *+Phacelia ramosissima* | - | - | P | P | - | - | - |
| *+Senecio blochmaniae* | - | - | - | - | P | - | P |
| *Dead Vegetation* | 0.03% | - | - | - | - | 0.75% | - |
| *Non-native species; Species not included in 2020 seed and plant installation; P=Present within Project Area but not on transect line | | | | | | | |

In 2025, the species with the highest vegetation cover across all treatments was beach bur with a mean cover of 2.9% in the FRA which surpassed red sand verbena which had previously shown the greatest cover. However, beach bur cover did decline in 2025 from a high of 3.96% in 2024. The species with the second highest cover in 2025 was red sand verbena with 1.96% down from its high of 4.11% in 2023. All other species had a cover below 1% with sea scale (*Atriplex leucophyla*) showing a decrease in cover each year and sea rocket showing an increase. None of the other species present showed a clear trend in cover change between years. The NOF followed a similar trend to the FRA with red sand verbena showing a greater than 50% reduction in cover from 2023 to 2025 with 9.88% in 2023 to 4.54% in 2025. Within the reference site, beach bur showed an increase from 4.16% in 2023 to 6.46% in 2024 and then a slight decrease in 2025 to 4.96%. Sea rocket also followed a similar trend between the FRA and the reference site with an increase each year that sampling occurred. Refer to Figure 1. Graph of trends in species cover within the FRA and the NOF.

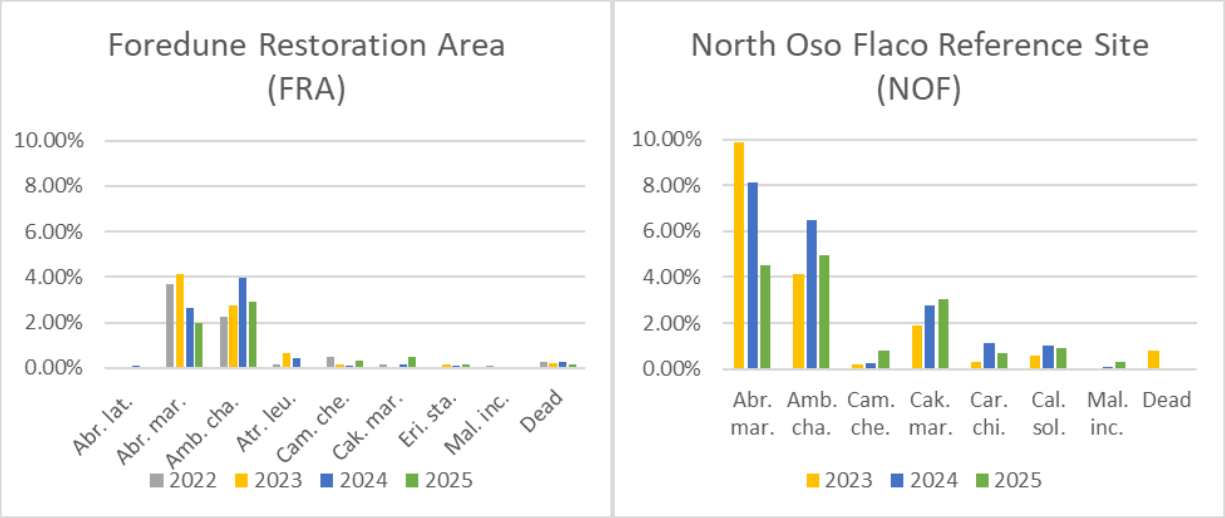



Figure 1. Trends in species cover within the FRA and the NOF. Note sampling did not occur in the NOF in 2022.

When comparing treatment areas, red sand verbena showed less cover in 2025 than in 2022 for all treatment areas except for TP1 (Control). Cover of sand verbena peaked in 2022 in both TP2 (Native Seed Only) and in TP3 (Native Seed and Sterile Grain Seed) and peaked in 2023 in the remaining treatment areas. This decline in red sand verbena is also seen in the NOF, indicating that it is caused by something within the broader area and is not unique to the FRA. This change in red sand verbena cover is also apparent in the photo documentation of the transect lines. From the photos, it appears that between 2023 to 2025 red sand verbena vegetation, across treatment areas and the NOF, begins to fragment as the nebkha build in height. More investigation would be needed to determine a cause, but the decline in vegetation could possibly be linked to extreme tidal events or changes in weather patterns in recent years. All of the treatment areas show beach bur cover increasing from 2022 to 2025 except for TP5 (High Density Nodes). However, in 2024, beach bur cover peaked in TP3 (Native and Sterile Seed), TP4 (Low Density Nodes) and TP6 (Parks Classic). Across all years and all treatment sites except for the TP1 (Control), either red sand verbena or beach bur had the highest cover. Within the TP1 (Control), sea rocket was the dominant species across all years, however, red sand verbena and beach bur were increasing cover to the point of detection on the transect lines in 2025. All other species varied in cover across years and are not showing strong trends in cover change across treatment areas. Refer to Figure 2. Comparison of species cover over time between treatment areas within the FRA, and Figures 3 through 16. Photos of FRA and NOF transects.

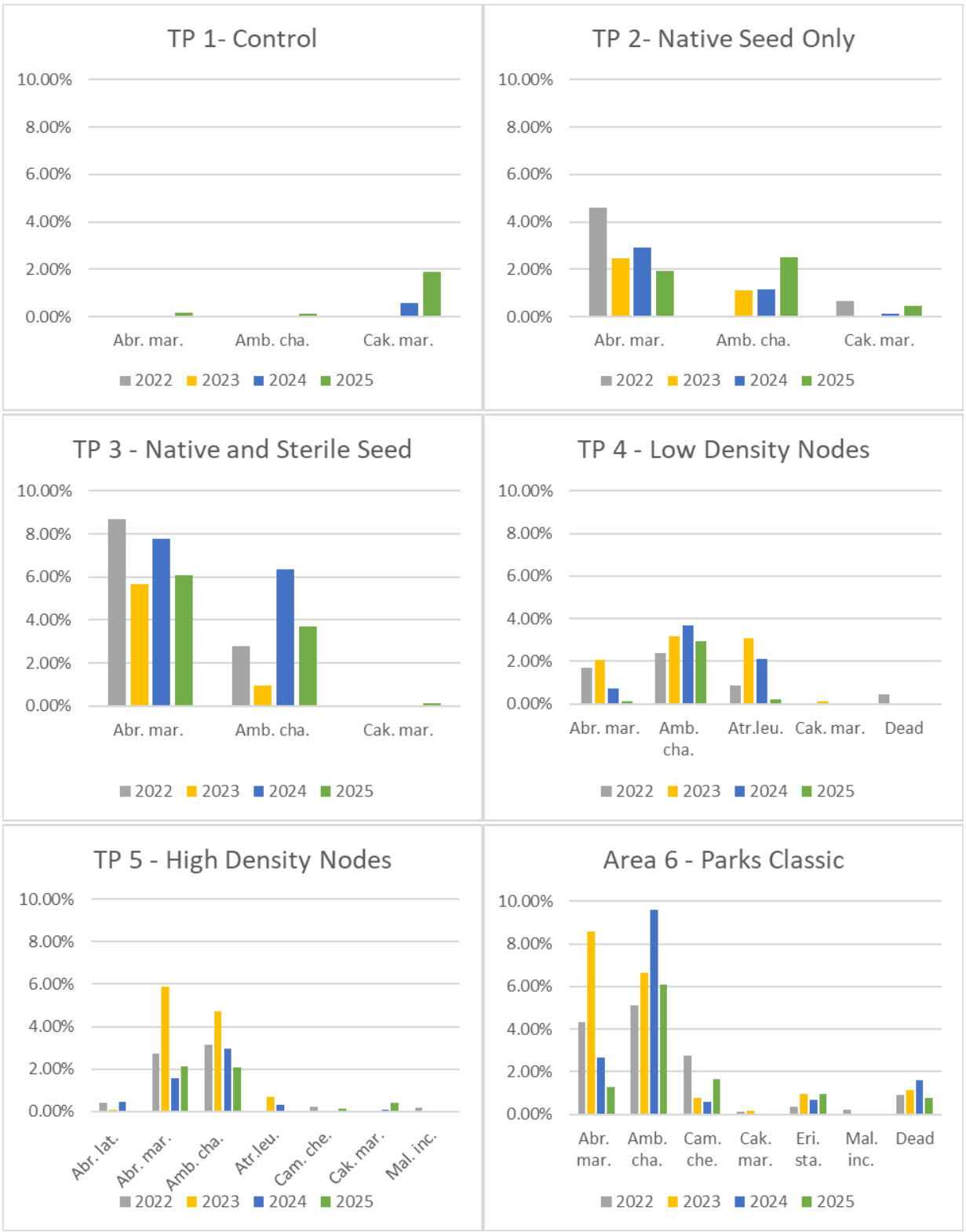



Figure 2. Comparison of species cover over time between treatment plots within the FRA.



Figure 3. TP1 (Control), Transect #3 in September 2024 facing north. Transect cover measured at 0.0% for all species.



Figure 4. TP1 (Control), Transect #3 in October 2025 facing north. Transect cover measured at 0.7% red sand verbena, 0.4% beach bur and 6.4% sea rocket.



Figure 5. TP2 (Native Seed), Transect #1 in September 2024 facing south. Transect cover measured at 11.7% red sand verbena and 4.6% beach bur.



Figure 6. TP2 (Native Seed), Transect #1 in October 2025 facing south. Transect cover measured at 7.77% red sand verbena and 9.73% beach bur. Note the decline in red sand verbena cover.



Figure 7. TP3 (Native Seed and Sterile Seed), Transect #2 in October 2024 facing southeast. Transect cover measured at 19.1% red sand verbena and 7.9% beach bur.



Figure 8. TP3 (Native Seed and Sterile Seed), Transect #2 in October 2025 facing southeast. Transect cover measured at 13.7% red sand verbena and 6.3% beach bur.



Figure 9. TP4 (Low Density Nodes), Transect #3 in October 2023 facing south. Transect cover measured at 7.47% red sand verbena, 4.17% beach bur and 11.5% sea scale.



Figure 10. TP4 (Low Density Nodes), Transect #3 in October 2025 facing south. Transect cover measured at 0.3% red sand verbena, 8.6% beach bur and 0.8% sea scale. Note the decline in red sand verbena.



Figure 11. TP5 (High Density Nodes), Transect #2 in October 2023 facing southeast. Transect cover measured at 23.6% red sand verbena and 7.03 % beach bur.



Figure 12. TP5 (High Density Nodes), Transect #2 in October 2023 facing southeast. Transect cover measured at 8.27% red sand verbena and 4.63% beach bur. Note the decline in red sand verbena cover.



Figure 13. TP6 (Parks Classic), Transect #3 in October 2023 facing east. Transect cover measured at 30.8% red sand verbena and 12.8 % beach bur.



Figure 14. TP6 (Parks Classic), Transect #3 in October 2025 facing east. Transect cover measured at 4.2% red sand verbena and 14.9 % beach bur. Note the decline in red sand verbena cover.



Figure 15. NOF Transect #2 in October 2024 facing east. Transect cover measured at 28.5% red sand verbena and 10.8% beach bur.



Figure 16. NOF Transect #2 in October 2025 facing east. Transect cover measured at 14.7% red sand verbena and 5.1% beach bur. Note the decline in vegetative from previous photo.

Back Dune Projects

Each of the back dune project areas that were surveyed showed healthy levels of vegetation cover, ranging from 24.2% to 31.4%. None of the project sites that were sampled met or exceeded the percent cover of the reference sites (67.2% for early seral and 78.5% for late seral) but they did show substantial levels of cover and are anticipated to increase over time as plantings continue to grow. Of the 22 native species present within the early seral and late seral reference sites, one back dune project (2022-VG-13) had 7 of the species present and the other two project areas (2023-VG-01 and 2022-VG-09) each had 14 present with a total richness (including non-native species) of between 12 and 25 species. The dominant species within the early seral reference site, dune bush lupine (*Lupinus chamissonis*), was also the dominant within all surveyed backdune projects with cover measurements of 21.14%, 21.10%, and 17.44% compared to 25.3% in the early seral reference site. Percent cover and richness are both anticipated to increase and approach the cover of the reference sites within the upcoming growing seasons. Refer to Table 2. Results from the back dune restoration project line intercept transect sampling.

Table 2. Results from the back dune restoration project line intercept transect sampling.

| **Back Dune Restoration Project Vegetation Assessment (Oct 2025)** | | | | | |
|---|---|---|---|---|---|
| *Non-native species<br>P=Present within project area | **Sand Highway (north) (2023-VG-01)** | **Eucalyptus Tree (center) (2022-VG-09)** | **Eucalyptus Tree (west) (2022-VG-13)** | **Reference - Early Seral (Oct 2024)** | **Reference - Late Seral (Oct 2024)** |
| **Age of Planting (years)** | **2.5** | **2.5** | **2.5** | **-** | **-** |
| **Species Richness** | **22** | **25** | **12** | **17** | **16** |
| **Transect 1** | **32.5%** | **25.9%** | **0.8%** | **60.0%** | **77.2%** |
| **Transect 2** | **29.4%** | **3.9%** | **54.2%** | **54.0%** | **82.4%** |
| **Transect 3** | **32.3%** | **44.2%** | **17.7%** | **87.8%** | **75.7%** |
| **Mean Percent Cover** | **31.4%** | **24.6%** | **24.2%** | **67.2%** | **78.5%** |
| **Species** | | | | | |
| *Abronia latifolia* | - | - | P | - | - |
| *Abronia umbellata* | - | P | - | - | - |
| *Achillea millefolium* | 0.16% | 0.12% | P | 2.2% | 0.4% |
| *Acmispon glaber* | 0.98% | 2.44% | | P | 2.4% |
| *Ambrosia chamissonis* | P | - | 0.57% | - | - |
| *Astragalus nuttallii* | P | P | - | - | - |
| *Baccharis pilularis* | - | - | - | 0.6% | P |
| *Cakile maritima* | - | - | 0.43% | - | |
| *Camissoniopsis cheiranthifolia* | 0.86% | P | 0.73% | - | - |
| *Carex praegracilis* | 0.02% | P | - | - | - |
| *Castilleja affinis* | P | 0.18% | - | P | - |
| *Chenopodium californicum* | - | - | - | - | 1.2% |
| *Cirsium occidentale* | - | - | - | P | - |
| **Conicosia pugioniformis* | - | - | - | 1.0% | 0.01% |
| *Corethrogyne filaginifolia* | 0.43% | - | - | P | 6.8% |
| *Cryptantha clevelandii* | - | - | - | - | 3.8% |
| *Dudleya lanceolata* | P | P | - | - | 0.17% |
| *Eriastrum densifolium* | P | P | - | - | - |
| *Ericameria ericoides* | P | P | - | 27.3% | 59.5% |
| *Erigeron blochmaniae* | P | P | - | 3.0% | - |
| *Eriogonum parvifolium* | 3.56% | 1.01% | 0.69% | - | 0.24% |

| Back Dune Restoration Project Vegetation Assessment (Oct 2025) | | | | | |
|---|---|---|---|---|---|
| *Non-native species<br>P=Present within project area | **Sand Highway (north) (2023-VG-01)** | **Eucalyptus Tree (center) (2022-VG-09)** | **Eucalyptus Tree (west) (2022-VG-13)** | **Reference - Early Seral (Oct 2024)** | **Reference - Late Seral (Oct 2024)** |
| *Eriophyllum staechadifolium* | 1.29% | P | 1.56% | - | - |
| *Erysimum suffrutescens* | P | P | - | 0.5% | 0.14% |
| *Horkelia cuneata* | P | P | - | - | - |
| *Juncus lescurii* | P | P | - | - | - |
| *Lupinus chamissonis* | 21.14% | 21.10% | 17.44% | 25.3% | P |
| *Monardella undulata crispa* | 2.49% | P | 2.98% | P | - |
| *Morella californica* | - | P | - | - | - |
| *Phacelia ramosissima* | 0.39% | - | 2.56% | 0.6% | - |
| *Populus trichocarpa* | - | P | - | - | - |
| *Pseudognaphalium biolettii* | - | P | | P | - |
| *Pseudognaphalium californicum* | - | - | - | - | 0.03% |
| *Pseudognaphalium ramosissimum* | - | P | P | p | 0.4% |
| *Rubus urisinus* | - | - | - | - | P |
| *Salix lasiolepis* | 0.57% | P | - | P | - |
| *Senecio blochmaniae* | 0.38% | P | P | 0.6% | 0.06% |
| *Dead woody vegetation* | - | 0.01% | - | 9.5% | 16.7% |

**Photo Point Monitoring**

State Parks has conducted on-the-ground photo point monitoring of the FRA since 2020. Initial photo point monitoring occurred before the installation of the FRA in February 2020. Follow-up photo point monitoring occurred in May 2020, October 2020, and each subsequent October since 2020. Photo points are located on all four corners of each treatment area. For each photo point, two photos are taken, each with one of the treatment area boundary lines on the outer edge of the photo with the interior of the treatment area centered in the photo. There is also one photo point overlooking the entire FRA. Select ground photo point monitoring examples are shown in Figures 17 through 28.

On-the-ground monitoring of back dune planting projects was conducted in 2025 to capture representative photos of the back dune project areas. Back dune ground photo monitoring was initiated in 2018 and is usually conducted in the summer and/or fall of each year. Photo points are positioned to capture changes within the general areas where back dune projects are located. The number of photos for each photo point and the number of photo points vary at each location to sufficiently capture each area. In total, 30 photo points were monitored in 2025. Select back dune ground photo point monitoring examples are shown in Figures 29 through 34.

UAS photo point monitoring of project areas has been conducted during the winter in past years but was not conducted in the winter of 2025/2026. State Parks plans to resume UAS photo point monitoring during the winter of 2026/2027.



Figure 17. Photo point of FRA TP 1 (Control) from the west fenceline facing south. Photo taken on November 4, 2024



Figure 18. Photo point of FRA TP 1 (Control) from the west fenceline facing south. Photo taken on October 22, 2025.



Figure 19. Photo point of FRA TP2 (Native Seed) from the east fenceline facing west, two weeks before treatment. Photo taken on February 4, 2020.



Figure 20. Photo point of FRA TP2 (Native Seed) from the east fenceline facing west. Photo taken on October 22, 2025.



Figure 21. Photo point of FRA TP3 (Native Seed and Sterile Grain Seed) from the east fenceline facing north, two weeks before planting treatment. Photo taken on February 4, 2020.



Figure 22. Photo point of FRA TP3 (Native Seed and Sterile Grain Seed) from the east fenceline facing north. Photo taken on October 22, 2025.



Figure 23. Photo point of FRA TP4 (Low Density Nodes) from the west fenceline facing south. Photo taken on October 18, 2022.



Figure 24. Photo point of FRA TP4 (Low Density Nodes) from the west fenceline facing south. Photo taken on October 22, 2025.



Figure 25. Photo point of FRA TP5 (High Density Nodes) from the west fence facing north. Photo taken on October 24, 2023.



Figure 26. Photo point of FRA TP5 (High Density Nodes) from the west fence facing north. Photo taken on October 22, 2025.



Figure 27. Photo point of FRA TP6 (Parks Classic) from the west fence facing south. Photo taken on October 24, 2023.



Figure 28. Photo point of FRA TP6 (Parks Classic) from the west fence facing south. Photo taken on October 22, 2025.



Figure 29. Photo point of La Grille Hill (2022-VG-03) facing south. Photo taken on October 20, 2022.



Figure 30. Photo point of La Grille Hill (2022-VG-03) facing south. Photo taken on October 23, 2025.



Figure 31. Photo point of Eucalyptus Tree (2021-VG-03 and 2022-VG-05) facing south. Photo taken on October 20, 2022.



Figure 32. Photo point of Eucalyptus Tree (2021-VG-03 and 2022-VG-05) facing south. Photo taken on November 6, 2025.



Figure 33. Photo point of Table Top Southeast (2024-VG-03) facing east. Photo taken on March 5, 2024.



Figure 34. Photo point of Table Top Southeast (2024-VG-03) facing east. Photo taken on October 22, 2025.

**ODSVRA Dust Control Program SAG Review Draft 2026 ARWP**

**ATTACHMENT 07**

**Increments of Progress Toward Air Quality Objectives, ODSVRA Dust Control 2025 Update**

- Increments of Progress Toward Air Quality Objectives, ODSVRA Dust Control 2025 Update (DRI Document)
- SAG Review of Desert Research Institute (DRI) "Increments of Progress Toward Air Quality Objectives, ODSVRA Dust Control 2025 Update" (SAG Memo)

*THIS PAGE WAS INTENTIONALLY LEFT BLANK.*

**Increments of Progress Towards Air Quality Objectives - ODSVRA Dust Controls, 2025 Update**

J.A. Gillies, G. Nikolich, E. Furtak-Cole, Division of Atmospheric Science, Desert Research Institute

Dust controls including temporary wind fences and vegetation projects have been used within the Oceano Dunes State Vehicular Area (ODSVRA) to reduce the emissions of $PM_{10}$ originating from the ODSVRA and to lower the regional $PM_{10}$ burden on the Nipomo Mesa. Beginning in 2014 and continuing through 2025, a total of 412.5 acres of managed dust control areas have been established in the ODSVRA (State of California, Department of Parks and Recreation, 2025).

Here we demonstrate that the $PM_{10}$ data measured at CDF and Mesa2 show that $PM_{10}$ measured at CDF and Mesa2 are lower now than prior to the establishment of dust controls. The reduction in $PM_{10}$ has scaled with the increase in acres of dust control upwind of these monitoring sites through to 2022 when the number of acres of managed dust control areas stabilized at 412.5 acres. Subsequent to 2022, there has been supplemental planting of vegetation to maintain or increase protective cover on the established management areas. In this report we use the $PM_{10}$ data in combination with wind data measured at the S1 tower (10 m above ground level, AGL) to update the ratio Total $PM_{10}$ ($TPM_{10}$):Total Wind Power Density (TWPD) for CDF and Mesa2 and acres of dust control with data from April to September 2025.

**Methods**

The metric used to evaluate the production of $PM_{10}$ from the ODSVRA is the ratio of the summation of the hourly $PM_{10}$ ($TPM_{10}$, $\mu g\ m^{-3}$ [measured with a Beta Attenuation Monitor or BAM]) operated by the San Luis Obispo County Air Pollution Control District (SLOAPCD) and the summation of thresholded hourly wind power density ($W\ m^{-2}$) as measured at the S1 tower within the ODSVRA, for winds that are expected to cause saltation and dust emissions during the spring-summer period (April through September). Only valid, paired hourly values of $PM_{10}$ ($\mu g\ m^{-3}$) and wind power density ($W\ m^{-2}$) are used for the summations.

Wind power density (WPD, $W\ m^{-2}$) is defined as (e.g., Kalmikov, 2017):

$$WPD=0.5\ \rho_a\ u^3 \quad (1)$$

where $\rho_a$ is air density ($kg\ m^{-3}$), and u ($m\ s^{-1}$) is wind speed at the measurement height above ground level (10 m AGL), a unit area of 1 $m^2$ is assumed in this application. For comparison among different locations and between different years, the height of measurement of wind speed and the lower limit of mean hourly wind speed for summation of Total Wind Power Density (TWPD) must be the same.

The following constraints were applied for the environmental data available:

1) A wind speed filter was applied based on screening for the conditions where it was most likely that the $PM_{10}$ reaching CDF and Mesa2 was due to the generation of dust by saltation within the ODSVRA. Only wind directions from 248° to 326° were used to ensure, conservatively, that the air flow that reached CDF and Mesa2 had most likely travelled across the ODSVRA.
2) Only wind speeds greater than a threshold value (see below) at which a visible trend between wind speed and increasing $PM_{10}$ at the CDF and Mesa2 sites were determined from data that relates $PM_{10}$ to wind speed measured at each of the sites.

3) Based on precipitation data from monitoring sites near the ODSVRA, the number of days where precipitation occurred prior to the hour of observation were identified. Observed data were removed from analysis if precipitation was observed less than 4 days prior (i.e., 3 days of drying with no precipitation).

To standardize the calculation of TWPD a lower limit of wind speed is chosen that corresponds with the lowest speed where the relation between increasing wind speed and simultaneous increase in $PM_{10}$ is observed at a monitoring station. As for previous years, a wind speed of 3.5 m $s^{-1}$ at 10 m AGL (WPD= 26 W $m^{-2}$) for CDF and Mesa2 defines the lowest value for the range over which $PM_{10}$ is summed at these stations to calculate $TPM_{10}$. TWPD is the summation of the hourly mean wind speed measured at the S1 tower for the hours identified at CDF or Mesa2 that correspond to hourly mean wind speed ≥3.5 m $s^{-1}$ (after screening for the wind direction and precipitation criteria).

The importance of using a consistent lower limit of mean hourly wind speed was demonstrated by Gillies et al. (2023) using the S1 tower wind and CDF $PM_{10}$ hourly concentration data for the lower wind speed limits of 3.5 m $s^{-1}$, 4.0 m $s^{-1}$, and 4.5 m $s^{-1}$ for each month, April through September 2024. As Gillies et al. (2023, their Fig. 1) showed, the strength of the relation between monthly $TPM_{10}$ and monthly TWPD remained unchanged ($R^2$=0.99) for all three lower limit wind speeds but changing the lower limit of wind speed does change the slope and intercept values. A change in the lower limit of wind speed also changes the seasonal $TPM_{10}$:TWPD (i.e., the summation of all [filtered] hours for the period April-September), hence it is important to maintain consistency for the lower limit wind speed value for comparison purposes to evaluate temporal change in the ratio.

The choice of using the lower limit of wind speed at CDF of 3.5 m $s^{-1}$ measured at 10 m AGL is that when this hourly wind speed is observed at CDF the wind speed at the S1 tower is likely above that needed for saltation and $PM_{10}$ dust emissions to be occurring within the ODSVRA.

**Results 2025**

**Total Wind Power Density, April-September 2011-2025**

To place the wind conditions into context across the available S1 tower data record, 2011-2025, TWPD for the period April-September in each year was calculated (Fig. 1). For 2025, TWPD for the period April-September 2025 (TWPD=313,490 W $m^{-2}$) is higher by a factor of 1.89 compared to the TWPD for the same period in 2024, and therefore 2025 had greater wind power to effect dust emissions within the ODSVRA. In the 15-year record from 2011 to 2025, 2025 had the second highest observed value of TWPD. 2022 had the highest TWPD 325,000 W $m^{-2}$, with the median TWPD for the period 2011-2025 being 205,883 W $m^{-2}$.

Figure 2 shows the distribution of wind direction at S1 tower for 2023, 2024 and 2025 after applying the directional filter of 248°-326°. 2023, 2024, and 2025 have the same median wind direction value of 280°.

**Total $PM_{10}$ and Total WPD April-September 2025, CDF**

As shown previously, TWPD measured at S1 correlates with total $PM_{10}$ at CDF and Mesa2 (Gillies et al., 2020, 2021, 2022a, 2022b, 2023, 2024). This relation was also observed for the 2025 data (Fig. 3).

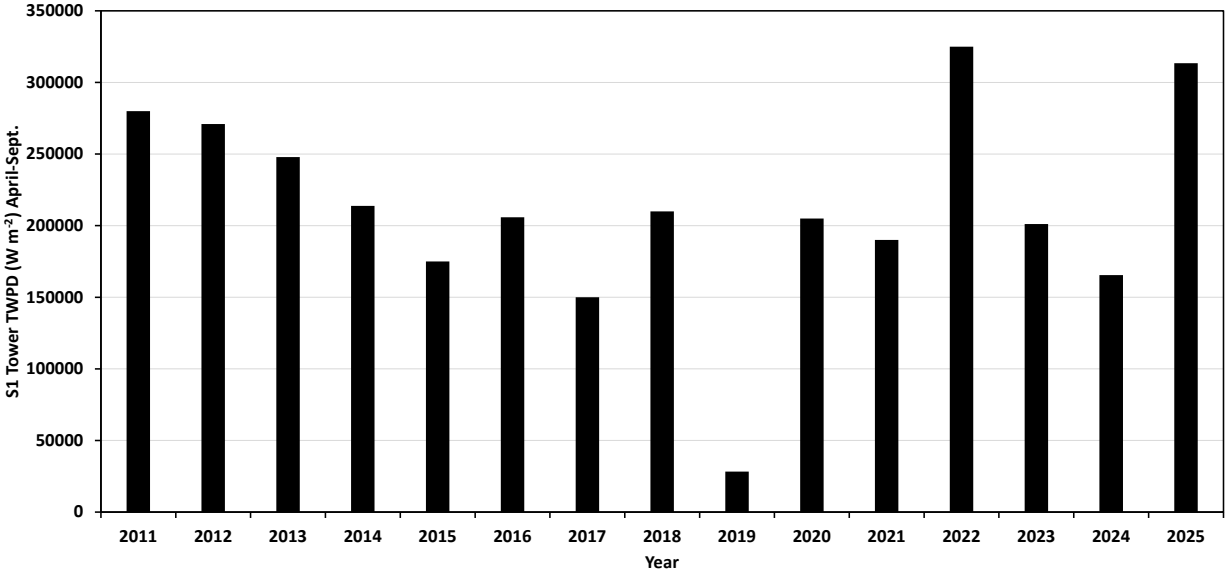



**Figure 1**. Total Wind Power Density (W $m^{-2}$) at the S1 tower for the period April-September 2011-2025. Data filtered for the wind direction range 248°-326°.

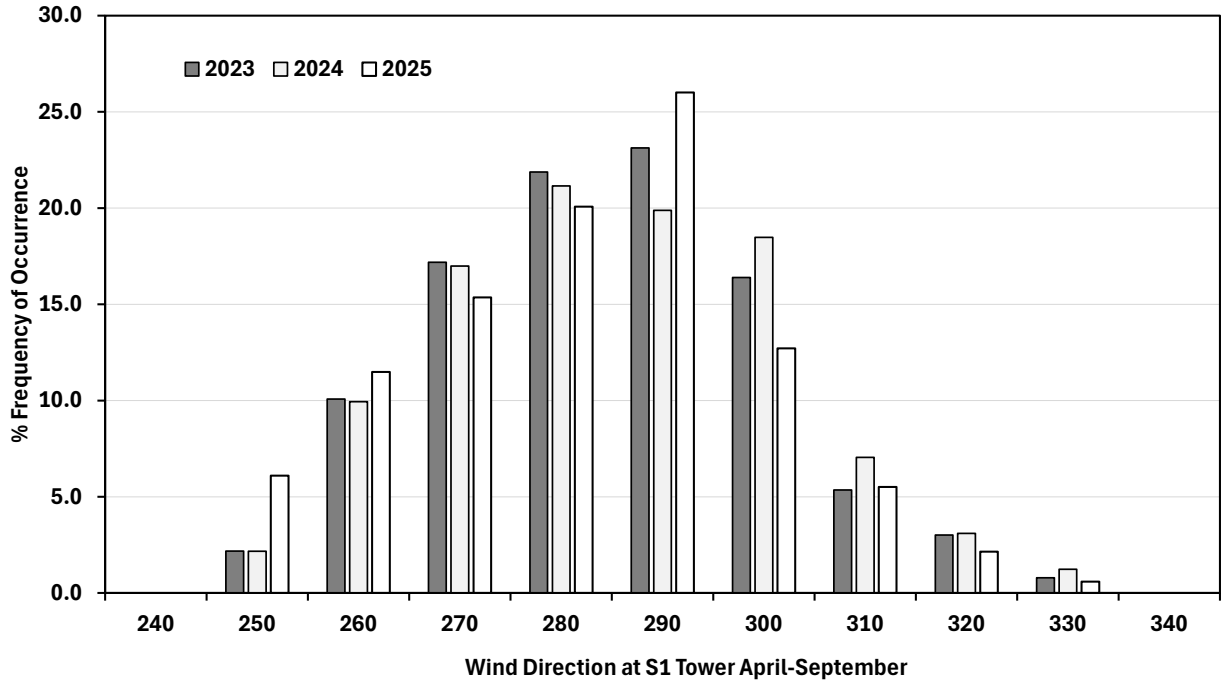



**Figure 2**. The distribution of wind direction at S1 tower for the period April-September 2023, 2024, and 2025, after applying the filtering criteria.

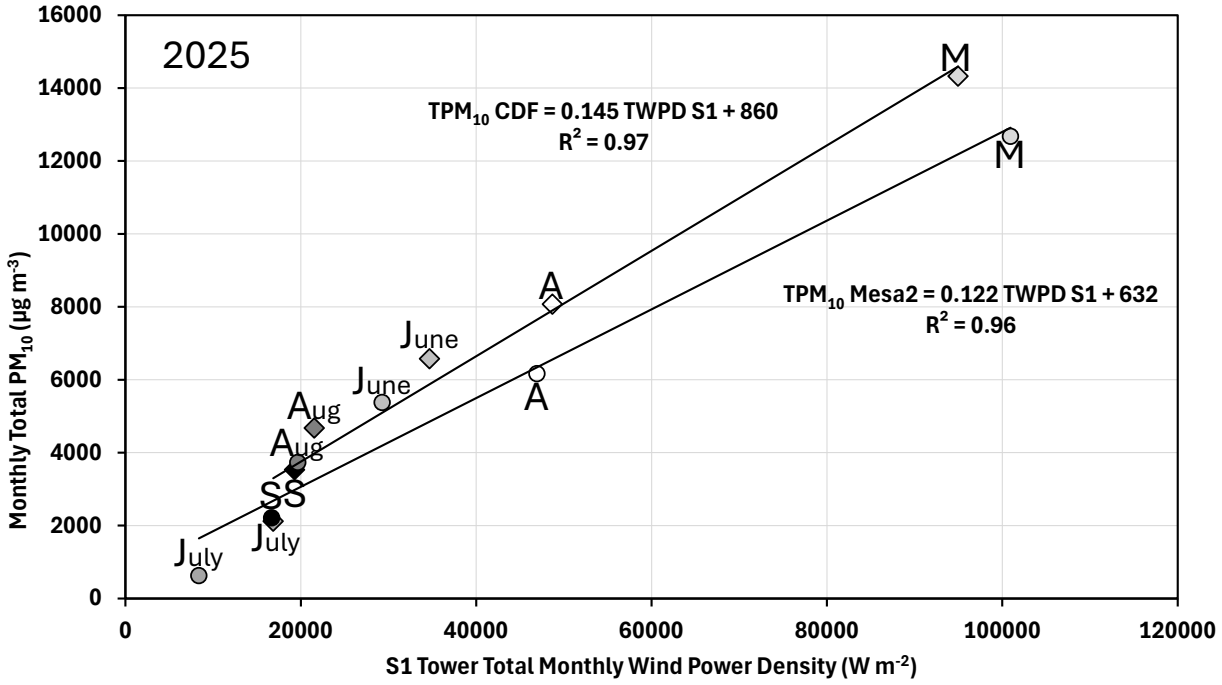



**Figure 3**. The relation between monthly Total $PM_{10}$ and monthly Total Wind Power Density for all hours when the wind direction was from 248°-326° observed at CDF (diamonds) and Mesa2 (circles), wind speeds were ≥3.5 m $s^{-1}$ (at CDF and Mesa2), and hours wherein there were <4 days since the last record of precipitation were removed. Monthly values are identified as April (A), May (M), June ($J_{une}$), $J_{uly}$ (July), August ($A_{ug}$), and September (S).

Based on the number of acres of dust control that were established directly upwind of CDF from 2013 (2 acres) through 2022 (330.7 acres), Fig. 4 shows that at CDF for the period April through September a downward trend in the $TPM_{10}$:TWPD ratio with increasing amounts of dust control acreage was observed through to 2022 when no further treatment projects were initiated. Note that the summation of acres of managed areas upwind of CDF lie within a directional range of 270° to 325° centered on CDF. Areas to the south of 270° will not have much influence on $PM_{10}$ concentrations at CDF as winds of <270° have a relatively low probability of occurrence and being above the speed needed for saltation and dust emissions. Similarly, so for winds approaching from >325°, which don't traverse the ODSVRA to any substantial degree before reaching CDF.

Since 2022 the $TPM_{10}$:TWPD ratio has varied between 0.15 (2023) and 0.17 (2024), with 2025 having a ratio value of 0.16. This may indicate that the ratio, representing the area upwind of CDF, has stabilized in the last four years and that the control measures in place have reached a quasi-equilibrium condition.

In Fig. 4, DRI reiterates from previous reporting (i.e., Gillies et al., 2022b, 2023, 2024) two years of data have not been included. In 2019 there were few hours where the winds exceeded the lower limit of wind speed to define the summation interval (i.e., ≥3.5 m $s^{-1}$ at CDF and Mesa2), which due to the paucity of higher wind speeds leads to an unstable ratio condition. The $TPM_{10}$:TWPD ratio for 2020 was also not included in the least squares regression as during April-September of that year OHV activity in the Park was restricted due to COVID19.

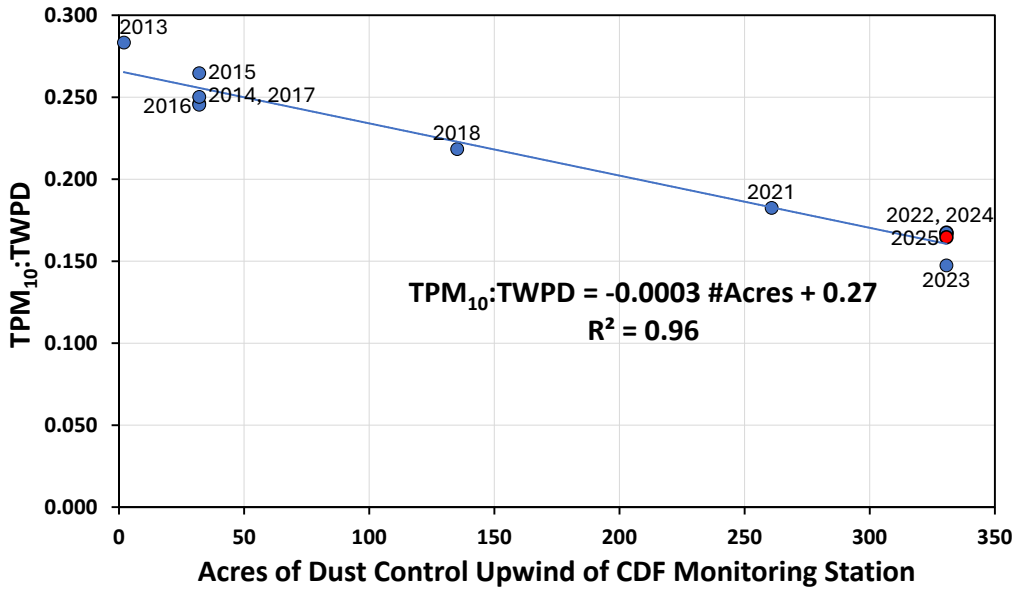



**Figure 4**. The $TPM_{10}$:TWPD ratio value measured at CDF and the acres of dust control from 2013 through to 2025 placed upwind of CDF in the directional range 270° to 325°. Note 2014 and 2017 data and 2022 and 2024 data align on top of each other. 2025 datum is represented by the red circle. Data from 2019 and 2020 were excluded as discussed elsewhere.

Figure 5 shows the change in the $TPM_{10}$:TWPD ratio for CDF as a function of year. This provides a more generalized representation of the ratio as a function of the state of the surface conditions upwind of CDF for the April-September period across the 13-year period of observation with the established filtering criteria applied in each year. The $TPM_{10}$:TWPD ratio has shown a steady decrease through time from 2013 through to 2022, with a leveling off between 2022 and 2025. This leveling off suggests that the dust emission system has stabilized with respect to the driving force of WPD producing similar levels of $PM_{10}$ concentrations across these last four years.

**Total $PM_{10}$ and Total WPD April-September 2025, Mesa2**

The ratio of $TPM_{10}$:TWPD for Mesa2 and S1 data for the period April through September for the years 2013-2025 as a function of acres of dust control upwind of Mesa2 is shown in Fig. 6. This figure shows that a downward trend in the $TPM_{10}$:TWPD ratio is observed with increasing acres of dust control for the period 2018-2022. Prior to 2018, there was no clear trend in the $TPM_{10}$:TWPD ratio data as there were few acres of dust control upwind of the Mesa2 monitoring station.

Figure 6 suggests a downward trend in the $TPM_{10}$:TWPD ratio through time for Mesa2 with the inclusion of the 2025 datum. The value of 0.14 in 2025, decreasing from 0.18 in 2024, is a promising indication of improvement in the dust management areas (e.g., increasing plant cover, supplemental planting) as the TWPD as measured at S1 increased in 2025 compared to 2024. The wind direction distributions at Mesa2 in 2024 and 2025 were similar (Fig. 7). The median wind directions were 284° in 2024, and 287° in 2025. The mean wind directions were 284° in 2024, and 286° in 2025.

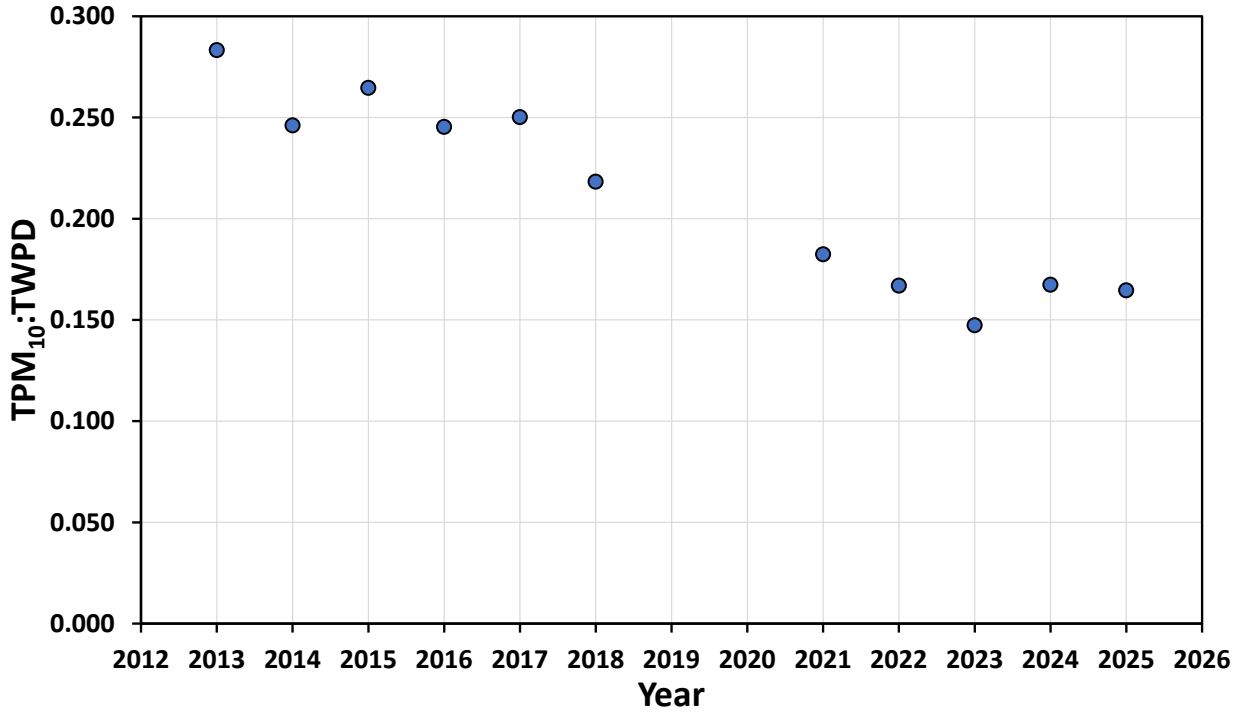



**Figure 5**. The $TPM_{10}$:TWPD ratio value measured at CDF as a function of the year of observation with the wind speed, wind direction, and precipitation day filters applied. Data from 2019 and 2020 were excluded as discussed elsewhere.

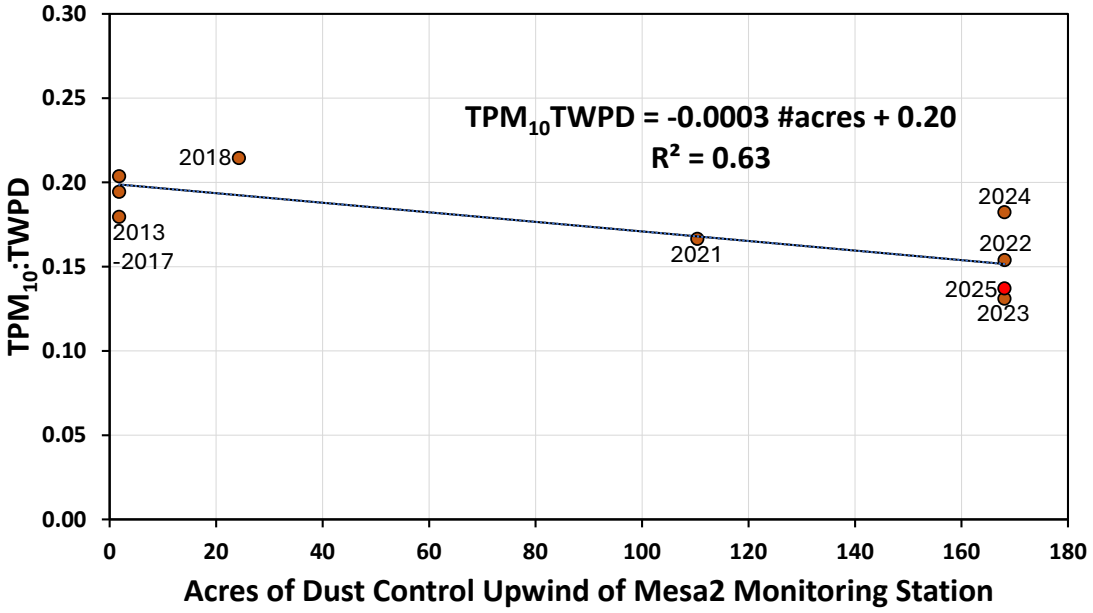



**Figure 6**. The relation between $TPM_{10}$:TWPD ratio value measured at Mesa2 and the acres of dust control from 2013 through to 2025 placed upwind of Mesa2 in the directional range 270° to 305°. Note for the 2013-2017 data points some years are aligned on top of one another. 2025 datum is represented by the red circle. Data from 2019 and 2020 were excluded as discussed elsewhere.

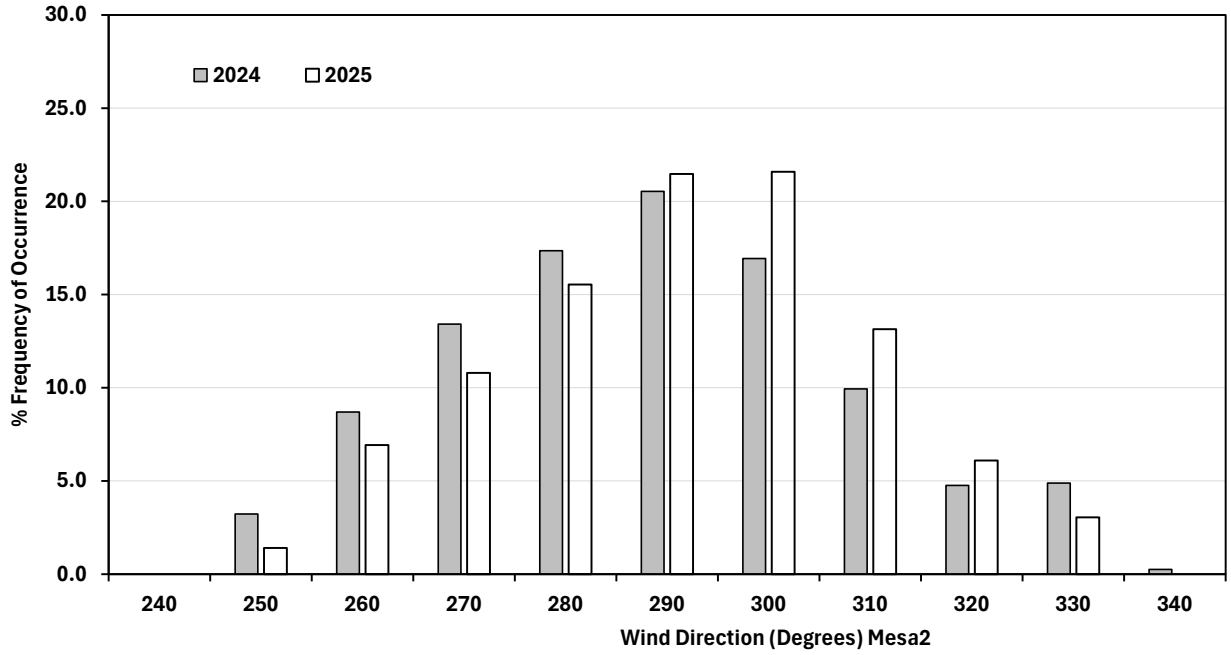



**Figure 7**. The distribution of wind direction at Mesa2 for the period April-September 2023, 2024, and 2025 after applying the filtering criteria.

Figure 8 shows the change in the $TPM_{10}$:TWPD ratio for Mesa2 as a function of year. This provides a more generalized representation of the ratio as a function of the state of the surface conditions upwind of Mesa2 for the April-September period across the 13-year period of observation with the established filtering criteria applied in each year. The $TPM_{10}$:TWPD ratio at Mesa2 has generally decreased from 2018 through 2025, but it has been more variable than has been observed at CDF.

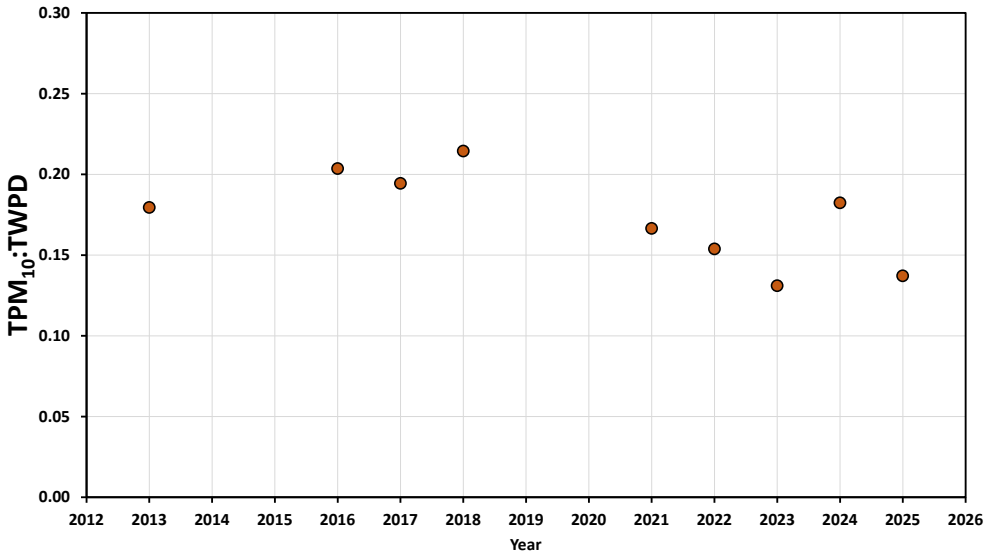



**Figure 8**. The $TPM_{10}$:TWPD ratio value measured at Mesa2 as a function of the year of observation with the wind speed, wind direction, and precipitation day filters applied. Data from 2019 and 2020 were excluded as discussed elsewhere.

**Discussions and Conclusions**

This analysis has demonstrated that TWPD is a robust metric for explaining the relationship between wind-driven saltation and the accompanying emission of $PM_{10}$ from the ODSVRA as measured at two key receptor sites, CDF and Mesa2. The TWPD and $TPM_{10}$ measurement-based metric indicates that the $PM_{10}$ originating from the ODSVRA has been reduced by approximately 43 % at CDF using the 4-year (2022 and 2025) mean value of 0.16 (±0.01) for equivalent WPD conditions compared with the baseline year of 2013 ($TPM_{10}$:TWPD = 0.28). For Mesa2, the TWPD and $TPM_{10}$ measurement-based metric indicates that the $PM_{10}$ originating from the ODSVRA has been reduced by approximately 13% using the 4-year (2022 and 2025) mean value of 0.16 (±0.03) for equivalent WPD conditions compared with the baseline year of 2013 ($TPM_{10}$:TWPD= 0.18) when there were few acres of dust control upwind of the Mesa2 station.

Figures 5 and 6 demonstrate that the $TPM_{10}$:TWPD ratio can be used to track the progress of the effect of dust controls on the dust emission system within the ODSVRA. It allows for quantification of the increments of progress as management efforts to limit dust emissions are further developed to meet the Stipulated Order of Abatement (SOA). It needs to be noted that the $TPM_{10}$:TWPD ratio is an indicator of the production potential of $PM_{10}$ as a function of WPD. An increase in WPD can result in more exceedances of the State or Federal standard even in the presence of increased amounts of dust controls because the $PM_{10}$ is produced from uncontrolled areas and it increases as a power function of wind speed, while the efficiency of the dust control does not. It should also be noted that the dust emission potential of the surfaces within the ODSVRA vary through time and across space and the wind climatology (wind speed and direction) in any given year is likely different compared to other years. This dynamism in the dust emission and wind climatology systems creates variability in the year-to-year $TPM_{10}$:TWPD metric. Without further modification or enhancement of the acres under dust control at the ODSVRA, there is every expectation that the value of this metric will fluctuate around a mean value that is currently 0.16 for CDF and Mesa2 based on the last four years of data. Even if the acres of dust control remain essentially unchanged, variability in the $TPM_{10}$:TWPD metric can be expected due to the vagaries of wind climatology and shifts in emissivity strength across space driven, in part, by changing patterns of off highway vehicle (OHV) activity as a function of location and frequency of disturbance within the ODSVRA.

**References**


Gillies, J.A., Furtak-Cole, E., Etyemezian, V. (2020). Increments of Progress Towards Air Quality Objectives - ODSVRA Dust Controls. Report prepared for California State Parks by the Desert Research Institute, December 2020.

Gillies, J.A., Furtak-Cole, E., Etyemezian, V. (2021). Increments of Progress Towards Air Quality Objectives - ODSVRA Dust Controls. Report prepared for California State Parks by the Desert Research Institute, December 2021.

Gillies, J.A., Furtak-Cole, E., Etyemezian, V. (2022a). Increments of Progress Towards Air Quality Objectives - ODSVRA Dust Controls. Report prepared for California State Parks by the Desert Research Institute, December 2022.

Gillies, J.A., Furtak-Cole, E., Nikolich, G. (2023). Increments of Progress Towards Air Quality Objectives - ODSVRA Dust Controls. Report prepared for California State Parks by the Desert Research Institute, December 2023.

Gillies, J.A., Furtak-Cole, E., Nikolich, G. (2024). Increments of Progress Towards Air Quality Objectives - ODSVRA Dust Controls. Report prepared for California State Parks by the Desert Research Institute, December 2024.

Gillies, J.A., E. Furtak-Cole, G. Nikolich, V. Etyemezian (2022b). The role of off highway vehicle activity in augmenting dust emissions at the Oceano Dunes State Vehicular Recreation Area, Oceano CA. *Atmospheric Environment: X*, 13, 100146, doi: 10.1016/j.aeaoa.2021.100146.

Kalmikov, A. (2017). Wind power fundamentals. In *Wind Power Engineering,* ed. T.M. Letcher. Elsevier Science Publishing Co., Inc.

State of California, Department of Parks and Recreation (2025). Oceano Dunes State Vehicular Recreation Area Dust Control Program, 2025 Annual Report and Work Plan.

*THIS PAGE WAS INTENTIONALLY LEFT BLANK.*

January 15, 2026

**Memo: SAG Review of DRI Report "Increments of Progress Towards Air Quality Objectives – ODSVRA Dust Controls 2025 Update" (11-2025 V1)**

**From**: Scientific Advisory Group (SAG)[1]

**To:** Jon O'Brien, California Department of Parks and Recreation

**Cc**: Ronnie Glick, California Department of Parks and Recreation

The SAG recently received (via email on January 6, 2026) a copy of the Desert Research Institute (DRI) report (*Increments of Progress Towards Air Quality Objectives – ODSVRA Dust Controls 2025 Update*, dated November 2024), and members have had the opportunity to review the document. This memo provides feedback on the DRI report.

As with the previous Increments of Progress (2022-2024) reports, the primary message of this 2025 update is that the dust-mitigation efforts instituted by CDPR since 2013 continue to be effective in reducing $PM_{10}$ concentrations at the CDF and Mesa2 monitoring stations. There has been a downward trend in the ratio of $TPM_{10}$/TWPD as a function of increases in the total acreage under dust control measures (between 2013 and 2022) at CDF. The most convincing aspect of this assessment is the fact that Total Wind Power Density (TWPD) has varied substantially from year-to-year, with particularly large values in 2025, and yet the $TPM_{10}$:TWPD ratio continues to fluctuate around a mean low value since 2022. This speaks to the **overall effectiveness of the dust control measures undertaken in the past decade as well as the ongoing efforts at supplemental planting by CDPR.**

The report is a straight-forward update of last year's Increments of Progress (2024) document with new data from 2025 added to the analysis, but retaining the same document structure and narrative as before. The SAG has identified a small number of editorial improvements for DRI to consider in revision, and a marked-up version of the original document will be delivered under separate cover.

In last year's review, the SAG had one substantive area of concern, with respect to the discussion of the trends for Mesa2. The results for CDF continue to be convincing in showing a decline in the $TPM_{10}$:TWPD ratio with increased acreage under dust control treatment followed by stabilization since 2022. But the results for Mesa2 are not nearly as compelling. The SAG encourages DRI to use more tentative language as regards the putative downward trends in the Mesa2 data, and suggests undertaking a rigorous statistical analysis to determine, for example, whether the ratio values for 2022-2025 are indeed different from those in earlier years. In addition, a deeper analysis of the influence of wind direction on the outcomes at Mesa2 might be revealing, and the SAG recommends that such an analysis be undertaken and reported on. DRI

[1] Standard procedure for SAG review of DRI reports is for Dr. Jack Gillies to recuse himself from the discussions due to a potential conflict of interest. Despite being a SAG member in good standing, Dr. Gillies did not participate in this review in any manner nor was DRI consulted about any aspect of this review.

is referred to the previous SAG review of the Increments Report for 2024 for additional details regarding related concerns.

The $TPM_{10}$:TWPD metric remains a practical tool to evaluate the long-term impacts of dust-mitigation efforts in the ODSVRA, and overall, the SAG concludes that this report provides a useful update for how dust controls are affecting downwind air quality..

Respectfully,

The Scientific Advisory Group

Bernard Bauer (Chair), Jenny Hand, Leah Mathews, Ian Walker

**ODSVRA Dust Control Program SAG Review Draft 2026 ARWP**

**ATTACHMENT 08**

**SAG Recommendations for Parameterizing Vegetative Grid Cells**

- Recommendations for Reconciling DRI Model Assumptions with Ground Evidence in Respect of Vegetated Grid Cells (SAG Memo)
- Incorporating Vegetation Cover into the DRI Model (SAG Memo)
- Contemplating DRI Model Refinements in Anticipation of the 2026 ARWP (SAG Memo)
- Synthetic Power Relations for Vegetation Islands (SAG Memo)
- Restoration Project Maturation Timeline (State Parks Memo)

*THIS PAGE WAS INTENTIONALLY LEFT BLANK.*

January 7, 2026

**Memo: <u>Recommendations for Reconciling DRI Model Assumptions with Ground Evidence in Respect of Vegetated Grid Cells</u>**

**From**: Scientific Advisory Group (SAG)

**To:** Ronnie Glick, California Department of Parks and Recreation (CDPR)

**CC**: Jon O'Brien, California Department of Parks and Recreation (CDPR)
Sarah Miggins, California Department of Parks and Recreation (CDPR)
Karl Tupper, SLO Air Pollution Control District (APCD)

At the recent SAG monthly meeting (December 15, 2025), a request was made by CDPR and APCD for the SAG to develop a set of recommendations regarding assumptions in the DRI (Desert Research Institute) model regarding the emissive properties of vegetated grid cells within polygons identified as Vegetation Islands (VI) and Treatment Areas (TA). There is need to reconcile the model assumptions with on-the-ground reality of percent vegetation cover (and hence dust emission potential) across the Oceano Dunes State Vehicular Recreation Area (ODSVRA). A prior SAG Memorandum (December 1, 2024) outlined the issue in detail, and suggested several action items that CDPR might take under consideration. Herein, the SAG offers updated recommendations for consideration by CDPR and APCD in view of the pending Stipulated Order of Abatement (SOA) compliance decision in October, 2028.

As background, the SAG notes that:

a) the most recent assessment of percent vegetation cover within grid cells in the ODSVRA is based on a 2024 vegetation mask produced by UCSB using imagery from the National Agricultural Imagery Program (NAIP);
b) the 2024 vegetation mask identifies both plants and straw cover based on image training algorithms, but not woody, dead shrub material; and
c) all grid cells have been classified accordingly in terms of percent vegetation cover in a GIS map produced by CDPR analysts.

Should a newly revised vegetation mask become available, depending on NAIP updates, it would seem prudent to base any future analysis on the most recent imagery. Very high-resolution imagery is also available from semi-annual UAS flights by UCSB, but is likely not suitable because the coverage is limited to only specific portions of the ODSVRA (e.g., Foredune Restoration Area).

The SAG has identified three possible action items for consideration by CDPR and APCD, as described below.

## Adaptive Management

In the December 1, 2024 SAG memo, it was noted that the most expeditious and simplest approach to reconciling model assumptions with ground reality was for CDPR to devise and actualize an adaptive management plan that provides reasonable assurance that each and every grid cell within mapped VI and TA polygons has sufficient vegetation cover to warrant an assumption of zero dust emission potential. Such management interventions would ensure that model assumptions align with ground truth, and this approach would require no modifications to the DRI model. **The first SAG recommendation is that CDPR proceed along this adaptive management path, to the extent feasible given limited resources, and to develop an operational plan that identifies target treatment areas and specific actions that will ultimately lead to a state of zero dust emission potential for all grid cells within VI and TA polygons**. Such a plan would be embedded in the annual ARWP process and is consistent with CDPR's transitioning to adaptive management principles. The plan should prioritize areas that are most likely to have long-term success as regards permanent plant cover rather than areas that are prone to inundation by blowing sand and therefore require on-going maintenance.

## Incremental Model Refinement

In parallel, **the SAG recommends that a scoping exercise be conducted that involves an incrementally refined DRI model for the purpose of assessing the degree to which SOA compliance is attained (or not) if model grid cells are parameterized for dust emission potential according to percentage vegetation cover (%VC), thereby reflecting present-day, on-the-ground realities rather than assuming that all VI and TA grid cells are non-emissive.** The objective is to retain relative simplicity within the model (given a range of inherent uncertainties, pro and con, that likely are balanced in the grand scheme), while more faithfully accounting for the influence of partial vegetation cover on dust emission potential across the entire ODSVRA rather than just the VI and TA grid cells.

The fundamental process steps in this approach are as follows:

1) Use the most recent vegetation mask (e.g., 2024 NAIP-based UCSB product) to quantify %VC in each model grid cell (product already available from CDPR)
2) Classify grid cells into two dust emission reduction categories based on %VC (with the threshold based on information from the scientific literature[1]), for example:
3)

Totally emissive: 0 – 15 %VC
Non-emissive: > 15 %VC

This binary approach (off-on) is the simplest, rather than having multiple categories with partial %VC and hence emission potential, and it is thought that any errors associated with emission potential in these binary categories are balanced by errors in the other category when averaged across large areas such as VIs and, ultimately, the entire ODSVRA. In cells that are categorized

[1] A synopsis of the literature on the effect of vegetation cover on wind erosion and dust emissions is provided as supplementary material at the end of this memorandum.

as totally emissive, the appropriate emissivity power relation would be applied (e.g., NRA North, NRA Central, NRA South, etc.). This requires only one extra layer of information attached to each grid cell within the DRI model.

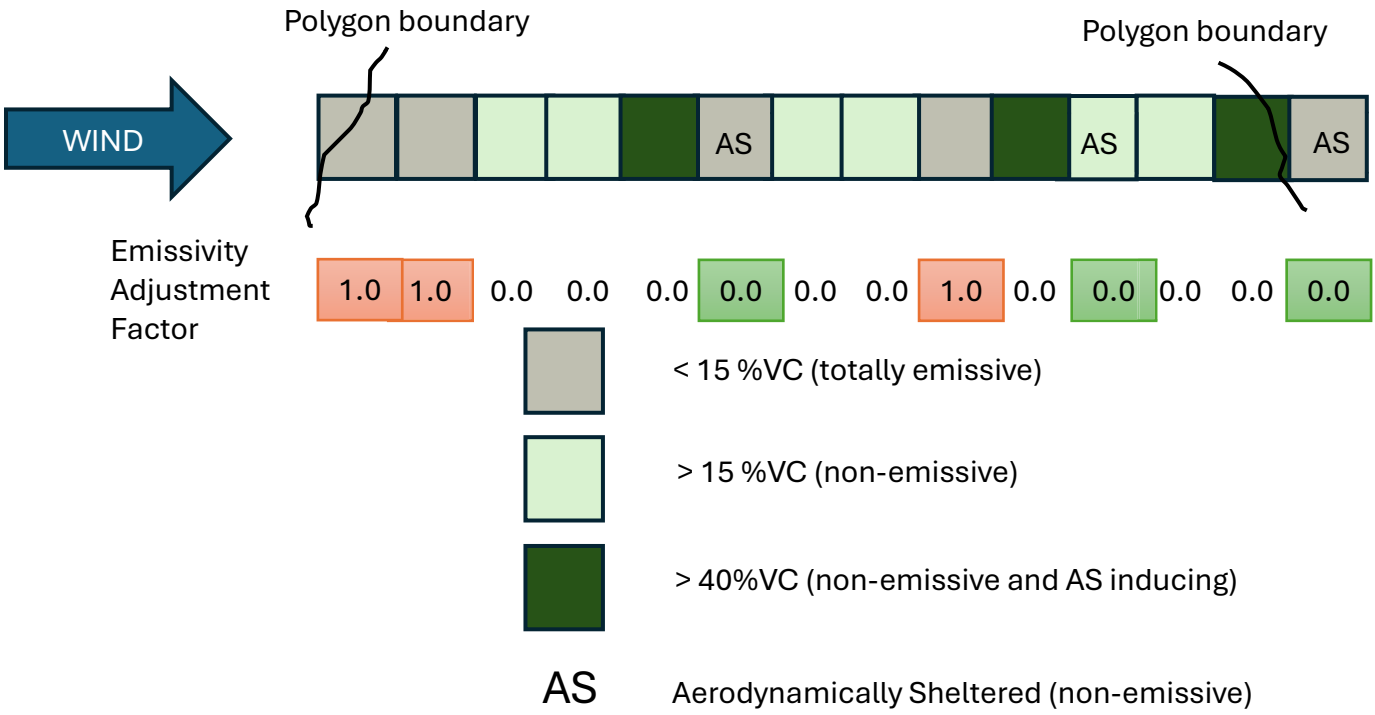
**Aerodynamic Sheltering Effect**

The scientific literature on boundary layer flow over a roughness transition from an aerodynamically rough surface (e.g., densely vegetated) to an aerodynamically smooth surface (e.g., open sand) indicates that a reduction in surface shear stress is induced over the downwind (smooth) surface as a new internal boundary layer develops in the downwind direction. A new equilibrium is achieved downwind of the transition in which the surface shear stress is controlled entirely by the characteristics of the smooth surface and is no longer influenced by the upwind roughness elements. Evidence in support of these trends derives from wind-tunnel results, Computational Fluid Dynamics (CFD) simulations, as well as field experimentation. The relaxation distance depends on the character of roughness elements on the upwind surface (in particular, plant height, h, and stem density), but it is reasonably estimated anywhere from 2h to 10h or more. Because of the reduced shear stress immediately downwind of the transition, there is an aerodynamic sheltering effect that creates a zone in which there is no sediment transport via saltation, and hence little potential for dust emission from the open sand surface. As the new internal boundary layer develops in the downwind direction and a new equilibrium surface shear stress is attained, the threshold for initiation of motion may be exceeded and saltation begins, thereby inducing dust emissions, initially at low levels but eventually at equilibrium rates. This process takes tens of meters to evolve, as per the literature dealing with the 'fetch' effect in aeolian transport systems.

To date, the aerodynamic sheltering effect has only been incorporated into the DRI model in relation to the topographic influences of the developing nebkha in the Foredune Restoration Area. **The third SAG recommendation is that consideration be given to including an aerodynamic sheltering effect, as controlled by densely vegetated grid cells across the entire ODSVRA.** Again, the objective is to develop a rule set that is relatively simple in terms of model implementation and consistent with the magnitude of uncertainties in other aspects of dust emission modeling. The following approach is suggested:

1) Use the most recent vegetation mask (e.g., 2024 NAIP-based UCSB product) to quantify %VC in each model grid cell (product already available from CDPR)
2) Identify grid cells that have >40 %VC, which is the threshold believed to be of sufficient coverage to reasonably induce an aerodynamic sheltering (AS) effect on a downwind grid cell.
3) For every grid cell within the ODSVRA that lies immediately to the east of an AS cell, assign it a zero for dust emission potential.

The following graphic provides an example of how this AS effect manifests itself in a fictitious model domain:




In the initial assignment of dust emission potential, all grid cells are categorized according to a 15 %VC threshold as either 'totally emissive' or 'non-emissive' and the corresponding emissivity adjustment factor is either 1.0 or 0.0, respectively. Grid cells identified as having >40 %VC are also non-emissive (factor of 0.0) but have the additional property of inducing an AS effect to the adjacent downwind grid cell.

In the diagram above, the first dark green cell (far left) is upwind of a cell that would normally be categorized as emissive (factor of 1.0), but due to the AS effect, the cell becomes non-emissive (factor of 0.0). The second dark green cell (from left to right) is upwind of a grid cell that would normally be categorized as non-emissive (factor of 0.0), and the AS effect does not alter this state. Finally, the third dark green cell (on the far right) lies along the polygon boundary but is more than 50% contained within the polygon. It lies upwind of a grid cell that is totally emissive (factor of 1.0) but because of the AS effect, the downwind cell becomes non-emissive (factor of 0.0) regardless of being situated in the riding area outside the polygon, but immediately adjacent to a cell that is within the polygon.

**Summary and Caveats**

The three SAG recommendations above regarding: (i) implementation of adaptive management interventions, (ii) undertaking a scoping exercise based on incremental model refinements, and (iii) including an AS effect in the dust emission modeling will lead to two significant outcomes. First, there will be improved air quality, as measured by downwind monitoring stations and

reflected in various performance metrics, because more grid cells in the ODSVRA (particularly within VIs and TAs) will be treated with supplemental planting and surface covers thereby reducing dust emission potential. Second, the modeling will provide a better understanding of the extent to which on-the-ground realities associated with grid cell vegetation cover (presence or absence) are represented faithfully in the DRI dust emission model. The information from the model scoping exercise can be useful in guiding future management decisions (how much? where?) and will be critical to assessing compliance with the SOA in 2028.

The SAG encourages CDPR and APCD to take these recommendations under advisement as potential next steps in the process of improving air quality conditions, while also remaining faithful to the mandate of the ODSVRA to provide unique recreational experiences for park visitor and users. Many of the details of the model scoping exercise remain to be firmed up, and this will require consensus among the parties. In addition, for consistency and scientific integrity, it will become necessary to consider whether the same model protocols (recommendations 2 and 3, above), which are to be applied to the current landscape scenario, should also be applied to the 1939 pre-disturbance scenario. Another scoping exercise should be undertaken to determine whether the low-resolution photogrammetric images from 1939 are conducive to assessing vegetation cover percentages to the same degree of fidelity as the 2024 NAIP imagery. This information will be critical in assessing how pre-disturbance baseline conditions can potentially be evaluated within the new modeling framework recommended above.

Respectfully,

The Scientific Advisory Group

Bernard Bauer (Chair), Jack Gillies, Jenny Hand, Leah Mathews, Ian Walker

## Literature Synopsis – Vegetation Cover Control on Wind Erosion

The presence of vegetation on sand surfaces has two primary effects: (1) a reduction in the rate of saltation and, hence, dust emission that becomes more effective with an increase in percent plant coverage; and (2) an alteration in the shear velocity ($u_*$) or stress distribution above the surface relative to a smooth, unvegetated surface. With respect to the latter, the mechanism of shear stress partitioning (Schlichting, 1968) modulates the shear stress acting on the surface between the roughness elements (i.e., plants) primarily as a function of the drag force generated by the roughness elements on the near-surface wind. This modulation of the surface shear velocity ($u_{s*}$) in the presence of the vegetation affects the magnitude of the $PM_{10}$ emissions.

Several alternative approaches are discussed in the literature to account for the role of vegetation to modulate wind shear, sand transport, and dust emissions, and they are of varying degrees of complexity (e.g., Marticorena and Bergametti, 1995; King et al., 2005; Okin, 2008). A pragmatic approach to consider for the emission modeling used to evaluate the state of excess emissions at the ODSVRA, as defined by the SOA, is to use the percent cover of vegetation data available from the National Agriculture Imagery Program (NAIP) and/or the UCSB UAS-derived vegetation survey data to set a limit on when a sand surface is protected by vegetation to effectively reduce the potential for sand transport and dust emissions to zero. Currently, the DRI emission model prescribes a threshold of 50% plant cover, but available information from the scientific literature suggests that considerably smaller percentages of plant cover will provide a large degree of protection. Information from the most-cited and easily-available literature is summarized below.

A commonality among peer-reviewed publications that have examined the relation between sand transport and differing amounts of vegetative cover (both wind tunnel and field-based studies) is that transport rate decreases exponentially with increasing amounts of vegetation (e.g., Buckley, 1987; Cheng et al., 2020; Lancaster and Baas, 1998; Li et al., 2022; Wasson and Nanninga, 1986). The effects of vegetation on wind flow and sediment transport are multiple and varied and depend on the vegetation type in question, as well as turbulence, porosity and pliability factors (Mayaud and Webb, 2017**). This complexity makes a universal relation between vegetation cover and its effect on sand transport and dust emission impossible to define.** The literature, however, suggests that bounds can be set that allow a high degree of confidence to identify the percent cover of vegetation, independent of plant characteristics, that will provide protection to the surface from erosive winds.

The physical basis of vegetation to provide protection to an erodible surface is shear stress partitioning as initially described by Schlichting (1968). Lee and Soliman (1977), provide a simpler framework based on the concept of flow regimes created by different amounts of roughness elements. They describe three types of flow regimes: isolated roughness, wake interference, and skimming flow. In isolated roughness the flow interacts with each element individually creating an isolated zone of protection on the lee side. Wake interference, as the term suggests, occurs when the wake created in the lee of an element interacts with the next element before it recovers to the undisturbed flow condition. Finally in skimming flow, the density of the roughness is sufficient to essentially act as a surface elevated above the ground and the flow does not reach the underlying surface. In the case of vegetation cover, each of the flow

regimes is attributed to a vegetation density as follows: isolated <16%, wake interference between 16% and 40%, and skimming >40% (Lee and Soliman, 1977; Wolfe and Nickling, 1993; Rotnicka et al., 2023).

According to theoretical considerations proposed by Musick and Gillette (1990), 16% cover should suppress wind erosion (i.e., sand transport and dust emissions). Field evidence supports that a high degree of protection to an erodible surface is provided by vegetation cover in the range 15% - 40%. An empirical study by Lancaster and Baas (1998) at Owens Lake, CA measured saltation flux for areas with different percent covers of salt grass and established the relation: $Q_n=0.95\ e^{-0.20\ C}$, where $Q_n$=saltation flux within the vegetation/saltation flux without vegetation present and C is percent cover [Supplemental Fig. 1]. **The Lancaster and Baas (1998) relation indicates that for a percent cover of ≈12%, saltation would be reduced by >90% compared to the same surface with no saltgrass present.**

NASEM (2020) using the wind erosion model of Okin (2008) report that for a simple plant model (diameter =0.5 m, aspect ratio=1), 25% shrub cover provides approximately 99% control efficiency to reduce saltation. NASEM (2025) using the Okin (2008) model and the more conservative plant property characteristics described in Mayaud et al. (2017) for shrub-like plants, report that 38% shrub cover provides approximately 99% control efficiency to reduce saltation. **For a percentage cover of 18%, NASEM (2025) reports a model predicted effectiveness of 95% using the Mayaud et al. (2017) parameterization**.

A different approach to estimate the effect of vegetation for protecting the surface from wind erosion can be done through knowledge of the characteristic drag coefficients ($Cd_p$) of plants (e.g., Gillies et al., 2000, 2002) within a shear stress partitioning model (e.g., Raupach et al., 1993). For example, assuming a shrub-like plant has a $Cd_p$=1.4 (greasewood [h=0.51 m, diameter=0.61 m] from Gillies et al., 2000), the Raupach et al. (1993) shear stress partitioning model can be used to quantify the shear velocity ($u_*$) required to exceed the threshold shear velocity (e.g., $u_{s*t}$=0.3 m $s^{-1}$) for the surface among the roughness elements [Supplemental Fig. 2]. **This drag coefficient-based evaluation of protection by shrub-like plants for the given dimensions and $Cd_p$ suggests that full protection for most wind conditions can be expected at a cover of 10%.**

Taking this approach one step further, using the relation between normalized sand flux (i.e., NSF=sand flux in the presence of the vegetation/sand flux in the absence of vegetation [Qn in Lancaster and Baas, 1998]) and roughness density from Gillies et al. (2018), and assuming the vegetative roughness elements are acting similar to the solid roughness elements used by Gillies et al. (2018) **sand flux would be 1% of the incoming flux with 15% cover** [Supplemental Fig. 3].

These different approaches to evaluate the protective role of vegetation to reduce sand flux and the associated dust emissions suggest that achieving a percent cover level of approximately 15%, independent of plant type, will result in a high degree of protection of the erodible sand surfaces within the ODSVRA. A caveat to this is that the plants should be relatively well distributed across space (i.e., uniform density across a grid cell). **Based on the available information presented, the SAG recommends that a value of 15% cover and greater be used to define a**

**grid cell within the modeling domain of the DRI emissions model that is non-emissive for $PM_{10}$.**

## References


Buckley, P.Y. (1987). The effect of sparse vegetation on the transport of dune sand by wind. *Nature* 325 (6103), 426–428, doi: 10.1038/325426a0.

Cheng, H., Liu, C., Zou, X., Li, H., Kang, L., Liu, B., Li, J. (2020). Wind erosion rate for vegetated soil cover: a prediction model based on surface shear strength. *Catena* 187, 104398, doi: 10.1016/j.catena.2019.104398.

Gillies, J.A., Etyemezian, V., Nikolich, G., Nickling, W.G., Kok, J.F. (2018). Changes in the saltation flux following a step-change in macro-roughness. *Earth Surface Processes and Landforms* 43, 1871-1884, doi: 10.1002/esp.4362.

Gillies, J.A., Green, H., McCarley-Holder, G., Grimm, S., Howard, C., Barbieri, N., Ono, D., Schade, T. (2015). Using solid element roughness to control sand movement: Keeler Dunes, Keeler, California. *Aeolian Research* 18, 35-46, doi: 10.1016/j.aeolia.2015.05.004.

Gillies, J.A., Lancaster, N., Nickling, W.G., Crawley, D.M. (2000). Field determination of drag forces and shear stress partitioning effects for a desert shrub (*Sarcobatus vermiculatus*, greasewood). *Journal of Geophysical Research* 105, 24871-24880, doi: 10.1029/2000JD900431.

King, J., Nickling, W.G., Gillies, J.A. (2005). Representation of vegetation and other non-erodible elements in aeolian sediment transport models. *Journal of Geophysical Research-Earth Surface* 110, F4, doi: 10.1029/2004JF000281.

Lancaster, N., Baas, A. (1998). Influence of vegetation cover on sand transport by wind: field studies at Owens Lake California. *Earth Surface Processes and Landforms* 25, 68-82, doi: 10.1002/(SICI)1096-9837(199801)23:1%3C69::AID-ESP823%3E3.0.CO;2-G.

Lee, B.E., Soliman, B.F. (1977). An investigation of the forces on three dimensional bluff bodies in rough wall turbulent boundary layers. *ASME Journal of Fluids Engineering* 99 (3), 503–509, doi: 10.1115/1.3448829.

Li, H., Liu, C., Cheng, H., Zou, X., Zhang, C., Liu, B., Li, J., Kang, L., Wu, W. (2022). A general model for predicting aeolian transport rate over sand surfaces with vegetation cover. *Earth Surface Processes and Landforms* 47, 2471-2482, doi: 10.1002/esp.5388.

Marticorena, B., Bergametti, G. (1995). Modeling the atmospheric dust cycle, 1, Design of a soil-derived dust emission scheme. *Journal of Geophysical Research* 100 (8), 16415-16430, doi: 10.1029/95JD00690.

Mayaud, J.R., Webb, N.P (2017). Vegetation in drylands: Effects on wind flow and aeolian sediment transport. *Land* 6 (64), doi:10.3390/land6030064.

Mayaud, J.R., Wiggs, G.F.S., Bailey, R.M. (2017). A field-based parameterization of wind flow recovery in the lee of dryland plants. *Earth Surface Processes and Landforms* 42, 378-386, doi: 10.1002/esp.4082.
Musick, H.B., Gillette, D.A., 1990. Field evaluation of relationships between a vegetated structural parameter and sheltering against wind erosion. *Land Degradation and Rehabilitation* 2, 87-94.

National Academies of Sciences, Engineering, Medicine (2020). Effectiveness and Impacts of Dust Control Measures for Owens Lake. The National Academies Press, Washington, DC, 184 p., doi: 10.17226/25658.

National Academies of Sciences, Engineering, Medicine (2025). Off-Lake Sources of Airborne Dust in Owens Valley, California. The National Academies Press, Washington, DC, 164 p., doi: 10.17226/27958

Okin, G. (2008). A new model of wind erosion in the presence of vegetation. *Journal of Geophysical Research - Earth Surface* 113, F02S10, doi: 10.1029/2007JF000758.

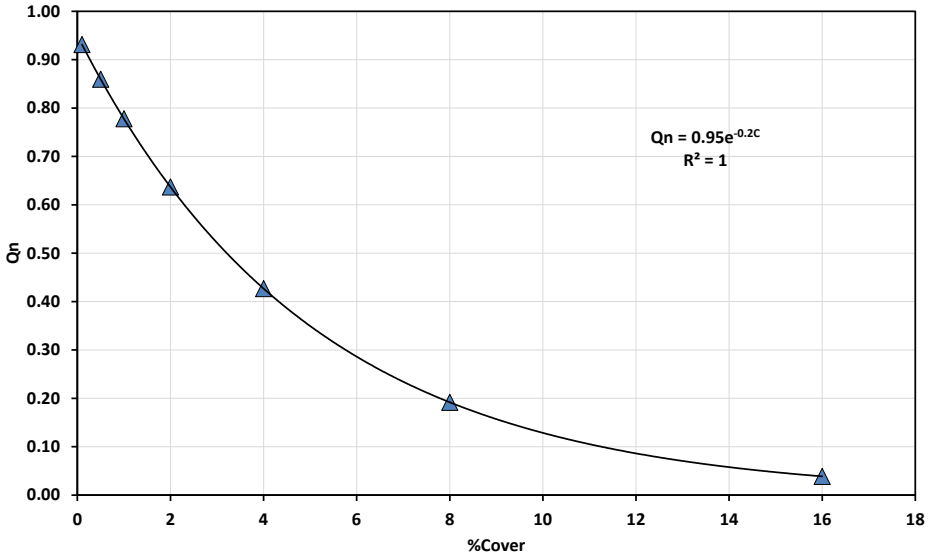
Raupach, M.R., Gillette, D. A., Leys, J. F. (1993). The effect of roughness elements on wind erosion threshold. *Journal of Geophysical Research* 98, 3023-3029, doi: 10.1029/92JD01922.

Rotnicka, J., Dluzewski, M., Hesp, P.A., Tomczak, J.O. (2023). Skimming flow and sand transport within and above Ammophila (Marram) grass on a foredune. *Journal of Geophysical Research-Earth Surface* 128, e2023JF007143, doi: 10.1029/2023JF007143.

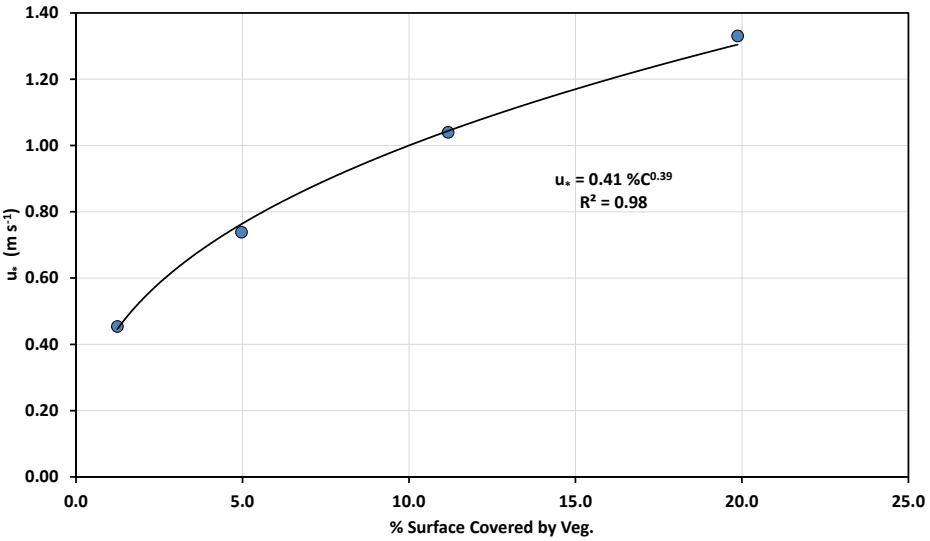
Schlichting, H. (1968). Boundary Layer Theory. McGraw Hill, New York, 747 p.

Wasson, R.J., Nanninga, P.M. (1986). Estimating wind transport of sand on vegetated surfaces. *Earth Surface Processes and Landforms* 11, 505-514, doi: 10.1002/esp.3290110505.

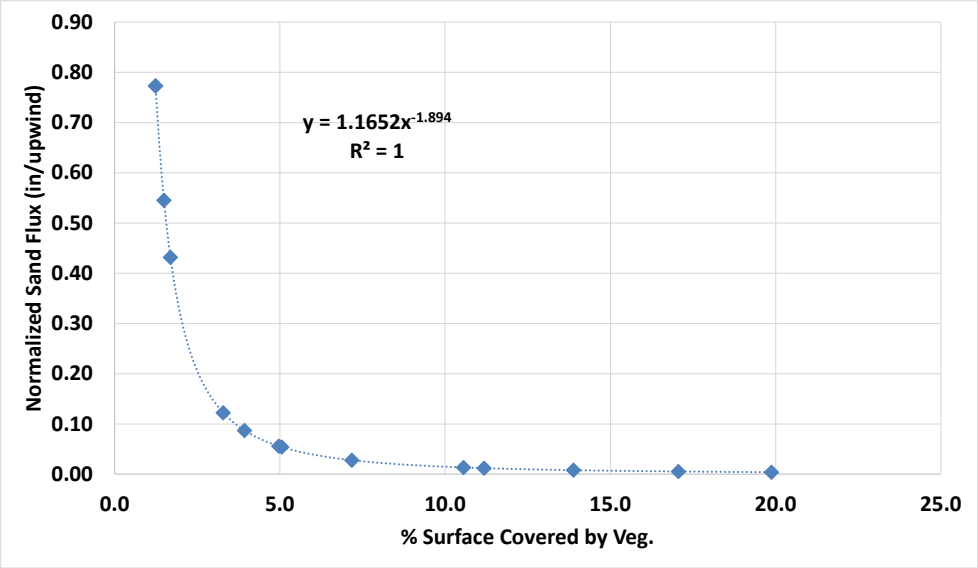
Wolfe, S., Nickling, W. (1993). The protective role of sparse vegetation in wind erosion. *Progress in Physical Geography* 17 (1), 50–68, doi: 10.1177/030913339301700010.




**Supplemental Figure 1**. Normalized sand flux (Qn) as a function of % cover from Lancaster and Baas (1998).




**Supplemental Figure 2**. Shear velocity (above roughness) required to reach the threshold shear velocity ($u_{*t}$=0.3 m $s^{-1}$) on the surface among the roughness elements as a function of % surface covered and the plant dimensions: h=0.5 m, diameter=0.6 m, and $Cd_p$=1.4.




**Supplemental Figure 3**. Normalized sand flux (NSF) as a function of % cover and the plant dimensions: h=0.5 m, diameter=0.6 m, and $Cd_p$

*THIS PAGE WAS INTENTIONALLY LEFT BLANK.*

April 9, 2026

**Memo: <u>Incorporating Vegetation Cover into the DRI Model</u>**

**From**: Scientific Advisory Group (SAG)

**To:** Jon O'Brien, California Department of Parks and Recreation
Karl Tupper, SLO Air Pollution Control District

**Cc**: Sarah Miggins, California Department of Parks and Recreation
Ronnie Glick, California Department of Parks and Recreation

The issue of incorporating vegetation cover and its impact on dust emissions into the DRI model in a manner that reflects on-the-ground realities has been a recurring topic of discussion amongst CDPR, APCD and SAG. Two recent SAG memos[1] [2] outlined several issues and made recommendations for consideration by CDPR and APCD. The over-riding objective is to improve the fidelity of the predictive model as regards dust emission potential from the Oceano Dunes State Vehicular Recreation Area (ODSVRA), and thereby lead to better outcomes for air quality improvements in the region, as well as to assist CDPR personnel to adaptively manage the ODSVRA accordingly.

Briefly, the concerns regarding the current approach to modeling dust emission potential are three-fold:

1. Currently, all model grid cells with greater than 50% plant cover are considered to be 'vegetated' and are modeled as having zero potential for dust emissions (i.e., non-emissive). Grid cells with less than 50% coverage are classified as 'bare sand' (i.e., emissive). A vegetation mask produced by UCSB based on the 2020 imagery from the National Agricultural Imagery Program (NAIP) was used to assess the 50% threshold condition for each grid cell in the modeling domain. On the basis of a thorough literature search, the SAG is of the opinion that a 15% threshold level is more appropriate to differentiate between a 'vegetated' (non-emissive) and 'bare sand' (emissive) classification. In addition, a more recent (2024) version of the NAIP imagery is now available.

2. Areas classified as "Vegetation Islands" (VI) or "Treatment Projects" (TP) were considered special management zones in the model, and they were identified by geo-referencing the physical fence lines using GPS and importing the vectors into the model as polygons. The entire area within these polygons was considered to be 'vegetated' and therefore having zero emissivity potential, regardless of actual plant cover percentage. Evidence from the field, as well as from remotely-sensed imagery (UAS flights, NAIP) indicates that there are patches of open sand and sparse vegetation within VIs and TPs, in

[1] SAG Memo – ***Management of Vegetated Areas in Respect of Zero Emissions*** (December 1, 2024)
[2] SAG Memo – ***Recommendations for Reconciling DRI Model Assumptions with Ground Evidence in Respect of Vegetated Grid Cells*** (January 7, 2026).

some cases quite extensive, and it seems unreasonable not to acknowledge and account for the dust-emitting potential of these within-polygon surfaces that are potentially dust emitting.

3. Unvegetated grid cells that lie downwind of heavily vegetated cells experience an aerodynamic sheltering (AS) effect, due to boundary-layer readjustments, that minimizes the potential for dust emissions from the downwind grid cell, even if there is no vegetation cover and only bare sand. The current version of the DRI model does not adequately incorporate this AS effect.

The SAG held a monthly meeting on March 9, 2026 during which members discussed a range of issues pertinent to the handling of vegetated areas in the DRI model. As a consequence of these discussion, the SAG recommends the following:

1. A revised threshold of 15% should be adopted to classify a grid cell as either 'vegetated' (non-emissive) or 'non-vegetated' (i.e., bare sand and, therefore, emissive). This replaces the 50% threshold that is currently used.
2. The most recent NAIP imagery should be used to develop a vegetation mask, and on the basis of this imagery, the classification of grid cells as 'vegetated' or 'non-vegetated' should be performed. UCSB has generated a vegetation mask using the 2024 NAIP imagery, and this 2024 vegetation mask should be used for modeling purposes until a new version of the NAIP imagery becomes publicly available. The DRI model should be updated accordingly.
3. The assessment of the vegetation status of model grid cells should be applied to the entire ODSVRA, including all management zones such as the Non-Riding Area North (Dune Preserve), the Non-Riding Area South (Oso Flaco), and all other zones in the central region (e.g., Riding Areas, Foredune Restoration Area, Plover Exclosure, etc.). The assessment should also be done for all VIs and TPs, which are no longer to be treated separately as non-emissive polygons in the DRI model.
4. To identify grid cells that are aerodynamically sheltered, a 40% threshold for vegetation cover should be applied to the immediately adjacent, upwind grid cell. Details are provided in a SAG memo.[3]
5. For consistency, the same rule sets (outlined above) should be applied to the Pre-Disturbance scenario in the DRI model. Although the 1939 photogrammetric imagery used to develop the Pre-Disturbance scenario is over-exposed and grainier than the NAIP imagery, an analysis by UCSB indicates that the uncertainty levels are within the error bounds implicit to the complete modeling exercise (personal communication). In short, it is technically feasible to apply the same rule sets to both vegetation masks for the Pre-Disturbance and Current modeling scenarios without significant source of error.
6. Given that there are no PI-SWERL measurements within the various polygons labelled as VI and TP, there is a need to create power emissivity relations for the grid cells internal to each of the polygons that are classified as 'non-vegetated' or 'bare sand' (i.e., below the 15% cover threshold). A possible procedure is outlined below.

[3] SAG Memo – ***Recommendations for Reconciling DRI Model Assumptions with Ground Evidence in Respect of Vegetated Grid Cells*** (January 7, 2026).

7. Future PI-SWERL campaigns should include sampling of bare-sand surfaces within VI and TP polygons in order to generate power emissivity curves that are directly applicable to each of the polygons (rather than inferring dust emission potential based on measurements in nearby areas).

As noted above, the areas inside the VI and TP polygons are not completely vegetated, as is currently assumed in the DRI model. Figure 1 shows the central portion of the ODSVRA with VI polygons outlined in dark blue, and various TP polygons filled with shades of blue (most recent in dark blue and progressively lighter colors indicating projects dating back to 2022). Grid cells colored in green indicate vegetation cover >40% and pink cells indicate vegetation cover >15%, both having zero emissivity potential on the basis of the revised threshold (recommendation #1). Yellow grid cells are aerodynamically sheltered (as per recommendation #4) and are also considered non-emissive.

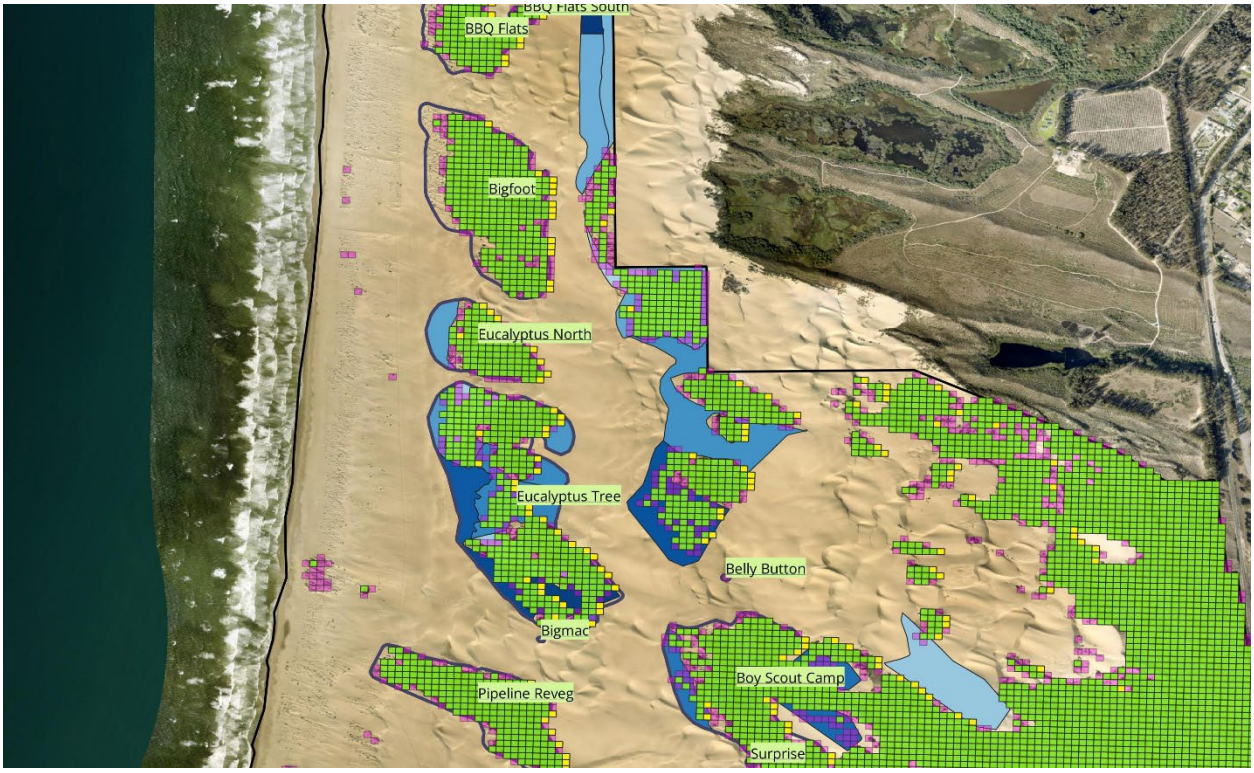



**Figure 1: Central sections of the ODSVRA with vegetated islands (VI) outlined in dark blue, and treatment projects (TP) shown in various shades of blue, as of early 2025. See text for additional information.**

There are numerous grid cells <u>within</u> VI and TP polygons that are not vegetated (i.e., <15% cover) and, therefore, they are reasonably expected to have some dust emitting potential. Some of these cells were treated recently (dark blue shades) and have not had time to evolve to full coverage, whereas others were treated several years ago but have failed to evolve for a number of reasons, mostly associated with wind disturbance and sand inundation. Table 1 (created by Tamar Carmona, CDPR) provides a sense of the extent of the challenge, showing that a total of 20% of grid cells within VI polygons are not vegetated to the level required to consider them non-emissive (as is assumed in the current version of the DRI model). A similar analysis for the

TP polygons has not been conducted, in part because the TP polygons are to be modeled separately with credit given for adaptive management efforts that anticipate the future vegetation states as plantings grow and fill in.

**Table 1: Distribution of vegetated (>15%) and non-vegetated (<15%) grid cells within vegetated island polygons in the ODSVRA.**

| | Number of Grid Cells | | | |
|---|---|---|---|---|
| **Name** | **Total** | **>15% cover** | **<15% cover** | **% of total with <15% cover** |
| | | | | |
| 7.5 Revegetation | 34 | 16 | 18 | 53% |
| APCD Test Plot | 8 | 8 | | 0% |
| BBQ Flats | 193 | 158 | 35 | 18% |
| BBQ Flats South | 8 | 8 | | 0% |
| Belly Button | 1 | 1 | | 0% |
| Bigfoot | 372 | 311 | 61 | 16% |
| Bigmac | 1 | | 1 | 100% |
| Boy Scout Camp | 311 | 277 | 34 | 11% |
| Crescent | 11 | 11 | | 0% |
| Enigma | 12 | 7 | 5 | 42% |
| Eucalyptus North | 137 | 101 | 36 | 26% |
| Eucalyptus Tree | 584 | 380 | 204 | 35% |
| La Grille Hill | 57 | 51 | 6 | 11% |
| Moymell | 13 | 9 | 4 | 31% |
| Pavilion Hill | 129 | 102 | 27 | 21% |
| Pipeline Reveg | 234 | 219 | 15 | 6% |
| Schnauzer | 194 | 167 | 27 | 14% |
| Surprise | 2 | 2 | | 0% |
| Worm Valley | 45 | 41 | 4 | 9% |
| | | | | |
| **Grand Total** | **2346** | **1869** | **477** | **20%** |

Given that there are numerous grid cells within VI polygons (i.e., 477 in total, amounting to roughly 74 acres), and that these are unlikely to be treated effectively to a state of zero dust emission in the next year (given other project areas already planned for treatment), it seems prudent to classify these grid cells as currently emissive in the DRI model for purposes of the 2026 ARWP. In order to do so, a power emissivity relation needs to be applied to each of these grid cells. Since there are no existing PI-SWERL measurements within the VI perimeters, a synthetic relation needs to be constructed and applied.

In keeping with previous SAG guidelines, all relevant data should be considered for inclusion in constructing a power emissivity curve, if it makes logical sense to do so. In this instance, the

strategy would be to recognize that areas inside VI polygons have not been exposed to OHV disturbance in recent times, and therefore all PI-SWERL measurements taken in nearby areas considered to be "non-riding" should be evaluated for inclusion. All areas with riding disturbance, whether annual or seasonal, should not be considered for inclusion.

Previous studies have indicated that there are geographic controls on the dust emitting potential of the ODSVRA surface, in particular a north-south gradient in grain size and emissivity. Given that most VIs are in the central portion of the ODSVRA, mostly embedded within and bounded by designated riding areas, it makes little sense to include the PI-SWERL measurements taken in the NRA North (Dune Preserve) and NRA South (Oso Flaco). This leaves the NRA Central as the primary data source. Nevertheless, most PI-SWERL measurements within the NRA Central are to the east of the VIs, in inland locations where grain sizes are known to be smaller than near the coast. PI-SWERL measurements in the Foredune Restoration Area (FRA) and Plover Exclosure (PE) are also candidates for inclusion because: (i) there has been no riding in these areas since about 2019 and 2020, respectively; (ii) there are a large number of PI-SWERL measurements taken in 2022 and beyond, which adequately characterize the emissive properties of the sand surfaces in the broad area of the foredunes; and (iii) the measurement locations in the FRA and PE are actually closer to the windward side of the VIs than those taken in the NRA Central (on the leeward side of the VIs). Figure 2 shows the distribution of PI-SWERL measurements in the FRA and PE since 2022 and in the NRA Central since 2013 relative to the major VIs. Accordingly, the SAG makes the following recommendation:

8. For the northerly VIs (i.e., Bigfoot and north), construct a synthetic power emissivity relation based on PI-SWERL measurements taken in the FRA (2022-2025 inclusive) pooled with the measurements taken since 2013 in the northern half of the NRA Central (roughly north of the orange dashed line in the map). Apply this relation to all grid cells inside each of the VI polygon outlines to determine the dust contribution from these 'bare sand' cells.
9. For the southerly VIs (i.e., Eucalyptus Tree and south), construct a synthetic power emissivity relation based on PI-SWERL measurements taken in the PE (2022-2025 inclusive) pooled with the measurements taken since 2013 in the southern half of the NRA Central (roughly south of the orange dashed line in the map). Apply this relation to all grid cells inside each of the VI polygon outlines to determine the dust contribution from these 'bare sand' cells.




**Figure 2: Distribution of PI-SWERL measurements in the Foredune Restoration Area (FRA) and Plover Exclosure (PE) since 2022, and in the Non-Riding Area (NRA) Central since 2013.**

The question of how to model the TPs (areas that have been treated with plantings) also needs to be addressed at this stage. At the moment, any TP that has been documented by CDPR is considered to have zero dust-emitting potential. The rationale for this is that such treatments are often accompanied by straw broadcasting, which effectively protects bare sand surfaces from wind erosion until plants are able to establish. However, some TPs have enjoyed only limited success as regards plant cover establishment, and after a period of a few years, the straw is no longer effective in preventing dust emission. Given that TPs are of varying vintage (with some dating back to 2020 or earlier), it seems judicious to evaluate the TPs in terms of percent vegetation cover as well as their stage of evolution. This is a complex undertaking, and it will demand lengthy discussion with CDPR personnel familiar with TP planting, but there seem to be several cases that need to be considered, as follows: (a) recent projects (i.e., 1-2 years old) that can be considered to be non-emitting; (b) maturing projects (3-5 years) that may or may not have

significant dust-emitting potential depending on how vegetation has evolved; (c) fully mature projects (>5 years) for which vegetation cover is >15% and are therefore non-emitting; and (d) fully mature projects (>5 years) in which a significant vegetation cover has failed to evolve (i.e., <15%), and therefore there is some level of dust emission likely. Prior to establishing a rule set by which to model the TPs in the DRI model, the SAG makes the following recommendation:

10. CDPR personnel familiar with TPs are asked to develop a short report on the status of the TPs in the ODSVRA with respect to vegetation cover percentage and stage of evolution. This information on which TPs have been successful, which have failed, and timelines would be most useful in developing a strategy for how to realistically portray TPs in the DRI model with respect to potential dust emissions.

Once such a report is in hand, further discussions will be required to finalize an approach that can be reasonably implemented into the DRI model for purposes of the 2026 ARWP.

Respectfully,

The Scientific Advisory Group

Bernard Bauer (Chair), Jack Gillies, Jenny Hand, Leah Mathews, Ian Walker

*THIS PAGE WAS INTENTIONALLY LEFT BLANK.*

May 31, 2026

**SAG Memo: <u>Contemplating DRI model refinements in anticipation of the 2026 ARWP</u>**

**From**: Scientific Advisory Group (SAG)

**To:** Karl Tupper, SLO Air Pollution Control District (APCD)
Jon O'Brien, California Department of Parks and Recreation (CDPR)
Ronnie Glick, California Department of Parks and Recreation (CDPR)

**Cc**: Sarah Miggins, California Department of Parks and Recreation (CDPR)

Significant progress toward dust mitigation in the Oceano Dunes State Vehicular Recreation Area (ODSVRA) has been achieved since the filing of the Stipulated Order of Abatement (SOA 2017-01) in May, 2018. Approximately 700 acres (inclusive of the 293-acre Plover Exclosure) have been subjected to dust control measures leading to a reduction in the number of hours of $PM_{10} > 300$ μg $m^{-3}$ at CDF and Mesa2, a reduction in annual violations of Rule 1001, a reduction in the number of exceedances of the California Ambient Air Quality Standard (CAAQS) of 50 μg $m^{-3}$ (averaged over 24 hours), and continued decrease in various indicators such as the SAG metric, the difference-in-difference analysis, and the ratio of Total $PM_{10}$ over Total Wind Power Density. In the past three years, no new treatment projects were undertaken, and the indicators have stabilized accordingly, as documented in the 2025 ARWP. These are the tangible touchstones against which progress toward improved air quality can be judged in the most meaningful way. However, **the SOA evaluates regulatory compliance not according to these indicators but, rather, according to the current levels of dust emissions being less or equal to those from a pre-disturbance landscape scenario.**

A simulation model developed and curated by the Desert Research Institute (DRI) is relied upon to quantify the levels of dust emissions from both the pre-disturbance and current landscape scenarios. PI-SWERL measurements taken since 2013 are used to assess dust emission potential from the current landscape surface, with increasing confidence in the results given the large number of measurements that are now available. **The pre-disturbance surface, in contrast, has no measurements of dust emission potential, and therefore model simulations must depend on a number of assumptions about what the likely surface characteristics were prior to intensive human disturbance**. It is critical to appreciate that the primary objective in modeling the pre-disturbance landscape is not to be absolutely accurate (i.e., know with certainty how much dust might have been emitted in 1939) because there is no way to verify the model results. Instead, the approach is to use sound scientific judgement as to the likely conditions that existed at that time, and then to come to agreement about the predicted dust emissions as a baseline value against which current progress can be evaluated. **The baseline value is an operational target that cannot be assessed for absolute accuracy.** In this memo, the SAG strives to provide sufficient background material in support of a collegial discussion about parameterization (and updating) of the pre-disturbance scenario baseline value.

Over the past five years, on-going discussions between CDRP, APCD, and the SAG regarding quantification of dust emission potential from the ODSVRA have led to a series of modifications

to the DRI simulation model, which is continually being updated as new information becomes available. Last year, for example, a new modeling grid was constructed that covers the entire ODSVRA and new information was incorporated into simulation of the wind field. With respect to dust emissions from grid cells within Vegetated Islands (VIs), all of which were previously modeled as non-dust-emitting, consensus was reached recently regarding a revised rule set, as outlined in a previous SAG Memo[1] and agreed to during the SAG Semi-Annual meeting held via Zoom on April 13, 2026. The manner in which Treatment Projects (TPs) are to be parameterized remains a work in progress as of mid-May, 2026, awaiting a summary report with recommended guidelines from CDPR.

This memo deals specifically with concerns raised by APCD regarding how the pre-disturbance scenario is to be parameterized relative to the current landscape scenario. In particular, APCD has expressed concerns that zones (i.e., grid cells) that are unvegetated and classified as non-riding in the current landscape scenario are allocated emissivity profiles that yield less dust than equivalent areas in the pre-disturbance scenario. This applies specifically to the footprint of the Plover Exclosure (PE). Below, we outline what we believe are relevant points for consideration as well as some historical context that may inform discussions regarding a path forward.

## Background

All prior model simulations (reported extensively in previous ARWPs) were based on the 1939 pre-disturbance landscape being sub-divided into three primary zones (NRA North, NRA Central, NRA South). In contrast, the current landscape is sub-divided into ten zones that reflect the complexity inherent to the ODSVRA due to a range of management imperatives as informed by spatial differentiation of dust emission potential based on PI-SWERL measurements. A SAG memo[2] provides a detailed explanation of the SAG-recommended zonation as well as the emissivity power relations to be applied to each of the zones. These recommendations were adopted in late 2023, and the 2024 ARWP was the first to provide simulation results from the DRI model based on the new zonation and approach. The 2025 ARWP was similarly predicated on this approach, with incremental changes to the emissivity curves (i.e., power relations) as new PI-SWERL measurements were acquired, as per established protocols.

Most aspects of the modeling framework, as currently implemented, are non-controversial. For example, the emissivity curves developed for the NRA North (Dunes Preserve) and the NRA South (Oso Flaco) using all PI-SWERL data collected since 2013 are applied to these respective zones in both the pre-disturbance scenario and current landscape scenario. The only change in dust emission potential for each of these zones arises because of changes in vegetation cover (quantified using vegetation cover masks developed by UCSB) rather than dust-emitting potential of non-vegetated, bare sand surfaces, then versus now.

The primary difference between the pre-disturbance and current landscape scenarios in the DRI model is that the large central region of the ODSVRA—identified as NRA Central in the pre-disturbance scenario—has been sub-divided into many sub-units in the current landscape

[1] SAG Memo – ***Incorporating Vegetation Cover in the DRI Model***_April 9, 2026.
[2] SAG Memo - ***Updated SAG Recommendations for Establishing Emissivity Grids to be used in Modeling of Pre-Disturbance Conditions and Future Excess Emissions Reductions***_December 19, 2023.

scenario. The largest sub-units are the RA-Central North and RA-Central South, which have been, and continue to be, exposed to year-round human disturbance (OHV riding, camping, hiking, etc.) and are parameterized, accordingly, with emissivity curves specific to those areas in the contemporary environment. The footprint of both these management sub-units falls within the NRA Central zone of the pre-disturbance scenario, which is parameterized using the emissivity curve developed from PI-SWERL measurements made in the areas designated as non-riding in the central portions of the contemporary ODSVRA. This approach is also non-controversial, reflecting the fact that the grid cells in the currently-designated RAs are continually disturbed by OHV traffic and have greater dust emission potential than a pre-disturbance surface that was not exposed to OHV traffic.

The parameterization of several of the remaining management sub-zones (e.g., Foredune Restoration Area (FRA), Plover Exclosure (PE)) is less certain. Updated information from recent PI-SWERL measurements on dust emission potential across these sub-zones compels a re-examination of original assumptions regarding how these sub-zones were parameterized. Each of these zones (in the current landscape scenario) has a specific emissivity power relation assigned to it based on PI-SWERL measurements taken since 2022 in each of the respective sub-zones. In contrast, these areas in the pre-disturbance landscape are all assigned an emissivity curve based on PI-SWERL measurements taken in the NRA Central zone beginning in 2013. Several points are noteworthy in this respect.

1. The currently-implemented approach was adopted for the 2024 ARWP and utilized for the 2025 ARWP, with conditional approval from APCD in both years. Nevertheless, the APCD expressed early concern with the assumptions regarding the PE, as outlined in a letter dated February 9, 2024 (from Gary Willey to Sarah Miggins, regarding approval of the 2023 ARWP), which stated that,

   *"The proposed methodology is rational and improves upon the previous approach; however, as noted in our comments on an earlier version of the recommendations, we have concerns about some assumptions for the Plover Exclosure, specifically, that the area has lower emissivity today than it did prior to disturbance by off-roading. Nonetheless, we defer to the SAG's expertise and hereby approve the proposed emissions assumptions for use in the current modeling."*

   With respect to the 2024 ARWP, the final approval letter (October 31, 2024) from APCD did not mention this issue of applying different emissivity curves, although it expressed concerns with potential re-opening of the PE to OHV access. The same was true for the final approval letter (October 16, 2025) for the 2025 ARWP. Thus, it seems that a precedent has been set that sanctions the current modeling approach (as originally proposed in the December 19, 2023 SAG Memo). But, it is also apparent that APCD has expressed consistent and long-standing concerns (documented in review materials for draft ARWPs, as well as in verbal and written correspondence) with the use of different power relations applied to certain zones in the pre-disturbance and current landscape scenarios.[3]

[3] The APCD requested additional simulation runs that modeled the PE with an emissivity curve based on the NRA Central measurements in the current landscape scenario (i.e., ignoring the actual PI-SWERL measurements in the PE since 2022), and these results were incorporated into a table in the ARWP.

Specifically, APCD questions why the footprint of the PE in the pre-disturbance scenario is assigned a dust emission potential (based on the NRA Central measurements) that yields greater emissivity in 1939 relative to today, despite significant human disturbance in the decades between.

2. At the time of the reframing of the DRI model structure in late 2023 (to include various zones, each with a specific emissivity curve), there was sparse information and understanding of the surface emissivity of the PE and FRA. The PE was closed to OHV traffic and recreational use in October, 2021, which effectively dates back to March 1, 2021 given seasonal riding restrictions associated with breeding/nesting of the Western Snowy Plover before closure. Thus, at the time of the September, 2022, PI-SWERL campaign (the first to quantify emission potential in the PE footprint since closure), the area was only in its initial stages of landscape adjustment (i.e., vegetation growth, foredune development, textural sorting). Given documented annual variations in dust emissions within the ODSVRA, it was not known with any degree of certainty whether the 2022 PI-SWERL measurements were representative of a 'mature' surface that had not been recently disturbed. Similarly, the FRA was officially closed on January 1, 2020 (fencing efforts were initiated in mid-December 2019) and subsequently treated with experimental plantings, with each of the sub-units evolving differently. More PI-SWERL measurements were needed in subsequent years to better understand the emissive characteristics of the evolving surfaces, but the 2022 measurements were all that were available at the time of the 2023 ARWP.

   For the model simulation results that informed the 2024 ARWP, APCD stipulated (with SAG support and CDPR approval) that the 2022 PI-SWERL measurements were to be applied to the current landscape scenario in the PE and FRA because they most accurately reflected surface conditions at that time (rather than using a synthetic curve derived from other zones). However, **given the uncertainty associated with knowing whether the power relations derived from the 2022 measurements were stable and representative, it was agreed that the NRA Central power relation would be used when modeling the dust emissions from the pre-disturbance scenario in all the grid cells in the central portion of the ODSVRA**. The effect of this assignment of power relations to the footprint areas of the FRA and PE was that greater dust emissions were predicted from the pre-disturbance grid cells than for the same grid cells in the current landscape scenario in the PE and the FRA. APCD is of the opinion that this approach does not yield sensible results, and that any unvegetated grid cells where there are riding restrictions today should have the same (or greater) emissivity potential than for the pre-disturbance landscape.

3. In the SAG Memo[2] that made recommendations for establishing the zones, some justification was provided for treating the FRA and PE (and also the Seasonal Exclosure, SE) differently in the pre-disturbance scenario relative to the current landscape. Specifically, it was argued that the FRA, PE, and SE areas have all experienced modifications by human actions in one way or another, for lengthy periods of time. All three areas have been subject to OHV traffic up until fairly recently (and even today in the case of the SE), and the FRA has been modified with experimental planting. Since closure, the PE has also been modified with emplacement of large woody debris and broadcasting of wood chips and wrack in certain spots (personal communication with CDPR personnel).

Given this history of surface disturbance and modification in the FRA, PE, and SE, it is not unreasonable to conclude **that the current landscape might have a different dust emission potential than in 1939. In other words, there is no *a priori* reason to assume that they would be the same.** This is most clearly applicable to the SE (currently managed with seasonal opening/closure), for which there is no counterpart in the pre-disturbance landscape. In other words, we should expect that the emissive properties of the pre-disturbance surface could differ from what they are today in the SE footprint. Similarly, the experimental plantings in the FRA have no analog in the pre-disturbance landscape, despite the expectation that each of the six treated areas will ultimately equilibrate to some 'natural' state. Whether this evolving surface will mimic the conditions in 1939 can never be known with certainty. Thus, in the case of the FRA, we can similarly expect that the pre-disturbance emission potential might differ from that of the current landscape scenario.

The situation in the PE is more nuanced and less certain because the intensity of recent human disturbance in the PE has been relatively minimal. However, there is little empirical evidence to indicate that the current surface has achieved a stable equilibrium state that mimics that of the pre-disturbance surface (in terms of vegetation cover, textural sorting vertically and horizontally) nor is there a robust method to ascertain what the dust-emitting potential was in the pre-disturbance landscape. We can never know with certainty whether the dust emission potential of the pre-disturbance surface was greater or lesser than it is today. APCD believes that the pre-disturbance surface was less emissive than (or equal to) what it is now. The SAG does not disagree but also allows for the possibility that the emissivity could have been greater in the pre-disturbance landscape given that the PE surface has been treated routinely in recent years.

4. Of all the zones that have been characterized by PI-SWERL measurements, the NRA Central is, perhaps, the one subject to most sampling bias. There are relatively few measurements from the thin, eastern strip along the northern portions of the NRA Central, in part because most of that zone has been replanted and is categorized as Treatment Projects (i.e., no longer in the NRA Central and therefore not sampled). In contrast, there is an extensive cluster of repeat measurements in the more southerly zone that extends much farther inland than the rest of the ODSVRA. Overall, the vast majority of NRA Central measurements were taken in locations that are at significantly large distances from the beach and foredune. Why is this important?

   It is generally understood (although difficult to prove unequivocally for the ODSVRA given existing data) that aeolian transport leads to a grain-size fining trend in the inland direction. In other words, foreshore and beach sediments tend to be poorly sorted with a substantial coarse fraction and a long tail of fines, foredune sediments tend to be finer on average, and sediments in the lee of the foredune and farther inland are typically the finest. There can be considerable variability in this general trend depending on the history of deposition over decades as well as recent process suites that modify the surface. However, if we take this fining-landward gradational sequence to be generally applicable to the ODSVRA (recognizing that there are intervening complexities associated with the non-riding areas adjacent to and immediately upwind of the NRA Central), and if we further assume that the

surfaces with the finest grain sizes are typically more emissive than those with coarse sediments, then it is reasonable to conclude that the power relation developed using the NRA Central measurements should yield greater dust emissions for the same wind speed as a power relation developed using PI-SWERL measurements taken in areas where there are coarse sediments, such as the beach and foredune. In other words, **applying the NRA Central power relation to sub-zones close to the beach (e.g., FRA, PE, SE) would likely lead to an over-prediction of the true dust-emitting potential from those areas**. This is why actual PI-SWERL measurements taken in the FRA, PE, and SE since 2022 are used to parameterize dust emissions from those zones in the current landscape scenario. There is no need to change this aspect of the model.

There are, however, implications for how the pre-disturbance scenario has been (and is being) modeled using the currently-implemented approach. The inland regions of the NRA Central are modeled using the NRA Central power relation, as is appropriate, but **it becomes less obvious that this is the power relation that is best suited to parameterize the areas closer to the beach, where grain sizes were undoubtedly coarser in the pre-disturbance scenario as they are today**. The challenge is to reach agreement on how to refine the DRI model, if at all, to accommodate this likelihood. In point #2 above, it was noted that there were insufficient data in 2023 to make any attempt to accommodate this putative landward trend in emissivity potential, so the default position was, by necessity, to use the NRA Central emissivity curve. The situation has changed in the intervening years with the acquisition of many more PI-SWERL measurements in the FRA, PE, and SE. These could be used to inform the construction of new power relations that may be more suitable in characterizing portions of the pre-disturbance landscape.

5. In terms of procedures, the SAG has consistently embraced the principle to use all applicable data that are available to construct power relations, unless there are explicit reasons to eliminate some data from consideration. This principle has been articulated in many documents and used consistently in the past, and it should continue to be respected when contemplating the parameterization of power relations for the FRA, PE, SE, NRA Central, and all other zones. However, the specific mix of available data included in specific power relation applicable to the pre-disturbance scenario depends not simply on spatial location but also on reasoned arguments for why data from some zones are included while others are precluded.

## Recommendations

The SAG appreciates that any changes to the modeling framework will have consequences for total modeled dust emissions from the ODSVRA, and hence for SOA compliance assessments that may, in turn, have real-world consequences for park operations and management. Nevertheless, it is the SAG's responsibility to provide the best advice to CDPR and APCD based on scientific principles, theoretical reasoning, and empirical evidence, and also to respond to concerns expressed by either party to the SOA. The SAG considers the continually evolving nature of dust emissions from the ODSVRA as well as any new information that is relevant to the management challenge. We know much more about dust emissions from the ODSVRA than

we did in 2022 when the SOA was first re-framed to assess compliance on the basis of reductions of mass-based $PM_{10}$ emissions within the ODSVRA to a level consistent with the pre-disturbance conditions. This new understanding leads us to make the following recommendations.

**The SAG does not support a suggestion from APCD to apply the power relation from the NRA Central (or NRA South) to the entire footprint of the zone identified as the PE for BOTH the pre-disturbance and current landscape scenarios equally.** This violates the general principle that all available data should be used unless there is a reason to exclude a portion of the data from consideration on reasoned grounds. The FRA, PE, and SE areas have been monitored since 2022, and those PI-SWERL measurements are the best indicator of dust-emitting potential from those zones in the current condition. These data should be utilized to parameterize the emission potential from the PE and not be ignored.

**The SAG does not support the suggestion from CDPR to continue to model the entire NRA Central in the pre-disturbance scenario with the NRA Central power relation.** Despite the precedent that has been set in prior ARWPs, the decision to apply the NRA Central power relation to the pre-disturbance scenario was the only viable option at the time. It was appreciated by all that this was an expedient solution to an uncertain problem, even though there was awareness amongst SAG members that there was likely an inland-fining trend in grain size that could influence dust emission potential. Unfortunately, there was little empirical evidence at hand to support the trend. Indeed, an attempt was made to investigate whether there were statistically-significant differences between PI-SWERL measurements in the western versus eastern portions of the ODSVRA (see page 18 and Appendix II of SAG Memo: Update SAG Recommendations for Establishing Emissivity Grids to be used in Modeling of Pre-Disturbance Conditions and Future Excess Emissions Reductions, December 19, 2023) but this line of inquiry, focused mainly on the RA, proved unfruitful at the time and was not pursued further.

A large number of PI-SWERL measurements from the PE are now available, and these indicate that there are statistical differences between the emissivity potential along the beach relative to farther inland in the lee of the foredunes. The limited number of samples from within the foredunes are not statistically different from those on the beach nor from those in the lee areas, suggesting that the foredunes are intermediary between two, more distinct populations (beach vs lee). Although a rigorous analysis has yet to be performed, the emission profile of the lee sediments appears similar to the NRA Central and NRA South, both of which comprise mostly inland measurement locations. To the extent that the pre-disturbance landscape had a similar landward-fining trend in sediment texture, it would be reasonable to conclude that even in the pre-disturbance landscape the emission potential of the beach and foredune surfaces would have been less than farther inland. Thus, **it seems inappropriate to apply the NRA Central emissivity power relation (based on inland only measurements) to the entire zone outlined as NRA Central in the pre-disturbance scenario (i.e., including those areas now identified as the FRA, PE, and SE).**

The SAG makes the following recommendation with respect to refining the dust emission potential of the pre-disturbance landscape.

**The NRA Central region of the pre-disturbance landscape should be divided into two large sub-zones to better reflect the inland-fining trend that is likely to have existed in 1939, and as is found on most natural beach-dune systems across the world.** There are two options to consider.

**Option 1: A new sub-zone for the pre-disturbance scenario would comprise the footprint of the current management zones known as the Plover Exclosure, Foredune Restoration Area, and Seasonal Exclosure Area.** The combination of these zones into one large pre-disturbance sub-zone accommodates the need to isolate these beach-proximal and foredune areas from the rest of the inland areas that likely have finer grain sizes and greater dust-emitting potential. Use of existing polygon boundaries for the PE, FRA, and SE will facilitate ease of modeling. However, this new sub-zone does not cover the full extent of the beach and foredune area in the ODSVRA to the north of the FRA.

**Option 2: A new beach-foredune zone could be carved out of the NRA Central zone, and it would consist of a north-south trending strip of land bounded by the ocean shoreline to the west and an eastern boundary line placed approximately 200 - 400 m inland from the shore.** Nominally, the north-south extent of the new zone covers the distance between Arroyo Grande Creek on the north to southern boundary of the Plover Exclosure (where it abuts with the Oso Flaco management zone). Thus, it most accurately reflects the entire latitudinal extent of the beach and foredune areas in the ODSVRA. A maximum width of 400 m for this new zone follows recommendations provided by a report from Swet et al., (2022; see Figure 1 on page 11)[4] that indicates that this is the average maximum width of the foredune zone along this stretch of coastline. However, a narrower width of this new sub-zone could be agreed to as long as it captures most of the foredune extent and doesn't cover too much of the landward lee area. Recent PI-SWERL measurements in the PE could be used to determine an appropriate average width. There are certain locations where the width of the new zone will be quite narrow, such as in the north where a wide strip would overlap substantially with the Dunes Preserve. The width of the sub-zone in the north would need to follow the fenced boundary of the Dune Preserve, which partitions it from the strip of beach that is currently used mainly as an access/egress corridor for OHV and street-legal traffic. Similarly in the south, the proposed zone will need to accommodate the fact that the North Oso Flaco management zone occupies a beach-foredune position and is not part of the NRA Central in the pre-disturbance scenario. **The detailed outline of such a new sub-zone would require further discussion.**

**Under either Option 1 or Option 2 (creating a new sub-zone in the pre-disturbance scenario), the remainder of the NRA Central portion of the pre-disturbance scenario will continue to be modeled as it is now—i.e., using the power relation derived from PI-SWERL measurements from the NRA Central designated areas since 2013.**

The new sub-zone will require the development of a synthetic power emission relation, and this will require additional discussion. Specifically, it will be important to decide which PI-SWERL measurements will be considered for inclusion, and which data to eliminate from consideration. For example, the SE has no direct analogue in the pre-disturbance scenario, and this area is

[4] Swet, N., Hilgendorf, Z., Walker, I., 2022. UCSB Historical Vegetation Cover Change Analysis (1930-2020) within the Oceano Dunes SVRA.

disturbed seasonally by OHV riding on an annual basis, which was not the case in the pre-disturbance era. For this reason, it seems reasonable to exclude PI-SWERL measurements taken in the SE from further consideration. In developing a synthetic power emission relation for the new sub-zone in the pre-disturbance scenario, there are two sensible options to consider, as follows:

**Option A: Include all measurements taken since 2022 in both the PE and the FRA, and create a synthetic power relation based on these data.** As noted above, both the PE and FRA have been closed to OHV and camping access since about 2021 and 2020, respectively, and therefore surface conditions have begun to return to a largely undisturbed state (despite sporadic management interventions). Whether this evolving state reflects a 'natural' condition that mimics what was there in 1939 is not known, but the PI-SWERL measurements in the PE and FRA since 2022 are the best representation of what might have been the pre-disturbance surface state in the new sub-zone. The NRA Central PI-SWERL measurements that were originally used are no longer under consideration because they represent the emissivity potential at inland locations where grain sizes are finer than the beach and foredunes.

**Option B: Include all measurements taken since 2022 in the PE, but only those measurements from the control area (Treatment 1) within the FRA**. The control area of the FRA was, in fact, not treated with plantings, despite being referred to as Treatment 1. It reflects how the foredune area would evolve naturally in the absence of OHV activity in terms of vegetation cover, foredune growth, sediment capture, and textural sorting. The five other treatment areas were subjected to a variety of surface modifications (e.g., sheepsfoot texturing, straw broadcasting), seeding strategies, and planting assemblages. Arguably, none of these five treatment areas has a direct analogue in the pre-disturbance landscape, although Treatment 6 ("Parks Classic") used randomly planted seedlings and native seeds and may therefore mimic a 'natural' foredune surface in the ODSVRA.

An analysis of the PI-SWERL data included in Option A and Option B was conducted, and despite a reduction in the total number of available data points for Option A (n = 286) to Option B (n =136), there is virtually no difference in the power emissivity relations. This also applies to a case where PI-SWERL measurements from both Treatment 1 and Treatment 6 were considered (n = 176). The medians for each of the three PI-SWERL speeds were essentially the same (see Table 1), although the means and standard deviations differed slightly, which reflects the fact that the FRA is generally characterized by a larger data range and greater extremes (especially in Treatments 2 – 5) than for the PE. Table 1 presents the medians and the coefficients (a) and exponents (b) for the power emissivity relations derived using the medians, as per established protocols. Figure 1 is a graphical representation of the three curves, demonstrating the negligible difference between Option A and Option B (both T1 and T1+T6).

**Table 1: Median dust flux values (mg $m^{-2}$ $s^{-1}$) as a function of the three PI-SWERL speeds for Option A (PE + FRA) and Option B (two approaches). Regression parameters for the power relation $F = a\ (u_*)^b$ where F is the flux (emissivity) magnitude (mg $m^{-2}$ $s^{-1}$) are included at the bottom of the table. Power regression results calculated using SigmaPlot© software.**

| u* | PE + FRA | PE + T1 + T6 | PE + T1 |
|---|---|---|---|
| ***n* =** | *286* | *176* | *136* |
| | | | |
| | median | median | median |
| **0.381** | 0.005 | 0.004 | 0.003 |
| **0.534** | 0.066 | 0.064 | 0.063 |
| **0.607** | 0.180 | 0.180 | 0.180 |
| | | | |
| **a** | 8.929 | 10.150 | 10.890 |
| **b** | 7.821 | 8.076 | 8.218 |
| | | | |
| **Rsqr** | 1 | 1 | 1 |

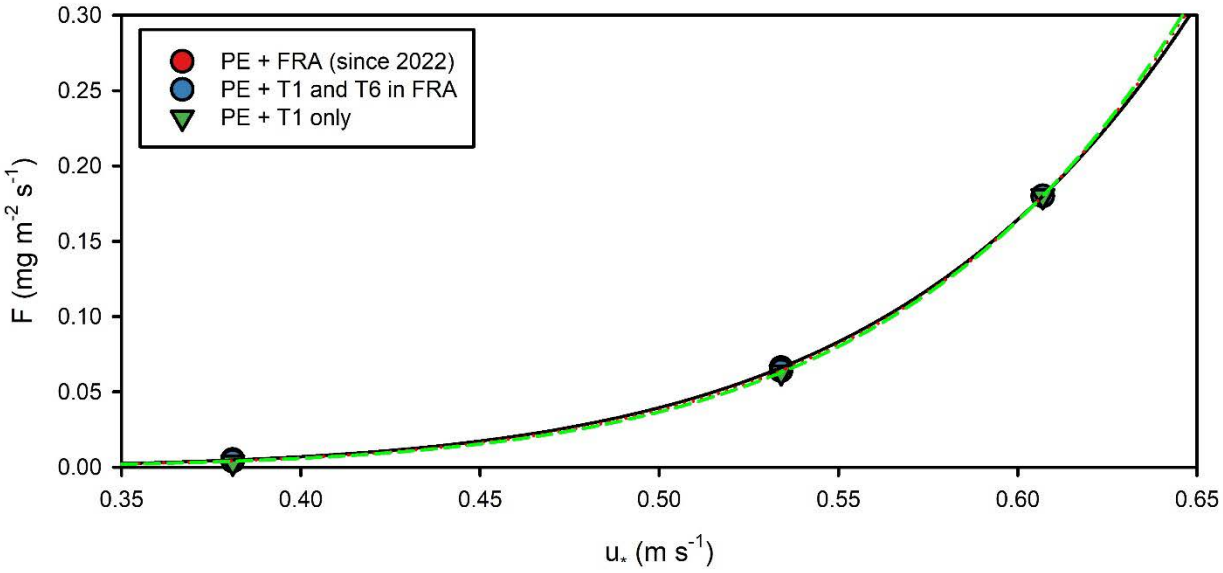



**Figure 1: Graphical representation of the three power relations for which the regression parameters appear in Table 1.**

Figure 2 shows the power relation derived using Option A data (PE and FRA since 2022) relative to power relations for other management zones in the ODSVRA. Not surprisingly, the Option A curve sits approximately half-way between the curves for the PE (lowest) and the FRA (higher).

All three curves have emissivity potentials less than the three Non-Riding Areas (NRA South, NRA Central, NRA North). As described above, the current DRI model parameterizes the footprints of the PE and FRA in the pre-disturbance scenario using the NRA Central curve, which yields and outcome where the pre-disturbance surface yields greater modelled dust emissions than today. With the adoption of Option A (or Option B), the outcome will be that there will be slightly greater dust emissions from the FRA today than in the pre-disturbance era BUT the reverse will be true for the PE. That is, there will continue to be smaller dust emissions from the PE today than from the pre-disturbance landscape, although the difference will be significantly smaller than when the NRA Central curve was used. As noted above, the SAG does not find this to be problematic given on-going management interventions in the PE.

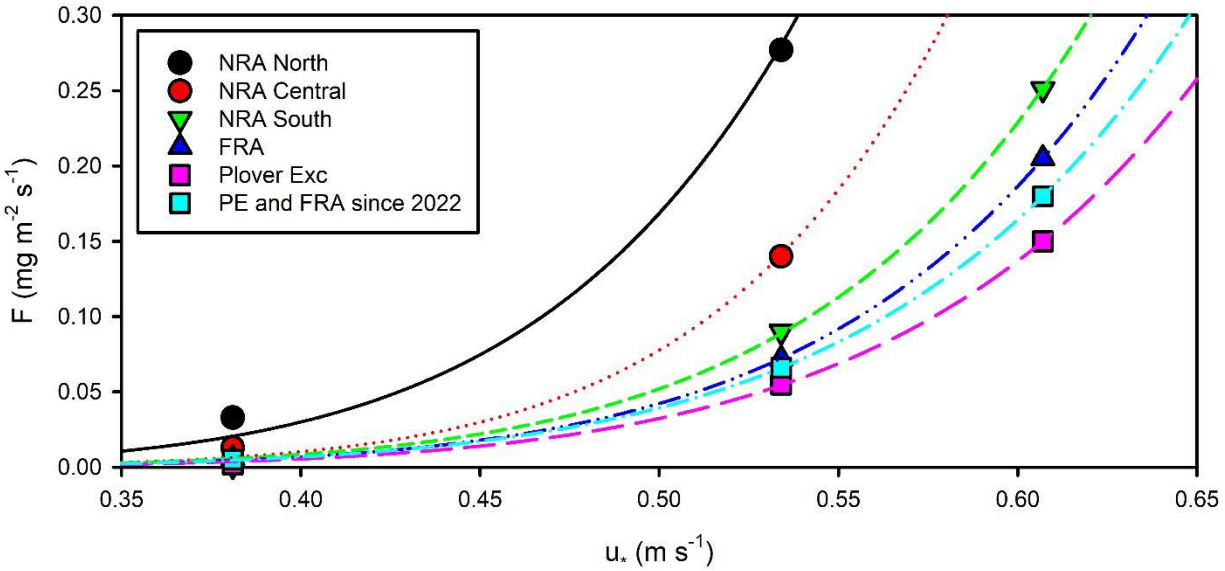



**Figure 2: Comparison of the power relation for Option A with those from other management zones in the ODSVRA.**

Should CDPR and APCD agree to adopting Option 1 or Option 2 (with respect to a new sub-unit within the pre-disturbance scenario), the complexity of the DRI model increases only marginally. The SAG believes it will improve the reliability and acceptance of the results as regards establishing a defensible pre-disturbance emission baseline, as required by the SOA. We anticipate fruitful and collegial discussion on this matter in advance of the 2026 ARWP.

Respectfully,

The Scientific Advisory Group

Bernard Bauer (Chair), Jack Gillies, Jenny Hand, Leah Mathews, Ian Walker

*THIS PAGE WAS INTENTIONALLY LEFT BLANK.*

June 10, 2026

**Memo: Synthetic Power Relations for Vegetation Islands**

**From**: Scientific Advisory Group (SAG)

**To:** Karl Tupper, SLO Air Pollution Control District (APCD)
Jon O'Brien, California Department of Parks and Recreation (CDPR)

**Cc**: Ronnie Glick, California Department of Parks and Recreation (CDPR)

In a series of memos[1], the SAG has discussed the parameterization of vegetated grid cells in the simulation model developed and curated by the Desert Research Institute (DRI), which is the primary tool used to assess compliance with the Stipulated Order of Abatement (SOA). In the April 9, 2026 memo, a series of recommendations were made, and these were adopted in a subsequent SAG Semi-Annual meeting held on April 13, attended by personnel from CDPR and APCD.

This memo deals specifically with the need to develop synthetic power relations that are applicable to grid cells within Vegetation Islands (VIs) that are classified as 'emissive' in respect of their potential to release dust during wind events. Whether a grid cell receives a designation of 'emissive' or 'non-emissive' depends, in the first instance, on whether there is less than or greater than 15% plant cover, respectively. If deemed 'emissive', a power relation has to be assigned to each such grid cell in the DRI model. The particulars were specified in the April 9, 2026 memo, as follows:

> For the northerly VIs (i.e., Bigfoot and north), construct a synthetic power emissivity relation based on PI-SWERL measurements taken in the FRA (2022-2025 inclusive) pooled with the measurements taken since 2013 in the northern half of the NRA Central (roughly north of the orange dashed line in the map). Apply this relation to all grid cells inside each of the VI polygon outlines to determine the dust contribution from these 'bare sand' cells.
>
> For the southerly VIs (i.e., Eucalyptus Tree and south), construct a synthetic power emissivity relation based on PI-SWERL measurements taken in the PE (2022-2025 inclusive) pooled with the measurements taken since 2013 in the southern half of the NRA Central (roughly south of the orange dashed line in the map). Apply this relation to all grid cells inside each of the VI polygon outlines to determine the dust contribution from these 'bare sand' cells.

PI-SWERL measurements in the Foredune Restoration Area (FRA) and Plover Exclosure (PE) are easily identified because these are separate management units that have been routinely

[1] SAG Memo – ***Management of Vegetated Areas in Respect of Zero Emissions*** (December 1, 2024)
SAG Memo – ***Recommendations for Reconciling DRI Model Assumptions with Ground Evidence in Respect of Vegetated Grid Cells*** (January 7, 2026).
SAG Memo – ***Incorporating Vegetation Cover into the DRI Model*** (April 9, 2026)

monitored since 2022. In contrast, PI-SWERL measurements applicable to the northerly and southerly VIs within the NRA Central were more challenging to separate from the master spreadsheets. QGIS was used to locate the applicable measurements, and these were extracted from the master spreadsheet and pasted into two new spreadsheets for subsequent analysis. Table 1 shows the number of measurements used in the analysis and their temporal distribution. A total of 224 values were in the data set for the Northerly VIs (Bigfoot and northward), and 357 values were in the data set for the Southerly VIs (Eucalyptus Tree and southward).

**Table 1: Enumeration of the number of PI-SWERL measurement locations used for the two synthetic power relations (Northerly VIs; Southerly VIs)**

| | **Northerly VIs** | | | **Southerly VIs** | |
|---|---|---|---|---|---|
| | FRA | NRA Central | | PE | NRA Central |
| **DATE** | | | | | |
| Aug 2013 | | 6 | | | 21 |
| Sept 2014 | | | | | 35 |
| June 2015 | | 2 | | | |
| Oct 2015 | | 6 | | | |
| Mar 2016 | | 12 | | | 22 |
| May 2019 | | 19 | | | 60 |
| Oct 2019 | | 2 | | | |
| May 2022 | | | | | 17 |
| Sept 2022 | 67 | | | 23 | |
| May 2024 | | | | | 46 |
| Sept 2024 | 110 | | | 30 | 46 |
| Sept 2025 | | | | 57 | |
| **TOTAL** | **177** | **47** | | **110** | **247** |

As per established procedures, the median values for each of the three PI-SWERL shear velocities were determined and used in a power regression procedure to generate coefficients and exponents for the power law. Table 2 provides the relevant parameters, and Figure 1 shows the curves for the Northerly and Southerly VIs in relation to the curves for the NRA Central, FRA, and PE.

**Table 2: Power relation coefficients (a, b) for the two synthetic power relations to be applied to grid cells in the Northerly (Bigfoot & North) and Southerly (Eucalyptus & South) VIs.**

| | **Bigfoot & North** | **Eucalyptus & South** |
|---|---|---|
| ***n =*** | ***224*** | ***357*** |
| $u_*$ (m $s^{-1}$) | median | median |
| **0.381** | 0.007 | 0.009 |
| **0.534** | 0.092 | 0.100 |
| **0.607** | 0.270 | 0.320 |
| | | |
| **a** | 17.64 | 28.81 |
| **b** | 8.372 | 9.017 |
| **Rsqr** | 1 | 1 |

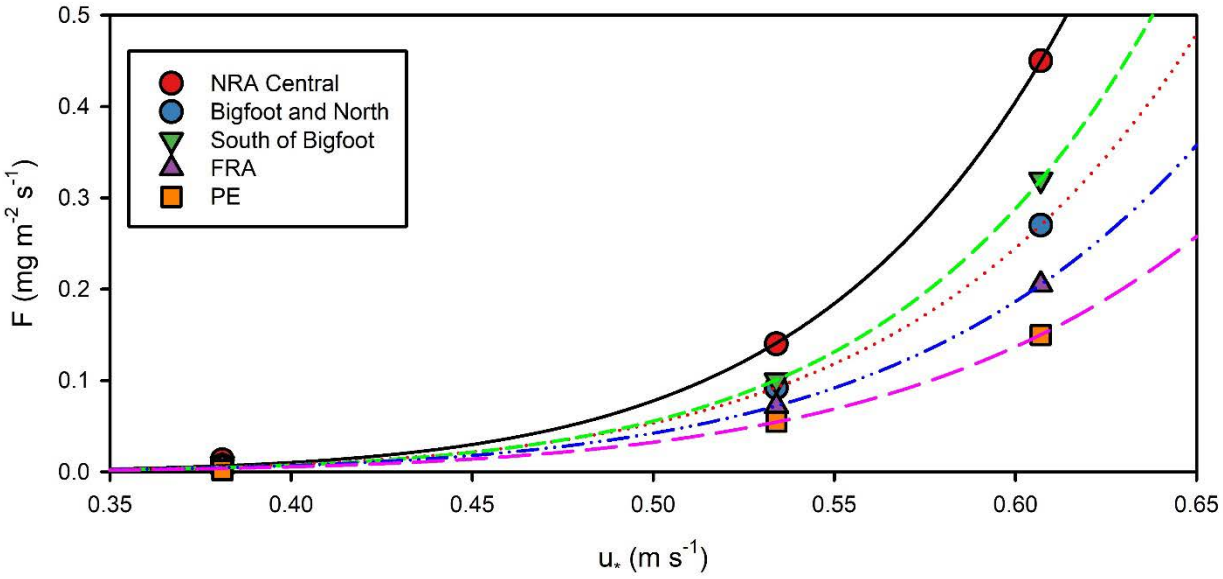



Figure 1. Emissivity curves for the two synthetic power relations (Bigfoot and North; South of Bigfoot) in relation to curves for the NRA Central, FRA, and PE using all data in each of those zones.

The two synthetic curves fall between their 'parent' curves, with the NRA Central showing greater emission potential and both the FRA and PE showing lesser emission potential than the synthetic curves. The curve for Bigfoot and Northerly VIs falls slightly below that of the Eucalyptus and Southerly VIs, in large part because the proportion of NRA Central to PE or FRA measurements is greater (347 vs 110) in the Southerly VI data mix than for the Northerly VI mix (177 vs 47), implying that the effect of the more-emissive NRA Central measurements may be over-represented in the south and under-represented in the north. There is no easy way to resolve this because the entire area designated NRA Central in the north has been subject to treatments, and PI-SWERL sampling of those areas concluded in 2019. In contrast, there remain wide open sand areas in the south of the NRA Central, and these were sampled extensively in 2024. Despite these minor shortcomings, the two new synthetic curves have the desirable property of balancing the surface emission potentials from the beach-foredune area (less emissive) with those from inland locations (more emissive). The difference between the two synthetic curves is small enough to be inconsequential to the overall emissions predictions from the DRI model.

Respectfully,

The Scientific Advisory Group

Bernard Bauer (Chair), Jack Gillies, Jenny Hand, Leah Mathews, Ian Walker

*THIS PAGE WAS INTENTIONALLY LEFT BLANK.*

# Restoration Project Maturation Time

## Purpose

To determine the time necessary for a dune restoration project to mature.

## Methods

A grid of 25x25 meter cells was placed over the Oceano Dunes SVRA. For each cell, the following categories were compiled:

- Restoration project boundaries: if a grid cell contains at least 50% of the project within it, it is tagged with that project's name
    - The project's name includes the year it was treated with straw and planted with vegetation (seeds and seedlings if available) in this format: 2022-VG-01. Some projects had seedlings planted in future years, based on greenhouse capacity, and all projects are tagged with the year that the seedlings were planted.
- 2024 vegetation layer from UCSB derived from 2024 NAIP aerial imagery: used to quantify the percentage cover within each grid cell
    - Vegetation cover greater than 15% is considered effective dust control within the dune environment.

Accordingly, each grid cell within restoration project boundaries was tagged with the year greenhouse plants were physically installed, and a percentage cover at the time that the imagery for the 2024 cover was taken. The age of a restoration project is generated by subtracting the planting year from 2024, the year of the imagery (Table 1, Figure 4). The count of grid cells >15% vegetation cover divided by the total count of grid cells for each project year results in a ratio of effective dust control mitigation in the total area of the restoration projects (Figure 1).

## Results

Figure 1 shows the ratio of grid cells with vegetation coverage percentage at >15% over total grid cells in the restoration project footprints by project year. Acreages planted per year are included to give an indication of sample sizes. Those acreages are from the actual project acreages (not from multiplying grid cells by a constant). The density of greenhouse seedlings planted per acre is also included.

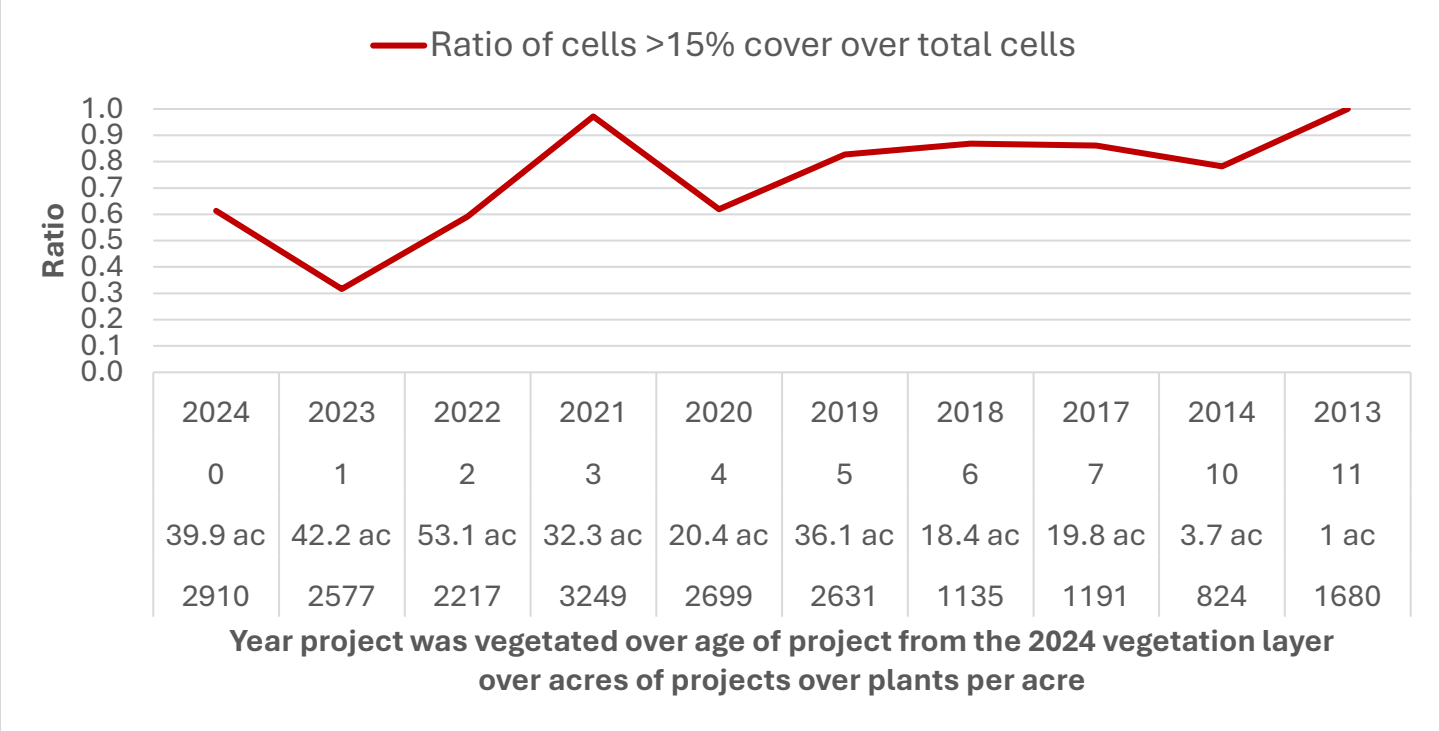



Figure 1. Ratio of effective project vegetation cells over total cells by project age from 2024.

At Year 0 (i.e., the initial year of restoration), the straw accounts for the coverage, as UCSB included it as coverage in their vegetation model. Crews installed plants and broadcast seed, but these are too small to be visible in the 2024 NAIP aerial imagery used by UCSB to quantify vegetation cover. When the project enters its first year, Year 1, the straw can be covered by sand and is not visible or accounted for in the percent cover estimate, despite holding the sand in place and allowing the newly planted native plants to establish their deep root systems.

Visual evidence of plant growth shows up in Years 1 and 2 ,-when coverage doubles from 30% of cells meeting or exceeding 15% coverage (in Year 1) to 60% of cells in Year 2. Year 3 and Year 4 are anomalous in that the 2021 projects were mainly protected by upwind vegetation (Figure 5) and were planted at a higher density per acre compared to other years.  Projects in 2020 (Year 4) were mainly the upwind edge projects (Also note that the 2020/Year 4 plots do not include the 48 acre foredune project). In Figure 2, the discrepancy between planting success of upwind (the right side in each image) vegetation versus the downwind protected vegetation is clear.

Year 5 shows 80% of grid cells within a project with 15% or greater plant cover. This appears to remain steady to the limit of the 11 year data record. The trend indicates that a project reaches a coverage plateau of approximately 80% at 5 years and holds at that 80%. The 100% at Year 11 is more a factor of the small trial project size of those early projects. The coverage at 80% might be a reflection of the sparsity in the upwind edges, which are replanted regularly to maintain the vegetation in the region where wind and sand move fastest.

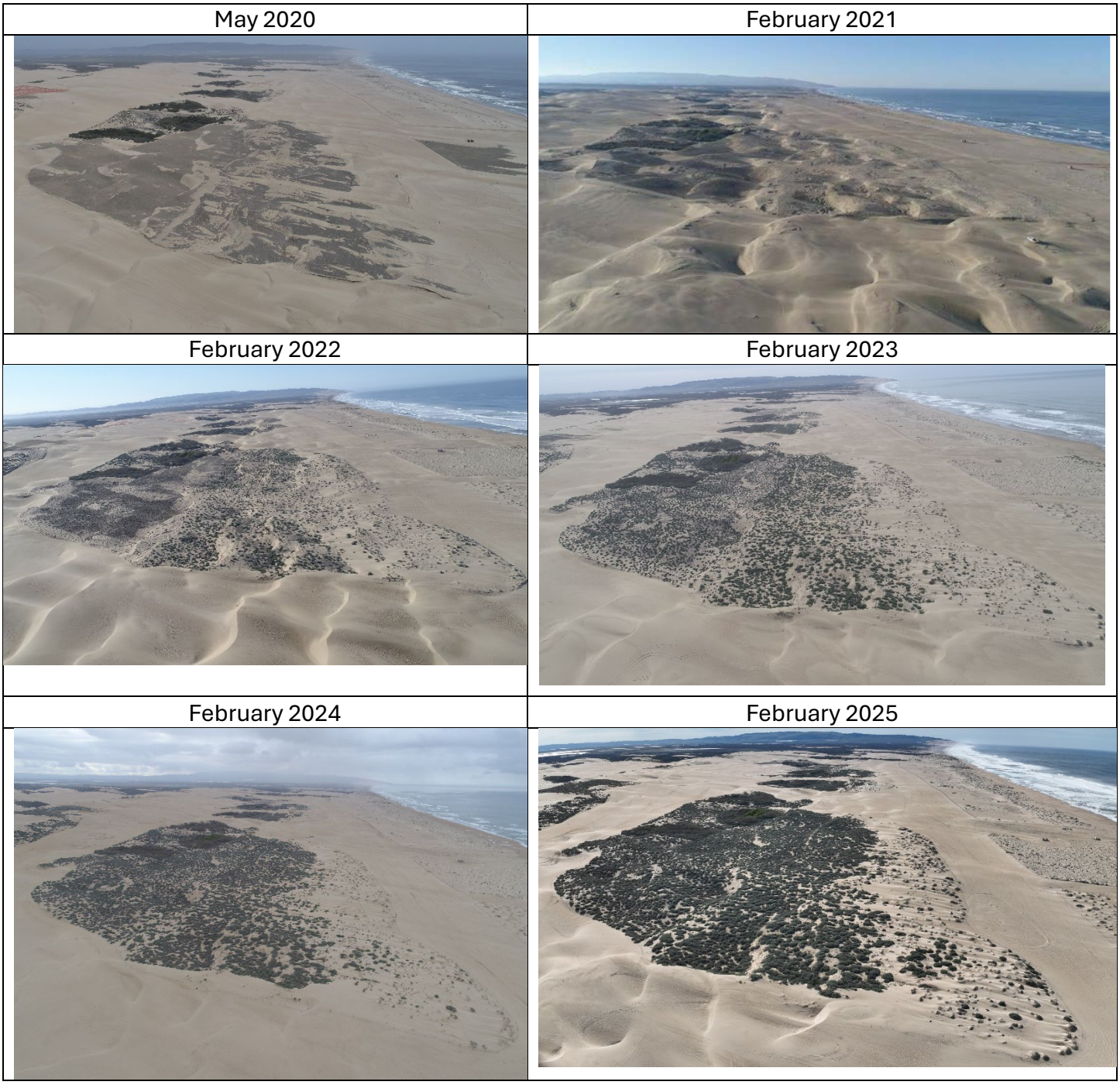



Figure 2. Example of northern portion of Bigfoot (2020-VG-04, 2021-VG-01) showing vegetation cover maturation in restoration projects.

## Discussion

Up to 2025, the DRI Emissions model treated all vegetation restoration plots as non-emissive after the first year of installation. This approach was initially supported by the SAG because there was an understanding that these projects would take time to develop and provide full emissions control. In 2025, the SAG and APCD noted that some of these vegetation plots had not achieved a minimum amount of cover and developed a recommendation to assign these areas some non-riding area emissivity until they reach a threshold cover of 15%.

This analysis demonstrates that it takes about five years post plant installation for projects to reach a plateau of more than 80% of the cells reaching 15% cover. For that reason, State Parks recommends assigning all areas that have been treated with vegetation zero emissions for the first five years post-planting and only after this time assigning an appropriate non-riding area emissivity to the remaining cells that remain below 15% cover, while also allowing for some downwind sheltering effect as discussed during regular SAG meetings during 2025 and early 2026. This approach provides some assurances that projects receive some credit once installed. After this five-year period post planting, once the plants have matured and ground surfaces are allowed to adjust, then cells with less than 15% cover can be factored back into the model with the appropriate non-riding area values to estimate their contributions to total PM10 emissions.

These projects take multiple years to plan for and execute:

- Determining the location using SAG data, getting approvals,
- straw purchasing and spreading,
- plant growing and planting (including by Cal Poly), working with CCC and ACE and RCD.

They also take multiple years to mature (Figure 2).

Note, some reviewers may note that Figure 1 shows vegetation projects that range from 36-53 acres per year rather than 42 acres as reported in Annual Report and Work Plans. This is mainly related to the availability of straw and the need for supplemental plantings. Straw availability limits the amount of new acreage that can be planted each year. In some years extra straw is spread while in others straw is more limited.

Figure 3 shows that some years have fewer acres of new vegetation plantings (full straw) but more acres of supplemental plantings. As reported in numerous ARWP's, the total areas treated each year is 42 acres, but for the purposes of this analysis, we only look at age of a project from the point where it is treated with straw and seedlings/native plantings. Supplemental plantings and plantings when straw is not available (No Straw) are not factored into the analysis in Figure 1.

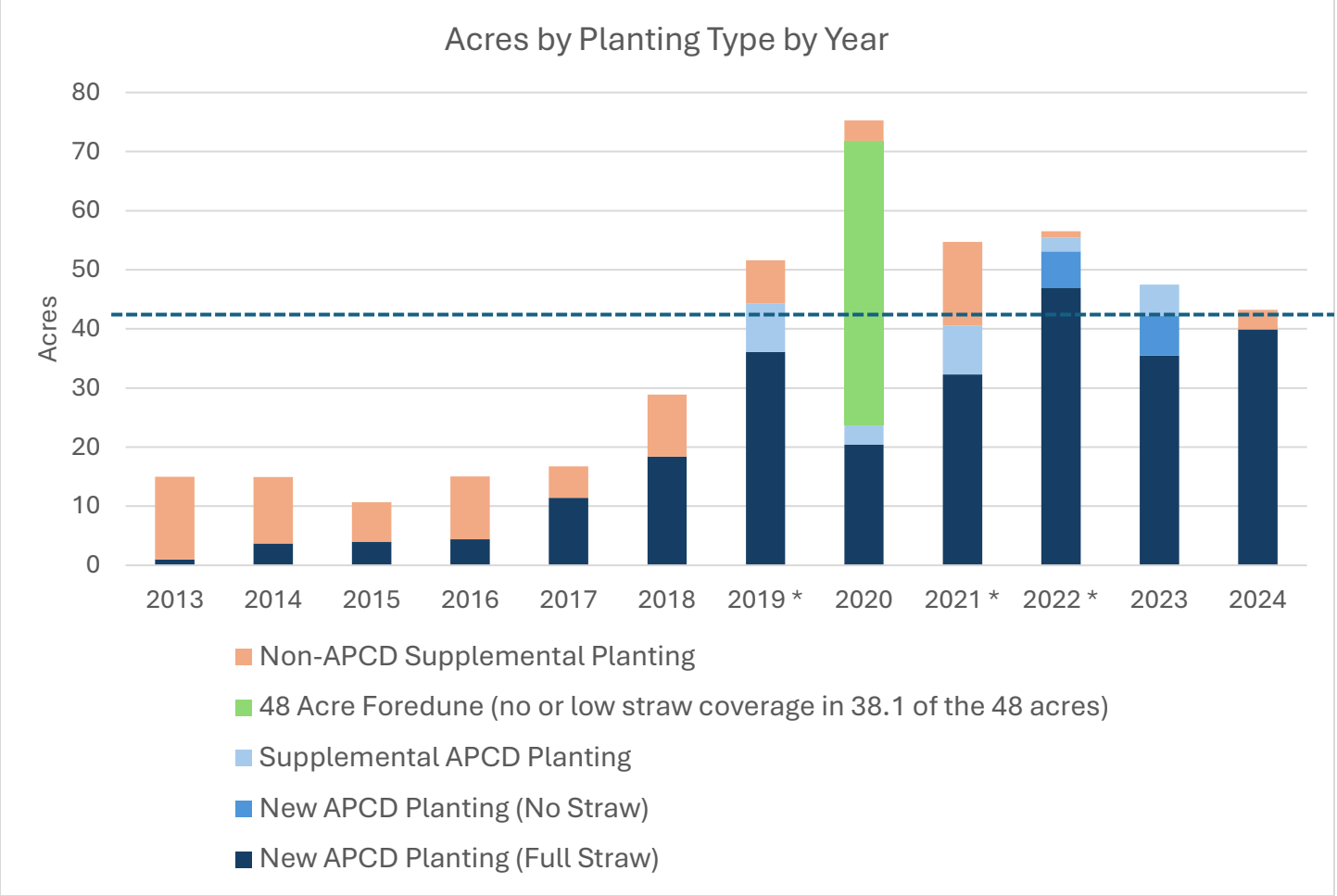



Figure 3. Acres planted with greenhouse plants each year, and the type of. * Straw applied previous year or spring in extra acreage.

## Conclusion

This analysis shows that it takes about five years post planting for vegetation treatments to reach a plateau of 80% of the cells reaching 15% cover. For the purposes of modeling emissions from vegetation treatment areas, State Parks advocates for using zero emissions for the first full five years post planting, and after that assigning the appropriate non-riding area emissions to the remaining cells that have less than 15% cover.

Table 1. Project ID, its year established, its age, and the count of grid cells within that project's boundary.

| Project ID | Year Planted | Age from 2024 | Count of Grid Cells | Count of Grid Cells >15% Cover | Ratio of >15% over total Grid Cells | Total Acres | Seedlings Planted per Acre |
|---|---|---|---|---|---|---|---|
| 2012-VG-01 | 2013 | 11 | 8 | 8 | 100% | 1 | 1680 |
| 2013-VG-01 | 2014 | 10 | 12 | 7 | 58% | 1.9 | 741 |
| 2013-VG-02 | 2014 | 10 | 11 | 11 | 100% | 1.8 | 912 |
| 2015-VG-01 * | 2015 | 9 | 194 | 167 | 86% | 30 | 936 |
| 2016-VG-01 * | 2016 | 8 | | | | | 1428 |
| 2017-VG-01 * | 2017 | 7 | | | | | 1190 |
| 2018-VG-01 | 2018 | 6 | 57 | 51 | 89% | 9.1 | 1569 |
| 2018-VG-02 | 2018 | 6 | 57 | 48 | 84% | 9.3 | 711 |
| 2019-VG-01 | 2019 | 5 | 178 | 143 | 80% | 27 | 2671 |
| 2019-VG-02 | 2019 | 5 | 59 | 53 | 90% | 9.1 | 2512 |
| 2020-VG-04 | 2020 | 4 | 134 | 83 | 62% | 20.4 | 2699 |
| 2021-VG-01 | 2021 | 3 | 102 | 102 | 100% | 14.8 | 3407 |
| 2021-VG-02 | 2021 | 3 | 25 | 23 | 92% | 4.1 | 2677 |
| 2021-VG-03 | 2021 | 3 | 53 | 51 | 96% | 7.9 | 3202 |
| 2021-VG-04 | 2021 | 3 | 33 | 31 | 94% | 5.5 | 3321 |
| 2022-VG-03 | 2022 | 2 | 128 | 115 | 90% | 19.9 | 2922 |
| 2022-VG-04 | 2022 | 2 | 31 | 1 | 3% | 4.6 | 2583 |
| 2022-VG-05 | 2022 | 2 | 34 | 22 | 65% | 5.5 | 2156 |
| 2022-VG-06 | 2022 | 2 | 20 | 2 | 10% | 3.3 | 1075 |
| 2022-VG-08 | 2022 | 2 | 20 | 2 | 10% | 2.9 | 1265 |
| 2022-VG-11 | 2022 | 2 | 42 | 22 | 52% | 6.3 | 2290 |
| 2022-VG-12 | 2022 | 2 | 33 | 17 | 52% | 4.9 | 1450 |
| 2022-VG-13 | 2022 | 2 | 37 | 23 | 62% | 5.7 | 1242 |
| 2022-VG-09 | 2023 | 1 | 97 | 44 | 45% | 14.9 | 2556 |
| 2023-VG-01 | 2023 | 1 | 136 | 43 | 32% | 20.5 | 2497 |
| 2023-VG-02 | 2023 | 1 | 42 | 0 | 0% | 6.8 | 2861 |
| 2022-VG-10 | 2024 | 0 | 18 | 10 | 56% | 2.4 | 2963 |
| 2024-VG-01 | 2024 | 0 | 142 | 88 | 62% | 21.7 | 2894 |
| 2024-VG-02 | 2024 | 0 | 34 | 15 | 44% | 5 | 2675 |
| 2024-VG-03 | 2024 | 0 | 70 | 49 | 70% | 10.8 | 3040 |

* Projects were done in smaller dispersed patches over three seasons in this earlier iteration, so the entire project area is included as one, and set to the latest date (which was the largest total area planted).

Note: 48 acre foredune plots are excluded as they are of a different vegetation community unlikely to meet the 15% threshold.

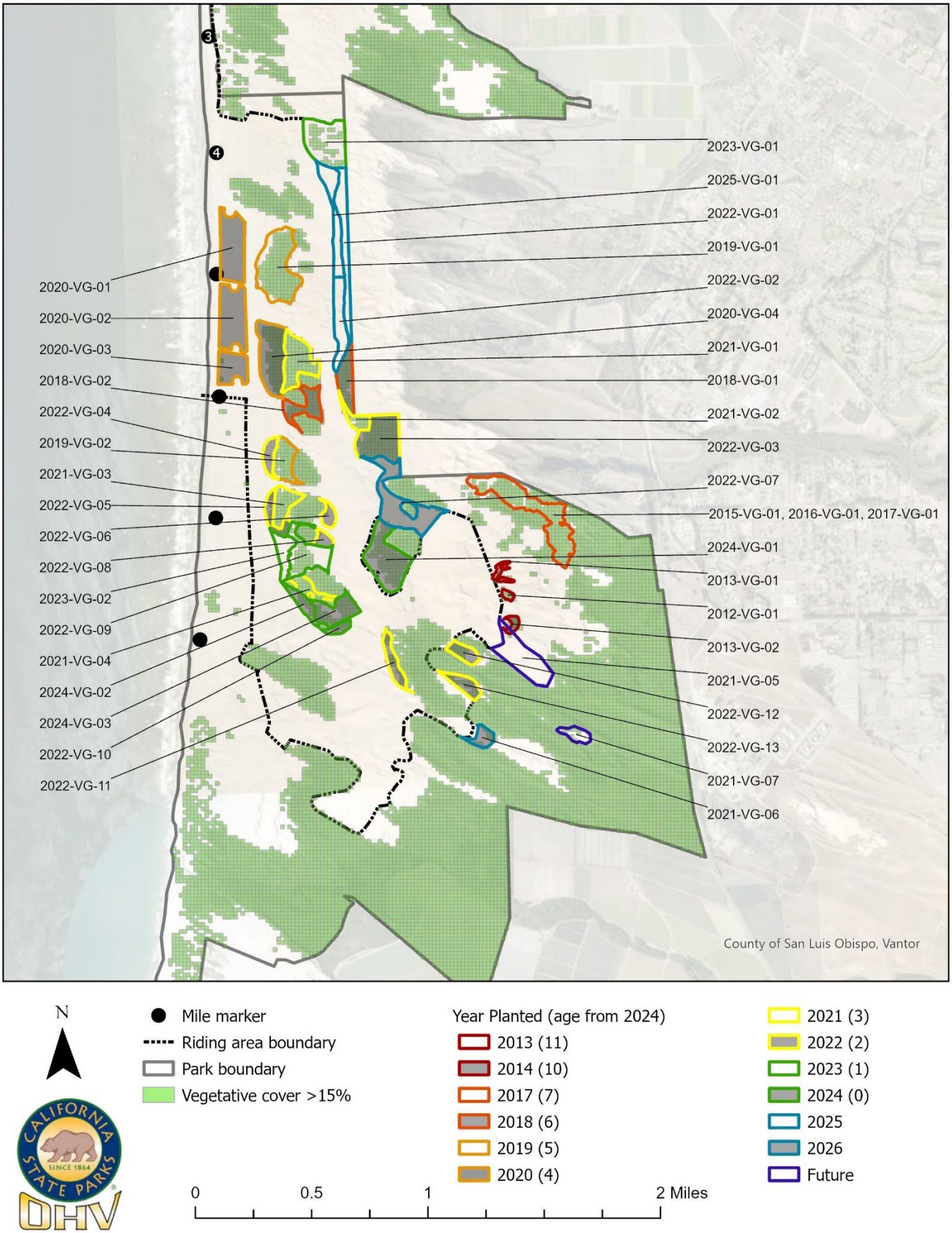



Figure 4. Dust control mitigation projects by location and year vegetated with a vegetation mask set at 15% and greater cover.

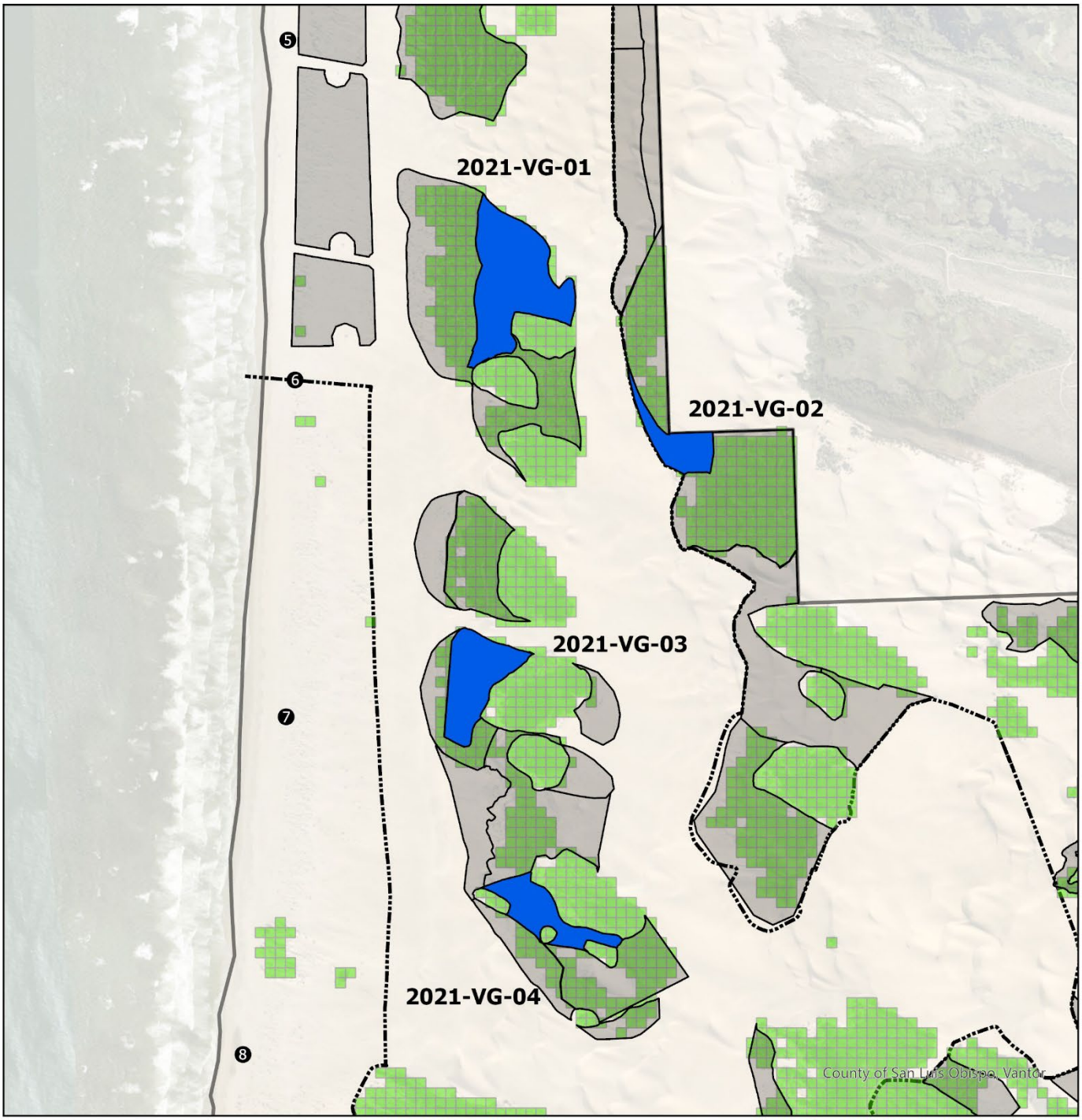



Figure 5. Dust control mitigation projects for 2021, which were more sheltered and had higher coverage success.

June 6, 2026

**Memo : Restoration Project Maturation Timeline**

From: California State Parks

To: Scientific Advisory Group (SAG)
Karl Tupper, San Luis Obispo Air Pollution Control District

This memo outlines the discussion with the Scientific Advisory Group, State Parks and San Luis Obispo Air Pollution Control District (APCD) on May 18, 2026 in reference to the State Parks Document "Restoration Project Maturation Time" Dated May 1, 2026.

After reviewing the methods and approach, APCD and State Parks agreed to the conclusion that it takes approximately five years post-planting for vegetation treatments to reach a condition where 80% of the grid cells reach 15% cover. The group agreed with the recommendation to assign all newly vegetated areas (both vegetation islands [VI] and other treatment areas [TA or TP]) zero emissions in the five years post-planting. After this five-year period, areas that do not reach a minimum of 15% cover will be assigned an appropriate SAG developed non-riding area emission curve.

This discussion represents a slight departure from the recommendation in the April 9, 2026 SAG Memo "Incorporating Vegetation Cover into the DRI Model." This memo recommended that VI polygons be assigned a new emissions curve immediately for the purpose of the 2026 ARWP. Instead, this will be implemented for a sub-set of the VI and TP polygons once they reach 5 years post initial planting. State Parks will provide Desert Research Institute an updated emissions zone map based on this agreement and will use the SAG generated emissions curve for new and existing emission zones for the 2026 Annual Report and Work Plan.

The issue of supplemental planting was not discussed specifically at the May 18 meeting. If supplemental planting occurs in a cell with less than 15% cover (or during the initial five-year period), State Parks recommends that those cells are again assigned zero emissions in the model until the supplemental planting reaches that five-year threshold. Until there is agreement on these supplemental planting areas, those cells that do not meet the 15% cover threshold will be modeled using the emissions curve suggested by the April 9, 2026 SAG Memo.

*THIS PAGE WAS INTENTIONALLY LEFT BLANK.*

**ODSVRA Dust Control Program SAG Review Draft 2026 ARWP**

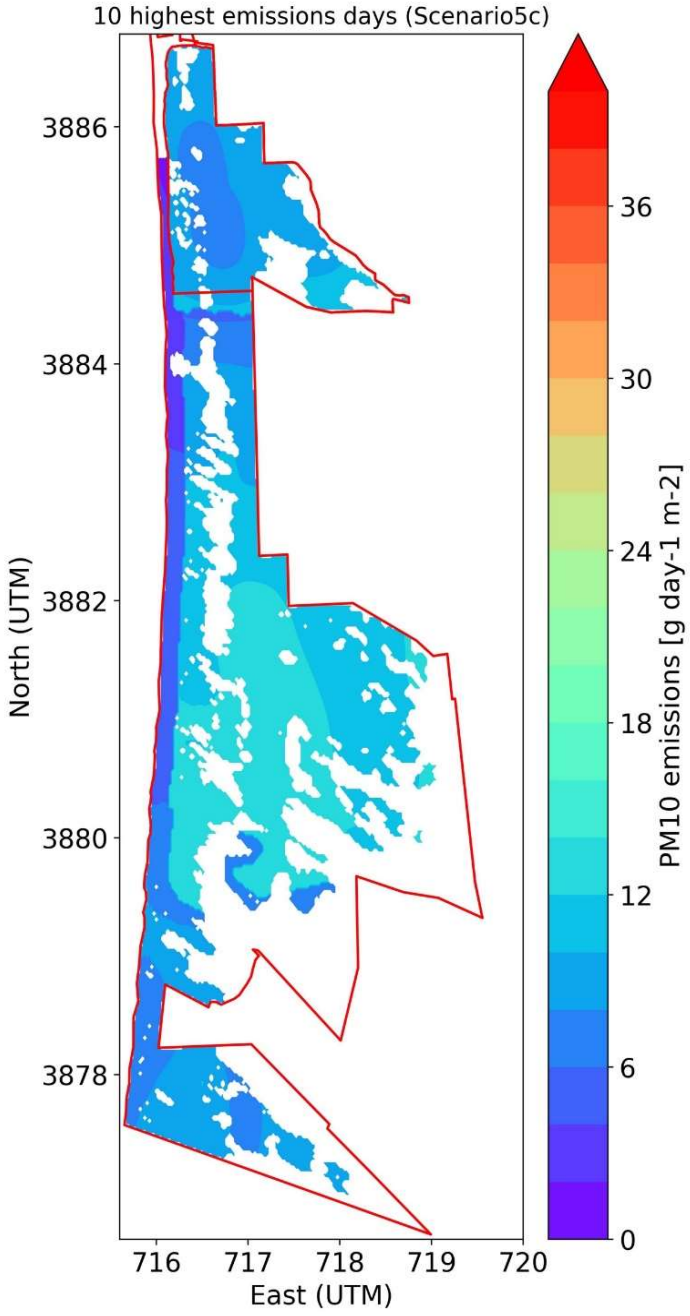
**ATTACHMENT 09**

**Modeling to Determine the Condition of Excess Emissions for 2026 ODSVRA (DRI Document)**

*THIS PAGE WAS INTENTIONALLY LEFT BLANK.*

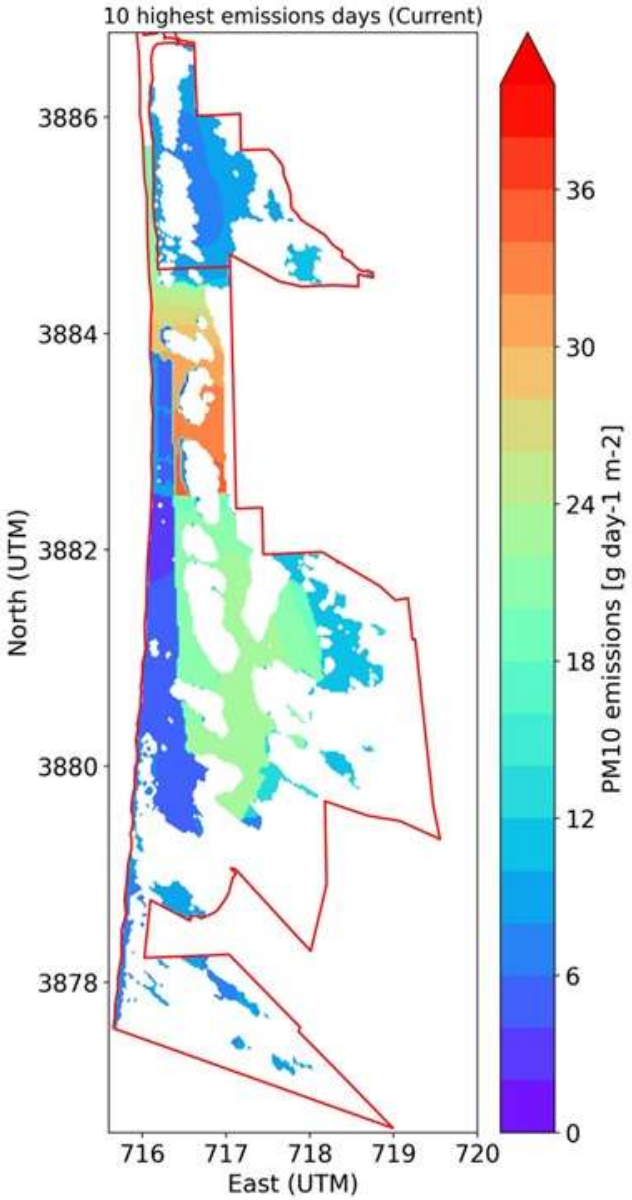
**Pre Disturbance (200m beach foredune)**

| Emissions by zone [Metric Tons/day] | Area of contributing grid points | 10 highest | 22-May |
|---|---|---|---|
| Non Riding Area Central | 1498.85 | 70.31 | 106.96 |
| Non Riding Area North | 570.35 | 20.04 | 22.4 |
| Non Riding Area South | 566.95 | 18.71 | 30.52 |
| Beach Foredune | 235.06 | 3.88 | 5.37 |
| Total | | 112.94 | 165.25 |



**Current**

| Emissions by zone [Metric Tons/day] | Area of contributing grid points | 10 highest |
|---|---|---|
| Foredune Restoration Area | 48.80 | 0.91 |
| Non Riding Area Central | 201.55 | 9.34 |
| Non Riding Area North | 368.34 | 12.87 |
| Non Riding Area South | 190.89 | 6.15 |
| Plover Exclosure | 303.94 | 5.19 |
| Riding Area Central-North | 241.39 | 28.13 |
| Riding Area Central-South | 527.72 | 46.42 |
| Seasonal Exclosure | 33.67 | 1.20 |
| NewN | 19.15 | 0.45 |
| NewS | 9.27 | 0.32 |
| Total | | 110.97 |



## Grid Cell Count 200m beach foredune

| Zone | Vegetated | Aerodynamically Sheltered | Non-vegetated | Total |
|---|---|---|---|---|
| Beach Foredune | 30 | 1 | 1522 | **1553** |
| Non Riding Area Central | 4920 | 196 | 9703 | **14819** |
| Non Riding Area North | 966 | 44 | 3693 | **4703** |
| Non Riding Area South | 3847 | 60 | 3673 | **7580** |
| **Grand Total** | **9763** | **301** | **18591** | **28655** |

## Acres 200m beach foredune

| Zone | Vegetated | Aerodynamically Sheltered | Non-vegetated | Total |
|---|---|---|---|---|
| Beach Foredune | 4.6 | 0.2 | 235.1 | **239.8** |
| Non Riding Area Central | 759.8 | 30.3 | 1498.5 | **2288.7** |
| Non Riding Area North | 149.2 | 6.8 | 570.3 | **726.3** |
| Non Riding Area South | 594.1 | 9.3 | 567.3 | **1170.7** |
| **Grand Total** | **1507.8** | **46.5** | **2871.2** | **4425.5** |

## Zone Totals 200m beach foredune

| Zone | Count | Acres |
|---|---|---|
| Beach Foredune | 1553 | 239.8 |
| Non Riding Area Central | 14819 | 2288.7 |
| Non Riding Area North | 4703 | 726.3 |
| Non Riding Area South | 7580 | 1170.7 |
| Unassigned | 81505 | 12587.7 |
| **Grand Total** | **110160** | **17013.2** |

*THIS PAGE WAS INTENTIONALLY LEFT BLANK.*

**ODSVRA Dust Control Program SAG Review Draft 2026 ARWP**

**ATTACHMENT 10**

**2026 PMRP Evaluation Metrics**

*THIS PAGE WAS INTENTIONALLY LEFT BLANK.*

**PMRP Evaluation Metrics – Annual Record 2025-26**

In 2021, the SAG, in consultation with State Parks, updated the PMRP evaluation metrics used to track dust control progress. The updated metrics provide a more streamlined dashboard that make it easier to track progress and to inform adaptative management. “Dust Mitigation Targets” refer to evaluation metrics with specific measurable endpoints. “Dust Mitigation Indicators” refer to values indicating progress but for which specific targets are not defined.

In 2022, the SOA amendments updated the metric for evaluating dust control progress, establishing a new excess emissions framework.

In October 2024, the SOA amendments extended the term of the SOA through December 2028, but did not materially change ARWP content or information requirements.

This attachment reports only on metrics both from the October 2022 and October 2024 amendments to the SOA (for the excess emissions framework, see Table 2).

Evaluation Metric table notes are provided at the end of this document.

| **DUST MITIGATION TARGETS TABLE 1: DUST CONTROL ACREAGE** | | | | | | | | | | |
|---|---|---|---|---|---|---|---|---|---|---|
| ***Dust mitigation treatments*** | | **2013 baseline** | **2019** | **2020** | **2021** | **2022** | **2023** | **2024** | **2025** | **2026[1]** |
| A. Cumulative area under treatment within ODSVRA, as of July 31 of current year, relative to 2013 baseline (acres) | A1. Total | 0 | 137.8 | 230.2 | 322.5 | 740.1 | 740.1 | 740.1 | 740.1 | 748.1 |
| | A2. Back dunes inside riding area | 0 | 103.1 | 195.5 | 213.2 | 288.3 | 288.3 | 288.3 | 288.3 | 288.3 |
| | A3. Back dunes outside riding area | 4.7 | 34.7 | 34.7 | 61.3 | 75.9 | 75.9 | 75.9 | 75.9 | 83.9 |
| | A4. Foredunes | 0 | 0.0 | 48.0 | 48.0 | 48.0 | 48.0 | 48.0 | 48.0 | 48.0 |
| | A5. Nesting exclosure | 0 | 0.0 | 0.0 | 0.0 | 293.3 | 293.3 | 293.3 | 293.3 | 293.3 |
| | A6. Foredune beach and corridor | 0 | 0.0 | 0.0 | 0.0 | 34.6 | 34.6 | 34.6 | 34.6 | 34.6 |

| **DUST MITIGATION TARGETS TABLE 2: EXCESS EMISSIONS FRAMEWORK** | | | | | | | | | |
|---|---|---|---|---|---|---|---|---|---|
| ***$PM_{10}$ mass emissions*** | | **2019** | **2020** | **2021** | **2022** | **2023** | **2024[2]** | **2025[3]** | **2026[4]** |
| A. Mean $PM_{10}$ emissions in all zones for 10 highest emission days – modeled (metric tons) | 1939 Pre-disturbance scenario | N/A | | | | | 166 | 135 | 113 |
| | Current scenario | N/A | | | | | 148 | 123 | 111 |

| **EVALUATION METRICS TABLE 3: DUST MITIGATION INDICATORS** | | | | | | | | | | |
|---|---|---|---|---|---|---|---|---|---|---|
| ***Air quality indicators*** | | **2013 baseline** | **2019** | **2020** | **2021** | **2022** | **2023** | **2024** | **2025** | **2026** |
| 1. Actual number of high wind event days[5] | | 59 | 30 | 55 | 51 | 64 | 72 | 51 | 71 | 27 |
| 2. Actual number of exceedances of California air quality standard[6] | 2a. at CDF | 58 | 12 | 30 | 54 | 54 | 16 | 13 | 22 | 22 |
| | 2b. at Mesa2 | 43 | 14 | 28 | 38 | 38 | 11 | 11 | 16 | 9 |
| 3. Actual number of exceedances of Federal air quality standard[7] | 3a. at CDF | 1 | 0 | 0 | 0 | 0 | 0 | 0 | 0 | 0 |
| | 3b. at Mesa2 | 0 | 0 | 0 | 0 | 0 | 0 | 0 | 0 | 0 |
| ***Foredune restoration*** | | **2013 baseline** | **2019** | **2020** | **2021** | **2022** | **2023** | **2024** | **2025** | **2026** |
| 4. Foredune plant fractional cover, at time of spring survey (%)[8] | 4a. Treatment 1 | N/A | N/A | N/A | 0 | 0 | 0 | 0 | 0.6 | -- |
| | 4b. Treatment 2 | | | | 0.1 | 1.9 | 2.7 | 3.1 | 3.6 | -- |
| | 4c. Treatment 3 | | | | 4.0 | 12.3 | 10.1 | 6.7 | 14.0 | -- |
| | 4d. Treatment 4 | | | | 0.8 | 5.7 | 5.1 | 7.9 | 6.0 | -- |
| | 4e. Treatment 5 | | | | 0.4 | 2.1 | 6.4 | 11.3 | 5.3 | -- |
| | 4f. Treatment 6 | | | | 3.6 | 12.7 | 13.8 | 17.8 | 15.0 | -- |
| 5. Foredune species richness index relative to Oso Flaco site (10 species in 2021)[9] | 5a. Treatment 1 | N/A | N/A | N/A | 0 | 0 | 20 | 80 | 40 | 50 |
| | 5b. Treatment 2 | | | | 33 | 40 | 30 | 50 | 30 | 40 |
| | 5c. Treatment 3 | | | | 50 | 50 | 40 | 70 | 50 | 80 |
| | 5d. Treatment 4 | | | | 100 | 60 | 70 | 100 | 90 | 100 |

| | | | | | | | | | | |
|---|---|---|---|---|---|---|---|---|---|---|
| | 5e. Treatment 5 | | | | 110 | 100 | 90 | 90 | 100 | 110 |
| | 5f. Treatment 6 | | | | 110 | 80 | 100 | 100 | 100 | 120 |
| 6. Foredune sand volume, current spring survey relative to previous fall survey ($m^3\ m^{-2}\ mo^{-1}$)[10] | 6a. Treatment 1 | N/A | N/A | N/A | 4 | 8 | -7 | 0 | 10 | 1 |
| | 6b. Treatment 2 | | | | 5 | 8 | 6 | 0 | 8 | 0 |
| | 6c. Treatment 3 | | | | 6 | 7 | 10 | 0 | 3 | 0 |
| | 6d. Treatment 4 | | | | 2 | 4 | 8 | 1 | 7 | 0 |
| | 6e. Treatment 5 | | | | 1 | 3 | 8 | 1 | 7 | 0 |
| | 6f. Treatment 6 | | | | 0 | 4 | 8 | 1 | 3 | 1 |

| ***Back dune stabilization*** | | **2013 baseline** | **2019** | **2020** | **2021** | **2022** | **2023** | **2024** | **2025** | **2026** |
|---|---|---|---|---|---|---|---|---|---|---|
| 7. Cumulative area of back dune stabilization within ODSVRA, as of July 31 of current year (acres) | 7a. Planting area | TBD[11] | 89.2 | 109.6 | 168.5 | 287.1 | 314.4 | 351.9 | 364.2 | 364.2 |
| | 7b. Fencing area | 0 | 48.6 | 53.7 | 72.8 | 53.0 | 32.5 | 0 | 0 | 0 |
| | 7c. Straw bales area | 0 | 0 | 18.9 | 27.3 | 24.1 | 17.3 | 12.3 | 0 | 0 |
| | 7d. Temporary vehicle exclusion areas | 0 | 0 | 0 | 5.9 | 0.0 | 0.0 | 0 | 0 | 0 |
| | 7e. Stabilized vegetation surface area | TBD[12] | 137.8 | 182.2 | 274.5 | 364.2 | 364.2 | 364.2 | 364.2 | 364.2 |
| 8. Native seed harvest for all plants during current ARWP reporting period (kilograms/year) | | N/A | 203.2 | 307.3 | 193.0 | 252.6 | 234.5 | 241.9 | 224.7 | 185.5 |
| 9. Plant species cultivation for all plants during current ARWP reporting period (#/year) | | | 106,350 | 89,433 | 127,464 | 125,380 | 121,724 | 116,112 | 121,013 | 109,657 |

**EVALUATION METRIC TABLE NOTES**

[1] 2026 dust mitigation treatment acreage values are based on State Parks 2026 ARWP, Chapter 3, and are subject to change.

[2] Pre-disturbance and current scenario emissions under the excess emissions modeling are from 2024 ARWP Table 2-9.

[3] Pre-disturbance and current scenario emissions under the excess emissions modeling are from 2025 ARWP Table 2-9.

[4] Pre-disturbance and current scenario emissions under the excess emissions modeling are from 2026 ARWP Table 2-10.

[5] Values are determined using the ARWP definition of "high wind event day", defined, in consultation with the SAG, as any day when the 3 p.m. PST hourly wind speed at CDF exceeds 8 mph and the 1 p.m. PST hourly wind direction is between 290 and 360°. The period of consideration is January 1 - July 31, 2026. Data may be preliminary and subject to change. The ARWP definition of high wind event days may differ from the SLOAPCD's definition used in SLOACPD reports and studies.

[6] The California Ambient Air Quality Standard is a mean value of 50 µg/$m^3$ over a 24-hour period. The period of consideration is January 1 – July 31, 2026. Data may be preliminary and subject to change.

[7] The National Ambient Air Quality Standard is a mean value of 150 µg/$m^3$ over a 24-hour period. The period of consideration is January 1 – July 31, 2026. Data may be preliminary and subject to change.

[8] Prior to 2025, State Parks used to evaluate percent cover of species, with the results of the line-intercept transect sampling compared to the UAS survey results to assess total vegetative cover within the FRA. State Parks, in consultation with the SAG, ceased the evaluation of percent cover during line-intercept transect sampling because it was determined to be redundant with the UAS surveys.

[9] The number of native plant species recorded for each treatment area as compared to reference site at Oso Flaco (10 species in 2021). Long term goal is to have a stable or increasing richness value versus reference site.

[10] 2021 – 2026 normalized volumetric change times 1,000 by total area per month obtained from 2026 ARWP Table 2-4. Values represent the change between spring (February UAS survey) of the column year and fall (October UAS survey) of the previous year. For example, the estimate of foredune sand volume for 2022 for treatment 2 (0.008 $m^3$ $m^{-2}$ $mo^{-1}$) is based on Table 2-4 column "Oct. 2021 – Feb. 2022".

[11] The baseline 2013 back dune stabilization "planting area" metric may be estimated from UCSB's historic vegetation report; however, the SAG has not established the methodology for establishing baseline vegetation conditions. State Parks will coordinate with the SAG to finalize the methodology for determining baseline 2013 back dune stabilization planting areas. Currently, the yearly estimates of planting area for the Dust Control Program (e.g., 89.2 acres in 2019) are based on the amount of back dune vegetation planted under the Dust Control Program (i.e., excludes foredune vegetation and non-vegetation projects such as wind fencing).

[12] The baseline 2013 back dune "stabilized vegetation surface area" metric may be estimated from vegetation coverage estimates determined from aerial imagery; however, the SAG has not established the methodology for establishing baseline vegetation conditions. State Parks will coordinate with the SAG to finalize the methodology for determining baseline 2013 back dune stabilization planting areas. Currently, the yearly estimates of stabilized vegetation surface area for the Dust Control Program (e.g., 137.8 acres in 2019) reflect the sum of the stabilization approaches in metrics 7a to 7d.

*THIS PAGE WAS INTENTIONALLY LEFT BLANK.*

**ODSVRA Dust Control Program SAG Review Draft 2026 ARWP**

**ATTACHMENT 11**

**2026/2027 ODSVRA Dust Control Program Vegetation Restoration Projects**

*THIS PAGE WAS INTENTIONALLY LEFT BLANK.*

2026-2027 APCD Planting Project List

| 2026-2027 Project List (subject to change) | | | | | | | |
|---|---|---|---|---|---|---|---|
| **Project Name** | **Project Acreage** | **Total Plants** | **Plants Per Acre** | **Native Seed (lbs)** | **Native Seed (lbs per Acre)** | **Sterile Grain Seed (lbs)** | **Large Straw Bales (3X4X8 ft)** |
| **Supplemental Areas (Initial Native Planting)** | | | | | | | |
| South Crescent (2021-VG-05) | 8.8 | 25,839 | 2,936 | 83 | 9.4 | 220 | 106 |
| **Supplemental Areas (Follow-up Native Planting)** | | | | | | | |
| Bigfoot West (2020-VG-04) | 7.9 | 21,248 | 2,690 | 76 | 9.6 | 200 | 95 |
| BBQ Flats (2019-VG-01) | 6.6 | 17,264 | 2,616 | 63 | 9.5 | 165 | 79 |
| Eucalyptus Table West (2023-VG-02) | 4.8 | 13,525 | 2,818 | 46 | 9.6 | 120 | 58 |
| LaGrille Hill South (2022-VG-07) | 4.4 | 11,840 | 2,691 | 42 | 9.5 | 110 | 53 |
| Boyscout Camp (2022-VG-11) | 3.2 | 8,040 | 2,513 | 30 | 9.4 | 80 | 38 |
| Eucalyptus Table East (2022-VG-09) | 2.7 | 7,055 | 2,613 | 25 | 9.3 | 70 | 32 |
| Paw Print 2018-VG-02) | 2.5 | 6,640 | 2,656 | 24 | 9.6 | 60 | 30 |
| Eucalyptus Tree West (2022-VG-05) | 1.2 | 3,048 | 2,540 | 11 | 9.2 | 25 | 14 |
| **Total** | **42.1** | **114,499** | **2,720** | **400** | **9.5** | **1,050** | **505** |

*THIS PAGE WAS INTENTIONALLY LEFT BLANK.*